Advances
in Clinical and Experimental Medicine

**WROCLAW
MEDICAL UNIVERSITY**

Contents

Monitoring the kynurenine system: Concentrations, ratios or what else?

Masaru Tanaka[A–F], László Vécsei[A–F]

Department of Neurology, Interdisciplinary Excellence Centre, Faculty of Medicine, University of Szeged, Hungary

A – research concept and design; B – collection and/or assembly of data; C – data analysis and interpretation;
D – writing the article; E – critical revision of the article; F – final approval of the article

Address for correspondence
Masaru Tanaka
E-mail: tanaka.masaru.1@med.u-szeged.hu

Abstract

The tryptophan-kynurenine metabolic pathway plays the most essential role in tryptophan metabolism, producing various endogenous bioactive molecules. The activation of the metabolic pathway is linked to the pathogenesis of a wide range of diseases. The calibration of the levels and the ratio of kynurenines has been attempted in search of biomarkers and diagnostic targets. This editorial introduces biosystems in close interaction with the kynurenine system and potential measures to assess a state of stress, which may lead to illnesses.

Key words: tryptophan, kynurenine, stress, neurological diseases, psychiatric diseases

Introduction

L-tryptophan (Trp) is the largest of the essential amino acids, the least abundant in the cell and the rarest in the proteome, which consumes the highest amount of energy in its biosynthesis among the 20 amino acids.[1] It is an essential component in the biosynthesis of proteins, muscle and enzymes, as well as an obligatory substrate for the production of neurotransmitters and hormones.[2] Acute Trp depletion causes increased pain sensitivity, acoustic startle, increased motor activity, and aggression, while chronic Trp deficiency causes ataxia, cognitive impairment and dysphoria with skin hyperpigmentation.[3,4] The Trp is broken down through the methoxyindole pathway leading to the production of serotonin (5-hydroxytryptamine) or through the kynurenine (KYN) pathway leading to the de novo synthesis of nicotinamide adenine dinucleotide (NAD$^+$). The KYN metabolic pathway consumes nearly 95% of Trp, being the controller of Trp metabolism while producing a wide range of multifarious and versatile bioactive molecules.[5] The molecules exhibit oxidant, antioxidant, anti-inflammatory, neurotoxin, neuroprotectant, and/or immunomodulating activity, but their actions depend on their concentrations and the cellular environment (Fig. 1).[6] Furthermore, the KYN system works in close interaction with other biosystems, including the oxidative stress complex, the antioxidant system, serotonin neurotransmission, glutamate neurotransmission, the tetrahydrobiopterin pathway, the cannabinoid system, the NAD$^+$/NADH redox system, and aryl hydrocarbon receptor (AHR) signaling.[2,5] The accelerated Trp metabolism is generally observed in clinical conditions such as infection, inflammation, cancer, aging, neurodegenerative diseases, and psychiatric disorders.[2,5,6,7–9]
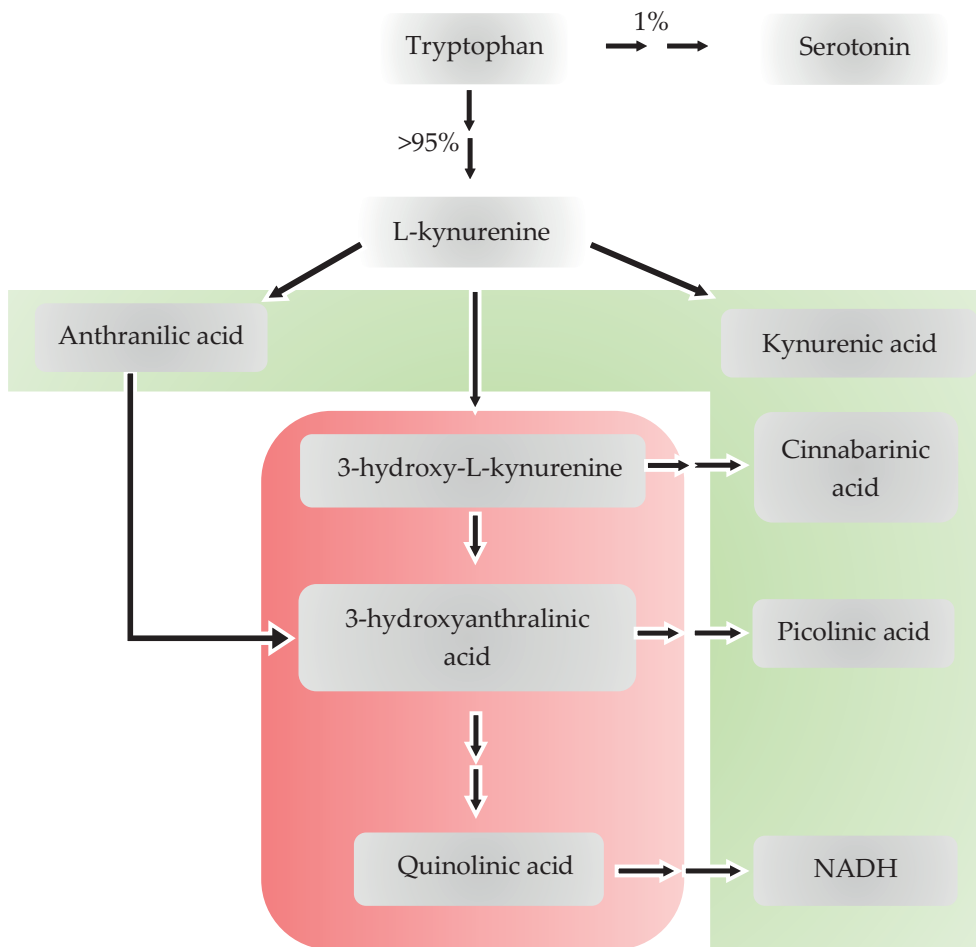
Fig. 1. Tryptophan (Trp) catabolism. More than 95% of Trp is broken down through the kynurenine (KYN) pathway, while only 1% of Trp is through the methoxyindole pathway. Protective KYN metabolites are marked green and toxic KYN metabolites are imarked red. The metabolites are endogenous molecules produced in balance in healthy conditions. However, the actions of the metabolites depend on the environment or their concentrations and the activation of the pathway generally leads to unfavorable consequences

The kynurenine system

In the KYN system, tryptophan 2,3-dioxygenase (TDO), indoleamine 2,3-dioxygenases (IDOs), kynurenine aminotransferases (KATs), kynureninase (KYNU), and kynurenine 3-monooxygenase (KMO) are the main enzymes in the Try degradation cascade. Among them, TDO and IDOs are responsible for the rate-limiting step of L-Trp to L-KYN. The TDO is stimulated by the stress hormone cortisol, while IDOs are upregulated by lipopolysaccharides and pro-inflammatory cytokines, and downregulated by antioxidant enzyme superoxide dismutase and anti-inflammatory cytokines. The KATs catalyze the conversion of KYN to kynurenic acid (KYNA) and 3-hydroxy-L-kynurenine (3-HK) to xanthurenic acid (XA), while KYNU converts L-KYN to anthranilic acid (AA). The KMO converts L-KYN to 3-HK. This enzyme is stimulated by oxygen molecules and pro-inflammatory cytokines, while it is inhibited by superoxide dismutase and anti-inflammatory cytokines. Thus, the KYN enzymes are under the constant influence of the hypothalamic–pituitary–adrenal axis, oxidative stress, the antioxidant system, and inflammatory responses.[2,5–9]

The 3-HK, 3-hydroxyanthranilic acid (3-HAA) and quinolinic acid (QA) are oxidants; however, 3-HK and 3-HAA may serve as antioxidants in certain conditions. Quinolinic acid stimulates glutamate receptors, while KYNA either stimulates or inhibits the glutamate receptors subgroups in a concentration-dependent manner. The L-KYN, KYNA, XA, and cinnabarinic acid (CA) are AHR agonists which relay the signal of immune tolerance. The AA serves as a water-soluble vitamin and its derivatives are nonsteroidal anti-inflammatory drugs such as diclofenac and mefenamic acid. Picolinic acid is thought to be a neuroprotectant (Fig. 1). The 3-HK stimulates TDO in vivo and NADH stimulates KMO, forming positive feedback loops; meanwhile, NADH inhibits TDO, forming a negative feedback loop within the KYN system.[2,5–9]

The molecules generated in the KYN system serve as components of and relay signals to the external biosystems: 3-HK, 3-HAA, and QA in the oxidative stress complex, 3-HK, 3-HAA, and KYNA in the antioxidant system, Trp in serotonin neurotransmission, QA and KYNA in glutamate neurotransmission, XA in the tetrahydrobiopterin pathway, KYNA and QA in the cannabinoid system, NADH in the NAD⁺/NADH redox system, and KYN, KYNA, XA, and CA in AHR signaling. Thus, stressors in general lead to the activation of the KYN system, and the presence of the positive feedback loops further amplifies stress loads, imposing a heavy burden on a wide range of biosystems.[2,5–9]

Monitoring the kynurenine system

Measurements of KYN metabolites and their ratios have been taken from clinical samples of patients with neurodegenerative diseases and psychiatric disorders in search of a correlation with diseases and thus to identify possible biomarkers.[2,10] Categorized analysis of neurotoxic KYNs and neuroprotective KYNs revealed higher levels of neurotoxic KYNs and higher ratios of neurotoxic KYNs in neurodegenerative and psychiatric diseases, but the levels and the ratios of neuroprotective KYNs remain unclear.[2,8,10] The levels of pro-inflammatory cytokines are invariably elevated in all diseases investigated, which therefore suggests that the elevation of neurotoxic KYNs is closely linked to the inflammatory response.[2,8] Furthermore, low-grade inflammation (LGI) is considered to participate in the pathogenesis of neurodegenerative diseases, but the role of LGI in psychiatric disorders remains unclear.[2] A meta-analysis of 101 studies of blood samples showed that decreased levels of Trp, KYN and KYNA, increased ratios of KYN/Trp, and decreased ratios of KYNA/KYN, KYNA/QA and KYNA/3-HK in patients with major depressive disorder (MDD), decreased levels of Trp and KYNA and decreased ratio of KYNA/QA in patients with bipolar disorder (BD), and the decreased level of Trp in patients with schizophrenia. This study confirms the activation of the Trp-KYN pathway and depletion of Trp in 3 major psychiatric disorders and the increased shunt toward the production of toxic KYNs in MDD and BD.[11] Further studies are expected to reveal the status of the KYN system and its interaction with functionally adjacent biosystems by assessing serotonin and glutamate neurotransmissions, tetrahydrobiopterin levels, antioxidant capacity, and immune tolerance.

Homeostasis, allostasis, far-from-equilibrium, entropy

The activation of the KYN system is at least partly a physiological reaction of the body to stressful events such as infection, inflammation, metabolic disturbance, aging, and anticipation, among others. The stability of le milieu intérieur (the internal environment) is essential to living independently of the external environment, as suggested by Claude Bernard, and homeostasis is the state within the physiological limits, proposed by Walter Cannon

(Fig. 2).[12,13] Selye conceptualized the process in which chronically harmful stimuli lead to disease in the general adaptation syndrome. Organisms attempt to maintain homeostasis against harmful stimuli up to the resistance stage but eventually surrender to the stressors in the exhaustion stage. Stress is an organized state of bodies in response to stressors, experienced by all patients during a period of illness. Harmful consequences are not due to exhaustion of defense mechanism, but the stress mediators themselves cause damage to the host, especially in the exhaustion stage (Fig. 2).[14] However, Selye's stress theory does not allow the measurements of stress or the evaluation of the reaction of systems under chronic stress.

Subsequently, Sterling and Eyer developed a concept of allostasis, which refers to the process of maintaining stability through change in the allostatic systems. The adaptational cost of chronic exposure to inappropriate response to the body, that is the allostatic load, eventually fails to perform normally, thus leading to diseases (Fig. 2).[15] However, the allostatic concept stands on the vague relationship between metabolism and energy consumption, which makes it difficult to sample and measure allostatic loads, thus limiting the application of the concept for stress measurement.

Researchers in the field of thermodynamics have attempted to quantify homeostasis, stress and allostasis. Life feeds on negative entropy. The second law of thermodynamics states the entropy of an isolated system can only increase. The body is an open thermodynamic system. Order within the body is maintained by an increase in the disorder of the environment through dissipating heat from the body.[16] It is supported in the nonequilibrium open system which prevails around us. The far-from-equilibrium system does not lead to turbulence, but indeed, it forms life.[17] Entropy is directional with time and thus it can be applied to physiological growth and aging.[18] A thermodynamic entropy-based model of the stress response has been proposed. Based on entropy production, the model describes the states of a living system under stress, and differentiates the states of health and disease by using measurable variables. Positive stress entropic load (SEL) leads to an adverse state, while negative SEL leads to a protective state of health. Furthermore, the model can predict not only the future failure of the living system but also the deterioration of the regulatory feedback (Fig. 2).[19] Improving energy balance may become a possible strategy for disease intervention.[20]

1850	1926	1936	1988	2016
Claude Bernard	Walter Cannon	Hans Selye	Sterling & Eyer	Bienertová-Vašků et al.
internal environment	homeostasis	adaptive stress response	allostasis	stress entropic load

Fig. 2. Conceptual evolution of stress

Conclusions and future perspective

Increasing amounts of evidence show the presence of KYN system activation in a wide range of diseases including neurodegenerative and psychiatric diseases. However, the levels and the ratios of KYN metabolites are equivocal among diseases and the actions of the metabolites are enigmatic depending on the environment and their concentrations.[21] Furthermore, the KYN system varies from cell or tissue where some enzymes are missing, and different bioactive molecules are predominantly produced.[10] Some metabolites can cross to the blood–brain barrier, but others cannot.[10] Nevertheless, the KYN metabolites potentially serve as biomarkers and the KYN system may be one possible target for disease intervention.[5,7,9,10] Very little is known about the interaction of the KYN system with adjacent biosystems. Understanding the interaction may open new diagnostic and interventional approaches toward various diseases.

Concepts of homeostasis, stress and allostasis have provided an intuitive insight into the action and effect of stress on the body and mind. Direct measurements of stressors, stress and the consequence remain far from feasible. Certainly, the KYN system is one of the major players under stress and in the pathogenesis of various diseases. Holistic approaches including understanding the interaction between other biosystems, theoretical reframing of the alteration of the KYN system under stress, and the application of empirical models to assess pathological processes and their consequences may provide a possible clue to understanding such a complex system.

The roles of the KYN system in physiological aging, the interaction of sex/gender factors, and nutritional and metabolic stress are of particular interest.[22,23] Animal research will certainly make a solid contribution to the area. Transgenic and pharmacological animal models of cognitive, emotional and/or social impairment may reveal the roles of the aging process, and/or sex/gender factors in the pathogenesis of mental illnesses. Transgenic mice such as KYNA, KYNU or KMO knock-out strains and double knock-out strains may help understand the role of the KYN system in physiological aging, discover potential diagnostic biomarkers and search for possible interventional targets in neurodegenerative diseases and psychiatric disorders.

ORCID iDs

Masaru Tanaka https://orcid.org/0000-0003-4383-4024
László Vécsei https://orcid.org/0000-0001-8037-3672

References

1. Barik S. The uniqueness of tryptophan in biology: Properties, metabolism, interactions and localization in proteins. *Int J Mol Sci.* 2020; 21(22):8776. doi:10.3390/ijms21228776
2. Tanaka M, Tóth F, Polyák H, et al. Immune influencers in action: Metabolites and enzymes of the tryptophan–kynurenine metabolic pathway. *Preprints.* 2021;2021:2021060344. doi:10.20944/preprints 202106.0344.v1
3. van Donkelaar E, Blokland A, Ferrington L, et al. Mechanism of acute tryptophan depletion: Is it only serotonin? *Mol Psychiatry.* 2011;16(7): 695–713. doi:10.1038/mp.2011.9
4. Blankfield A. A brief historic overview of clinical disorders associated with tryptophan: The relevance to chronic fatigue syndrome (CFS) and fibromyalgia (FM). *Int J Tryptophan Res.* 2012;5:27–32. doi:10.4137/IJTR.S10085
5. Tanaka M, Török N, Vécsei L. Editorial: Are 5-HT1 receptor agonists effective anti-migraine drugs? *Expert Opin Pharmacother.* 2021;12:1–5. doi:10.1080/14656566.2021.1910235
6. Encyclopedia. Available online: https://encyclopedia.pub/8633 (accessed on 21 June 2021).
7. Tanaka M, Bohár Z, Vécsei, L. Are kynurenines accomplices or principal villains in dementia? Maintenance of kynurenine metabolism. *Molecules.* 2020;25(3):564. doi:10.3390/molecules25030564
8. Tanaka M, Toldi J, Vécsei L. Exploring the etiological links behind neurodegenerative diseases: Inflammatory cytokines and bioactive kynurenines. *Int J Mol Sci.* 2020;21(7):2431. doi:10.3390/ijms21072431
9. Tanaka M, Török N, Vécsei L. Novel pharmaceutical approaches in dementia. Riederer P, Laux G, Nagatsu T, Le W, Riederer C, eds. *NeuroPsychopharmacotherapy.* Cham, Switzerland: Springer; 2021. doi:10.1007/978-3-319-56015-1_444-1
10. Török N, Tanaka M, Vécsei L. Searching for peripheral biomarkers in neurodegenerative diseases: The tryptophan–kynurenine metabolic pathway. *Int J Mol Sci.* 2020;21(24):9338. doi:10.3390/ijms21249338
11. Marx W, McGuinness AJ, Rocks T, et al. The kynurenine pathway in major depressive disorder, bipolar disorder, and schizophrenia: A meta-analysis of 101 studies [online ahead of print published on November 23, 2020]. *Mol Psychiatry.* 2020. doi:10.1038/s41380-020-00951-9
12. Bernard C. *An Introduction to the Study of Experimental Medicine.* Transl. H.C. Greene. New York, USA: Collier; 1865
13. Cannon WB. *The Wisdom of the Body.* New York, USA: Norton; 1932.
14. Selye H. *The Stress of Life.* 2nd ed. New York, USA: McGraw–Hill; 1976.
15. Sterling P, Eyer J. Allostasis: A new paradigm to explain arousal pathology. In: Fisher S, Reason JT. *Handbook of Life Stress, Cognition and Health.* Chichester, USA: Wiley & Sons; 1988.
16. Schrödinger E. *What is Life?* Cambridge, UK: Cambridge University Press; 1944.
17. Ornes S. Core Concept: How nonequilibrium thermodynamics speaks to the mystery of life. *Proc Natl Acad Sci U S A.* 2017;114(3):423–424. doi:10.1073/pnas.1620001114
18. Haddad WM. Thermodynamics: The unique universal science. *Entropy.* 2017;19:621. doi:10.3390/e19110621
19. Bienertová-Vašků J, Zlámal F, Nečesánek I, et al. Calculating stress: From entropy to a thermodynamic concept of health and disease. *PLoS One.* 2016;11(1):e0146667. doi:10.1371/journal.pone.0146667
20. Finger E. Thermodynamics as the driving principle behind the immune system. *Einstein (Sao Paulo).* 2012;10(3):386–388. doi:10.1590/s1679-45082012000300024
21. Rózsa E, Robotka H, Vécsei L, Toldi J. The Janus-face kynurenic acid. *J Neural Transm.* 2008;115:1087–1091. https://doi.org/10.1007/s00702-008-0052-5
22. Muntsant A, Jiménez-Altayó F, Puertas-Umbert L, et al. Sex-dependent end-of-life mental and vascular scenarios for compensatory mechanisms in mice with normal and AD-neurodegenerative aging. *Biomedicines.* 2021;9(2):111. doi:10.3390/biomedicines9020111
23. Giménez-Llort L, Marin-Pardo D, Marazuela P, Hernández-Guillamón M. Survival bias and crosstalk between chronological and behavioral age: Age- and genotype-sensitivity tests define behavioral signatures in middle-aged, old and long-lived mice with normal and AD-associated aging. *Biomedicines.* 2021;9(6):636. doi:10.3390/biomedicines9060636
24. Kordestani Moghadam P, Nouriyengejeh S, Seyedhoseini B, Pourabbasi A. The study of relationship between nutritional behaviors and metabolic indices: A systematic review. *Adv Biomed Res.* 2020;9:66. doi:10.4103/abr.abr_12_20
25. Kordestani-Moghadam P, Assari S, Nouriyengejeh S, Mohammadipour F, Pourabbasi A. Cognitive impairments and associated structural brain changes in metabolic syndrome and implications of neurocognitive intervention. *J Obes Metab Syndr.* 2020;29(3):174–179. doi:10.7570/jomes20021

MiR-let-7i inhibits CD4+ T cell apoptosis in patients with acute coronary syndrome

Boxin Zhao[A,B,D], Zhiyong Zhang[A,B,F], Lin Gui[C], Yingyu Xiang[B], Xueyuan Sun[E], Lijuan Huang[A]

The Second Affiliated Hospital of Harbin Medical University, China

A – research concept and design; B – collection and/or assembly of data; C – data analysis and interpretation;
D – writing the article; E – critical revision of the article; F – final approval of the article

Address for correspondence
Lijuan Huang
E-mail: hebhlj@sina.com

Abstract

Background. Abnormal CD4+ T cells appear in the peripheral blood of patients with acute coronary syndrome (ACS). Studies have confirmed that CD4+ T cells are resistant to apoptosis, but the specific mechanism has not been elucidated yet.

Objectives. The microRNA (miR)-let-7i plays an important regulatory role in the cardiovascular system and is widely involved in cell proliferation and apoptosis. In this study, we aimed to investigate its functional and regulatory roles in CD4+ T cell apoptosis.

Materials and methods. Apoptosis of CD4+ T cells was detected using TUNEL assay. Western blot analyses were used to detect the expression of Bcl-2 and Bax. Real-time polymerase chain reaction and western blot analyses were used to detect the expression of miR-let-7i, Fas and FasL. A miR-let-7i mimic or inhibitor was transfected into CD4+ T cells, and miR-let-7i activity was investigated using Cell Counting Kit-8 (CCK-8) and TUNEL assays.

Results. Apoptosis of CD4+ T cells in ACS patients was significantly decreased. Overexpression of miR-let-7i inhibited CD4+ T cell apoptosis and improved cell survival rates, while inhibition of miR-let-7i facilitated cell apoptosis. We also found that miR-let-7i negatively regulated Fas and FasL gene expression in CD4+ T cells.

Conclusions. The present study identified that miR-let-7i significantly reduces Fas and FasL expression in ACS CD4+ T cells and inhibits apoptosis in these cells. Therefore, miR-let-7i may serve as a possible therapeutic target for the treatment of ACS.

Key words: Fas, FasL, CD4+ T cell, apoptosis, miR-let-7i

Background

Acute coronary syndrome (ACS) refers to clinical conditions characterized by the rupture of atherosclerotic plaques and the secondary formation of complete or incomplete occlusive thrombosis. Atherosclerotic plaque rupture is the most important physiological and pathological mechanism in ACS, accounting for more than 70% of acute coronary events. The ACS-vulnerable plaques are characterized by thin, fibrous caps covering large lipid nuclei, inflammatory cell infiltration (including T cells, macrophages and other immune cells) and endothelial smooth muscle cell apoptosis. Studies have shown that T lymphocytes play an important role in the development of atherosclerosis, and inflammatory cytokines secreted by CD4⁺ T cells can directly affect the stability of atherosclerotic plaques by activating macrophages, thereby leading to the occurrence of ACS.[1] In addition to macrophage activation and cytokine secretion, CD4⁺ T cells have been reported to accumulate in early and advanced human atherosclerotic plaques and contribute to the progression and destabilization of these atherosclerotic lesions.[2] Studies have shown that CD4⁺ T cells in the peripheral blood of patients with ACS lack the co-stimulatory receptor CD28.[3] Furthermore, CD4⁺ T cells have a long life span and secrete large amounts of interferon gamma (IFN-γ) and tumor necrosis factor alpha (TNF-α), which leads to a chronic inflammatory response that causes plaque rupture.[4] It is currently believed that the longevity of CD4⁺ T cells is related to apoptotic resistance;[5,6] however, this specific mechanism needs further study.

MicroRNAs (miRNAs) are a class of non-coding small RNAs of about 18–25 nucleotides in length that can regulate gene expression after transcription through degradation or inhibition of translation of the target mRNA via base pairing specific to that mRNA.[7] MiR-let-7 was first discovered in *Caenorhabditis elegans* and is highly conserved in a variety of species, including flies and mammals.[8] The human miR-let-7 family includes 13 members – let-7a, let-7b, let-7c, let-7d, and miR-98 and other members. Recent studies have shown that let-7i plays an important regulatory role in tissue differentiation and tumorigenesis as well as cell proliferation and apoptosis.[9] MiR-let-7i can act on different apoptosis-related genes, such as insulin-like growth factor-1 receptor (*IGF1R*),[10] B-cell lymphoma-extra large (*Bcl-xl*)[11] and YAP1,[12] supporting its role in regulating apoptosis.

Cell apoptosis, as a part of the self-balancing mechanism of growth and development, maintains a constant number of cells in the body by eliminating damaged cells in tissues that are difficult to control for a prolonged time.[13,14] Apoptotic signal transduction includes 3 pathways: the Fas/FasL pathway, the mitochondrial pathway and the granulase B pathway,[15,16] among which is Fas/FasL the main pathway of apoptosis.

Objectives

Fas is the most representative death receptor in the TNF superfamily. After binding to its ligand FasL on the surface of the cell membrane, the Fas molecules aggregate and form a trimer that initiates apoptosis signal transmission leading to cell death with positive Fas expression.[17] Kovalcsik et al. found that CD4⁺ T cells resist apoptosis through the death receptor pathway (Fas-mediated) in ACS patients.[18] Furthermore, studies have shown that there are binding sites between miR-let-7i and Fas/FasL.[19,20] Nevertheless, how miR-let-7i and Fas/FasL mediate the anti-apoptotic effects of CD4⁺ T cells in ACS remains unclear. Therefore, the aim of this study was to explore whether miR-let-7i regulates the expression of the Fas/FasL genes to promote the anti-apoptotic effects of CD4⁺ T cells in the peripheral blood of ACS patients.

Materials and methods

Clinical study population

Based on patients' angina symptoms and the diagnostic criteria of the American Heart Association, we enrolled 36 patients (41–78 years old) diagnosed with ACS, 23 men and 13 women. The enrollment criteria were ACS confirmed with angiography at the time of enrollment and obvious clinical symptoms within 24 h before the consultation. Patients with infectious diseases, tumors, connective tissue diseases, and autoimmune diseases were excluded. A total of 30 healthy study participants (20 men and 10 women) were recruited from the physical examination center of Second Affiliated Hospital of Harbin Medical University, China. Stable angina pectoris (SAP) patients enrolled in this study experienced chest discomfort or pain that could be relieved with rest or administration of nitroglycerin; SAP patients (diagnosed via coronary angiography) were enrolled from our hospital. There was no statistically significant difference in gender or age of patients enrolled in this study (p > 0.05). In order to exclude the interference of other risk factors on experimental data, statistical analysis was conducted on triglycerides (TG), total cholesterol (TC), high-density lipoprotein (HDL), and low-density lipoprotein (LDL) (Table 1), and the results showed no statistical difference among each group (p > 0.05).

The present study was approved by the Research Ethics Committee of the Second Affiliated Hospital of Harbin Medical University and was performed in accordance with the Declaration of Helsinki and the guidelines of the Ethics Committee of the Second Affiliated Hospital of Harbin Medical University. Written informed consent was obtained from all patients for the use of their clinical tissues.

Table 1. Clinical and biochemical characteristics of the study subjects. Values are expressed as mean ±SD or median (Q1–Q3). TC and LDL were analyzed with ANOVA. Age, TG and HDL were analyzed using Kruskal–Wallis test. The χ^2 test was used for gender statistics

Variable	Total	Normal	SAP	ACS	p-value
Patients, n	97	30	31	36	–
Gender	62 male/35 female	20 male/10 female	19 male/12 female	23 male/13 female	0.91
Age [years]	58 (48–65)	54.5 (45.75–61)	60 (52–65)	57.5 (47–65.75)	0.24
TC [mmol/L]	4.38 ±0.80	4. 50 ±0. 72	4.31 ±1.06	4.34 ±0.58	0.61
TG [mmol/L]	1.65 (1.22–2.07)	1.65 (1.27–1. 97)	1.48 (0.98–1.97)	1.76 (1.34–2.14)	0.12
HDL [mmol/L]	1.13 (1.06–1.27)	1.13 (1.08–1.50)	1.13 (1.05–1.24)	1.13 (1.05–1.19)	0.19
LDL [mmol/L]	2.66 ±0.62	2.81 ±0.46	2.51 ±0.81	2.67 ±0.52	0.18

TC – total cholesterol; TG – triglyceride; HDL – high-density lipoprotein; LDL – low-density lipoprotein; SD – standard deviation; ANOVA – analysis of variance; ACS – acute coronary syndrome; SAP – stable angina pectoris.

CD4+ T cell isolation and culture

Peripheral blood mononuclear cells were isolated by density centrifugation using Human Peripheral Blood Lymphocyte Dissociation Solution (TBD Science, Tianjin, China). CD4+ T cells were purified from peripheral blood mononuclear cells using BD IMag™ anti-human CD4 Particles-DM (Becton Dickinson Biosciences, San Jose, USA) and a Cell Separation Magnet (Becton Dickinson Biosciences) according to the manufacturer's instructions. Cells were cultured at 37°C in a humidified incubator at 5% CO$_2$ in RPMI-1640 supplemented with 100 U IL-2, 2 µg/mL phytohemagglutinin (PHA), and 10% fetal bovine serum (FBS). Next, the cells were washed and subjected to flow cytometric analysis and RNA extraction.

Flow cytometry

CD4+ T cell purity determination

Isolated cells were stained with PE Mouse Anti-Human CD4 antibody (Elabscience Biotechnology, Wuhan, China) according to the manufacturer's instructions. Cells were subsequently analyzed using multicolor flow cytometry, and their purity was assessed. The purity of sorted CD4+ T cells was 90–95% (Fig. 1).

Perforin detection

Briefly, 100 µL of fresh EDTA anticoagulant whole blood was added to the test and control tubes, respectively. Then, 20 µL of FITC-CD4 and PEcy5-CD28 (BD Biosciences)
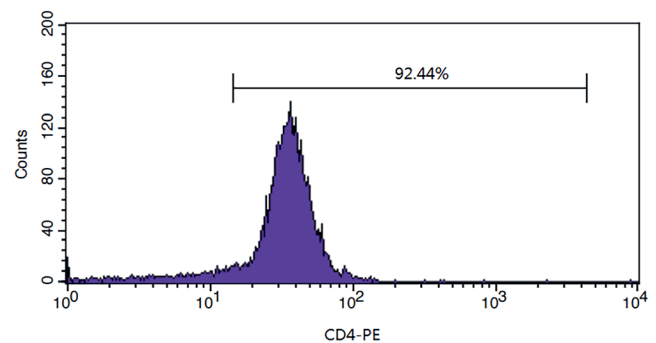
Fig. 1. The purity of sorted CD4+ T cells

were added to the test tube and 20 µL of isotype control antibody was added to the control tube; the tubes were incubated. The erythrocytes were lysed and perforated with FACS (Becton Dickinson Biosciences), 20 µL PE-Perforin mAb (Legend Biotech, USA) was added and the cells were incubated. Finally, paraformaldehyde was used to fix the cells, which were analyzed using flow cytometry.[21]

qRT-PCR

Total RNA was extracted from CD4+ T cells using Trizol reagent (Sigma–Aldrich, St. Louis, USA) and quantified using a NanoDrop spectrophotometer (Shimadzu, Kyoto, Japan) according to the manufacturer's instructions. The total RNA was then reverse-transcribed into complementary DNA (cDNA) using the Transcriptor First Strand cDNA Synthesis Kit (Roche, Mannheim, Germany). Quantitative real-time polymerase chain reaction (qRT-PCR) analysis was performed using FastStart Universal SYBR Green Master (Roche), with an initial denaturation step at 95°C for

Table 2. Primer sequence of the target gene

Gene name	Forward primer	Reverse primer
Fas	TCTGGTTCTTACGTCTGTTGC	CTGTGCAGTCCCTAGCTTTCC
FasL	ATCCTACCAAGGCAACCA	CCCTGTCCAACCTCTGTG
β-actin	GGACCTTCTAAGCCCTTTTGG	GCCTGCTCCTCTTACTCCTCAC
miR-let-7i	CGGGCTGAGGTAGTAGTTTG	CAGCCACAAAAGAGCACAAT
U6	GAGATACCGACTTGTTCCTTACG	CTCGCCTTTCTCAACCTCTTCTT

10 min, followed by 45 cycles of 95°C for 15 s and 60°C for 30 s. The sequences of the used primers (Shanghai Generay Biotech, Shanghai, China) are shown in Table 2. U6 small nuclear RNA was used as an internal control to normalize miR-let-7i levels. β-actin was used as an internal control to normalize Fas and FasL.

Western blot

The protein expressions of Fas, FasL, Bax, Bcl-2, and β-actin in cells were assayed with western blot analysis. Total protein of CD4⁺ T cells was extracted in RIPA lysis buffer (Beyotime, Shanghai, China) and then quantified using BCA assay (Beyotime). A total of 50 μg of protein was separated using 8% or 10% sodium dodecyl sulphate–polyacrylamide gel electrophoresis (SDS-PAGE). After electrophoresis, the proteins were transferred onto polyvinylidene fluoride (PVDF) membranes. The membranes were incubated with 5% skimmed milk at room temperature (20–25°C) for 1 h and then incubated with the corresponding primary antibody overnight at 4°C. Membranes were washed 3 times with Tris-buffered saline with Tween 20 (TBST), and then incubated with the appropriate secondary antibodies. Protein bands were visualized using the electrochemiluminescence (ECL) system. Beta-actin was used as an internal control.

Cell transfection

CD4⁺ T cells were transfected with miR-let-7i mimic or mimic negative control (NC) or with inhibitor or inhibitor NC, using Entranster™-R4000 (Engreen Biosystem Ltd, Beijing, China) according to the manufacturer's instructions. Cells were then collected and washed with ice-cold phosphate-buffered saline (PBS) for subsequent analysis.

CCK-8 assay

To test the CD4⁺ T cell survival ratio, we used the Cell Counting Kit-8 (CCK-8; Dalian Meilun Biotechnology, Dalian, China) according to the manufacturer's instructions. CD4⁺ T cells were digested and seeded into 96-well plates at a density of 1×10^5 per well in 100 μL of the medium. Cells were then transfected with mimic, mimic NC, inhibitor or inhibitor NC for 12 h 24 h or 36 h. The optical density (OD) value was read at 450 nm. Each experiment was repeated 3 times. The cell survival ratio was calculated as follows:

$$\text{cell survival ratio} = [(As - Ab)/(Ac - Ab)] \times 100\%.$$

As – the OD value of the treatment group; Ac – the OD value of control group; Ab – the OD value of the blank group.

TUNEL staining for DNA fragmentation

Poly-L-lysine was used to coat the cell culture plate (24-well plate) for 30 min, and the liquid was discarded. The transfected cells were inoculated and plated on the 24-well plate and cultured for 3 h to fix the cells on the plate. The air-dried cell samples were fixed with freshly prepared 4% paraformaldehyde in PBS for 1 h. The cells were incubated with 3% H_2O_2 in methanol for 10 min, incubated with 0.1% Triton X-100 for 2 min on ice and washed twice with PBS. A total of 50 μL of TUNEL reaction solution (Roche) was added to each well and incubated at 37°C for 1 h in the dark. Cell samples were analyzed using fluorescence microscopy.

Statistical analyses

Statistical analyses were performed using IBM SPSS v. 24.0 (IBM Corp., Armonk, USA) and GraphPad Prism v. 5.0 (GraphPad Software, San Diego, USA), and results were considered significant when p < 0.05. The results are presented as mean ± standard error of the mean (SEM) from 3 or more independent experiments. Student's t-test was used to analyze the data between 2 groups. Clinical and biochemical characteristics were analyzed using the Kruskal–Wallis test, analysis of variance (ANOVA) or χ² test. Parametric tests mentioned in this paper satisfy the assumptions.

Results

Percentage of CD4⁺ T cells between ACS patients and healthy subjects

We found that CD4⁺ T cells accounted for 63.7% in healthy subjects, while the percentage of CD4⁺ T cells was 58.4% in ACS patients.[22] These results indicate that there was no significant difference in the percentage of CD4⁺ T cells between normal subjects and ACS patients. It is possible that the absolute lymphocytosis was not significantly different between the studied groups.

The apoptosis level of CD4⁺ T cells was markedly decreased in ACS patients

The apoptosis level of CD4⁺ T cells was assessed using TUNEL staining (Fig. 2). TUNEL-stained images showed a greater number of TUNEL-positive cells (green) in cells from the healthy controls than in cells from ACS patients. Statistical analysis showed that the number of apoptotic CD4⁺ T cells in ACS patients was significantly decreased when compared with CD4⁺ T cells from healthy control individuals. Next, we detected the expression levels of apoptotic proteins, Bcl-2 and Bax with western blot. As shown in Fig. 3, the CD4⁺ T cells from ACS patients showed higher expression of the anti-apoptotic protein Bcl-2 (t = 6.585, degrees of freedom (df) = 4, p = 0.0028) and markedly lower expression of the pro-apoptotic protein Bax than those in healthy controls (t = 7.703, df = 4, p = 0.0015). This suggests that CD4⁺ T cells in peripheral blood of ACS patients are resistant to apoptosis.
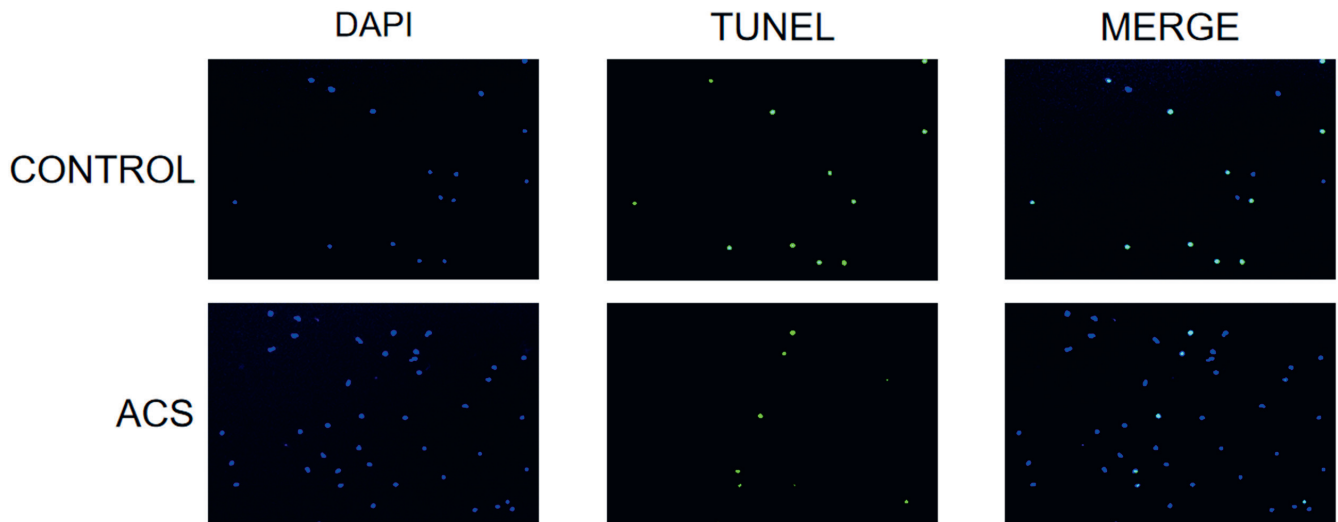
Fig. 2. TUNEL assay was used to detect the apoptosis in cells. Representative images of immunofluorescence staining showing expression of apoptotic cells (stained in green). Nuclei that labeled with DAPI (blue)
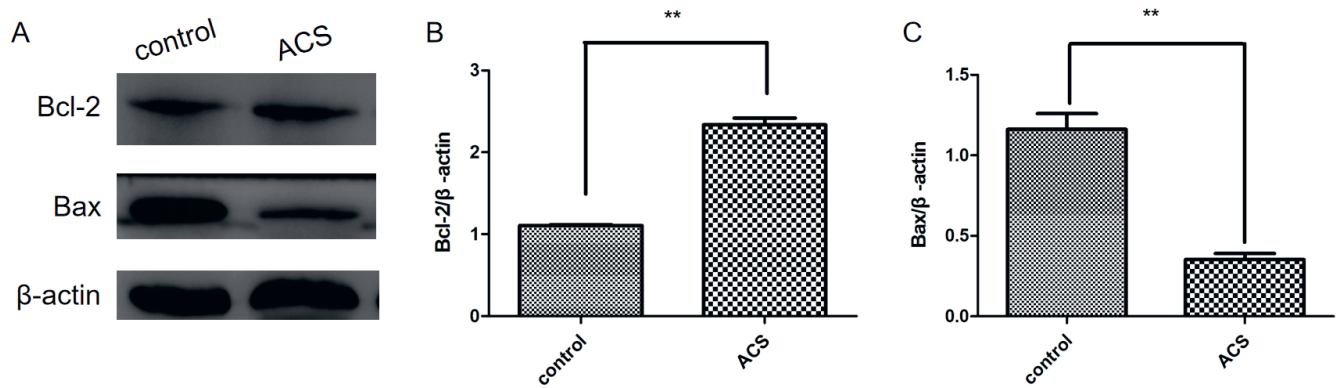
Fig. 3. A. Western blot analysis showing the expression levels of Bcl-2 and Bax proteins; B and C. Relative integrated density values were calculated using ImageJ (National Institutes of Health, Bethesda, USA) (n = 3). ** p < 0.01 compared to control. Data are expressed as mean ±standard error of the mean (SEM). Statistical analysis was done using Student's t-test.
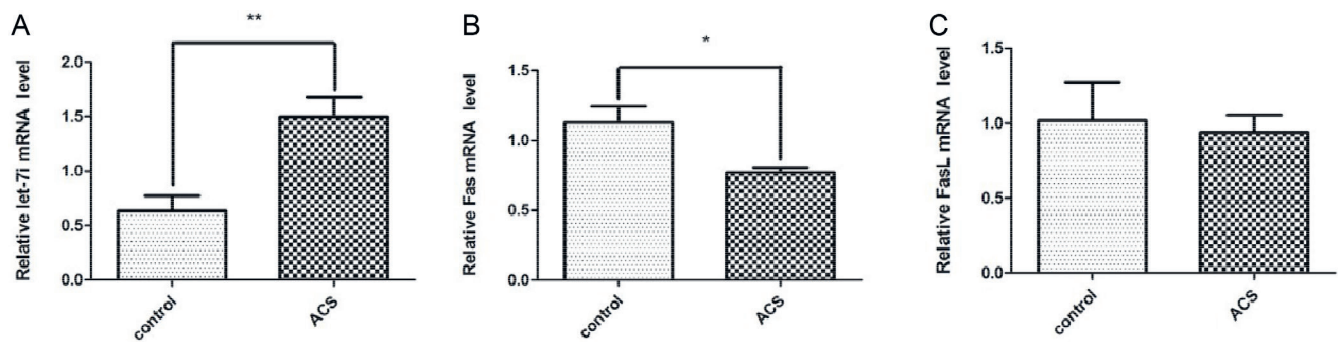
Fig. 4. The expression levels of miR-let-7i, Fas and FasL. Relative miR-let-7i (A), Fas (B) and FasL (C) expression levels in ACS CD4+ T cells compared with normal CD4+ T cells as determined using quantitative real-time polymerase chain reaction (qRT-PCR). *p < 0.05 and **p < 0.01 compared to control. Data are expressed as mean ±standard error of the mean (SEM). Statistical analysis was done using Student's t-test

MiR-let-7i was upregulated and Fas was downregulated in CD4+ T cells of patients with ACS

As shown in Fig. 4, miR-let-7i expression was markedly higher (t = 3.701, df = 8, p = 0.006) and Fas mRNA expression levels (t = 2.579, df = 11, p = 0.0257) decreased in ACS CD4+ T cells when compared with those of healthy controls. However, the expression of FasL (t = 0.9227, df = 12, p = 0.3743) was not significantly different from that of the healthy controls.

Fas and FasL were negatively regulated by miR-let-7i in ACS CD4+ T cells

The qRT-PCR results revealed that overexpression of ##miR-let-7i significantly reduced the mRNA expression levels of Fas (t = 3.509, df = 4, p = 0.0247) and FasL (t = 3.801, df = 7, p = 0.0067) when compared with that of mimic NC. In contrast, miR-let-7i inhibitors had the opposite effect and increased expression levels of Fas (t = 2.428, df = 12, p = 0.0319) and FasL (t = 5.550, df = 4, p = 0.0052) (Fig. 5). Similarly, the protein expression of Fas (mm: t = 3.392, df = 6, p = 0.0146; in: t = 2.417, df = 10, p = 0.0363) and FasL (mm: t = 4.927, df = 4, p = 0.0388; in: t = 3.773, df = 4, p = 0.0196) as determined with western blot analysis supported this finding (Fig. 6). Based on the obtained results, we conclude that miR-let-7i might negatively regulate the mRNA and protein expression of Fas and FasL.

MiR-let-7i enhanced the survival rate of ACS CD4+ T cells

Based on the miR-let-7i expression levels in CD4+ T cells determined with qRT-PCR, the cells were transfected with miR-let-7i mimic or mimic NC or with inhibitor or inhibitor NC to investigate the biological functions of miR-let-7i in CD4+ T cells. Next, the influence of miR-let-7i on CD4+ T cells was investigated using CCK-8 assays. The survival rate of CD4+ T cells transfected with miR-let-7i mimic was significantly higher than that of the miR-let-7i mimic NC group (12 h: t = 4.677, df = 6, p = 0.0034; 24 h: t = 10.17, df = 6, p < 0.001; 36 h: t = 10.74, df = 6, p < 0.001). In contrast, CD4+ T cells transfected with the miR-let-7i inhibitor (12 h: t = 6.295, df = 7, p = 0.0004; 24 h: t = 8.496, df = 8, p < 0.0001; 36 h: t = 3.725, df = 4, p = 0.0204) exhibited a notable decrease compared with those in the inhibitor
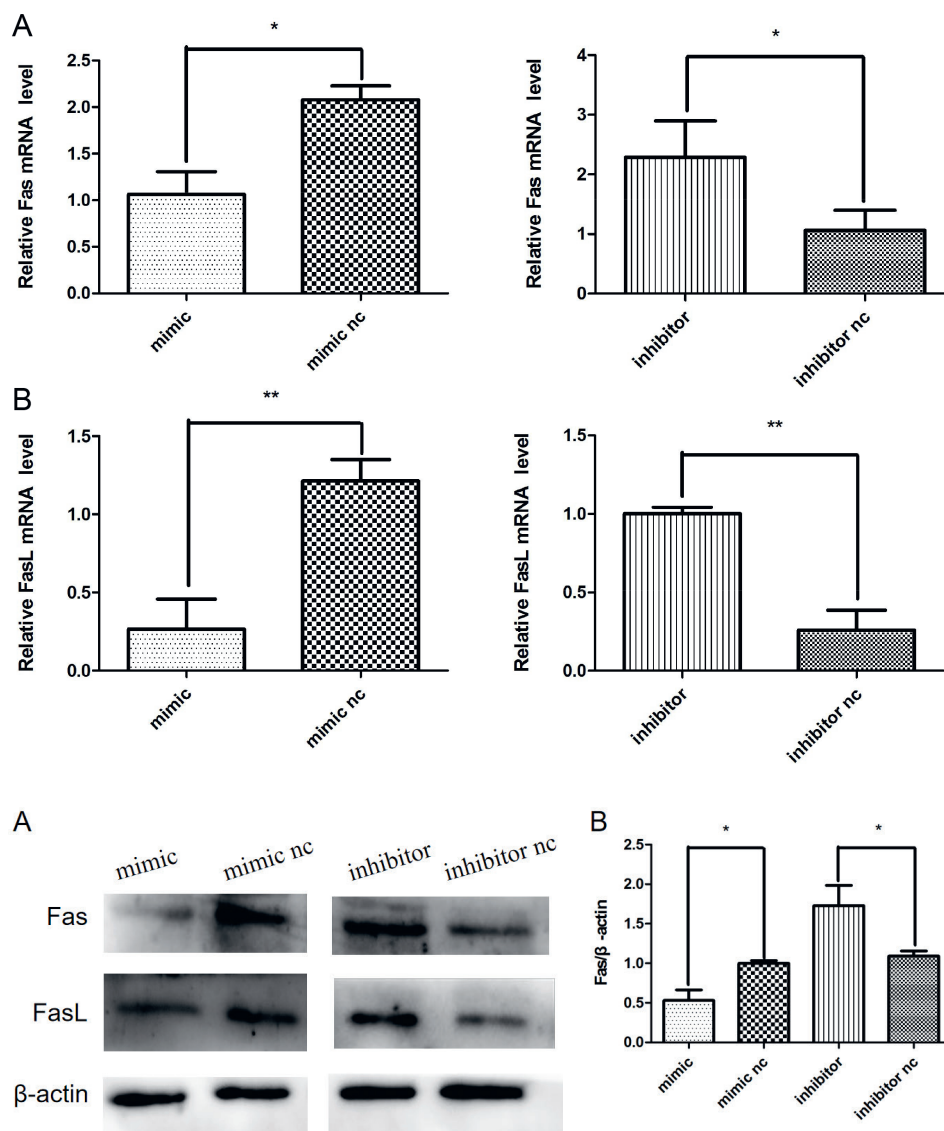
Fig. 5. Effect of miRNA-let-7i on the expression levels of Fas, FasL mRNA after transfection. ACS CD4+ T cells were transfected with miR-let-7i mimic, mimic NC, inhibitor, or inhibitor NC. The mRNA expression levels of Fas and FasL were decreased in cells transfected with miRNA-let-7i mimic compared with the mimic NC, but there was a higher expression in cells transfected with the miRNA-let-7i inhibitor compared with the inhibitor NC. *p < 0.05 and **p < 0.01 compared to control. Data are expressed as mean ±SEM. Statistical analysis was done using Student's t-test

Fig. 6. Transfected ACS CD4+ T cells with miR-let-7i mimic, mimic NC, inhibitor, or inhibitor NC. A. Western blot analysis showed the expression levels of Fas and FasL proteins; B and C. The miRNA-let-7i mimic group showed a significantly decreased expression of Fas and FasL, and the miR-let-7i inhibitor group showed a significantly increased expression of these proteins compared with those in control cells (n = 3); *p < 0.05 compared to control. Data are expressed as mean ±standard error of the mean (SEM). Statistical analysis was done using Student's t-test
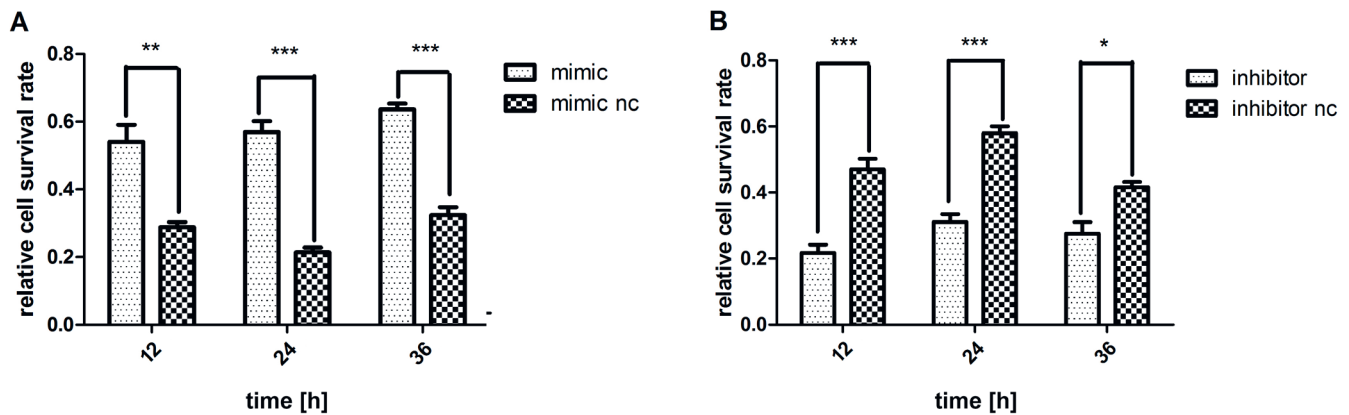
Fig. 7. Effect of miRNA-let-7i on the ACS CD4+ T cell survival ratio. CD4+ T cells were transfected with miR-let-7i mimic, mimic NC, inhibitor, or inhibitor NC for 12 h, 24 h or 36 h. CCK-8 assay was conducted to detect cell survival ratio (n > 3).*p < 0.05, **p < 0.01 and ***p < 0.001 compared to control. Data are expressed as mean ±standard error of the mean (SEM). Statistical analysis was done using Student's t-test

nc group (Fig. 7). These findings indicated that miR-let-7i might play a protective role in ACS CD4+ T cells.

MiR-let-7i inhibited apoptosis of ACS CD4+ T cells

To determine the effect of miR-let-7i on the apoptosis of CD4+ T cells, we transfected miR-let-7i mimic, mimic NC or inhibitor, inhibitor NC into CD4+ T cells. The apoptosis of CD4+ T cells was determined using TUNEL staining. As demonstrated in Fig. 8, TUNEL staining images showed a greater number of TUNEL-positive cells (green color) in the miR-let-7i-inhibitor-transfected group than in the inhibitor NC group. Interestingly, overexpression of miR-let-7i dramatically decreased the number of TUNEL-positive cells.

MiR-let-7i regulates the expression of the apoptosis proteins Bcl-2 and Bax in ACS CD4+ T cells

To further confirm that miR-let-7i can regulate CD4+ T cell apoptosis, the expression of apoptotic proteins was analyzed with western blot. As shown in Fig. 9, the expression of the anti-apoptotic protein Bcl-2 (t = 3.659, df = 4, p = 0.0216) was higher and the pro-apoptotic protein Bax (t = 5.466, df = 6, p = 0.0016) was lower in the mimic group compared with the mimic NC group. In contrast, miR-let-7i inhibitor reduced the expression of Bcl-2 (t = 7.008, df = 4, p = 0.0022) and increased the expression of Bax (t = 16.59, df = 4, p < 0.0001) when compared with the inhibitor NC group. In recent years, Bax has been found to interact with Bcl-2 to form a heterodimer or with itself to form a homodimer, and increased levels of the Bax homodimers often lead to apoptosis.[23] Accordingly, we examined the ratio of Bax/Bcl-2 (Fig. 9D). The results showed that miR-let-7i downregulated the Bax/Bcl-2 ratio. These results further confirmed that miR-let-7i plays a crucial role in regulating CD4+ T cell apoptosis.

Discussion

In this study, we demonstrate that compared with healthy control, the apoptosis rate of CD4+ T cells was reduced in ACS patients. We found high levels of miR-let-7i in CD4+ T cells in the peripheral blood of ACS patients. Upregulation of miR-let-7i inhibited apoptosis of CD4+ T cells in ACS, which may be one of the reasons for the resistance to apoptosis of these cells. The present study showed that Fas expression levels were reduced in ACS patients, while the expression of FasL was not significantly different from that in normal subjects, a finding which is consistent with previous results.[18] Our research confirms that miR-let-7i contributes to the partial protection of CD4+ T cells from apoptosis by targeting Fas/FasL.

Studies on T cells have confirmed the critical roles of miR-let-7i in the regulation of apoptosis. Zhang et al. found that miR-let-7i mediates CD4+ T cells to resist apoptosis through the IL-2 signaling pathway during HIV-1 infection.[24] Recent reports have indicated that miR-let-7i might protect T cells from apoptosis in ankylosing spondylitis by targeting IGF1R.[10] However, the regulatory mechanisms of miR-let-7i in CD4+ T cells in ACS are still unclear. In this study, we determined the expression of miR-let-7i. The expression level of miR-let-7i in CD4+ T cells in ACS was significantly upregulated when compared with the healthy control group. The abnormal expression of miR-let-7i may be associated with anti-apoptotic effects in CD4+ T cells. Therefore, the biological activity of miR-let-7i in CD4+ T cells was investigated by transfection and other tests. Our results showed that miR-let-7i overexpression facilitated cell survival and anti-apoptotic effects, while the opposite effects were observed in the miR-let-7i inhibitor group.

Apoptosis is a programmed and orderly cell death regulated by several genes. Cells undergo apoptosis via 'exogenous' (death receptor) or 'endogenous' (mitochondrial) pathways. The Fas/FasL signaling pathway plays an important role in apoptosis.[16] Fas, also known as Apo1 or CD95,
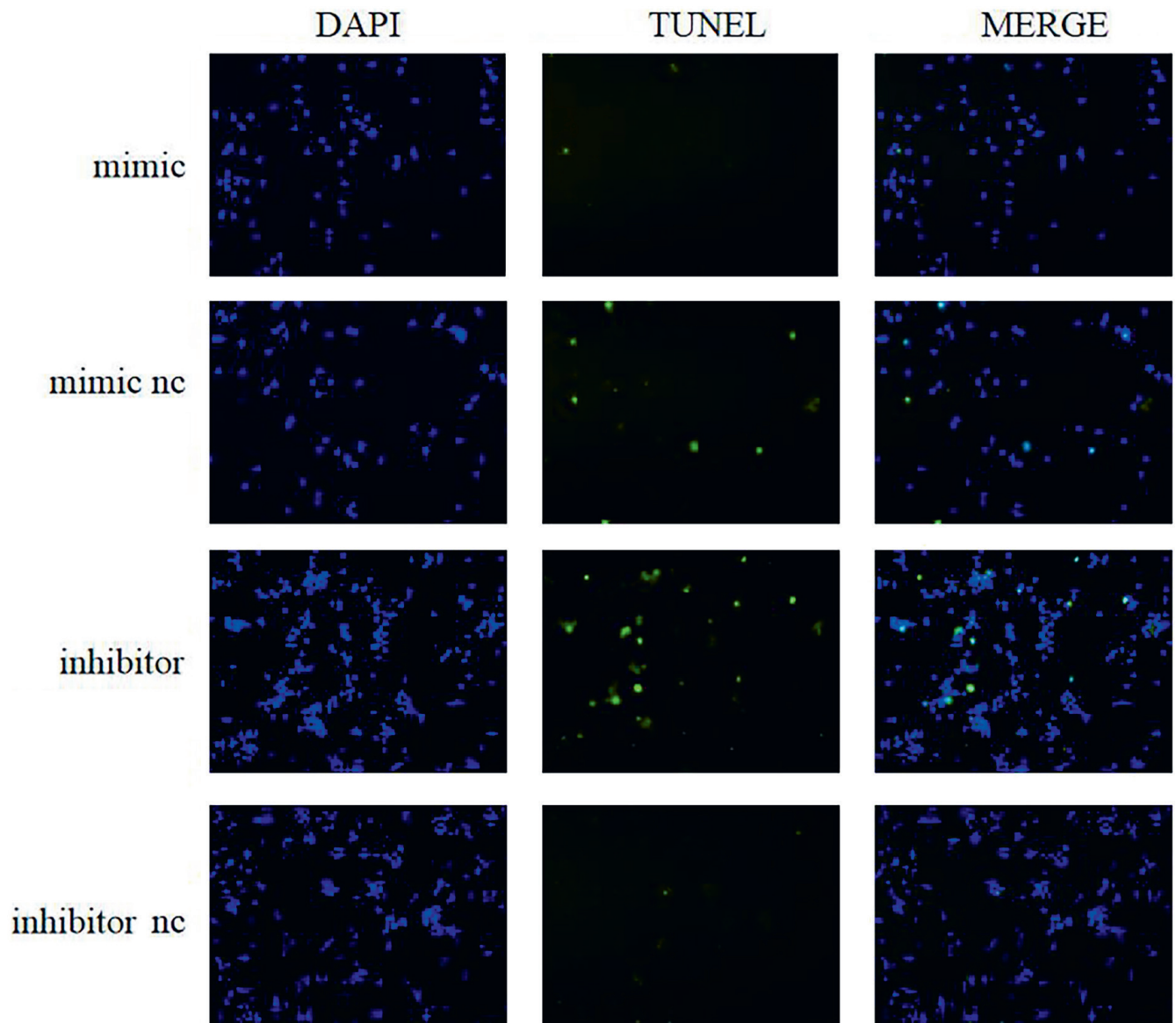
Fig. 8. Effect of miRNA-let-7i on ACS CD4+ T cell apoptosis. The number of TUNEL-positive cells transfected with miRNA-let-7i mimic was decreased compared with those with mimic NC. However, the number of TUNEL-positive cells transfected with miR-let-7i inhibitor was significantly increased. Representative images of immunofluorescence staining showing expression of apoptotic cells (stained in green). Nuclei were labeled with DAPI (blue)

belongs to the TNF receptor family and is a transmembrane glycoprotein widely distributed on the surface of different cells.[25] Fas initiates the extrinsic apoptotic pathway to induce apoptosis by interacting with its natural ligand, FasL.[26] Liu et al. found that Fas/FasL induced myocardial cell apoptosis in the process of myocardial cell ischemia-reperfusion (I/R) in a rat model.[25] Zhang et al. indicated that the upregulation of miR-25 inhibits cerebral I/R injury-induced apoptosis by downregulating Fas/FasL.[27] In this study, we identified the decreased expression of Fas and a slight difference in FasL in ACS patients when compared with healthy subjects.

MiR-let-7 is one of the largest and most highly expressed families of miRNAs.[28] All family members are considered to have similar functions because of the identical seed region (nucleotides 2 to 7) required for miR-target mRNA interaction.[9] It has been shown that miR-let-7i belongs to the let-7 family. Wang et al. first demonstrated that let-7 regulates Fas expression and the sensitivity of Fas-mediated apoptosis.[19] Furthermore, Zhang et al. indicated that miR-98, a member of the let-7 family, regulates Fas/FasL gene expression in myocardial cells and modulates cell apoptosis.[29] Zhang et al. also proved that Faslg, encoding the Fas ligand, is the target of let-7i-5p and plays an anti-apoptotic role.[20] Fas/FasL signaling is a major regulator of apoptosis.[30] We confirmed that miR-let-7i negatively regulates Fas/FasL at the RNA and protein levels and plays a significant role in the apoptosis of CD4+ T cells in ACS. However, the association between cell apoptosis and Fas/FasL expression and whether interference with

A
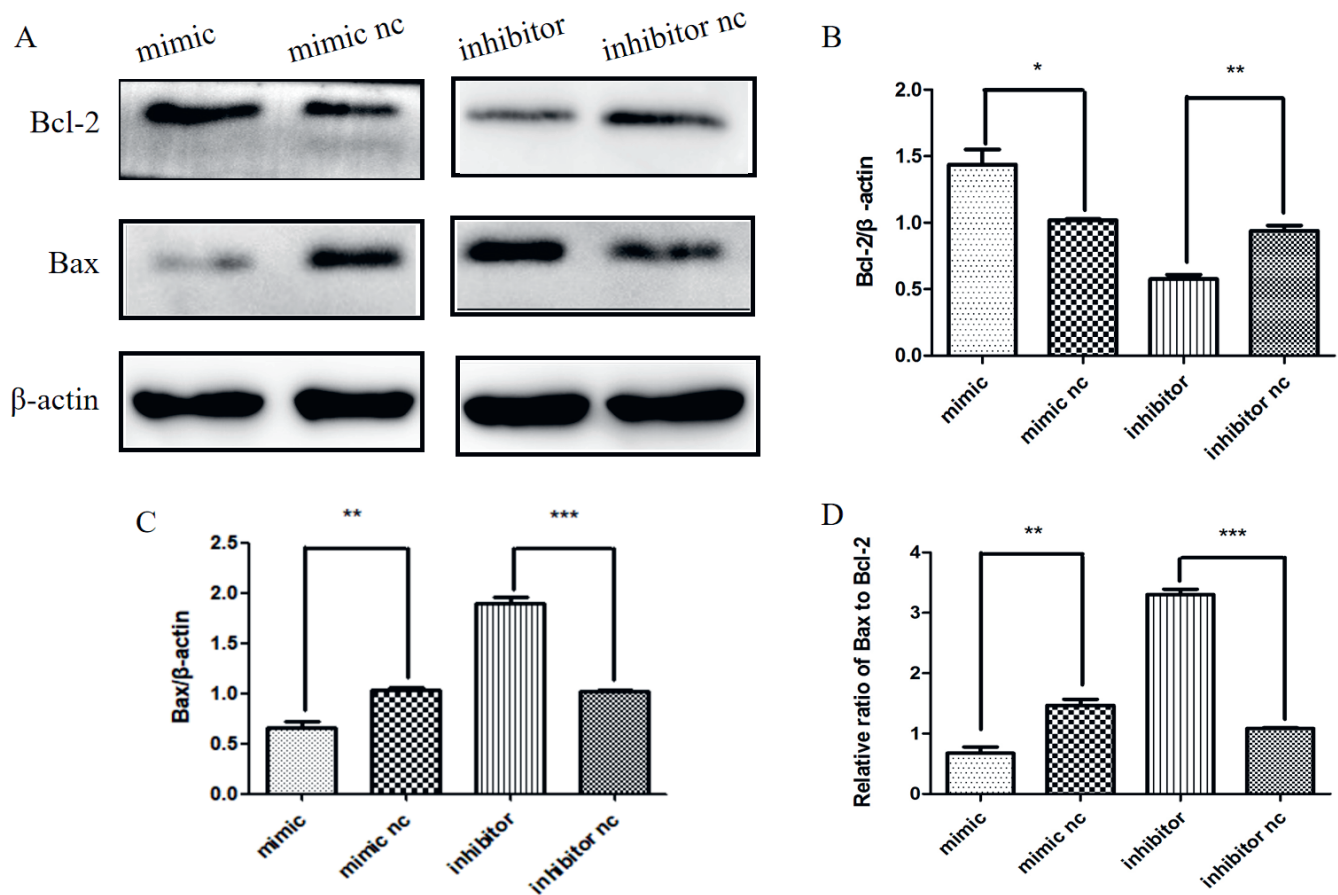
Fig. 9. Effect of miRNA-let-7i on ACS CD4+ T cell apoptosis proteins Bcl-2 and Bax and the ratio of Bax/Bcl-2. A. Western blot analysis shows the expression levels of Bcl-2 and Bax proteins; B and C. Relative integrated density values were calculated using ImageJ. The ratio of Bax/Bcl-2 (D) (n = 3); *p < 0.05, **p < 0.01 and ***p < 0.001 compared to control. Data are expressed as mean standard error of the mean (SEM). Statistical analysis was done using Student's t-test

the Fas/FasL signaling pathways affects the role of miR-let-7i in apoptosis remain to be established. Future studies are needed to clarify the molecular mechanisms involved.

Previous studies have found that CD4+ T cells lacking the costimulatory receptor CD28 are present in the peripheral blood of patients with ACS. It has also been shown that these CD28-deficient CD4+ T cells can accumulate preferentially in unstable ruptured atherosclerotic plaques. This particular subset of CD4+ T cells can selectively invade unstable plaques, indicating that they may have a direct role in plaque destabilization following the local activation by antigens.[31] These cells can also express killer cell immunoglobulin-like receptors (KIRs) that release IFN-γ.[32] Our study has shown that the majority of CD4+ T cells in ACS patients express perforin but lack CD28, while CD4+ T cells in both healthy controls and SAP patients express CD28 but lack perforin expression.[21] Thus, the decreased expression of the CD28 costimulatory molecule has an important effect on the function of CD4+ T cells. Because of the decreased expression of CD28 protein, the CD4+ T cells in ACS patients are resistant to apoptotic signals, and live longer in vivo. We will focus on the understanding of the relationship between the decreased protein expression of CD28 and the mechanisms of survival and apoptosis of CD4+ T cells in future research studies.

Limitations

In addition to CD4+CD28−T cells, there are many other subsets of CD4+T cells. In this study, we only study the CD4+T cells. Therefore, we need to further investigate the important role of CD4+T cells and their subsets in acute coronary syndromes.

Conclusions

In conclusion, our findings demonstrate that miR-let-7i significantly reduces Fas and FasL expression in ACS CD4+ T cells and inhibits apoptosis in these cells. Our work indicates that suppressing miR-let-7i may be a potential approach to treat atherosclerosis. Since a large number of genes are involved in apoptosis, we cannot exclude the possibility that miR-let-7i regulates cell apoptosis by targeting other apoptosis genes. Therefore, further studies are needed to confirm our findings.

ORCID iDs

Boxin Zhao ![ID] https://orcid.org/0000-0002-6011-0637
Zhiyong Zhang ![ID] https://orcid.org/0000-0002-4282-5970
Lin Gui ![ID] https://orcid.org/0000-0002-1019-7535
Yingyu Xiang ![ID] https://orcid.org/0000-0003-3180-0492
Yueyuan Sun ![ID] https://orcid.org/0000-0003-4548-8321
Lijuan Huang ![ID] https://orcid.org/0000-0003-4999-917X

References

1. Dumitriu IE, Kaski JC. The role of lymphocytes in the pathogenesis of atherosclerosis: Focus on CD4$^+$ T cell subsets. *Inflamm Resp Cardiovasc Surg*. 2013;2013:9–14. doi:10.1007/978-1-4471-4429-8_2

2. Cao M, Ruan L, Huang Y, et al. Premature CD4$^+$ T cells senescence induced by chronic infection in patients with acute coronary syndrome. *Aging Dis*. 2020;116(6):1471–1480. doi:10.14336/AD.2020.0203

3. Téo FH, de Oliveira RT, Mamoni RL, et al. Characterization of CD4$^+$CD28^{null} T cells in patients with coronary artery disease and individuals with risk factors for atherosclerosis. *Cell Immunol*. 2013;281(1):11–19. doi:10.1016/J.CELLIMM. 2013.01.007

4. Ye ZL, Lu HL, Su Q, Li L. Association between the level of CD4$^+$ T lymphocyte microRNA-155 and coronary artery disease in patients with unstable angina pectoris. *J Geriatr Cardiol*. 2018;15(10):611–617. doi:10.11909j.issn.1671-5411. 2018.10.003

5. Moro F, Morciano A, Tropea A, et al. CD4$^{(+)}$CD28$^{(null)}$ T lymphocyte frequency, a new marker of cardiovascular risk: Relationship with polycystic ovary syndrome phenotypes. *Fertil Steril*. 2012;98(6):1609–1615. doi:10.1016/j.fertnstert.2012.08.015

6. Dumitriu IE. The life (and death) of CD4$^+$CD28^{null} T cells in inflammatory diseases. *Immunology*. 2015;146(2):185–193. doi:10.1111/imm.12506

7. Wu T, Cao Y, Yang Y, et al. A three-dimensional DNA walking machine for the ultrasensitive dual-modal detection of miRNA using a fluorometer and personal glucose meter. *Nanoscale*. 2019;11(23):279–284. doi:10.1039/c9nr03588e

8. Lee H, Han S, Kwon CS, et al. Biogenesis and regulation of the let-7 miRNAs and their functional implications. *Protein Cell*. 2016;7(2):100–113. doi:10.1007/s13238-015-0212-y

9. Zhou Q, Frost RJA, Anderson C, et al. Let-7 contributes to diabetic retinopathy but represses pathological ocular angiogenesis. *Mol Cell Biol*. 2017;37(16):00001-17. doi:10.1128/MCB.00001-17

10. Hou C, Zhu M, Sun M, et al. MicroRNA let-7i induced autophagy to protect T cell from apoptosis by targeting IGF1R. *Biochem Biophys Res Commun*. 2014;453(4):728–734. doi:10.1016/j.bbrc.2014.10.002

11. Wu L, Wang Q, Yao J, et al. MicroRNA let-7g and let-7i inhibit hepatoma cell growth concurrently via downregulation of the anti-apoptotic protein B-cell lymphoma-extra large. *Oncol Lett*. 2015;9(1):213–218. doi:10.3892/ol.2014.2706

12. Ni J, Liu Y, Wang K, et al. Trophoblast stem-cell-derived exosomes improve doxorubicin-induced dilated cardiomyopathy by modulating the let-7i/YAP pathway. *Mol Ther Nucleic Acids*. 2020;22:948–956. doi:10.1016/j.omtn.2020.10.014

13. Raiders SA, Eastwood MD, Bacher M, et al. Binucleate germ cells in *Caenorhabditis elegans* are removed by physiological apoptosis. *PLoS Genet*. 2018;14(7):e1007417. doi:10.1371/journal.pgen.1007417

14. Brown JJ, Short SP, Stencel-Baerenwald J, et al. Reovirus-induced apoptosis in the intestine limits establishment of enteric infection. *J Virol*. 2018;92(10):e02062-17. doi:10.1128/JVI.02062-17

15. Czabotar PE, Lessene G, Strasser A, Adams JM. Control of apoptosis by the BCL-2 protein family: Implications for physiology and therapy. *Nat Rev Mol Cell Biol*. 2014;15(1):49–63. doi:10.1038/nrm3722

16. Rathore R, McCallum JE, Varghese E, Florea AM, Büsselberg D. Overcoming chemotherapy drug resistance by targeting inhibitors of apoptosis proteins (IAPs). *Apoptosis*. 2017;22(7):898–919. doi:10.1007/s10495-017-1375-1

17. Budisova Svandova E, Vesela B, Lesot H, Poliard A, Matalova E. Expression of Fas, FasL, caspase-8 and other factors of the extrinsic apoptotic pathway during the onset of interdigital tissue elimination. *Histochem Cell Biol*. 2017;147(4):497–510. doi:10.1007/s00418-016-1508-6

18. Kovalcsik E, Antunes RF, Baruah P, Kaski JC, Dumitriu IE. Proteasome-mediated reduction in pro-apoptotic molecule Bim renders CD4$^+$CD28^{null} T cells resistant to apoptosis in acute coronary syndrome. *Circulation*. 2015;131(8):709–720. doi:10.1161/circulationaha.114.013710

19. Wang S, Tang Y, Cui H, et al. Let-7/miR-98 regulate Fas and Fas-mediated apoptosis. *Genes Immun*. 2011;12(2):149–154. doi:10.1038/gene.2010.53

20. Zhang J, Ma J, Long K, et al. Overexpression of exosomal cardioprotective miRNAs mitigates hypoxia-induced H9c2 cells apoptosis. *Int J Mol Sci*. 2017;18(4):711. doi:10.3390/ijms18040711

21. Li-Juan H, Ying C, Wen-Ying S, et al. CD4$^+$CD28^{null} T cell numbers of peripheral blood in patients with coronary heart diseases. *Chinese Journal of Laboratory Medicine*. 2007;30:424–426. doi:10.3760/j.issn: 1009-9158.2007.04.017

22. Sun W, Cui Y, Zhen L, Huang L. Association between HLA-DRB1, HLA-DRQB1 alleles, and CD4$^{(+)}$CD28$^{(null)}$ T cells in a Chinese population with coronary heart disease. *Mol Biol Rep*. 2011;8(3):1675–1679.

23. Lu J, Lu S, Li J, Yu Q, Liu L, Li Q. MiR-629-5p promotes colorectal cancer progression through targeting CXXC finger protein 4. *Biosci Rep*. 2018;38(4):BSR20180613. doi:10.1042/BSR20180613

24. Zhang Y, Yin Y, Zhang S, Luo H, Zhang H. HIV-1 infection-induced suppression of the Let-7i/IL-2 axis contributes to CD4$^{(+)}$ T cell death. *Sci Rep*. 2016;6:25341. doi:10.1038/srep25341

25. Liu XM, Yang ZM, Liu XK. Fas/FasL induces myocardial cell apoptosis in myocardial ischemia-reperfusion rat model. *Eur Rev Med Pharmacol Sci*. 2017;21(12):2913–2918. PMID:28682425

26. Yang Y, Yang H, Xu M, et al. Long non-coding RNA (lncRNA) MAGI2-AS3 inhibits breast cancer cell growth by targeting the Fas/FasL signalling pathway. *Hum Cell*. 2018;31(3):232–241. doi:10.1007/s13577-018-0206-1

27. Zhang JF, Shi LL, Zhang L, et al. MicroRNA-25 negatively regulates cerebral ischemia/reperfusion injury-induced cell apoptosis through Fas/FasL pathway. *J Mol Neurosci*. 2016;58(4):507–516. doi:10.1007/s12031-016-0712-0

28. Madison BB, Jeganathan AN, Mizuno R, et al. Let-7 Represses carcinogenesis and a stem cell phenotype in the intestine via regulation of Hmga2. *PLoS Genet*. 2015;11(8):e1005408. doi:10.1371/journal.pgen.1005408

29. Zhang BY, Zhao Z, Jin Z. Expression of miR-98 in myocarditis and its influence on transcription of the FAS/FASL gene pair. *Genet Mol Res*. 2016;15(2). doi:10.4238/gmr.15027627

30. Song Q, Ma YL, Song JQ, et al. Sevoflurane induces neurotoxicity in young mice through FAS/FASL signaling. *Genet Mol Res*. 2015;14(4): 18059–18068. doi:10.4238/2015.December.22.32

31. Dumitriu IE, Baruah P, Finlayson CJ, et al. High levels of costimulatory receptors OX40 and 4-1BB characterize CD4$^+$CD28null T cells in patients with acute coronary syndrome. *Circ Res*. 2012;110(6):857–869. doi:10.1161/CIRCRESAHA.111.261933

32. Zal B, Chitalia N, Ng YS, et al. Killer cell immunoglobulin receptor profile on CD4$^+$ CD28$^-$ T cells and their pathogenic role in non-dialysis-dependent and dialysis-dependent chronic kidney disease patients. *Immunology*. 2015;145(1):105–113. doi:10.1111/imm.12429

Expression of *miR-9a-5p* in cirrhosis patients with recurrent portal hypertension after treatment

Cuifang Nie[1,A–C,E,F], Guangju Meng[1,A,C–F], Yongyun Wu[1,A,E,F], Li Liu[1,2,A–C,F], Li Chen[1,B–E], Shengqiang Yang[1,A–F], Yan Hu[1,A,B,E,F]

[1] Department of Infectious Disease, Tai'an Central Hospital, China

[2] Shanghai Key Laboratory of Tuberculosis, Shanghai Pulmonary Hospital, Tongji University School of Medicine, China

A – research concept and design; B – collection and/or assembly of data; C – data analysis and interpretation;
D – writing the article; E – critical revision of the article; F – final approval of the article

Address for correspondence
Yan Hu
E-mail: yanhu242424@outlook.com

Conflict of interest
None declared

Abstract

Background. MicroRNA (miR) influences the biological activities of cirrhotic patients with recurrent portal hypertension.

Objectives. The current study was designed to investigate risk factors related to the survival of cirrhosis patients and assessed the possibility of using *miR-9a-5p* predictability to prevent post-treatment portal hypertension.

Materials and methods. Patients with portal hypertension due to liver cirrhosis treated from January 2015 to September 2016 were included in this study. Patients without relapse after treatment were selected as the success group while patients with relapse after treatment were selected as the recurrence group. Serum samples from healthy people were also collected. The blood indexes of the 2 groups of patients before and after treatment were compared and the *miR-9a-5p* serum level in each group was determined. The Kaplan–Meier method was applied to analyze three-year survival, Cox univariate regression was used to analyze the risk factors for recurrence of cirrhotic portal hypertension, and the receiver operating characteristic curve (ROC) was used to evaluate the diagnostic value of serum *miR-9a-5p*, total bilirubin (TBIL) and platelet (PLT) levels in patients with recurrence.

Results. The *miR-9a-5p* level in the recurrence group was higher than that in the success group after treatment. In patients with recurrence, the *miR-9a-5p* level was negatively correlated with red blood cell count, TBIL, white blood cell count, and PLT count, and positively correlated with albumin. The *miR-9a-5p*, TBIL and PLT are potential markers of recurrent portal hypertension in liver cirrhosis. The *miR-9a-5p* had the highest area under the curve (AUC) value in patients with relapse.

Conclusions. The *miR-9a-5p* is a risk factor for the recurrence of cirrhotic portal hypertension after treatment. It may be used as a marker of recurrence, and so has potential clinical value for the diagnosis and treatment of recurrent portal hypertension.

Key words: *miR-9a-5p*, liver cirrhosis, portal hypertension, recurrence, risk factor

Background

Liver cirrhosis is a common and chronic liver disease that is caused by extensive fibrosis secondary to long-term liver cell inflammation and necrosis accompanied by the formation of pseudolobules and regenerative nodules, which deform and harden the liver.[1] The main causes of cirrhosis are viral hepatitis – a few cases of which are schistosomiasis cirrhosis – alcoholism, autoimmune conditions, and Budd–Chiari syndrome.[2,3] The disease progresses slowly and has no visible symptoms. Most patients have mild or no symptoms that can be relieved by rest. However, once liver function is decompensated, the symptoms become more obvious, and are mainly manifested as liver function decline and portal hypertension.[4,5] The clinical manifestation of cirrhotic portal hypertension is usually the opening of the communicating branch of the portal systemic vein, which results in a large amount of portal vein blood directly entering systemic circulation before entering the liver, resulting in venous dilatation, hypersplenism, splenomegaly, and ascites in the esophagus and abdominal wall.[6,7] Dilatation of the esophageal and gastric fundus veins can occur in severe cases. If rupture occurs, the patient will suffer from severe upper gastrointestinal hemorrhage, which endangers their life.[8] Massive hemorrhage of the digestive tract caused by rupture of collateral circulation of portal body is one of the main causes of death in patients with decompensated liver cirrhosis. Zhao et al. reported that the death rate after the first hemorrhage is about 20%, and the rebleeding rate can reach 45% within 24 h after hemorrhage, and is as high as 75% within 1 year.[7] If untreated, about 60% of patients suffer from rebleeding within 1–2 years after the first hemorrhage.[9,10] The most effective treatment for cirrhotic portal hypertension in patients complicated with esophageal and gastric varices bleeding is a transjugular intrahepatic portosystemic shunt (TIPS), which is minimally invasive and can effectively reduce the pressure of the portal vein. However, due to hemodynamic changes after TIPS and mechanical damage during the operation, complications such as liver function damage, hepatic encephalopathy and long-term stent stenosis may occur after TIPS.[11,12]

MicroRNA (miR), which is a kind of non-coding RNA containing approx. 22 nucleotides that is widely distributed in organisms, regulates the biological functions of cells by binding to target mRNA 3'UTR to inhibit translation.[13] MicroRNA has been found to play a role in many diseases including viral hepatitis,[14] liver fibrosis[15] and liver cancer.[16] It can regulate differentiation, proliferation, apoptosis, metabolism, tumorigenesis, and other biological processes, and has gradually attracted attention in the field of molecular biology.[17]

Objectives

In order to explore the role of *miR-9a-5p* in cirrhosis patients with recurrent portal hypertension after treatment, this study assessed *miR-9a-5p* levels in recurrent patients to explore three-year survival, identify risk factors related to survival, and discuss the possibility of using *miR-9a-5p* to predict the recurrence of liver cirrhosis portal hypertension after treatment.

Materials and methods

General patient data

From January 2015 to September 2016, 42 patients (28 males and 14 females, aged 49.8 ±12.1 years) who did not relapse (successful operation) after treatment and 35 patients (23 males and 12 females, aged 50.1 ±11.5 years) who suffered from relapse (operation failure) after treatment were selected for TIPS treatment due to liver cirrhosis portal hypertension in our hospital (Tai'an Central Hospital, Tai'an, China). The general characteristics of the 2 groups before treatment were comparable. The success criteria for the TIPS operation are: 1. The portal pressure should be reduced to 12 mm Hg (16 cm H_2O), or below 25% of the pressure for treatment of the anterior portal vein after the establishment of the hepatic vein (inferior vena cava of the hepatic segment) 2. Diversion between the portal veins should occur. The diagnostic criteria of shunt dysfunction in TIPS include any of the following signs indicating that shunt dysfunction may be present: 1) ultrasound indicates that the shunt blood flow velocity is >200 cm/s, <50 cm/s or no blood flow, or the shunt diameter is <50%; and 2) recurrence of portal hypertension, i.e., hemorrhage and ascites of the esophagogastric vein after treatment. In all cases, portosystemic pressure gradient (PSG) exceeded 12 mm Hg (16 cm H_2O). Suspected shunt dysfunction can only be diagnosed after the portal vein pressure exceeds 12 mm Hg, as determined using portal vein angiography. Data from 30 healthy people were collected during the same time to serve as a control group (18 males and 12 females, aged 50.3 ±10.8 years). All patients and healthy people participating in this study provided informed consent and the study was approved by the Ethics Committee of our institution.

Blood sample collection

Patients in each group received anticoagulants through the antecubital vein on an empty stomach in the morning. A blood sample was then collected and centrifuged at 4°C for 10 min at 3000 rpm. The upper serum was placed in a microcentrifuge tube sterilized with high pressure steam, centrifuged at 4°C for 15 min at 15,000 rpm, collected, divided into smaller samples, and stored in a refrigerator at 4°C.

Quantitative polymerase chain reaction

Serum samples frozen at –80°C were thawed at room temperature. Each microcentrifuge tube contained 100 µL of serum. Total RNA was extracted from serum according to the instructions of the miRNeasy Mini kit (Qiagen, Hilden, Germany). The concentration and purity of total RNA at 260–280 nm were detected using an ultraviolet spectrophotometer. An OD260/OD280 ratio of 1.8–2.0 indicated acceptable RNA purity. According to the instructions of the reverse transcription kit (Qiagen), a 20 µL reaction system was constructed and reverse transcription was carried out using a Gene AmpPCR System 9700 (37°C for 60 min and 95°C for 5 min). The following *miR-9a-5p* and U6 primers were designed and synthesized by Sangon Biotech (Shanghai, China): *miR-9a-5p*: F: 5'-GGGTCTTTGGTTATCTAGCT-3'; R: 5'- ATCCAGTGC-GTGTCGTGGA-3', U6: 5'-GCTTCGGCAGCACATATAC-TAAAAT-3'; R:5'-CGCTTCACGAATTTGCGTGTCAT-3'. The PCR kit was purchased from Ribo Bio (Guangzhou, China), and 20 µL of the reaction system was prepared according to the manufacturer's instructions. The standard three-step method was used: 95°C for 20 s, 95°C for 10 s, 60°C for 20 s, and 70°C for 10 s, for a total of 40 cycles. The serum miR-level was calculated using $2^{-\Delta\Delta Ct}$ method.

Patient follow-up

The non-recurrent group of patients visited the hospital for routine blood, liver function, kidney function, and hemagglutination testing at 1, 3, 6, and 12 months after TIPS treatment, and then they were examined once a year. During this period, if the patients suffer from gastrointestinal hemorrhage or ascites, they should return to hospital for examination and treatment at any time. For the relapse group, patients were followed-up by nurses every 6 months through outpatient or telephone visits for 3 years.

Data analyses

IBM SPSS v. 20.0 (IBM Corp., Armonk, USA) software was used for statistical analyses and GraphPad Prism v. 6 (GraphPad Software, San Diego, USA) software was used for visualizing the data. Measurement data are reported as the mean ± standard deviation (SD). Comparisons between groups were performed using the independent sample t-test, log rank test, and one-analysis of variance (ANOVA), and post hoc pair-wise comparisons were performed using the least significant difference (LSD) test. Count data are reported as n and comparisons were performed using the χ^2 test. Receiver operating curve (ROC) analysis was applied to explore the diagnostic value of *miR-9a-5p* for patients with recurrent cirrhosis portal hypertension after treatment. Cox regression analysis was applied to test the risk factors for recurrence. All data were tested using two-tailed tests. A value of 95% was used for the confidence intervals (95% CI). A difference was considered to be statistically significant when $p < 0.05$.

Results

Comparison of general data of patients before and after treatment

There were no significant differences in the routine blood index, liver function index, renal function index, Child–Pugh score, or grading before treatment between the 2 groups. After treatment, the routine blood index, liver function index, renal function index, and Child–Pugh score of patients in the recurrence group were significantly lower than those in the success group ($p < 0.05$; Table 1,2).

Expression of *miR-9a-5p* and its influence on prognosis

Comparison of miR-9a-5p levels in patients with different Child–Pugh grades revealed higher levels in patients with liver cirrhosis than in controls, and it was expressed differentially by distinct high Child–Pugh grade ($p < 0.05$, Fig. 1A). The *miR-9a-5p* level in the recurrence group was significantly higher than that in the success group after treatment ($p < 0.05$, Fig. 1B). Combined with the expression level of *miR-9a-5p* in patients' serum samples, the Kaplan–Meier method was applied to analyze the three-year survival of the 77 patients with liver cirrhosis portal hypertension (Fig. 1C) and Cox univariate regression was used to test the risk factors of these patients. The results showed no significant difference in three-year survival between the high and low *miR-9a-5p* groups. Cox univariate analysis showed that *miR-9a-5p*, serum TBIL, PLT, Child–Pugh score before treatment, and hepatic encephalopathy before treatment were all risk factors for three-year survival in patients with recurrent cirrhotic portal hypertension.

Correlation between serum *miR-9a-5p* and various indicators in recurrent patients

The *miR-9a-5p* levels in patients with recurrent liver cirrhosis portal hypertension were negatively correlated with red blood cell count, TBIL, white blood cell count, and PLT count, and positively correlated with albumin, as shown in Fig. 2.

Evaluation of *miR-9a-5p*, TBIL, and PLT as diagnostic markers of recurrence

In order to determine whether *miR-9a-5p*, TBIL or PLT can be used as markers for the treatment of recurrent portal

Table 1. General data of patients before treatment

Variable	Success group (n = 42)	Recurrence group (n = 35)	χ^2/t	p-value
Gender, n (%)	–	–	0.0077	0.9299
Male	28	23	–	–
Female	14	12	–	–
Age [years]	49.8 ±12.1	50.1 ±11.5	0.1108	0.9121
Red blood cell count [×10^{12}/L]	4.46 ±1.86	4.39 ±1.91	0.1624	0.8713
White blood cell count [×10^9/L]	3.56 ±1.03	3.48 ±1.08	0.3269	0.7446
Platelet count [×10^9/L]	50.35 ±15.23	53.25 ±16.98	0.7896	0.4322
Albumin [g/L]	31.65 ±3.26	31.58 ±3.03	0.0969	0.9231
TBIL [μmol/L]	23.75 ±5.98	23.52 ±5.85	0.1697	0.8657
Alanine transaminase [U/L]	52.06 ±10.74	51.97 ±10.82	0.0365	0.9710
Thrombin activity [%]	60.03 ±8.26	59.56 ±8.74	0.2421	0.8093
INR	1.15 ±0.12	1.16 ±0.09	0.4067	0.6854
Blood creatinine [μmol/L]	59.8 ±2.96	58.7 ±3.12	1.5843	0.1173
Child–Pugh score	6.85 ±1.02	6.73 ±1.16	0.4829	0.6306
Child–Pugh grading (A/B/C)	32/10/0	26/7/0	0.0711	0.7897

TBIL – total bilirubin; INR – International Normalized Ratio.

Table 2. Comparison of indexes after treatment

Variable	Success group (n = 42)	Recurrence group (n = 35)	χ^2/t	p-value
Red blood cell count [×10^{12}/L]	5.23 ±1.36	4.39 ±1.91	2.2482	0.0275
White blood cell count [×10^9/L]	8.06 ±1.75	3.48 ±1.08	13.4827	<0.0001
Platelet count [×10^9/L]	305.36 ±20.36	137.98 ±12.03	42.7823	<0.0001
Albumin [g/L]	23.85 ±3.72	28.63 ±3.16	6.0061	<0.0001
TBIL [μmol/L]	30.06 ±6.32	24.36 ±4.53	4.4631	<0.0001
Alanine transaminase [U/L]	41.05 ±5.23	49.85 ±10.82	4.6619	<0.0001
Thrombin activity [%]	78.69 ±8.03	64.26 ±7.84	7.9363	<0.0001
INR	1.89 ±0.36	1.30 ±0.18	8.8144	<0.0001
Blood creatinine [μmol/L]	55.3 ±1.29	58.7 ±2.85	6.9326	<0.0001
Child–Pugh score	6.03 ±0.71	6.89 ±1.05	4.2673	<0.0001

TBIL – total bilirubin; INR – International Normalized Ratio.
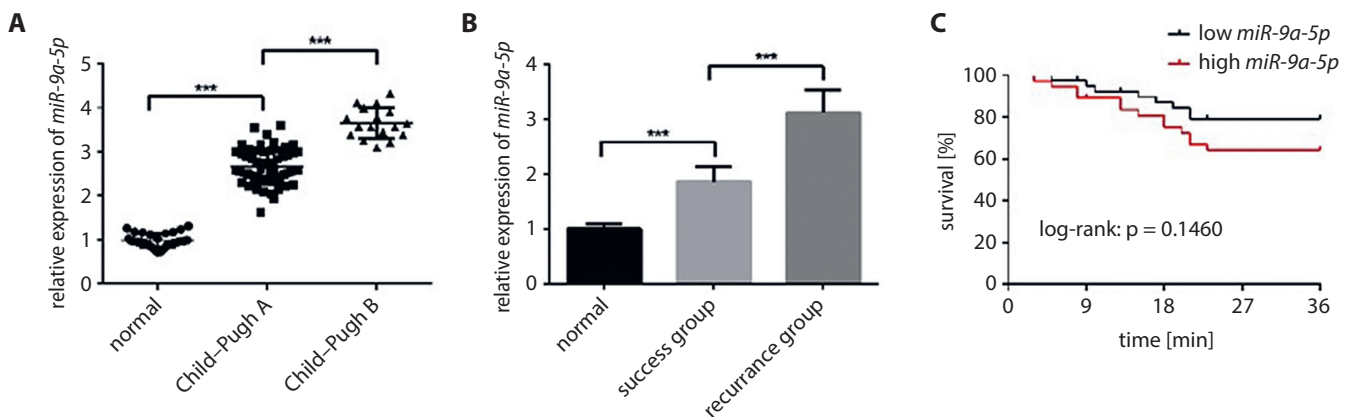
Fig. 1. Expression of *miR-9a-5p* and its relationship with prognosis. A. Expression of *miR-9a-5p* in serum of patients with different Child–Pugh grades; B. Expression of *miR-9a-5p* in serum of different groups of patients; C. Prognosis of patients with different *miR-9a-5p* expression levels

*** significant intergroup differences; p < 0.001
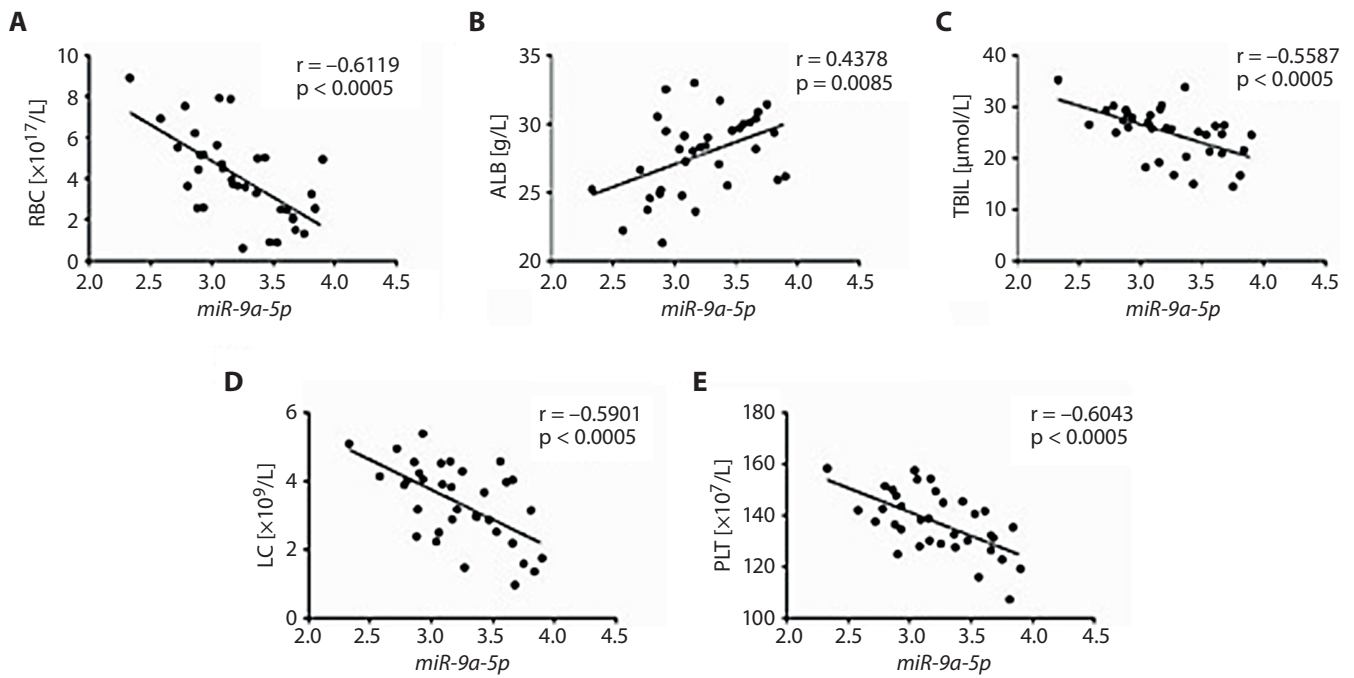
Fig. 2. Correlation between serum *miR-9a-5p* and various indexes in relapsed patients. A. Correlation between *miR-9a-5p* and red blood cell count; B. Correlation between *miR-9a-5p* and albumin; C. Correlation between *miR-9a-5p* and total bilirubin (TBIL); D. Correlation between *miR-9a-5p* and leukocyte count; E. Correlation between *miR-9a-5p* and platelet (PLT) count
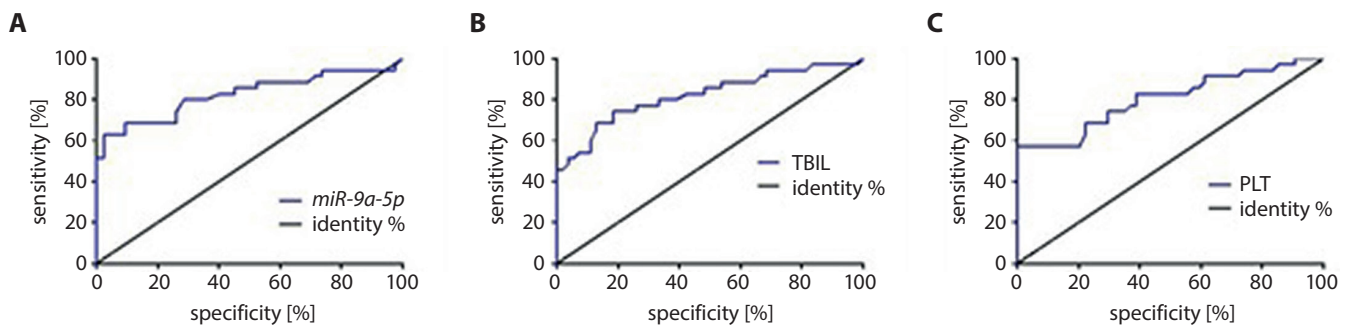
Fig. 3. Use of *miR-9a-5p*, total bilirubin (TBIL) and platelet (PLT) for diagnosis of recurrence. A. Use of *miR-9a-5p* for diagnosis of recurrent patients; B. Use of TBIL for diagnosis of recurrent patients; C. Use of PLT for diagnosis of recurrent patients

Table 3. Results of COX regression analysis

Variable	HR	95% CI	p-value
miR-9a-5p	1.032	1.001–1.062	0.034
Gender	1.385	0.921–2.052	0.192
Age	1.521	0.943–2.522	0.083
Serum TBIL	1.236	1.026–1.273	0.010
Platelet count	0.972	0.932–1.009	0.035
Child–Pugh score before treatment	1.125	1.001–1.043	0.027
HE before treatment	1.018	0.905–0.973	0.007

TBIL – total bilirubin; HE – hepatic encephalopathy; 95% CI – 95% confidence interval; HR – hazard ratio.

hypertension in cirrhosis, the ROC curves of *miR-9a-5p*, TBIL and PLT were constructed (Fig. 3). The area under the curve (AUC) values of *miR-9a-5p*, TBIL and PLT were 0.8252, 0.8209 and 0.8040, respectively. The above results revealed that *miR-9a-5p* had the best diagnostic value (Tables 3,4).

Discussion

Cirrhosis, as a common liver disease, has a rising incidence rate.[18] The liver function of patients with early cirrhosis is normal and there are no obvious clinical symptoms.

Table 4. Diagnostic value of *miR-9a-5p*, TBIL and PLT for recurrence of portal hypertension

Variable	AUC	SE	95% CI	p-value
miR-9a-5p	0.8252	0.052	0.7240–0.9263	<0.0001
TBIL	0.8209	0.049	0.7248–0.9170	<0.0001
PLT	0.8040	0.050	0.7050–0.9030	<0.0001

AUC – area under the curve, SE – standard error; 95% CI – 95% confidence interval; TBIL – total bilirubin; PLT – platelet level.

However, patients with late cirrhosis may experience a portal vein pressure increase and other phenomena that induce portal hypertensive gastropathy, gastrointestinal hemorrhage and other complications. Liver cirrhosis and portal hypertension can further induce splenomegaly and hyperfunction.[19] Although drug therapy can alleviate the disease to a certain extent, long-term medication use can lead to a drug withdrawal reaction, low hemostasis rate and other complications. Surgery is a commonly used method for clinical treatment of liver cirrhosis and portal hypertension, but the possibility of recurrence of portal hypertension is high due to the development of liver cirrhosis.[20] Studies have shown that although microRNA accounts for only 2% of human genes, it regulates the expression of more than 30% of human genes, and is closely related to the occurrence and development of diseases. Clinically, miR-130a and miR-130b are helpful for the diagnosis and prognosis of liver cirrhosis and can be applied as a joint detection method for liver cirrhosis or for a general survey of liver cirrhosis.[21]

In the present study, *miR-9a-5p* in patients with recurrent cirrhosis and portal hypertension after treatment was studied. The results revealed higher *miR-9a-5p* serum levels in patients with recurrent cirrhosis and portal hypertension than in patients in the success group after treatment. Previous research has revealed that *miR-9a-5p* is enhanced in rats with liver fibrosis portal hypertension.[22] The serum *miR-9a-5p* level in patients with recurrent liver cirrhosis portal hypertension showed a negative correlation with red blood cell count, TBIL, white blood cell count, and PLT count, and a positive correlation with albumin. About $1/3$ of platelets in the normal blood system are stored in the spleen, while 50–90% of platelets in patients with cirrhosis are stored there; if metabolism of the spleen is enhanced, damage to blood cells is increased and the proliferation of monocytes and macrophages is over-activated, thus leading to a decreased PLT level in peripheral blood.[23] Albumin plays a decisive role in maintaining blood volume and plasma colloid osmotic pressure. It can expand the blood volume, inhibit the aggregation of leukocyte components, reduce blood consistency, and improve blood flow, which are beneficial for tissue repair and the control of ascites formation. However, albumin also controls ascites and increases portal vein blood flow, thus increasing the risk of esophageal and gastric varices bleeding.[24] Serum bilirubin is a metabolite of heme in hemoglobin and other heme proteins in macrophages or other reticuloendothelial cells and hepatocytes. Blood detection indexes include indirect bilirubin level (IBIL) combined with albumin in blood, and direct bilirubin level (DBIL) combined with glucuronic acid in liver. The increase in bilirubin is likely caused by a related increase in bilirubin production or issues with the uptake, binding or excretion of bilirubin.[25] The *miR-9a-5p*, TBIL and PLT are potential markers for diagnosis of recurrent portal hypertension in liver cirrhosis. Previously, several investigations have found that platelet count is an independent factor affecting the survival rate of patients with refractory ascites.[26] Therefore, PLT count is related to postoperative liver function and survival rate, and a higher PLT count is beneficial to liver function.[27] In the present study, *miR-9a-5p* had the highest AUC value in patients with relapse.

Limitations

Although the most optimal care possible has been provided by the researchers during every step of this study, still some limitations exist.

This was a clinic-based study and only hematological analysis was carried out; therefore, futher investigation is required in this aspect. Due to time constraints, the collected sample size was not adequate to represent all patients' characteristics. The result might be area-specific and might not necessarily represent the community scenario. Finally, the study might lack external validity.

Conclusions

Overall, by studying the expression of *miR-9a-5p* in the serum of patients with recurrent cirrhosis portal hypertension, this study has identified factors associated with recurrence after treatment of cirrhosis portal hypertension. The *miR-9a-5p* may be used as a marker of recurrence, and so has clear potential clinical value for the diagnosis and treatment of recurrent portal hypertension.

ORCID iDs
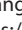
Cuifang Nie https://orcid.org/0000-0002-8919-773X
Guangju Meng https://orcid.org/0000-0002-3252-6379
Yongyun Wu https://orcid.org/0000-0003-2139-7097
Li Liu https://orcid.org/0000-0002-5886-9978
Li Chen https://orcid.org/0000-0003-1011-9673
Shengqiang Yang https://orcid.org/0000-0003-2028-5480
Yan Hu https://orcid.org/0000-0002-9699-6441

References

1. Barnett R. Liver cirrhosis. *Lancet*. 2018;392(10144):275. doi:10.1016/S0140-6736(18)31659-3
2. Nishikawa K, Osawa Y, Kimura K. Wnt/β-catenin signaling as a potential target for the treatment of liver cirrhosis using antifibrotic drugs. *Int J Mol Sci*. 2018;19(10):3103. doi:10.3390/ijms19103103
3. Iliescu L, Toma L, Mercan-Stanciu A, et al. Budd–Chiari syndrome: Carious etiologies and imagistic findings. A pictorial review. *Med Ultrason*. 2019;21(3):344–348. doi:10.11152/mu-1921
4. D'Amico G, Morabito A, D'Amico M, et al. Clinical states of cirrhosis and competing risks. *J Hepatol*. 2018;68(3):563–576. doi:10.1016/j.jhep.2017.10.020
5. Acharya C, Sahingur SE, Bajaj JS. Microbiota, cirrhosis, and the emerging oral–gut–liver axis. *JCI Insight*. 2017;2(19):e94416. doi:10.1172/jci.insight.94416
6. Jiang XW, Gao F, Ma Y, Feng SF, Liu XL, Zhou HK. Percutaneous microwave ablation in the spleen for treatment of hypersplenism in cirrhosis patients. *Dig Dis Sci*. 2016;61(1):287–292. doi:10.1007/s10620-015-3732-7
7. Zhao R, Lu J, Shi Y, Zhao H, Xu K, Sheng J. Current management of refractory ascites in patients with cirrhosis. *J Int Med Res*. 2018;46(3):1138–1145. doi:10.1177/0300060517735231
8. Zacharias AP, Jeyaraj R, Hobolth L, Bendtsen F, Gluud LL, Morgan MY. Carvedilol versus traditional, non-selective beta-blockers for adults with cirrhosis and gastroesophageal varices. *Cochrane Database Syst Rev*. 2018;10(10):CD011510. doi:10.1002/14651858.CD011510.pub2
9. Moodley J, Lopez R, Carey W. Compliance with practice guidelines and risk of a first esophageal variceal hemorrhage in patients with cirrhosis. *Clin Gastroenterol Hepatol*. 2010;8(8):703–708. doi:10.1016/j.cgh.2010.02.022
10. Sauerbruch T, Mengel M, Dollinger M, et al; German Study Group for Prophylaxis of Variceal Rebleeding. Prevention of rebleeding from esophageal varices in patients with cirrhosis receiving small-diameter stents versus hemodynamically controlled medical therapy. *Gastroenterology*. 2015;149(3):660-8.e1. doi:10.1053/j.gastro.2015.05.011
11. Lv Y, Zuo L, Zhu X, et al. Identifying optimal candidates for early TIPS among patients with cirrhosis and acute variceal bleeding: A multicentre observational study. *Gut*. 2019;68(7):1297–1310. doi:10.1136/gutjnl-2018-317057
12. Qi X, Han G, Fan D. Management of portal vein thrombosis in liver cirrhosis. *Nat Rev Gastroenterol Hepatol*. 2014;11(7):435–446. doi:10.1038/nrgastro.2014.36
13. Lu TX, Rothenberg ME. MicroRNA. *J Allergy Clin Immunol*. 2018;141:1202–1207. doi:10.1016/j.jaci.2017.08.034
14. Yang X, Li H, Sun H, et al. Hepatitis B virus-encoded miRNA controls viral replication. *J Virol*. 2017;91(10):e01919-16. doi:10.1128/JVI.01919-16
15. Chen J, Yu Y, Li S, et al. MicroRNA-30a ameliorates hepatic fibrosis by inhibiting beclin1-mediated autophagy. *J Cell Mol Med*. 2017;21(12):3679–3692. doi:10.1111/jcmm.13278
16. Sandbothe M, Buurman R, Reich N, et al. The microRNA-449 family inhibits TGF-β-mediated liver cancer cell migration by targeting SOX4. *J Hepatol*. 2017;66(5):1012–1021. doi:10.1016/j.jhep.2017.01.004
17. Acunzo M, Romano G, Wernicke D, Croce CM. MicroRNA and cancer: A brief overview. *Adv Biol Regul*. 2015;57:1–9. doi:10.1016/j.jbior.2014.09.013
18. Ascione T, Di Flumeri G, Boccia G, De Caro F. Infections in patients affected by liver cirrhosis: An update. *Infez Med*. 2017;25(2):91–97. PMID:28603226
19. Dunne RM, Shyn PB, Sung JC, et al. Percutaneous treatment of hepatocellular carcinoma in patients with cirrhosis: A comparison of the safety of cryoablation and radiofrequency ablation. *Eur J Radiol*. 2014;83(4):632–638. doi:10.1016/j.ejrad.2014.01.007
20. Reverter E, Lozano JJ, Alonso C, et al. Metabolomics discloses potential biomarkers to predict the acute HVPG response to propranolol in patients with cirrhosis. *Liver Int*. 2019;39(4):705–713. doi:10.1111/liv.14042
21. Lu L, Wang J, Lu H, et al. MicroRNA-130a and -130b enhance activation of hepatic stellate cells by suppressing PPARγ expression: A rat fibrosis model study. *Biochem Biophys Res Commun*. 2015;465:387–393. doi:10.1016/j.bbrc.2015.08.012
22. Qi F, Hu JF, Liu BH, et al. MiR-9a-5p regulates proliferation and migration of hepatic stellate cells under pressure through inhibition of Sirt1. *World J Gastroenterol*. 2015;21(34):9900–9915. doi:10.3748/wjg.v21.i34.9900
23. Bucsics T, Hoffman S, Grünberger J, et al. ePTFE-TIPS vs repetitive LVP plus albumin for the treatment of refractory ascites in patients with cirrhosis. *Liver Int*. 2018;38(6):1036–1044. doi:10.1111/liv.13615
24. Ruohoniemi DM, Taslakian B, Aaltonen EA, et al. Comparative analysis of safety and efficacy of transarterial chemoembolization for the treatment of hepatocellular carcinoma in patients with and without pre-existing transjugular intrahepatic portosystemic shunts. *J Vasc Interv Radiol*. 2020;31(3):409–415. doi:10.1016/j.jvir.2019.11.020
25. Allegretti AS, Frenk NE, Li DK, et al. Evaluation of model performance to predict survival after transjugular intrahepatic portosystemic shunt placement. *PLoS ONE*. 2019;14(5):e0217442. doi:10.1371/journal.pone.0217442
26. Wang J, Zhang M, Zhou T, Zhao S, Zhenguo S, Liu X. Role of platelet infiltration as independent prognostic marker for gastric adenocarcinomas. *J Clin Lab Anal*. 2020;34(8):e23320. https://doi.org/10.1002/jcla.23320
27. Zhang F, Zhuge Y, Zou X, et al. Different scoring systems in predicting survival in Chinese patients with liver cirrhosis undergoing transjugular intrahepatic portosystemic shunt. *Eur J Gastroenterol Hepatol*. 2014;26(8):853–860. doi:10.1097/MEG.0000000000000134

The chest radiographic scoring system in initial diagnosis of COVID-19: Is a radiologist needed?

Marta Rorat[1,A–F], Tomasz Jurek[1,C–F], Krzysztof Simon[2,C,E,F], Maciej Guziński[3,B–F]

[1] Department of Forensic Medicine, Wroclaw Medical University, Poland
[2] Department of Infectious Diseases and Hepatology, Wroclaw Medical University, Poland
[3] Department of General Radiology, Interventional Radiology and Neuroradiology, Wroclaw Medical University, Poland

A – research concept and design; B – collection and/or assembly of data; C – data analysis and interpretation;
D – writing the article; E – critical revision of the article; F – final approval of the article

Address for correspondence
Tomasz Jurek
E-mail: tomasz.jurek@umed.wroc.pl

Abstract

Background. Lung imaging, next to a polymerase chain reaction (PCR) test, is a key diagnostic tool in severe acute respiratory syndrome coronavirus 2 (SARS-CoV-2) infection. The degree of abnormalities correlates with clinical outcome. Imaging of the lungs using chest radiography (CXR) at the peak of a pandemic is considered a basic diagnostic tool at the triage stage. The CXR images are less characteristic than computed tomography (CT) and should be interpreted with a combination of clinical findings.

Objectives. Comparison of the usefulness of 2 CXR severity scores to evaluate the presence/severity of inflammation in the course of COVID-19 and the possibility of a non-radiologist to interpret the image independently.

Materials and methods. Retrospective analysis of the medical records of 152 consecutive patients (aged 19–96, 73 men), infected with SARS-CoV-2, confirmed using real-time PCR (RT-PCR). Five-point and twelve-point CXR severity scoring systems were used (independently by a radiologist and a referring physician) to assess the severity of inflammation.

Results. In 77 of 152 cases, the CXR revealed features of inflammation. Bilateral abnormalities were found in 48/77 (62.3%) cases. Statistically, the lower lobes were involved more often than the upper ones ($p < 0.001$) and the left lobe more often than the right one ($p < 0.001$). The intensity of the abnormalities using both scales correlated with the persistence of symptoms ($p = 0.0133$ and $p = 0.0403$). A positive and statistically significant correlation was found between both scales and dyspnea, decreased oxygen saturation, elevated C-reactive protein (CRP), ferritin, D-dimer, lactate dehydrogenase, and alanine aminotransferase activity. The interobserver agreement analysis did not show a statistically significant difference in the CXR severity score using the five-point (B = 0.8345, kappa = 0.82; $p = 0.1480$) or the twelve-point scale (B = 0.8219, kappa = 0.77; $p = 0.0502$).

Conclusions. The CXR severity score is a useful tool to assess the inflammation in the initial diagnosis of coronavirus disease 2019 (COVID-19). Quantifying lung abnormalities accurately may be performed by a referring physician. Both CXR severity scales correlate well with clinical parameters.

Key words: chest X-ray, imaging, viral infection, COVID-19, lung opacities

Background

Lung imaging, next to PCR testing, is a key diagnostic tool in severe acute respiratory syndrome coronavirus 2 (SARS-CoV-2) infection. So far, computed tomography (CT) has been a widely validated method in coronavirus disease 2019 (COVID-19). In CT tests, inflammatory lesions can be detected in symptomatic and asymptomatic patients, which significantly increases the sensitivity of this diagnostic method.[1] The abnormalities present in patients with COVID-19 are diverse, depend on the severity of infection and the duration of symptoms, and undergo dynamic changes.[2–4] Lung abnormalities appear the earliest, within the first days of infection, but the most severe abnormalities appear about 10 days after the onset of initial symptoms.[3] The lack of visible changes on a CT or the presence of atypical changes does not exclude SARS-CoV-2 infection.[5]

Although assessment based on a CT test is characterized by high sensitivity and substantially expands the knowledge on the severity of inflammation, in many medical centers, access to this test is restricted, used mainly for epidemiological and logistic reasons. This is usually the case at the peak of the pandemic, in field hospitals and in countries where health services are insufficient. In such situations, the use of a portable chest X-ray (CXR) is sufficient in the triage stage as this method is fast and carries a low risk of cross-infection. This procedure is consistent with recommendations from the American College of Radiology (ACR), the British Society of Thoracic Imaging, and the Polish Agency for Health Technology Assessment and Tariff System.[6–8]

As the literature-based data suggests, the CXR image is less characteristic and requires more careful interpretation.[9] Test sensitivity is estimated to be 68.1–89% and the specificity is 60.6%.[10–12] Data concerning CXR itself are still limited. There are no standards for evaluating a CXR in patients with COVID-19, and reports on the frequency of occurrence and the type of changes are still scarce. The reports published so far indicate that the lesions found most commonly in the early phase of COVID-19 are ground-glass opacities, reticular alterations, and consolidations that gradually increase as the illness progresses.[13] Abnormalities on a CXR are found less frequently than with CT, which is why the CXR image should be interpreted with a combination of clinical and laboratory findings.[7]

Objectives

This study aimed to explore the correlation with laboratory results and to compare the usefulness of 2 scoring scales to assess the presence and severity of inflammation in the course of COVID-19 using CXR, as well as to evaluate the possibility of a non-radiologist (referring physician) interpreting the presence and degree of inflammation in the lungs independently.

Materials and methods

A retrospective analysis of X-ray images of 152/165 consecutive patients (48% male, average age 56.6 ±16.8 years) infected with COVID-19 (confirmed using real-time polymerase chain reaction – RT-PCR), in which an anteroposterior chest X-ray was performed on admission. The patients were hospitalized in the period between March 6 and April 16, 2020. Patients who had undergone thoracic surgery in the 2 weeks beforehand (7 patients), those with active tuberculosis (2 patients), disseminated cancer of the lungs (3 patients), or who underwent an incorrectly performed CXR (1 patient) were excluded from the analysis. Another study based on the same group of medical records using only a five-point severity scoring system to assesses the correlation of CXR with patients' health conditions was performed.[9]

Table 1 presents the baseline characteristics of study patients.

Chest X-rays were interpreted and described independently by 2 doctors – an experienced radiologist and a referring physician (infectious diseases specialist who diagnoses and treats patients infected with SARS-CoV-2 daily).

Table 1. Baseline characteristics of study patients (n = 152)

Variable	Value
Age [years]	19–96, average 56.6; SD = 16.8 women average 58.1; SD = 16.5 men average 55.1; SD = 16.8
Sex	M 73; F 79
Comorbidities cardiovascular diseases (including hypertension) pulmonary diseases malignant neoplasm obesity diabetes other (autoimmune diseases, liver cirrhosis)	83 (54.6%) 66 (43.4%) 14 (9.2%) 19 (12.5%) 22/83 (26.5%) 19 (12.5%) 8 (5.3%)
Duration of hospitalization [days] (mean)	1–69 (14)
Deaths, n (%)	16 (10.5%)

SD – standard deviation.

The infectious diseases specialist had a short training session on using the 2 scoring systems based on validated radiological images. The 1st one (five-point scale) is a chest X-ray severity scoring system proposed by Taylor et al. CXR findings were categorized as: 1 – normal; 2 – patchy atelectasis and/or hyperinflation and/or bronchial wall thickening; 3 – focal consolidation, no more than 1 lobe; 4 – multifocal and bilateral consolidation; and 5 – diffuse alveolar changes.[14] The 2nd scoring system (twelve-point scale) is our modification of a system proposed by Borghesi et al.[15] The assessment of the severity of abnormalities was performed in 4 quadrants, similar to the system used in the radiographic assessment of lung edema (RALE), using a scoring system with 1–3 points for each of the 4 quadrants based on the percentage of the quadrant with opacification: 1 – normal, 2 – lesions <50% of the pulmonary field and 3 – lesions involving ≥50% of the pulmonary field. All CXRs were performed with the use of a portable device in an isolated room.

The results from the use of the 2 scales by a radiologist and non-radiologists were compared. The twelve-point scale results were contrasted with those from the five-point scale.[9] The correlation between clinical parameters: the presence of comorbidities, dyspnea and cough, saturation and laboratory test results (morphology, capillary blood gas test, C-reactive protein – CRP, lactate dehydrogenase – LDH, serum alanine aminotransferase – ALT activity, D–dimer, and ferritin level) was analyzed.

Statistical analyses

Given the ordinal nature of the scores compared, we used non-parametric statistics when comparing levels between groups. To compare the scores between the 2 groups, we used the Mann–Whitney test. The correlation between scores and quantitative variables was assessed using Spearman's rank correlation coefficient. Assessment of the presence of inflammation among various positions was performed using Pearson's χ^2 test of independence. The optimal cut-off point for CXR scores to predict death was performed by maximizing the Youden's index in a receiver operating characteristic (ROC) curve analysis. All tests were considered significant when the p-value was lower than 0.05. Calculations were performed using the R statistical program for Windows (v. 4.0; https://www.r-project.org/)).[16] B-statistics and kappa statistics were used to quantify the agreement between the 2 observers.

The following R packages were used:

1. Psych package – Revelle W. (2020) psych: Procedures for Personality and Psychological Research, Northwestern University, Evanston, USA, https://CRAN.R-project.org/package=psych, v. 2.1.3. (for Cohen's kappa),

2. vcd package – David Meyer, Achim Zeileis and Kurt Hornik (2020). vcd: Visualizing Categorical Data. R package v. 1.4-8. (for B-statistic),

3. Rstatix package – Alboukadel Kassambara (2021). rstatix: Pipe-Friendly Framework for Basic,

4. Statistical Tests. R package v. 0.7.0. https://CRAN.R-project.org/package=rstatix (for games Howell test),

5. Cut-point package – Christian Thiele (2021). cutpointr: Determine and Evaluate Optimal Cutpoints in Binary Classification Tasks. R package v. 1.1.0. https://CRAN.R-project.org/package=cutpointr (for ROC analysis).

The rest of the tests were performed using built-in tests.

Results

In the research group, the severity of inflammation in CXR images was assessed using a five-point scale (Table 2) and a twelve-point scale (Table 3).

Among 77 patients with features of pneumonia detected on CXR, bilateral changes were found in 48/77 (62.3%), peripheral (±central) opacities in 44/77 (57.1%), heart

Table 2. Severity of inflammatory changes in chest X-ray (CXR) expressed in five-point scale, where 1 shows no inflammatory changes and 5 means diffuse alveolar changes, in assessment of a radiologist and a referring physician (n = 152)

Assessment		Number of points				
		1	2	3	4	5
Assessment of a radiologist	number of patients (%)	75 (49.3)	11 (7.2)	21 (13.8)	38 (25)	7 (4.6)
Assessment of a referring physician		73 (48)	10 (6.6)	20 (13.2)	40 (26.3)	9 (5.9)

Table 3. Severity of inflammatory changes in chest X-ray (CXR) expressed in twelve-point scale assessment in 4 quadrants in 1 to 3 points, where 1 means no inflammatory changes and 3 means lesions involving ≥50% pulmonary field, in assessment of a radiologist and a referring physician (n = 152)

Assessment		Number of points								
		4	5	6	7	8	9	10	11	12
Assessment of a radiologist	number of patients (%)	75 (49.3)	27 (17.8)	25 (16.4)	7 (4.6)	5 (3.3)	9 (5.9)	4 (2.6)	0	0
Assessment of a referring physician		73 (48)	25 (16.4)	23 (15.1)	10 (6.6)	6 (3.9)	10 (6.6)	5 (3.3)	0	0

enlargement in 22/77 (28.6%), pleural effusion in 6/77 (7.8%), and emphysema in 1 case as a complication of vena cava catheterization. We observed a statistically significant presence of inflammation in the lower than the upper lobes (48.03% compared to 15.3%; $p < 0.001$; Pearson's χ^2 test) and in the left lobes rather than the right ones (44.74% compared to 34.87%; $p < 0.001$; Pearson's χ^2 test). The frequency of pleural effusions (mean 2.27 ±1.39 compared to 2.67 ±1.86, $p = 0.565$; Mann–Whitney test, Shapiro–Wilk W statistics 381) was not statistically significant in contrast to heart enlargement (mean 3.42 ±0.85 compared to 3.82 ±0.79, $p = 0.0477$; Mann–Whitney test, W statistics 442) and peripheral opacities (mean 3.06 ±0.89 compared to 3.85 ±0.67, $p = 0.0001$; Mann–Whitney test, W statistics 373). Patients reported to the hospital with symptoms having evolved over 1–23 days (6.5 days on average). The severity of abnormalities measured using both scales remained in relation with the duration of symptoms (five-point scale: $r = 0.21$, $p = 0.0133$; twelve-point scale $r = 0.17$, $p = 0.0403$; Spearman's rank correlation coefficient). Patients in which symptoms persisted for more than 7 days had a significantly higher score using both scales (five-point scale: <7 days mean 1.99 ±1.32, ≥7 days 2.68 ±1.45, $p = 0.04$; twelve-point scale: <7 days mean 4.93 ±1.54, ≥7 days 5.57 ±1.78, $p = 0.009$; Spearman's rank correlation coefficient).

The interobserver agreement analysis did not show a statistically significant difference in CXR assessment using the five-point scale (B = 0.8345, kappa = 0.82; $p = 0.148$) or the twelve-point scale (B = 0.8219, kappa = 0.77; $p = 0.0502$). High compliance of assessments between the radiologist and referring physician was observed (Tables 2,3). An almost perfect interobserver agreement and substantial agreement were detected. The first researcher (radiologist) obtained lower results on average using the twelve-point scale.

We demonstrated, like in the other papers where the five-point scale had been used,[9] the correlation between scores using the twelve-point scale – presence/severity of inflammation changes in CXR – and age ($r = 0.45$, $p < 0.001$; Spearman's rank correlation coefficient), obesity (mean 4.92 ±1.38 compared to 6.77 ±2.05, $p < 0.001$; Mann–Whitney test, W statistics 290), cardiovascular system diseases (mean 5.77 ±1.19 compared to 6.70 ±1.71, $p = 0.0222$; Mann–Whitney test, W statistics 494), increased level of CRP > 6 mg/L ($r = 0.61$, $p < 0.001$), D-dimers >500 ng/mL ($r = 0.52$, $p < 0.001$; Spearman's rank correlation coefficient), ferritin level >291 ng/mL ($r = 0.49$, $p = 0.0081$; Spearman's rank correlation coefficient), ALT activity >48 IU/L ($r = 0.57$, $p < 0.001$; Spearman's rank correlation coefficient), LDH > 246 U/L ($r = 0.69$, $p < 0.001$; Spearman's rank correlation coefficient), decreased O_2 saturation <94% (mean 4.60 ±1.09 compared to 6.49 ±1.86, $p < 0.001$; Mann–Whitney test, W statistics 927), and finally, dyspnea (mean 4.69 ±1.23 compared to 5.63 ±1.82, $p = 0.0002$; Mann–Whitney test, W statistics 1916). We did not observe statistical significance between the presence of fever or cough and other concomitant diseases. On both scales, the higher scores occurred in patients with longer durations of hospitalization (five-point scale: $r = 0.32$, $p = 0.001$; twelve-point scale: $r = 0.29$, $p = 0.0036$; Spearman's rank correlation coefficient) and the deceased (five-point scale: mean 2.15 ±1.34 compared to 3.44 ±1.46, $p = 0.0005$; twelve-point scale: mean 4.98 ±1.40 compared to 6.94 ±2.32, $p = 0.0003$; Mann–Whitney test, W statistics 534). We did not find any significant differences between the scales within this range. The ROC analysis on death prediction was used to establish the cut-off point for the five-point scale at 2 points and the twelve-point scale at 7 points.

The above data are also presented in Fig. 1,2.
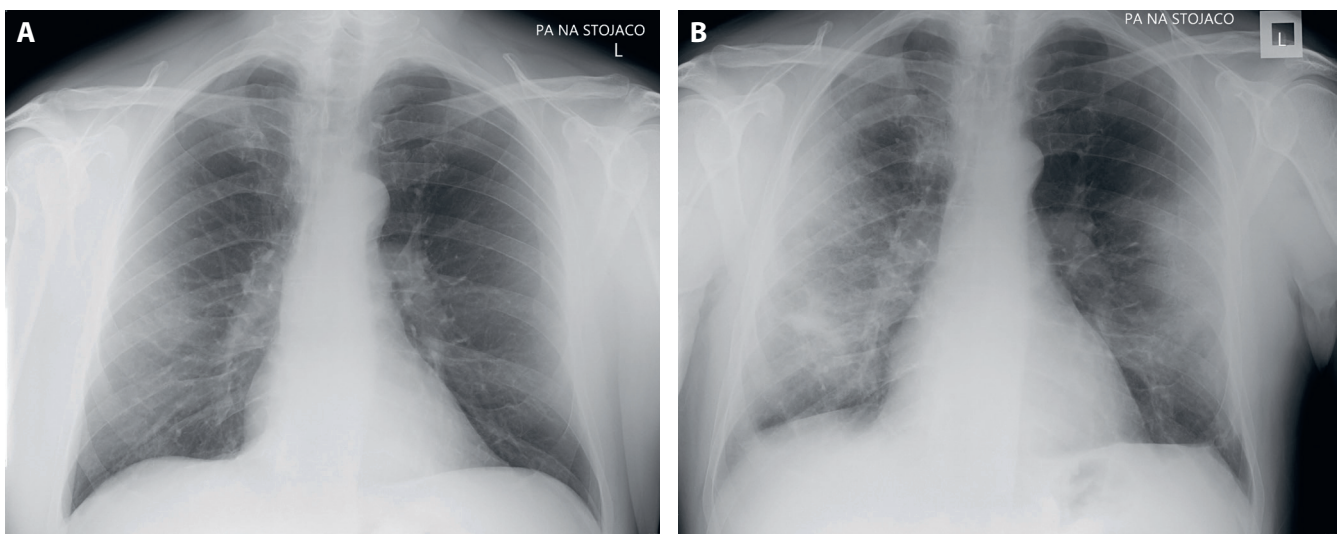
Fig. 1. A. April 10, a 53-year-old man, 4th day after the onset of symptoms; cough, fever, oxygen saturation 97%; chest X-ray (CXR): unilateral, focal, peripheral patchy consolidation – ground-glass opacity in the right lung; five-point scale score: 3; twelve-point scale score: 5 (1+2+1+1); B. April 17, CXR: peripheral multifocal diffuse patchy consolidations in the right and left lung; five-point scale score: 4; twelve-point scale score: 8 (2+3+1+2)
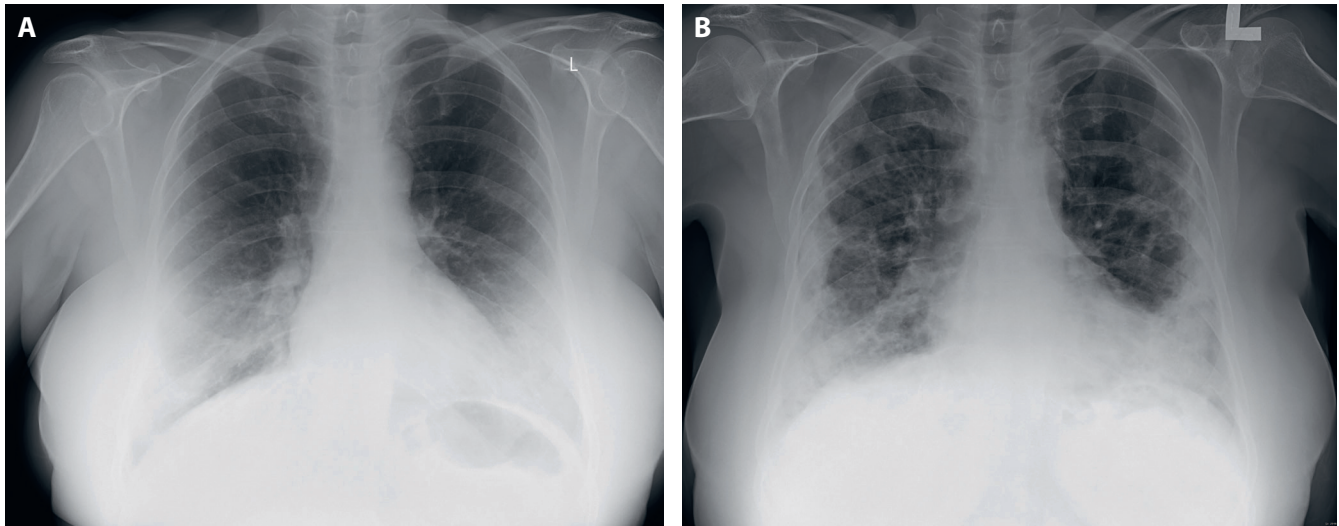
Fig 2. A. April 15, a 54-year-old woman; 4th day after the onset of symptoms; cough, fever, tachypnea, dyspnea, oxygen saturation 86%; chest X-ray (CXR): bilateral consolidation of lower lobes; five-point scale score: 4, twelve-point scale score: 8 (1+1+2+2); B. April 29, CXR: progression of consolidations and patchy opacities; five-point scale score: 4; twelve-point scale score: 10 (2+3+2+3)

Discussion

According to the literature, the overall rate of a positive CXR in COVID-19 is between 43.4% and 94.4%,[10–13,17] and is higher in patients with a long-lasting course of the disease.[13] Our research paper revealed the presence of alterations in CXR, regardless of their type, in 50.7% of patients at the time they reported to the hospital. A lower number of positive results compared to Italian studies may be due to the fact that younger patients, often in a better general state of health, attended the hospital at an earlier stage of the disease and with a milder course thereof.

It is well known that community bacterial pneumonia is usually unilateral and involves 1 lobe. However, in infections with SARS-CoV-2, lung opacities are typically multifocal, bilateral and peripheral.[10,12,13,17,18] In our study, alterations were bilateral in 62.3% of patients – in other papers, they were reported in 50–73.3% of cases,[10,12,13,17,18] which, as is well known, depends on the persistence of the disease. Our research shows a statistically significant occurrence of heart enlargement compared to patients with no inflammation, which corresponds to reports by Cozzi et al.[10] Peripheral involvement took place in over ½ of the cases, which is consistent with other reports.[10,13,18] Just like other researchers, we detected that the involvement of the lower fields was more predominant.[10,13,19,20] There was also a predominance of the left side over the right side in contrast to research by Vancheri et al., where neither side presented prevalence,[13] or research by Cozzi et al. and Toussie et al., where the right side was predominant (58% and 42%, respectively).[10,20] From a clinical point of view, this feature does not seem to be significant. Pleural effusions were present in <10% of those infected, similar to the research by Wong et al. and Vancheri et al.,[12,13] whereas higher percentages were noted by Cozzi et al. – 16.7% and Ippolito et al. – 12.2%.[10,18]

We considered a variety of CXR results in patients with COVID-19 at the moment of admission to the hospital – ranging from reticular alterations, more or less intensified ground-glass opacities co-occurring with reticular alterations or alone, to single or multiple, sometimes massive consolidations. In some patients, the changes were restricted to 1 lobe and in others, they were disseminated. According to the literature, the picture of changes depends, among others, on the phase of the disease. Consolidations are detected less frequently than other lesions, especially in the initial phase of the illness and they tend to increase over time.[10,13,18] However, there is no research on the correlation between the type of changes with the clinical picture. In our opinion, the assessment of the severity of abnormalities is more important than the analysis of an individual alteration occurrence. The amount of involved lung tissue has a direct influence on lung impairment and clinical status. Therefore, we believe it is vital for a referring physician to perform a fast initial scoring of the severity of abnormalities using CXR. As our paper shows, the results obtained are highly consistent with an evaluation by a radiologist. In situations where a radiologist is unavailable to provide a quick evaluation, the interpretation of the severity of inflammatory abnormalities by a referring doctor serves as a valuable diagnostic and prognosticative guideline.

Scoring to assess the severity of inflammation in the lungs does not require the use of calculators. It is comprehensive and easy for any physician to do. We did not detect superiority in any of the scales. Both scales were equally correlated with many clinical parameters. The five-point scale is easy to use and to interpret, it informs about the progression of the illness, it has mainly qualitative and, to a lesser extent, quantitative features; it is also less subjective. In turn, the twelve-point scale, which is similar to the RALE score (Radiographic Assessment of Lung Edema) used by other

802

M. Rorat et al. CXR of COVID-19: Is a radiologist needed?

researchers, is used for a semi-quantitative evaluation and in this range, better presents the severity of inflammatory changes. However, the aggregated number of points does not reflect the distribution of abnormalities in given quadrants as an 8/12 point evaluation might show involvement of 2 (3+3+1+1), 3 (3+2+2+1) or 4 quadrants (2+2+2+2).

In our opinion, scoring according to one of the scales is clinically more useful than a description on its own and should be an essential component of a structured reporting strategy. As no scale was deemed superior, it is more legitimate to use an easier tool in the form of a simpler and clearer five-point scale. The more complex the scale, the more uncertain the assessment. The authors' experience in treating COVID-19 patients allows them to highlight the importance of interpreting the image and not just the description. Our paper proves that the five-point and twelve-point scales for CXR scoring in COVID-19 patients can be used by a referring physician with the risk of error not exceeding 10%. This is vital in situations when an urgent decision about subsequent treatment for a patient is required (to send them home, to admit them to a hospital or to perform further diagnostics with more tests, including imaging tests). A RALE score was used in research by Wong et al. and Cozzi et al.[10,12] It is marginally more complex as it requires assessment of consolidations on a scale of 0–4 and density on a scale of 0–3 with the values then being multiplied by each other. The assessment is carried out in 4 quadrants and the sum thereof gives the final result.[19] The greater complexity of the scale the less useful it is in emergency situations. In our research, the five-point scale produced a marginally greater consistency between the results of a radiologist and a referring physician.

The use of these scales also has prognostic importance as shown in the research by Toussie et al. In this research, a zonal scale was used to reveal that CXR severity scores represent an independent prognostic indicator of outcomes in COVID-19 patients.[20] In this case, the lungs were divided into 6 zones and it was demonstrated that if opacities were present in at least 2 lung zones, the patient was more likely to require hospitalization, but if the changes were present in at least 3 lung zones, they required intubation.

Limitations

Our study has several limitations. Firstly, it is a retrospective research study. Secondly, the time between the onset of symptoms and reporting to the hospital was highly variable. The number of patients with a positive CXR result is too small to divide the patients into groups based on the duration of symptoms in order to perform a comparative analysis between the groups. The lower quality of portable X-ray images should also be taken into account.

Conclusions

The CXR severity score is a useful tool to assess the severity of inflammatory changes in the initial diagnosis of COVID-19. At the peak of a pandemic, when the system is overwhelmed, quantifying lung abnormalities accurately can be performed by a referring physician with a substantial agreement in respect to radiological evaluation. In such a situation, the function of a radiologist should be to conduct training for referring clinicians as well as being helpful in cases of uncertain images. Simple and complex CXR severity scales correlate well with clinical parameters thus the less complex five-point scale should be recommended as an essential component of a structured reporting strategy. The presence of inflammatory changes in CXR, even non-severe ones, is an independent factor of worse prognosis in COVID-19.

ORCID iDs

Marta Rorat ⓘ https://orcid.org/0000-0002-5318-4945
Tomasz Jurek ⓘ https://orcid.org/0000-0003-0110-0276
Krzysztof Simon ⓘ https://orcid.org/0000-0002-8040-0412
Maciej Guziński ⓘ https://orcid.org/0000-0002-9781-2114

References

1. Hu Z, Song C, Xu C, et al. Clinical characteristics of 24 asymptomatic infections with COVID-19 screened among close contacts in Nanjing, China. *Sci China Life Sci.* 2020;63(5):706–711. doi:10.1007/s11427-020-1661-4
2. Chung M, Bernheim A, Mei X, et al. CT imaging features of 2019 novel coronavirus (2019-nCoV). *Radiology.* 2020;295(1):202–207. doi:10.1148/radiol.2020200230
3. Pan F, Ye T, Sun P, et al. Time course of lung changes at chest CT during recovery from coronavirus disease 2019 (COVID-19). *Radiology.* 2020;295(3):715–721. doi:10.1148/radiol.2020200370
4. Bernheim A, Mei X, Huang M, et al. Chest CT findings in coronavirus disease-19 (COVID-19): Relationship to duration of infection. *Radiology.* 2020;295(3):685–691. doi:10.1148/radiol.2020200463
5. Kanne JP. Chest CT Findings in 2019 novel coronavirus (2019-nCoV) infections from Wuhan, China: Key points for the radiologist. *Radiology.* 2020;295(1):16–17. doi:10.1148/radiol.2020200241
6. American College of Radiology (ACR). ACR recommendations for the use of chest radiography and computed tomography (CT) for suspected COVID-19 infection. https://www.acr.org/Advocacy-and-Economics/ACR-Position-statements/Recommendations-for-Chest-Radiography-and-CT-for-Suspected-COVID19-Infection. Published March 22, 2020. Accessed August 5, 2020.
7. Nair A, Rodrigues JCL, Hare S, et al. A British Society of Thoracic Imaging statement: Considerations in designing local imaging diagnostic algorithms for the COVID-19 pandemic. *Clin Radiol.* 2020;75(5):329–334. doi:10.1016/j.crad.2020.03.008
8. Agency for Health Technology Assessment and Tariff System. Zalecenia w COVID-19: Polskie zalecenia diagnostyczno-terapeutyczne oraz organizacyjne w zakresie opieki nad osobami zakażonymi lub narażonymi na zakażenie SARS-CoV-2 (v. 1.0). https://www.aotm.gov.pl/www/zalecenia-covid-19-2/. Published April 24, 2020. Accessed August 5, 2020.
9. Rorat M, Zińczuk A, Szymański W, Simon K, Guziński M. Usefulness of portable chest radiography in initial diagnosis of COVID-19. *Pol Arch Intern Med.* 2020;130(10):906–909. doi:10.20452/pamw.15512
10. Cozzi D, Albanesi M, Cavigli E, et al. Chest X-ray in new coronavirus disease 2019 (COVID-19) infection: Findings and correlation with clinical outcome. *Radiol Med.* 2020;125(8):730–737. doi:10.1007/s11547-020-01232-9

11. Schiaffino S, Tritella S, Cozzi A, et al. Diagnostic performance of chest X-ray for COVID-19 pneumonia during the SARS-CoV-2 pandemic in Lombardy, Italy. *J Thorac Imaging.* 2020;35(4):W105–W106. doi:10.1097/RTI.0000000000000533

12. Wong HYF, Lam HYS, Fong AH, et al. Frequency and distribution of chest radiographic findings in patients positive for COVID-19. *Radiology.* 2020;296(2):E72–E78. doi:10.1148/radiol.2020201160

13. Vancheri SG, Savietto G, Ballati F, et al. Radiographic findings in 240 patients with COVID-19 pneumonia: Time-dependence after the onset of symptoms. *Eur Radiol.* 2020;30(11):6161–6169. doi:10.1007/s00330-020-06967-7

14. Taylor E, Haven K, Reed P, et al; SHIVERS Investigation Team. A chest radiograph scoring system in patients with severe acute respiratory infection: A validation study. *BMC Med Imaging.* 2015;15:61. doi:10.1186/s12880-015-0103-y

15. Borghesi A, Zigliani A, Masciullo R, et al. Radiographic severity index in COVID-19 pneumonia: Relationship to age and sex in 783 Italian patients. *Radiol Med.* 2020;125(5):461–464. doi:10.1007/s11547-020-01202-1

16. R Foundation for Statistical Computing; R Core Team. A language and environment for statistical computing. https://www.R-project.org/. Published February 29, 2020. Accessed August 10, 2020.

17. Israelsen SB, Kristiansen KT, Hindsberger B, et al. Characteristics of patients with COVID-19 pneumonia at Hvidovre Hospital, March–April 2020. *Dan Med J.* 2020;67(6):A05200313. PMID:32448405

18. Ippolito D, Maino C, Pecorelli A, et al. Chest X-ray features of SARS-CoV-2 in the emergency department: A multicenter experience from northern Italian hospitals. *Respir Med.* 2020;170:106036. doi:10.1016/j.rmed.2020.106036

19. Warren MA, Zhao Z, Koyama T, et al. Severity scoring of lung oedema on the chest radiograph is associated with clinical outcomes in ARDS. *Thorax.* 2018;73(9):840–846. doi:10.1136/thoraxjnl-2017-211280

20. Toussie D, Voutsinas N, Finkelstein M, et al. Clinical and chest radiography features determine patient outcomes in young and middle age adults with COVID-19. *Radiology.* 2020;297(1):E197–E206. doi:10.1148/radiol.2020201754

Cancer patients and internal medicine patients attitude towards COVID-19 vaccination in Poland

Joanna Kufel-Grabowska[1,2,A–D,F], Mikołaj Bartoszkiewicz[3,B–D], Rodryg Ramlau[4,E,F], Maria Litwiniuk[5,6,E,F]

[1] Department of Electroradiology, Poznan University of Medical Sciences, Poland

[2] Department of Chemotherapy, University Hospital of Lord's Transfiguration, Poznań, Poland

[3] Department of Immunobiology, Poznan University of Medical Sciences, Poland

[4] Department and Clinic of Oncology, Poznan University of Medical Sciences, Poland

[5] Department of Chemotherapy, The Greater Poland Cancer Center, Poznań, Poland

[6] Department of Cancer Pathology and Prevention, Poznan University of Medical Sciences, Poland

A – research concept and design; B – collection and/or assembly of data; C – data analysis and interpretation;
D – writing the article; E – critical revision of the article; F – final approval of the article

Abstract

Background. The initial approval of the Pfizer/BioNTech and Moderna vaccines by the European Medicines Agency (EMA) and Food and Drug Administration (FDA) marked a milestone in the fight against the COVID-19 pandemic. The increased public debate about the vaccine development process and vaccine side effects has activated the anti-vaccine community, which has begun to spread conspiracy theories about vaccine safety.

Objectives. Our study is the first to investigate the awareness of Polish patients suffering from various chronic diseases, mainly cancer, about vaccination against SARS-CoV-2.

Materials and methods. An anonymous survey was made available from November 2020 to February 2021 to representatives of patient organizations through social media (Facebook) and to patients in the Chemotherapy Department of the Clinical Hospital in Poznań. The survey was completed by 836 patients. The majority of the survey respondents had cancer (77%, n = 644), and almost $1/5$ of the respondents indicated hypertension (15.7%, n = 131) as well as depression and/or anxiety disorders (11.1%, n = 93).

Results. Less than half of the respondents (43.5%, n = 364) believed that SARS-CoV-2 vaccines were safe (40.4%, n = 260, among cancer patients; 53.9%, n = 104, among patients with other medical conditions). More than half of the respondents (60.5%, n = 506) intended to be vaccinated against SARS-CoV-2 (58.8%, n = 378, among cancer patients; 66.3%, n = 128, among patients with other medical conditions). Fear of vaccine complications and lack of belief in vaccine effectiveness were prevalent among both cancer patients and patients with other medical conditions.

Conclusions. The vast majority of cancer and medical patients wanted to be vaccinated against COVID-19. More than half of the respondents did not believe that the COVID-19 vaccine would be safe for them. Education of cancer and medical patients on the safety and effectiveness of the vaccine, as well as the use of additional protective measures against infection, is an extremely important element of prevention during the COVID-19 pandemic.

Key words: infection, vaccine, cancer patients, COVID-19

Background

Since the outbreak of the COVID-19 pandemic until February 13, 2021, nearly 108 million people worldwide have been infected with the coronavirus and 2.4 million have died. In Poland, 1.6 million cases have been confirmed and 41,000 people have lost their lives.[1] Each year there are about 10 million cancer deaths worldwide. In Poland, 155,000 new cases are diagnosed and 93,000 die from cancer each year.[2,3]

On December 11, 2020, the United States Food and Drug Administration (FDA) approved the Pfizer vaccine against COVID-19 and on December 18, 2020, it approved the Moderna vaccine. In January 2021, the Astra Zeneca vaccine was approved for use in European Union countries.[4,5]

The risk of severe infection with SARS-CoV-2 is several times higher among patients with hematological malignancies, lung cancer, tumors at the stage of dissemination, and solid tumors up to 1 year after a diagnosis of cancer. In the general population, the risk is about 2–3%, while among cancer patients it is 5–61%.[6]

Vaccines based on viral RNA (Comirnaty, Moderna) and vector vaccines (Astra Zeneca) can be safely used in cancer patients, even during cancer treatment. Their effectiveness depends on the current therapy (chemotherapy, immunotherapy, hormone therapy, targeted therapy), the general condition of the patient, coexisting diseases, and the type and severity of the cancer. Patients on cytostatic therapy may have lower immunization levels, whereas patients on immunotherapy and hormone therapy should have immune responses comparable to the healthy population.[7,8]

Optimally, vaccination should take place at least 14 days before beginning cancer therapy, but this should not be a reason to delay its initiation. The use of cytostatic drugs has an immunosuppressive effect; however, vaccination may be administered between courses of therapy, preferably after the time of the greatest decrease in white blood cell count and at least 2–3 days before the next dose, when there is the greatest risk of post-vaccination deterioration. During immunotherapy and hormone therapy, the use of vaccines is independent of the timing of drug administration.[9,10]

This study presents a survey of attitudes about vaccination against COVID-19 among cancer and internal medicine patients in Poland in the early stages of the COVID-19 vaccination program.

Objectives

The aim of the conducted survey was to gather the opinions of Polish cancer patients and internal medicine patients about the SARS-CoV-2 vaccine and to study the consequences resulting from their decisions.

Materials and methods

Study design

This cohort study included 836 patients suffering from various chronic diseases. Data were collected from November 2020 to February 2021 from representatives of patient organizations through social media (Facebook) and patients from the Department of Chemotherapy at the University Hospital of Lord's Transfiguration in Poznań, Poland.

An anonymous survey entitled "Vaccination against SARS-CoV-2 causing COVID-19" was used for this study. The survey was divided into 2 parts. The 1st part (epidemiological) included questions about the patient (gender, age, place of residence, education, employment, coexisting diseases, and chronic treatment), whereas the 2nd part asked about the patient's attitudes toward SARS-CoV-2 vaccination (willingness to be vaccinated, concerns about vaccines and effectiveness of protective measures in the face of the COVID-19 pandemic). The questionnaire was designed by the study authors and has not been validated.

Inclusion criteria

Patients in Poland with various diseases were eligible for this study. Completion of the survey was voluntary. Data were collected for 4 months without limiting the population.

Statistical analyses

IBM SPSS Statistics v. 26 (IBM Corp., Armonk, USA) software was used for the analysis. A p-value <0.05 was adopted as the level of statistical significance. The Shapiro–Wilk test was used to test the normality of the distribution. The χ^2 test was used to investigate the interdependence of the data. The z-test was used to test for significant differences between percentages (Bonferroni correction was used to correct for multiple comparisons). The binomial test was used to compare whether the proportion of success on a two-level categorical dependent variable differed significantly from a hypothesized value. To study whether the distribution of quantitative data in more than 2 groups originated from the same distribution, the nonparametric Kruskal–Wallis test was chosen with the Bonferroni test used for post hoc tests (pairwise Mann–Whitney U test with Bonferroni correction).

Ethics

The survey was submitted to the bioethics commission, which ruled that, in the case of an anonymous survey, the approval of the bioethics commission is not needed. Each patient was informed about the voluntary nature study of the questionnaire survey and expressed verbal

consent. All procedures were performed in accordance with the 1964 Declaration of Helsinki and its later amendments or comparable ethical standards.

Results

Participants

The survey was completed by 836 participants, and it included significantly more women (92.1%, n = 770, binomial test p < 0.01 more than 50%) than men (7.9%, n = 66, binomial test: p < 0.01, less than 50%).

Most respondents came from cities with more than 250,000 residents (34.9%, n = 292), followed by villages (22.0%, n = 184) and cities with up to 50,000 residents (20.3%, n = 170); the fewest respondents were from cities with up to 100,000 residents (13.5%, n = 113) and then cities with up to 250,000 residents (9.2%, n = 77). The vast majority of respondents were employed (71.8%, n = 600), almost 15% of the respondents were retired and 10.8% (n = 90) declared being unemployed. Almost all respondents had at least secondary education (60% higher, 32.1% secondary), 7.2% had vocational education and 0.7% had primary education (Fig. 1).

More than 3/4 of the survey participants had cancer (77.0%, n = 644), and almost $^1/_5$ of the respondents indicated hypertension (15.7%, n = 131) as well as depression and/or anxiety disorders (11.1%, n = 93). Less than 10% of respondents had the following conditions: migraine or frequent headaches (9.4%, n = 79), obesity (9.0%, n = 75), bronchial asthma (5.3%, n = 44), osteoporosis (4.9%, n = 41), hypothyroidism (4.5%, n = 38), insulin resistance (4.2%, n = 35), acne (3.2%, n = 27), rheumatoid arthritis (2.8%, n = 23), Hashimoto's thyroiditis (2.6%, n = 22), kidney disease (1.7%, n = 14), allergies (1.4%, n = 12), atherosclerosis (0.6%, n = 5), gout, epilepsy (each n = 4, 0.5%), hepatitis, thrombosis, pneumonia (each n = 3, 0.4%), stroke, endometriosis (each n = 2, 0.2%), and other diseases (5.8%, n = 48). The vast majority of patients were receiving chronic treatment (78.6%, n = 657) (Table 1).
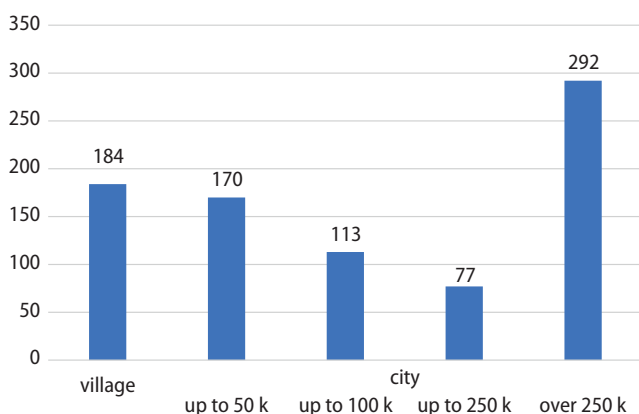
Fig. 1. Place of residence of the respodents

Table 1. The most common diseases by respondents

Disease	Frequency	Percent
Allergies	12	1.4%
Bronchial asthma	44	5.3%
Depression, anxiety disorders	93	11.1%
Cardiovascular disease	35	4.2%
Cancer	644	77.0%
Kidney disease	14	1.7%
Diabetes	35	4.2%
Gout	4	0.5%
Endometriosis	2	0.2%
Epilepsy	4	0.5%
Hashimoto	22	2.6%
Insulin resistance	35	4.2%
Migraine or frequent headaches	79	9.4%
Atherosclerosis	5	0.6%
Hypertension	131	15.7%
Hyperthyroidism	1	0.1%
Hypothyroidism	38	4.5%
Osteoporosis	41	4.9%
Obesity	75	9.0%
Rheumatoid arthritis	23	2.8%
Acne	27	3.2%
Stroke	2	0.2%
Viral hepatitis	3	0.4%
Thrombosis	3	0.4%
Pneumonia	3	0.4%

Main part of the survey

Less than half of the respondents (43.5%, n = 364) believed that SARS-CoV-2 vaccines were safe (40.4% among cancer patients, 53.9% among patients with other medical conditions), while 13.5% (n = 113) had the opposite opinion and 42.9% (n = 359) could not determine vaccine safety (Table 2, Q1). More than half of the respondents (60.5%, n = 506) intended to be vaccinated against SARS-CoV-2 (58.8% among cancer patients, 66.3% among patients with other medical conditions), 17.5% (n = 146) did not plan to be vaccinated and more than $^1/_5$ (22.0%, n = 184) had not yet made a decision (Table 2, Q2). Undecided individuals and vaccine opponents were most concerned about vaccine complications (32.1%, n = 268), did not believe in vaccine effectiveness (12.0%, n = 100) or believed that they did not need the vaccination because of their history of SARS-CoV-2 infection 3.9% (n = 33) (Table 2, Q3). Fear of vaccine complications (33% compared to 29%) and lack of belief in vaccine effectiveness (12.6% compared to 9.8%) were prevalent among both cancer patients and patients with other medical conditions (Table 2).

Table 2. Main part of survey – analysis of patients' responses

Question	Answer	Frequency (n)	Percentage
Q1. Do you think the coronavirus vaccine is safe?	No	113	13.5
	I don't know	359	42.9
	Yes	364	43.5
Q2. Are you planning to vaccinate against the coronavirus?	No	146	17.5
	I don't know	184	22.0
	Yes	506	60.5
Q3. If not, why not? (multiple choice question)	I don't believe the vaccine will be effective	100	12.0
	I am concerned about post-vaccination complications	268	32.1
	I have had COVID-19 and do not need a vaccination	33	3.9
Q4. If you are concerned about vaccine complications, what are they? (multiple choice question)	Anaphylactic shock	313	37.4
	Fever	48	5.7
	Pain, redness at the injection site	33	3.9
	Rash	8	1.0
Q5. Why are you planning to get vaccinated? (multiple choice question)	I am worried about COVID-19	430	51.4
	I am afraid that I might infect someone from my relatives or patients	349	41.7
	I want to get back to my social life/trips	382	45.7
	I have had COVID-19 and want to avoid getting it again	78	9.3
Q6. Do you think that vaccination against coronavirus should be mandatory? (multiple choice question)	Yes, for everyone	273	32.7
	Yes, but only for people at risk (medics, police, army, teachers, chronically ill people)	64	7.7
	Yes, for people traveling abroad	51	6.1
	No, everyone should have a choice	502	60.0
Q7. What do you think can significantly reduce the number of coronavirus cases? (multiple choice question)	Vaccinating entire societies	579	69.3
	Use of personal protective equipment (masks, disinfection, gloves)	564	67.5
	Limiting interpersonal contacts to the necessary minimum	276	33.
	Closing the state borders	128	15.3

When asked about vaccine complications, respondents were most often concerned about anaphylactic shock (37.4%, n = 313), followed by fever (5.7%, n = 48), pain and redness at the injection site (3.9%, n = 33), and rash (1.0%, n = 8) (Table 2, Q4).

More than half of the patients (51.4%, n = 430) wanted to be vaccinated against SARS-CoV-2 due to fear of getting sick, 45.7% (n = 382) wanted to return to social life and/or travel and 41.7% (n = 349) wanted to be vaccinated due to fear of infecting a loved one; some patients (3.9%, n = 78) wanted to avoid reinfection with a new variant of coronavirus 2 (Table 2, Q5).

More than half of the respondents (60.0%, n = 502) believed that everyone should be able to decide individually whether to participate in the SARS-CoV-2 vaccination program, while more than $1/4$ of the respondents (32.7%, n = 273) stated that vaccination should be mandatory for everyone, and 6.1% (n = 51) that it should be mandatory for international travelers (Table 2, Q6). A comparable number believed that vaccinating the public (69.3%, n = 579) and using personal protective equipment (masks, disinfectants, gloves) (67.5%, n = 564) could significantly reduce COVID-19 incidence (Table 2, Q7).

Relationships of attitudes with respondent characteristics

Age

We compared responses to the question if the coronavirus vaccine was safe between young people and the elderly. There was a significant difference between the age groups (Kruskal–Wallis test, p = 0.0142). To further investigate the differences, the Bonferroni post hoc test was used:

– The average age among those who do not believe the coronavirus vaccine is safe was significantly lower than among the group who believe it is safe (response "yes", Bonferroni post hoc test, B = –70.938, p = 0.006, M = 45, n = 364) and who have no opinion (response "don't know", Bonferroni post hoc test, B = –71.952, p = 0.0066, M = 45, n = 112).

– There were no significant difference in age distribution between the groups that answered "yes" and "I don't know" (Bonferroni post hoc test, B = 1.015, p = 0.9555).

– The younger the respondents, the more often they indicated that they would not be vaccinated because they had already been sick with COVID-19 (r = –0.073, p = 0.0364). Respondents who indicated that they would

Table 3. Prerequisites for vaccination

Prerequisite	No cancer (n = 193)	Cancer (n = 643)	z-test statistic	p-value
I am afraid of catching COVID-19	n = 101 52.3%	n = 329 51.2%	0.284	0.7795
I am afraid I might infect a relative or a patient	**n = 102** **52.8%**	**n = 247** **38.4%**	**3.567**	**0.0004**
I want to get back to my social life/travels	**n = 104** **53.9%**	**n = 278** **43.2%**	**2.605**	**0.0091**
I have had COVID-19 and want to avoid getting it again	n = 18 9.3%	n = 60 9.3%	0.000	1.0000

Values in bold are statistically significant.

not be vaccinated because they had already been sick with COVID-19 were significantly younger (Mann–Whitney U test; U = 9685.000, p = 0.0375).

– The younger the respondents, the more often they cited the desire to return to a social life and travel as the reason for vaccination (r = −0.082, p = 0.017). Respondents who cited the desire to return to a social life and travel as the reason for vaccination were significantly younger (Mann–Whitney U test; U = 11814.500, p = 0.0424).

– The older the respondents, the more often they cited fear of contracting COVID-19 as a reason for vaccination (r = 0.119, p = 0.0013). Respondents who cited fear of contracting COVID-19 as a reason for vaccination were significantly older (Mann–Whitney U test; U = 100007.000; p = 0.000).

Place of residence

There was a significant relationship between place of residence and answers given to the survey question (χ^2 = 24.263, p = 0.0022):

– Respondents from bigger cities gave the fear of COVID-19 disease as a reason for vaccination significantly more often than people from smaller cities (χ^2 = 22.050, n = 430; p = 0.000).

– Respondents from bigger cities gave the desire to return to a social life as a reason for vaccination significantly more often than people from smaller cities (χ^2 = 17.116, p = 0.002, n = 382).

Educational level

There was a significant relationship between education level and answers given to the survey question (χ^2 = 37.234):

– Respondents with higher education were significantly more likely to believe that the coronavirus vaccine was safe than those with a vocational education (z-test with Bonferroni correction, z = 2.773, p = 0.0056) or a secondary education (z-test with Bonferroni correction, z = 4.524, p < 0.0001, n = 364).

– Respondents with higher education significantly more often perceived population vaccination as an effective means to reduce coronavirus incidence than those with

vocational education (z-test with Bonferroni correction, z = 4.136 p < 0.0001) or secondary education (z-test with Bonferroni correction, z = 4.772, p < 0.0001, n = 579).

Cancer

There was a significant relationship between the presence of cancer and concerns about the safety of the coronavirus vaccine (χ^2 = 11.400, p = 0.0031). In particular:

– Cancer patients were significantly less likely to believe that coronavirus vaccines are safe than non-cancer patients (z-test: z = 3.305, p = 0.0009, n = 364).

– No significant relationship between willingness to be vaccinated against coronavirus and presence of cancer was observed (χ^2 = 3.875, p = 0.1444, n = 506).

– Cancer patients were significantly less likely to intend to get vaccinated due to a desire to return to a social life than non-cancer patients (z-test: z = 2.605, p = 0.0091, n = 382).

The above data are summarized in Table 3.

Discussion

Our study is the first to investigate the awareness of Polish patients suffering from various chronic diseases, mainly cancer, about vaccination against SARS-CoV-2. Its results highlight the importance of this problem and draw attention to the need to educate these communities about the severe course and complications of coronavirus infection.

The successful completion of clinical trials for the use of SARS-CoV-2 vaccines was one of the highlights of 2020. The initial approval by the European Medicines Agency (EMA) and FDA of the Pfizer/BioNTech and Moderna vaccines marked a milestone in the fight against the COVID-19 pandemic. However, the increased public debate about the vaccine development process and vaccine side effects have activated the anti-vaccine community, which has begun to spread conspiracy theories about vaccine safety.

Previous studies analyzing morbidity and mortality due to COVID-19 confirm that the groups most vulnerable to severe SARS-CoV-2 infection are the elderly, those burdened with chronic diseases and cancer patients. In our

study, all respondents were burdened with coexisting conditions, among which cancer predominated (77%), followed by cardiovascular diseases (heart disease 4.2%, hypertension 15.7%), psychiatric diseases (depression, anxiety disorders 11.1%), internal medicine and metabolic disorders (kidney disease 1.7%, diabetes 4.2%, gout 0.5%, hypothyroidism 4.5%, obesity 9%), and other conditions, although only 43.5% thought the SARS-CoV-2 vaccine was safe. A report by the Centre for Countering Digital Hate (CCDH) published in early October 2020 warned that more than 7 million users have joined anti-vaccine groups since 2019. The study found that people who used social media to search for information about the pandemic were more hesitant in their decision to vaccinate.[11]

Individuals with coexisting chronic diseases should take special care of their health due to the higher risk of severe SARS-CoV-2 infection. More than 60.5% of the respondents in our study planned to be vaccinated against SARS-CoV-2. Similar results were obtained in a study conducted in the USA by Fisher et al. among 991 adults, with 571 (57.6%) stating their intention to be vaccinated against SARS-CoV-2.[12]

Our study showed that almost ⅔ of patients wanted to be vaccinated against SARS-CoV-2, while more than $1/5$ of the respondents were undecided. The most common reason mentioned by Polish patients was fear of post-vaccination complications (32.1%). Respondents were most concerned about anaphylactic shock (37.4%). Fear of severe post-vaccination complications is one of the most frequently addressed issues by anti-vaccine groups, which aim to discourage the public from vaccinating. A CDC report dated January 6, 2021, indicates that after 1.9 million doses of the Pfizer/BioNTech vaccine were administered, there were 21 cases of severe allergic reaction, which is a 0.001105% probability of such an adverse event. To a large extent, the benefits outweigh the risks.[13]

Among the motivations reported by respondents to vaccinate against SARS-CoV-2, the main reason was fear of getting COVID-19 (51.4%), while young people were more likely to indicate the desire to return to a social life (45.7%). A survey by Larson et al. of a group of 65,819 individuals from 67 countries indicated that education increases awareness about the importance and effectiveness of vaccination, but not about its safety.[14]

Our study showed that patients with higher education were significantly more likely to report willingness to participate in the SARS-CoV-2 vaccination program and significantly more likely to believe in vaccine effectiveness. Individuals with higher education were more afraid of getting COVID-19 than those without an academic education, and they regarded vaccination as an opportunity to return to a social life.

Similar views as educated respondents were held by younger respondents, who were more likely to believe that vaccines should be voluntary and that the main rationale for vaccination was to return to a social life.

Older respondents, on the other hand, were more concerned about being infected with COVID-19 and were more likely to believe that vaccines should be mandatory for everyone. The respondents, depending on their age, place of residence and education, were motivated to get vaccinated in different ways. This suggests that education of all individuals, especially those at higher risk for severe SARS-COV-2 infection, is extremely important and may increase their awareness of the role and importance of vaccination.

The largest group of respondents were cancer patients (77%). As mentioned earlier, this group is particularly at risk of severe SARS-CoV-2 infection due to immunosuppressive oncological treatment. The recommendations of Polish and global scientific societies emphasize that cancer patients and people involved in their therapeutic process should be vaccinated as a priority, regardless of age or coexisting diseases.[13]

Due to the innovative nature of vaccines, there are discussions about their safety and vaccine feasibility in cancer patients. Cancer patients have not participated in clinical trials on vaccine effectiveness. However, based on previous experience with vector vaccines against the influenza virus, it should be assumed that vaccines against SARS-CoV-2 are safe for them.[15,16]

Among the respondents, oncology patients were less likely to believe in the safety of vaccines than patients with other conditions (40.4% compared to 53.9%), thus their education is extremely important. It is worth emphasizing that vaccines are safe and do not impair cancer treatment, nor should they be a reason for vaccine postponement. Their effectiveness may be limited during immunosuppressive therapy (chemotherapy), but in combination with the use of personal protective equipment, they are an effective strategy in the fight against coronavirus. Immunotherapy, hormonal therapy and targeted therapy do not impair patients' immune response.Their effectiveness in cancer patients is on the same level as in the general population.

Our study found that cancer patients were less likely than patients with other conditions to report willingness to be vaccinated against coronavirus (58.8% compared to 66.3%), although the difference was not statistically significant. The same reasons for not wanting to vaccinate dominated in both groups: fear of complications (33% compared to 29%) and disbelief in vaccine effectiveness (12.6% compared to 9.8%). It is also worth mentioning that the motivation for vaccination in internal medicine patients was the desire to return to a social life and the fear of exposing relatives to coronavirus infection significantly more often than in cancer patients.

Limitations

Our study has several limitations. Firstly, we did not verify that the patients actually suffered from the diseases indicated. Secondly, a small proportion of respondents

were men and the vast majority of respondents were cancer patients. Lastly, the questionnaire used in the survey was not validated.

Conclusions

The vast majority of cancer and medical patients want to be vaccinated against COVID-19. More than half of the respondents did not believe that the COVID-19 vaccine would be safe for them. The most common fear was the occurrence of anaphylactic shock following the administration of the vaccine. Educating cancer and other patients about the safety and effectiveness of the vaccine, as well as the use of additional protective measures against infection, is an extremely important element of prevention during the COVID-19 pandemic.

ORCID iDs

Joanna Kufel-Grabowska ● https://orcid.org/0000-0002-5724-9961
Mikolaj Bartoszkiewicz ● https://orcid.org/0000-0002-8728-5998
Rodryg Ramlau ● https://orcid.org/0000-0002-3199-2298
Maria Litwiniuk ● https://orcid.org/0000-0001-8428-3877

References

1. World Health Organization (WHO). Coronavirus (COVID-19) Dashboard, https://covid19.who.int. Accessed April 1, 2021.
2. Sung, H, Ferlay, J, Siegel, RL, et al. Global Cancer Statistics 2020: GLOBOCAN estimates of incidence and mortality worldwide for 36 cancers in 185 countries. *CA Cancer J Clin*. 2021;1(3):209–249. doi:10.3322/caac.21660
3. Krajowy Rejestr Nowotworów. Nowotwory złośliwe w Polsce w 2018 roku. http://onkologia.org.pl/wp-content/uploads/Nowotwory_2018.pdf. Accessed April 1, 2021.
4. Federal Drug Administration. Pfizer-BioNTech COVID-19 vaccine. https://www.fda.gov/emergency-preparedness-and-response/coronavirus-disease-2019-covid-19/pfizer-biontech-covid-19-vaccine. Accessed March 8, 2021.
5. European Medicines Agency. EMA recommends COVID-19 Vaccine AstraZeneca for authorisation in the EU. https://www.ema.europa.eu/en/news/ema-recommends-covid-19-vaccine-astrazeneca-authorisation-eu. Accessed March 8, 2021.
6. European Society for Medical Oncology (ESMO). COVID-19 vaccination in cancer patients: ESMO statements. https://www.esmo.org/covid-19-and-cancer/covid-19-vaccination. Accessed April 1, 2021.
7. Dooling K, McClung N, Chamberland M, Marin M, Wallace M, Bell BP, et al. The Advisory Committee on Immunization Practices' interim recommendation for allocating initial supplies of COVID-19 vaccine – United States, 2020. *MMWR Morb Mortal Wkly Rep*. 2020;69(49): 1857–1859. doi:10.15585/mmwr.mm6949e1
8. Ribas A, Sengupta R, Locke T, et al. Priority COVID-19 vaccination for patients with cancer while vaccine supply is limited. *Cancer Discov*. 2021;11(2):233–236. doi:10.1158/2159-8290.CD-20-1817
9. El-Shakankery KH, Kefas J, Miller R. COVID-19, the future vaccine and what it means for cancer patients on immunotherapy. *Front Oncol*. 2021;10:631611. doi:10.3389/fonc.2020.631611
10. Chong CR, Park VJ, Cohen B, Postow MA, Wolchok JD, Kamboj M. Safety of inactivated influenza vaccine in cancer patients receiving immune checkpoint inhibitors. *Clin Infect Dis*. 2020;70(2):193–199. doi:10.1093/cid/ciz202
11. Burki T. The online anti-vaccine movement in the age of COVID-19. *Lancet Digit Health*. 2020;2(10):e504–e505. doi:10.1016/S2589-7500(20)30227-2
12. Fisher KA, Bloomstone SJ, Walder J, Crawford S, Fouayzi H, Mazor KM. Attitudes toward a potential SARS-CoV-2 vaccine: A survey of U.S. adults. *Ann Intern Med*. 2020;173(12):964–973. doi:10.7326/M20-3569
13. Centers for Disease Control and Prevention (CDC). COVID-19 Vaccination. https://www.cdc.gov/vaccines/covid-19/index.html. Accessed April 1, 2021.
14. Larson HJ, de Figueiredo A, Xiahong Z, et al. The state of vaccine confidence 2016: Global insights through a 67-country survey. *EBioMedicine*. 2016;12:295–301. doi:10.1016/j.ebiom.2016.08.042
15. Polack FP, Thomas SJ, Kitchin N, et al. Safety and efficacy of the BNT162b2 mRNA Covid-19 vaccine. *N Engl J Med*. 2020;383(27): 2603–2615. doi:10.1056/NEJMoa2034577
16. National Institutes of Health (NIH). Peer-reviewed report on Moderna COVID-19 vaccine publishes. https://www.nih.gov/news-events/news-releases/peer-reviewed-report-moderna-covid-19-vaccine-publishes. Accessed April 1, 2021.

The sense of coherence and sense of satisfaction with life in patients hospitalized in Polish and Irish surgical departments

Krzysztof Kamil Kotulski[1,A,B,D], Joanna Bartczak-Kotulska[2,B,C],
Julia Rudno-Rudzińska[1,E], Wojciech Kielan[1,E,F], Ewelina Frejlich[1,C], Wojciech Hap[1,B]

[1] Clinic of General and Oncological Surgery, Jan Mikulicz-Radecki University Teaching Hospital, Wrocław, Poland

[2] Joanna Bartczak-Kotulska Center for Psychoeducation and Therapy, Ostrowina, Poland

A – research concept and design; B – collection and/or assembly of data; C – data analysis and interpretation;
D – writing the article; E – critical revision of the article; F – final approval of the article

Address for correspondence
Krzysztof Kotulski
E-mail: k.kotulski@mp.pl

Abstract

Background. The concept of the sense of coherence (SOC) – the global orientation of life, created by Aaron Antonovsky – is increasingly popular. This study within the field of health psychology examines the situation of patients awaiting surgery in Poland and Ireland.

Objectives. To investigate the relationship between the strength of the SOC and its components (comprehensibility, manageability and meaningfulness) and the level of satisfaction with life (SWL) of patients hospitalized in surgical departments in hospitals in Poland and Ireland.

Materials and methods. The research was conducted in a group of 60 surgical patients, including 30 hospitalized in Poland and 30 in Ireland. The tools utilized were the Sense of Coherence Questionnaire for Adults SOC-29 and the Satisfaction with Life Scale (SWLS). Polish versions of both questionnaires were also used.

Results. We obtained the following results:
– for comprehensibility: in patients undergoing surgery in hospitals in Poland, the mean (M) = 46.3, standard deviation (SD) = 9.8, minimum value (Min) = 28, and maximum value (Max) = 63; in Irish patients, M = 50.8, SD = 9.2, Min = 33, and Max = 71;
– for manageability: in patients undergoing surgery in hospitals in Poland, the M = 49.7, SD = 5.07, Min = 37, and Max = 58; in Irish patients, M = 49.3 SD = 6.39, Min = 38, and Max = 63;
– for meaningfulness: in patients undergoing surgery in hospitals in Poland, M = 45.5, SD = 4.24, Min = 37, and Max = 54; in Irish patients, M = 44.9 SD = 5.74, Min = 34, and Max = 56.

Conclusions. The results of the study confirmed the assumption that a general SOC correlates with SWL. However, they did not confirm the hypothesis that differences in the strength of patients' SOC, its components and their level of SWL depend on the country of hospitalization.

Key words: life satisfaction, sense of coherence, salutogenesis, surgical patient

Background

The sense of coherence as the central concept of salutogenesis

The sense of coherence (SOC) has been a concept in psychology for over 30 years. The originator of the concept is Aaron Antonovsky, a medical sociologist.[3] The inspiration for this concept was his analysis of the living situation (including health) of the survivors of concentration camps. Antonovsky sought an answer to the question of why some people, despite extremely difficult experiences, survived and lived long lives, maintaining optimism and serenity, while others lost their desire to live, became bitter and, after regaining freedom, became ill and died. Antonovsky sought to explain what determines that some people maintain their health, living a long and active life, while others are more likely to fall ill, recover with difficulty and live shorter lives as a result. The answer Antonovsky found was that the observed differences are caused by the way we comprehend ourselves and the world, by a sense of the meaningfulness of our lives and our actions, and a sense of possessing qualities that enable us to manage life successfully. These 3 elements are the ingredients of the notion of the SOC – the most important

concept in Antonovsky's concept of health, which is called salutogenesis.

In this approach, health is considered the current position on a continuum of health–illness, where the left pole is characterized as a state of full mental, physical and social health, while the right pole is the state of profound, life-threatening illness.[4] There are 2 types of approaches in the concepts of health: consideration and examination of health determinants (the salutogenic approach) and consideration and examination of the factors responsible for the appearance of disease (pathogenetic approach). Based on the research questions listed in the text, we formulated the research hypotheses presented in Table 1. Table 2 presents the essential features of the salutogenic paradigm in comparison with the pathogenetic paradigm.

The notion of health in the salutogenic paradigm is related to the ability to cope with external and internal demands and burdens while maintaining a dynamic balance.[5] Antonovsky outlines 4 key elements that affect an individual's health. These are: generalized resistance resources, stressors, SOC, and behavior and lifestyle.[4]

Antonovsky uses these concepts to explain why people maintain health despite experiencing stress and difficult conditions, or why – in the event of health problems – they quickly regain it. The answer is in the existence

Table 1. Hypotheses and detailed hypotheses

SN	Hypotheses	Detailed hypotheses
1	H0: There is no correlation between the strength of the sense of coherence (SOC) and the level of satisfaction with life (SWL). H1: There is a correlation between the strength of the sense of coherence (SOC) and the level of satisfaction with life (SWL).	Hypothesis 1A: H0: There is no correlation between the comprehensibility component of the SOC and the level of SWL. H1: There is a correlation between the comprehensibility component of the SOC and the level of SWL.
		Hypothesis 1B: H0: There is no correlation between the manageability component of the SOC and the level of SWL. H1: There is a correlation between the manageability component of the SOC and the level of SWL.
		Hypothesis 1C: H0: There is no correlation between the meaningfulness component of the SOC and the level of SWL. H1: There is a correlation between the meaningfulness component of the SOC and the level of SWL.
2	H0: There is no difference between the strength of the SOC in Polish and Irish patients. H1: There is a difference between the strength of the SOC in Polish and Irish patients.	Hypothesis 2A: H0: There is no difference between the levels of the comprehensibility component of the SOC in Polish and Irish patients. H1: There is a difference between the levels of the comprehensibility component of the SOC in Polish and Irish patients.
		Hypothesis 2B: H0: There is no difference between the levels of the manageability component of the SOC in Polish and Irish patients. H1: There is a difference between the levels of the manageability component of the SOC in Polish and Irish patients.
		Hypothesis 2C: H0: There is no difference between the levels of the meaningfulness component of the SOC in Polish and Irish patients. H1: There is a difference between the levels of the meaningfulness component of the SOC in Polish and Irish patients.
3	H0: There is no difference between the levels of SWL in Polish and Irish patients. H1: There is a difference between the levels of SWL in Polish and Irish patients.	–

Table 2. A comparison between the salutogenic paradigm and the pathogenic paradigm

Pathogenic paradigm	Salutogenic paradigm
Thinking about people: either healthy or sick	Thinking about health and illness within the continuum from health to disease
Concentration on one specific pathological unit	Communicating with all who work on exploring the mystery of health
Studying the causes of disease	Focus on resources to help deal with stress
All the stressors are bad	How to learn to live in health with stressors and take advantage of them
It is important to declare war on the disease and overcome it	An open road to cooperation between scientists and practitioners and to making a significant contribution to the social system
Priority for individual cases and high-risk groups	People should be taken care of at every point of the health–disease continuum

of so-called generalized resistance resources, understood as "[…] characteristics of the natural, material and socio-cultural environment, characteristics of the organism and psychological characteristics of the individual that are beneficial for the management of stress".[1] The functional value of generalized resistance resources is that they allow the individual to avoid stressors and influence the ability to cope with internal and external demands by preventing the transformation of tension into stress while promoting health care.[6] Initially, the author defines stressors as the conditions for which there are no ready responses. Due to the lack of ready responses, tension appears.[5] He then adds, however, that stressors are linked to overburden, a low level of involvement or a lack of involvement in decision-making. Antonovsky proposes that stressors should be perceived in relation to the continuum of resistance resources – as resource deficits. The more resistance resources a person possesses, i.e., the closer they are to the resources on the continuum, the more their experience will foster the development of a SOC.[1] Therefore, Antonovsky regards as a stressor any factor that causes tension by increasing demands or creating new ones, necessitating a new way of responding. He emphasizes that a stressor can also act as a mobilizer, mobilizing and releasing energy, and strengthening resistance as a result. In a situation when the resources and the individual's own energy are inadequate and ineffective in coping with demands (stressors), then tension transforms into stress, which leads to a health breakdown and the occurrence of disorders.[6]

According to Antonovsky, the key element influencing the method and quality of functioning of generalized resistance resources is the SOC. The SOC has a motivational function in the active handling of demands, and a regulatory function, controlling the selection of resources relevant to current requirements.[6] The greater the intensity of the SOC, the more efficient and adequate is the use of resources and coping strategies. Therefore, coping with stress and tension depends on the adequate use of resources, which is linked to the strength of one's SOC.

In Antonovsky's concept, SOC is defined as "a global orientation that expresses the extent to which one has a pervasive, enduring yet dynamic feeling of confidence that one's internal and external environments are structured and predictable, and the feeling of the probability of a positive turn of events, expected on the basis of rational premises".[1] He goes on to broaden the definition by adding that the SOC is related to the fact that "1) the stimuli deriving from one's internal and external environments in the course of living are structured, predictable and explicable; 2) the resources to meet the demands posed by these stimuli are available to one; and 3) these demands are challenges, worthy of investment and engagement". The author does not equate the SOC with a personality trait. He uses the phrase "dispositional orientation", which is correlated with comprehensibility, manageability and meaningfulness.[1]

Describing in detail the dynamics of coherence in the human development cycle, Antonovsky emphasizes the importance of the process of socialization. According to the author, achieving a certain level of the SOC is a result of individual coherent life experiences created in interaction with the environment. However, the SOC can be defined as a relatively constant trait only at the beginning of adulthood, when a socio-cultural context is established, related to (among other things) the roles one takes on, the work one undertakes and lasting relationships.[1]

Antonovsky initiated a new processual understanding of the notion of health. He defined health as a process of balancing requirements (stressors) and resources. Health maintenance is therefore the use of available resources to meet external and internal requirements without permanently disrupting the dynamic balance between burdens and possibilities.[1] The most important factor – "the key to health", as the author puts it – is the SOC, which is a meta-resource of the individual.[6]

The concept of satisfaction with life in literature and psychological research

The concept of satisfaction with life (SWL) has been discussed in numerous works and is often associated with such concepts as quality of life (QOL), prosperity and happiness. Since the mid-20th century, it has been of interest to many scientific disciplines, including medicine, sociology, economics, and psychology. The literature on the subject cites many definitions of levels of SWL and QOL viewed from different perspectives, e.g., Cummins, Dieber, Czapiński, Sęk and Heszen, Schipper, Levin, Argyle, de Walden-Gałuszko, and many other researchers. However, no single

coherent definition has yet been established that would address the issue from an interdisciplinary perspective.[3]

The state of health can be assessed objectively, from the point of view of an observer (e.g., a doctor) or subjectively, from the perspective of the individual.[6] One element of a subjective evaluation is the level of SWL, also called the QOL, happiness or prosperity. The concept of the "quality of life" is rooted in positive psychology, which focuses primarily on the promotion and multiplication of happiness.[7] As emphasized by R.A. Kane, for some the QOL is a very broad concept in which almost everything is significant, while for others it includes only some elements of life.[8]

According to the findings of the International Society for Quality of Life Research (ISOQOL), the concept of the "quality of life" has 2 main underlying principles:

1. The concept of QOL as a practical (not necessarily strictly defined) concept in social policy and in evaluating services offered by it, as well as useful in evaluating various initiatives and programs undertaken at the local, national and international levels.

2. The overriding importance of individual perception and the subjective perspective of the individual regarding their QOL.[9]

The multidimensional nature of the concept of the QOL is also emphasized, highlighting the link between QOL and individual and environmental factors, such as intimacy, family life, friendship, work, neighborhood, place and living conditions, education, health, standard of living, and nationality.[10]

An interesting definition was put forward by Raphael et al., who defined QOL as "the degree to which a person enjoys the important possibilities of his/her life".[11] The authors list 3 main areas from the perspective of which they study the concept of QOL: being – individual attributes of the individual; belonging – matching the person and the environment; and becoming – realizing oneself (see Table 3 for details).

According to the assumptions formulated by Schalock, QOL consists of 8 components: emotional well-being,
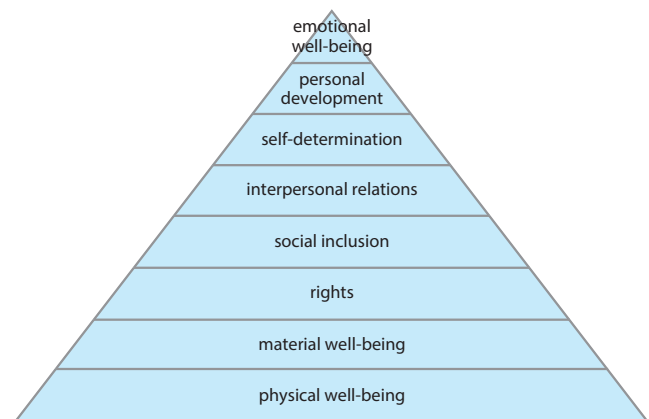
Fig. 1. Quality of life in a hierarchical perspective

interpersonal relations, material well-being, personal development, physical well-being, self-determination, social inclusion, and individual rights.[12] The author presents QOL in a multidimensional and dynamic perspective, emphasizing the hierarchical dependence of these 8 factors, as shown in Fig. 1. At the same time, the author draws attention to the interactions of the individual with the environment, including the educational and medical contexts.[12]

Cummins, on the other hand, points to both the objective and subjective dimension of QOL, each of which is characterized by 7 identical factors. These are: standard of living, health, life achievements, relationships with other individuals, personal security, relationships with the community, and securing the future. The subjective dimension is related to the sense of SWL. The researcher proposed a homeostatic model of the subjective QOL, presented in Fig. 2, according to which 3 groups of factors determine the degree of SWL:

1. Determinants of the 1st order: personality, i.e., extraversion and neuroticism, strongly correlated to one's sense of QOL.

2. Determinants of the 2nd order: so called internal buffers, i.e., control, self-esteem and optimism, which have

Table 3. Areas of the quality of life (QOL)

Main areas	Sub-areas	Detailed description
Being	physical	health, personal hygiene, nutrition, movement, care, dress, exterior appearance
	mental	mental health and adaptation, perception, emotions, self-evaluation and self-control
	spiritual	personal values, lifestyle, beliefs
Belonging	physical	relationship with the physical environment, e.g., home, workplace, neighborhood, school, community
	social	relationship with the environment regarding the acceptance and kindness of others, e.g., family, friends, co-workers, neighbors
	local	equal and adequate access to social resources such as income, healthcare, social welfare, employment, education, recreation, celebrations
Becoming	productivity	planning and regular activities taking into account the needs of the individual, concerning, e.g., home, work, education
	free time	rest, relax, stress reduction
	personal development	classes developing knowledge and skills

Fig. 2. Homeostatic model of the subjective quality of life (QOL)

the function of alleviation in the event of the deterioration of external conditions.

3. Determinants of the 3rd order: the personal experience of the individual.

According to Shin and Johnson, SWL is an "overall assessment of QOL in relation to selected criteria".[2] If the assessment is positive, it is assumed that the person feels satisfied with his/her life. Diener, on the other hand, lists SWL, in addition to the presence of positive feelings and the absence of negative feelings, as elements of so-called well-being.[2] According to Sęk and Heszen, QOL can be associated with the predominance of positive emotions, the level of satisfaction of needs, an abundance of goals, activity, commitment, and a positive attitude towards life. These concepts can be considered from an objective and a subjective perspective. The objective perspective refers to a person's living and working conditions, i.e., to their physical, material and socio-cultural conditions. The subjective determinants, on the other hand, are the evaluation of life as a whole and its individual elements. It should be noted that there are no simple relations between these 2 perspectives. Sęk points to persons who, despite difficult objective conditions, value life positively, due to a sense of influence over their own life and the skillful use of resources.[4]

Discussing the relationship between the SOC and the level of SWL, we will refer to the subjective perception of QOL. The aim of the study was an attempt to answer the question of whether there is a link between the strength of the SOC in patients undergoing surgery in Poland and Ireland and the level of their SWL.
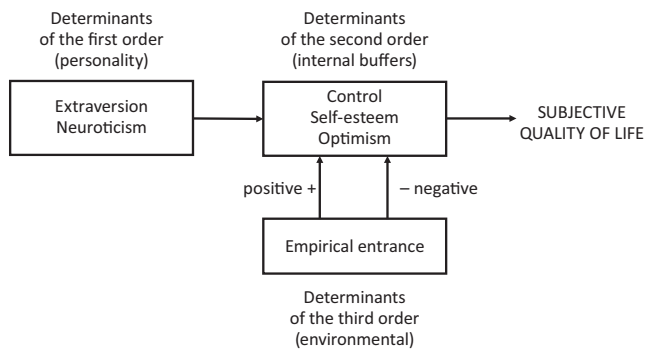
Objectives

The main goal of the study was to examine the relationship between the SOC and its components (comprehensibility, manageability and meaningfulness), and the level of SWL in patients hospitalized in surgical departments in hospitals in Poland and Ireland. The main assumptions were:

1. the hypothesis that there is a relationship between the variables tested; and

2. the hypothesis that there is a difference in the SOC and SWL between the 2 study groups, with higher values assumed for the Irish patients, as a result of higher living standards, including medical and social care.

Also, so-called contextual variables, such as age, sex, place of residence, level of education, marital status, and the reason for hospitalization, the length of the hospital stay, the number of stays, and medical history were considered important factors in the study.

Materials and methods

The research was conducted in a group of 60 surgical patients, including 30 hospitalized in Poland and 30 in Ireland. The tools utilized were:

1. the Sense of Coherence Questionnaire for Adults SOC-29 and

2. the Satisfaction with Life Scale (SWLS).

Polish versions of both questionnaires were also used. Based on the literature, the following specific questions were asked:

1. Is there a correlation between the level of an individual's SOC and their level of SWL?

2. Is there a difference between the strength of the SOC in Polish and Irish patients?

3. Is there a difference between the level of SWL in Polish and Irish patients?

Taking into account the variables being tested, it was assumed that people with a stronger SOC as a global orientation in life, along with its components (comprehensibility, manageability and meaningfulness), experience a relatively higher level of SWL. In addition, it was assumed that in patients hospitalized in Ireland, the levels of both tested variables are higher than in Polish patients, due to better medical care.

Structure of the variables

The variables included in the study were divided into dependent, independent, categorical, and contextual data. The main dependent variable is the level of SWL. The independent variable is the strength of the SOC and its components. The categorical variable is the country of residence (Poland or Ireland). Contextual variables included age, sex, place of residence, level of education, marital status, the reason for hospitalization, the length of the hospital stay, the number of stays, and medical history.

Stages of the research

In the research, the correlation model was applied. The research plan consisted of the following stages:

1. Defining the objective and research problems, selecting the variables to be tested:
   – SOC,
   – SWL.

2. Selecting appropriate research tools:

– Sense of Coherence Questionnaire – SOC-29 (Polish version),

– Sense of Coherence Questionnaire – SOC-29 (English version),

– SWLS (Polish version),

– SWLS (English version).

3. Psychometric analysis of the tools.

4. Research, conducted in 2 stages:

– pilot studies – May 2011,

– research on patients undergoing surgical treatment using selected research tools – June–August 2011.

5. Analysis of the data obtained, verification of hypotheses.

6. Conclusions.

Selection and characteristics of the research sample

The study was conducted between May and August 2011 in surgical departments in the Jan Mikulicz-Radecki University Teaching Hospital in Wrocław (Poland), the District Hospital Complex in Oleśnica (Poland) and St. Michael's Hospital in Dun Laoghaire (Ireland).

The primary criterion for selecting the research sample was the waiting period for surgery. Each time before the research, the patients were asked about their physical and mental health, well-being and willingness to participate in the research. The subjects were informed of the voluntary nature of their participation, the aim of the research and that they could withdraw from it at any time. There were 3 patients who did not consent. Prior to the beginning of the research, consent was obtained from the directors of the hospitals and department heads.

The research included 60 patients, 30 in hospitals in Poland and 30 in the hospital in Ireland. All the questionnaires were correctly completed by the participants, in accordance with the instructions attached to the questionnaires, which allowed us to include all of them in our analysis.

The following variables were included in the characteristics of the research sample: the participant's age, sex, level of education, place of residence, marital status, the reason for the hospitalization, the length of the hospital stay, the number of stays, and medical history.

The number of men and women was evenly distributed (50% from each group). The average age was 47 years. The largest number of people had secondary or higher education (33% each). The majority of the respondents lived in rural areas or small towns (33% each), and the majority (61.7%) were married. The most common causes of hospitalization were gallbladder disease (20%), hernia (15%) and fracture (11.7%). The majority of the patients remained in the hospital for 2 days (36.7%). The most common diseases in the respondents' medical histories were hypertension, hernia and heart problems.

Statistical analyses

SPSS PL v. 19 software (Predictive Solutions Sp. z o.o., Kraków, Poland) was used for the statistical calculations. The level of correlations between variables was determined using the Pearson's correlation coefficient, and differences between the groups (country of residence: Poland or Ireland) were determined using Student's t-test. In addition, the following analyses were performed on the general characteristics of the research group: descriptive statistics, minimum and maximum value (Min and Max), mean (M), standard deviation (SD), frequency, and the Kolmogorov–Smirnov test. P-values <0.05 were regarded as statistically significant.

Results

The independent variable in the research was the SOC and its components (comprehensibility, manageability and meaningfulness). The strength of the SOC was assessed on the basis of the SOC-29 questionnaire, in which one can score in total between 29 and 203 points. In the research group, the following values were obtained (Table 4):

– for comprehensibility: in patients undergoing surgery in hospitals in Poland, M = 46.3, SD = 9.8, Min = 28, Max = 63; in Irish patients, M = 50.8, SD = 9.2, Min = 33, Max = 71;

– for manageability: in patients undergoing surgery in hospitals in Poland, M = 49.7, SD = 5.07, Min = 37,

Table 4. Breakdown of the level of the components of the sense of coherence (SOC) in the 2 groups

Component	Group	Number of participants	Min	Max	Mean	SD
Comprehensibility	PL	30	28	63	46.3667	9.85930
	IE	30	33	71	50.8000	9.23785
Manageability	PL	30	37	58	49.7333	5.07144
	IE	30	38	63	49.3667	6.39765
Meaningfulness	PL	30	37	54	45.5000	4.24873
	IE	30	34	56	44.9000	5.74966

SOC – sense of coherence; PL – Polish participants; IE – Irish participants; SD – standard deviation.

Table 5. Breakdown of the level of the sense of coherence (SOC) in the 2 groups

SOC		Results	Polish patients	Irish patients	In total
Level of the SOC	low (below 117 points)	number of persons	0	0	0
		% of persons	0	0	0
	medium (117–156 points)	number of persons	23	21	44
		% of persons	76.7	70	73.7
	high (over 156 points)	number of persons	7	9	16
		% of persons	23.3	30	26.7

Max = 58; in Irish patients, M = 49.3 SD = 6.39, Min = 38, Max = 63;

– for meaningfulness: in patients undergoing surgery in hospitals in Poland, M = 45.5, SD = 4.24, Min = 37, Max = 54; in Irish patients, M = 44.9 SD = 5.74, Min = 34, Max = 56.

Table 5 shows a breakdown of the strength of the SOC. Average scores (117–156 points) were reported by 23 of Polish patients (76.7%) and 21 of Irish patients (79%). High results (above 156 points) were scored by 7 of Polish patients (23.3%) and 9 of Irish patients (30%). A low SOC (below 117 points) did not occur. In general, 44 patients (73.7%) had mean SOC scores and 16 (26%) had high SOC scores. The results are shown in Fig. 3–5.

The dependent variable was the level of SWL, tested using the SWLS questionnaire. The respondents could get between 5 and 35 points. As can be seen from the data in Table 6, the following values were obtained in the researched group:

– in patients undergoing surgery in hospitals in Poland, M = 24.6, SD = 5.1, Min = 15, Max = 33;

– in patients undergoing surgery in hospitals in Ireland, M = 23.9, SD = 6.1, Min = 8, Max = 35.

According to the data, the mean level of SWL is similar in the 2 groups. The overall average level of SWL in patients in both countries is M = 24.25, which in standardized units corresponds to a sten score of 7. This result indicates that the subjects of the research are characterized by a high level of SWL.

The results of the distribution of the dependent and independent variables tested in both groups are presented in Fig. 6.

Statistical verification of the hypotheses

The study posited main hypotheses with detailed hypotheses. Their verification on the basis of the results of the research is presented below.

Fig. 3. Distribution of results for the sense of coherence (SOC) in Polish patients in terms of the number of persons
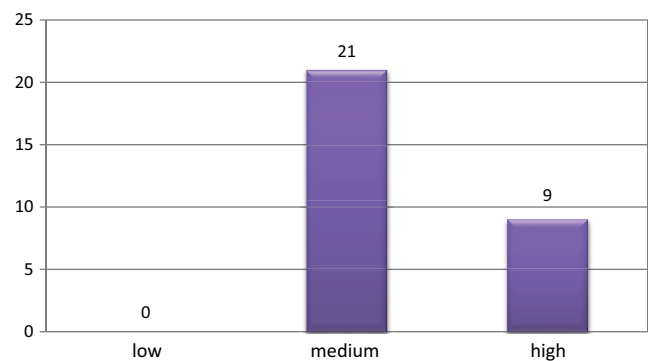
Fig. 4. Distribution of results of the sense of coherence (SOC) in Irish patients in terms of the number of persons
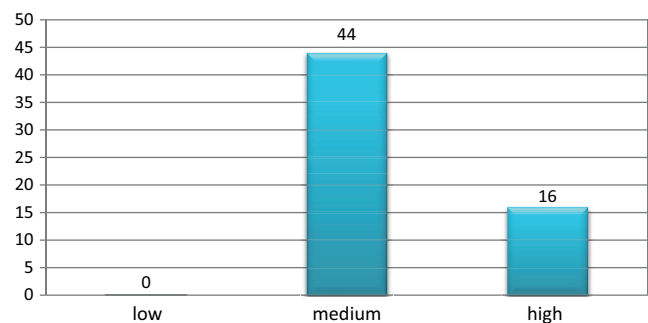
Fig. 5. Distribution of the results of the overall sense (SOC) of coherence in terms of the number of persons

Table 6. Breakdown of the level of SWL in the 2 groups

Variable	Country	Number	Min	Max	Mean	SD	SEM
SWLS	L	0	5	3	24.6000	5.10308	0.93169
	E	0	8	5	23.9333	6.11912	1.11719

Min – minimum; Max – maximum; SD – standard deviation; SEM – standard error of the mean; SWLS – Satisfaction with Life Scale.
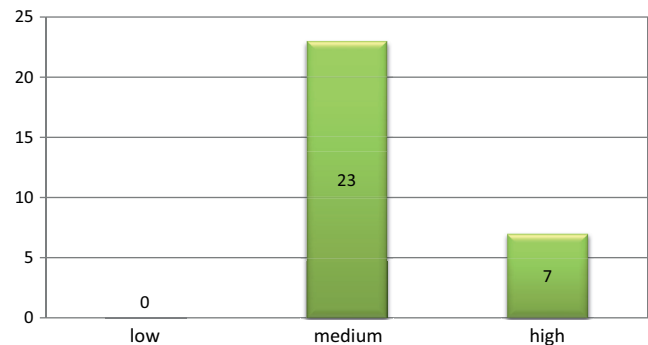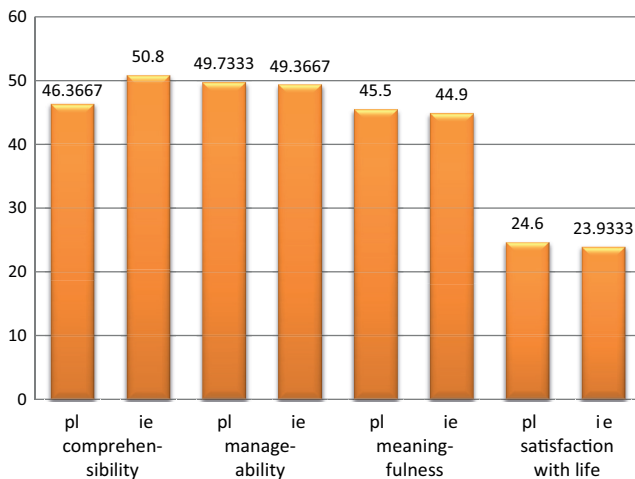
Fig. 6. Distribution of the results of the variables examined in Polish and Irish patients

Hypothesis 1

In order to verify the first hypothesis, correlations between the results of the SOC-29 and SWLS questionnaires were examined using Pearson's correlation coefficient. The results (presented in Table 7) show that the correlations between the subcategories of the SOC and SWL in the examined patients are as follows.

There was a statistically significant positive correlation between the overall result of the SOC and SWL ($p < 0.01$; $r = 0.36$). The results show that with an increase in one variable, the second variable increases too, and that with a decrease in one variable, the second variable also decreases.

In addition, the following statistically significant positive correlations were observed:

– between comprehensibility and manageability ($p < 0.01$; $r = 0.36$),

– between comprehensibility and meaningfulness ($p < 0.01$; $r = 0.37$),

– between comprehensibility and SWL ($p < 0.05$; $r = 0.26$).

In each case, the results again show that with an increase in one variable, the second variable increases too, and that with a decrease in one variable, the second variable also decreases.

There was a statistically significant positive correlation between manageability and meaningfulness ($p < 0.001$; $r = 0.61$). Once more the results show that with an increase in one variable, the second variable increases too, and that with a decrease in one variable, the second variable also decreases.

Thus, there is a connection between all the variables except manageability and SWL. It can be stated that for the first major hypothesis, the detailed hypotheses H0A and H0C can be rejected in favor of hypotheses H1A and H1C. However, there is no reason to reject hypothesis H0B.

Hypothesis 2

In order to test differences in the level of comprehensibility in the groups of patients hospitalized in Poland and Ireland, Student's t-test for independent samples was used ($t[58] = -1.797$, $p = 0.078$). The result of the analysis indicates that there are no differences between the 2 groups in terms of comprehensibility. This means there are no grounds for rejecting the zero hypothesis. The data obtained are presented in Table 8.

Student's t-test for independent samples was also used to test differences in the level of manageability in the groups of patients hospitalized in Poland and Ireland ($t[58] = 0.246$, $p = 0.807$). The result again indicates that there are no differences between the 2 groups in terms of manageability, and that there are no grounds

Table 7. Correlations between particular subscales of the sense of coherence (SOC) and the satisfaction with life (SWL)

| Variable	Parameter	Comprehensibility	Manageability	Meaningfulness	SOC	SWL
Comprehensibility	Pearson's correlation	1	0.360	0.374	0.836	0.257
	significance (bilateral)	–	0.005	0.003	0.000	0.048
	number of persons	60	60	60	60	60
Manageability	Pearson's correlation	0.360	1	0.605	0.752	0.234
	significance (bilateral)	0.005	–	0.000	0.000	0.071
	number of persons	60	60	60	60	60
Meaningfulness	Pearson's correlation	0.374	0.605	1	0.750	0.403
	significance (bilateral)	0.003	0.000	–	0.000	0.001
	number of persons	60	60	60	60	60
SOC	Pearson's correlation	0.836	0.752	0.750	1	0.357
	significance (bilateral)	0.000	0.000	0.000	–	0.005
	number of persons	60	60	60	60	60
SWL	Pearson's correlation	0.257	0.234	0.403	0.357	1
	significance (bilateral)	0.048	0.071	0.001	0.005	–
	number of persons	60	60	60	60	60

Table 8. Results of Student's t-test for independent samples for the variable comprehensibility

T	df	Significance
−1.797	58	0.78

T –Student's t-test; df – degrees of freedom.

Table 9. Results of Student's t-test for independent samples for the variable manageability

T	df	Significance
0.246	58	0.807

T –Student's t-test; df – degrees of freedom.

Table 10. Results of Student's t-test for independent samples for the variable meaningfulness

T	df	Significance
0.406	58	0.647

T –Student's t-test; df – degrees of freedom.

Table 11. Results of Student's t-test for independent samples for the variable satisfaction with life

T	df	Significance
0.458	58	0.648

T –Student's t-test; df – degrees of freedom.

for rejecting the zero hypothesis. The data obtained are presented in Table 9.

When Student's t-test for independent samples was used to test differences in the level of meaningfulness in the 2 groups of patients, the result (t[58] = 0.46, p = 0.647) once again indicated that there are no differences between the 2 groups in terms of meaningfulness. Again, this means there are no grounds for rejecting the zero hypothesis. The data obtained are presented in Table 10.

Therefore, the results of the analysis indicates, therefore, that there are no differences between the groups of Polish and Irish patients in terms of the SOC and its components.

Hypothesis 3

In order to test differences in the level of SWL in the compared groups of patients hospitalized in Poland and Ireland, Student's t-test for independent samples was used. The result of the analysis (t[58] = 0.458, p = 0.648) indicates that there are no differences between the 2 groups in terms of SWL. This means there are no grounds for rejecting the zero hypothesis H30. The data obtained is presented in Tables 11,12.

Conclusions

Analyzing the results of our research, we formulated the following conclusions:

1. The study group has a high average level of SWL.
2. Most of the respondents got an average score for the SOC.
3. There are relationships between particular subscales of the SOC, i.e., comprehensibility, manageability and meaningfulness, with the highest correlation between manageability and meaningfulness (r = 0.61).
4. Patients who are characterized by a strong SOC are probably also characterized by a high level of SWL.
5. Patients who are characterized by an average SOC are probably also characterized by an average level of SWL.
6. In the study group, increases in the SOC were accompanied by increases in the level of SWL, and decreases in the SOC mean the level of SWL decreases too.
7. Correlations were demonstrated among the components of the SOC (comprehensibility, manageability and meaningfulness).
8. There is no significant correlation between the manageability component of the SOC and SWL.
9. None of the patients had a low level of the SOC.
10. There were no significant differences between patients hospitalized in Polish and Irish hospitals in terms of the SOC and its components.

Table 12. Significance of the differences in the level of satisfaction with life (SWL) for independent groups: Polish participants compared to Irish ones

Method	Variables	Levene's test of the equation of variance		t-test of the equality of means						
		F	significance	t	df	significance (bilateral)	difference in means	standard error of the difference	95% CI for the difference in means	
									lower limit	upper limit
SWLS	equation of variance is assumed	1.019	0.317	0.458	58	0.648	0.66667	1.45471	−2.24524	3.57858
	equation of variance is not assumed	–	–	0.458	56.187	0.649	0.66667	1.45471	−2.24724	3.58058

CI – confidence interval; df – degrees of freedom; SWLS – Satisfaction with Life Scale.

11. There were no significant differences between patients hospitalized in Polish and Irish hospitals in terms of the level of SWL.

12. Therefore, the country of hospitalization does not significantly differentiate the remaining variables analyzed in the study.

References

1. Antonovsky A. *Rozwikłanie tajemnicy zdrowia. Jak radzić sobie ze stresem i nie zachorować*. Warszawa, Poland: Instytut Psychiatrii i Neurologii; 2005:7–8,11,34,43,106–107,175–178.
2. Juczyński Z. *NPPPZ – Narzędzia pomiaru w promocji i psychologii zdrowia*. 2nd ed. Warszawa, Poland: Pracownia Testów Psychologicznych Polskiego Towarzystwa Psychologicznego; 2009.
3. Trzebiatowski J. Jakość życia w perspektywie nauk społecznych i medycznych – systematyzacja ujęć definicyjnych. *Hygeia Public Health*. 2011;46(1):25–31.
4. Heszen I, Sęk H. *Psychologia zdrowia*. Warszawa, Poland: Wydawnictwo Naukowe PWN; 2008:56–57,78.
5. Antonovsky A. *Health, Stress and Coping*. San Francisco, USA: Jossey-Bass Inc.; 1979:49,72.
6. Sęk H. *Psychologia kliniczna*. Tom 1. Warszawa, Poland: Wydawnictwo Naukowe PWN; 2005.
7. Turosz AM. Zasoby osobiste i deficyty a jakość życia studentów Akademii Wychowania Fizycznego w Warszawie. *Probl Hig Epidemiol*. 2011:92(2):204–210.
8. Kane RA. Quality of life. In: Breslow L. ed. *Encyclopaedia of Public Health*. Vol. 3. 2nd ed. New York, USA: Macmillan Library Reference; 2002:1003–1006.
9. Zawiślak A. Koncepcja jakości życia osób z upośledzeniem umysłowym w niektórych współczesnych ujęciach teoretycznych. In: Palak Z, Lewicka A, Bujnowska A. *Jakość życia a niepełnosprawność*. Lublin, Poland: Wydawnictwo UMCS; 2006:149–158.
10. Schalock RL, Brown I, Brown R, et al. Conceptualization, measurement, and application of quality of life for persons with intellectual disabilities: Report of an international panel of experts. *Ment Retard*. 2002;40(6):457–470. doi:10.1352/0047-6765(2002)040<0457:CMAAOQ>2.0.CO;2
11. Raphael D, Brown I, Renwick R. Psychometric properties of the full and short versions of the Quality of Life Instrument Package: Results from the Ontario province-wide study. *Intl J Disabil Dev Educ*. 1999;46(2):157–168. doi:10.1080/103491299100605
12. Schalock RL. Three decades of quality of life. *Focus Autism Other Dev Disabl*. 2000;15(2):116–127. doi:10.1177/108835760001500207
13. Cummins RA. The subjective well-being of people caring for a severely disabled family member at home: A review. *J Intellect Dev Disabil*. 2001;26(1):83–100. doi:10.1080/13668250020032787
14. Diener E. Subjective well-being. *Psychol Bull*. 1984;95(3);542–575.
15. Shin C, Johnson DM. Avowed happiness as an overall assessment of the quality of life. *Soc Indic Res*. 1978;5:475–492. doi:10.1007/BF00352944

GP6 promotes the development of cerebral ischemic stroke induced by atherosclerosis via the FYN-PKA-pPTK2/FAK1 signaling pathway

Ye Gu[1,A–C,F], Yihua Wu[1,B,C,F], Liang Chen[2,A,D–F]

[1] Shanghai International Medical Center, China

[2] Xinhua Hospital affiliated to Shanghai Jiaotong University School of Medicine, China

A – research concept and design; B – collection and/or assembly of data; C – data analysis and interpretation;
D – writing the article; E – critical revision of the article; F – final approval of the article

Address for correspondence
Liang Chen
E-mail: l_chen15@21cn.com

Abstract

Background. Cerebrovascular disease is currently a serious threat to human health and life, commonly including cerebral infarction, cerebral hemorrhage and transient cerebral ischemia, among others.

Objectives. To explore the role and e molecular mechanism of *GP6* in the development of cerebral ischemic stroke (CIS) induced by atherosclerosis (AS).

Materials and methods. Forty-five male New Zealand white rabbits were randomly divided into 3 groups: the control, CIS model and anti-*GP6* group. Carotid artery tissues and blood of the white rabbits were collected for analysis. Hematoxylin and eosin (H&E) staining was used to analyze the pathological characteristics of vascular endothelial injury. Flow cytometry (FCM) was performed to analyze the content of *Th1* and *Th17* in blood. Immunohistochemistry was used to analyze the distribution and relative expression of *FCER1G*, *ITGA2* and *GP6* proteins in the carotid artery and cerebrovascular tissues. Western blot was applied to determine the protein expression of *GP6*, *FYN*, *PKA*, *pPTK2*, and *pFAK1* in carotid artery tissues of the rabbits.

Results. In the CIS model group, there was lymphocyte infiltration, fibrous tissue formation, and the formation of thrombus and lipid plaques. In the anti-*GP6* group, scattered thin plaques were observed, and no obvious foam cell deposition was observed. The *Th1* and *Th17* content was significantly decreased in the CIS model group compared to the control and anti-*GP6* group. The relative expression of *FCER1G*, *ITGA2* and *GP6* in the CIS model group was significantly higher compared to those in the control group and anti-*GP6* group. The protein expression of *GP6*, *FYN*, *PKA*, *pPTK2*, and *pFAK1* in the CIS model group were markedly higher compared to those in the control group and anti-*GP6* group.

Conclusions. *GP6* can promote the development of CIS by activating the *FYN-PKA-pPTK2*/FAK1 signaling pathway.

Key words: CIS, AS, *GP6*, thrombus, vascular endothelial cells

Background

Cerebrovascular disease is currently a serious threat to human health and life, the most common being cerebral infarction, cerebral hemorrhage and transient cerebral ischemia, among others.[1] It mainly occurs in middle-aged and elderly people, but the age of onset has shown a trend of decreasing, often occurring in people 30–50 years old.[2] The disease often leads to cognitive disorders or disorders affecting the physical activity of patients. Many patients are unable to take care of themselves after onset and quality of life is seriously reduced, resulting in them becoming a heavy burden to their families and society.[3] At present, there is no radically effective cure for the disease, and the prognosis is often closely related to the initial severity of the disease.[4] Even if patients survive, most of them are accompanied by lifelong sequelae, and cerebrovascular diseases can occur repeatedly, causing far more pain to the patients and their families than malignant tumors and cardiovascular diseases. Therefore, how to prevent and treat cerebrovascular disease more effectively is the most serious problem that neurology faces presently.[5] Cerebral ischemic stroke (CIS) is ischemic necrosis or softening of localized brain tissue due to cerebral blood circulation disorder, ischemia or hypoxia. It is the most common type of cerebrovascular disease, accounting for about 70% of all acute cerebrovascular diseases. About 30–40% of CIS is caused by carotid atherosclerotic stenosis.[6]

Extracellular matrix (ECM) contact exposed at the site of platelet and vascular injury is the first line of defense for repairing damaged tissue and stopping bleeding. Collagen, one of the macromolecular components of ECM, can not only adhere to platelets through direct and indirect channels but also cause platelet aggregation and expression of pro-coagulant activity. The interaction between platelets and collagen in arteries or damaged vessels with high shear stress is particularly important. Current research suggests that platelets have 2 types of collagen receptors on their surfaces, α2β1 and glycoprotein 6 (*GP6*). It is a glycoprotein receptor that acts on collagen and is located on the long arm of chromosome 19 (19q13.4). It contains 8 exons and has a molecular weight of 62 kDa. In humans, *GP6* is encoded by the *GP6* gene. *GP6* mediates the initial adhesion of platelets to collagen, generates signal transduction, improves the binding affinity of integrin receptors, and causes platelet aggregation, platelet release and thrombosis.[7] When serum *GP6* concentration is increased, it can promote the initial adhesion of collagen and platelets, improving the affinity of the integrin receptor, which induces platelet aggregation and thrombosis.[8] Kubisz et al. found that a variation of the *GP6* gene was related to platelet aggregation.[9] Sokol et al. found that a *GP6* gene polymorphism may be related to the heightened aggregation ability of platelets.[10] Despite the complex composition of the ECM, the adhesion of platelets and collagen plays an important role in initiating hemostasis and thrombus in the body. Inhibition of *GP6* function can significantly inhibit collagen-induced platelet adhesion, aggregation and platelet thrombosis under high shear stress in vitro.[11] Therefore, we believe that atherosclerotic CIS is closely related to the structural and functional integrity of *GP6*, but the mechanism of action of *GP6* in atherosclerosis (AS) has rarely been studied.

Objectives

In this paper, we wanted to investigate the mechanism of action of *GP6* in AS. Helper T (Th) cell content, *Th1* and *Th17*, was significantly decreased in the CIS model group compared to the control group, while having no marked differences compared to the anti-*GP6* group. Immunohistochemistry showed that the proteins *FCER1G*, *ITGA2* and *GP6* were all distributed in the cell membrane. *GP6* can promote the formation of cerebral ischemic stroke via upregulating the expression of *FCER1G*, *ITGA2*, *FYN*, *PKA*, *pPTK2*, and *pFAK1*. This may be a new target for treating cerebral ischemic stroke.

Materials and methods

Model establishment and grouping

Forty-five male New Zealand white rabbits (~16–18 weeks old, weight: ~1.5–2.0 kg) were obtained from the Naval Medical Institute Animal Center (Shanghai, China). They were randomly divided into 3 groups (n = 15 in each group): the control group, CIS group and anti-*GP6* group. In the CIS group and the anti-*GP6* group, rabbits were first fed with a specific high-fat diet for 8 weeks, and then 3% hydrogen peroxide solution was applied to perfuse the bilateral common carotid arteries of the rabbits, causing vascular endothelial oxidative stress injury. In the anti-*GP6* group, the rabbits were given anti-*GP6* antibody via the tail vein. Carotid artery tissues of the white rabbits were collected and rapidly stored in –80°C liquid nitrogen for further use.

In this study, atherosclerotic stenosis injury rabbit models were constructed and separated into 3 groups: the control group, CIS group and anti-*GP6* group. Hematoxylin and eosin (H&E) staining was used to analyze the pathological features of vascular endothelial injury. Flow cytometry (FCM) was used to determine the concentration of *Th1* and *Th17* cells in blood samples. The expressions of *GP6*, *FYN*, *PKA*, *pPTK2*, and FAK1 were also assessed.

The animal experiments were approved by the Ethics Committee of Xinhua Hospital affiliated with Shanghai Jiaotong University School of Medicine (Shanghai, China).

Hematoxylin and eosin staining

After the rabbits were sacrificed by the cervical dislocation method, hippocampal tissue was taken from their brains. The tissues were fixed with 4% formaldehyde for 24 h, embedded in paraffin and sectioned into 5 μm-thick sections. Histopathological changes were observed under a light microscope (Olympus Corp., Tokyo, Japan) after H&E staining.

Flow cytometry

Cells were digested with trypsin, washed twice with phosphate-buffered saline (PBS) and collected into a centrifuge tube. Binding buffer was added to prepare cell suspensions with a final concentration of 1×10^6/mL. Annexin V-FITC kit (BioVision, Milpitas, USA) instructions were used for labeling, which was performed according to the instructions of Annexin V-FITC kit. Annexin V was added for staining at room temperature in the dark for 15 min.

Western blot

Cells were lysed with cell lysis buffer on ice for 30 min and then centrifuged at 12,000 rpm for 25 min. Supernatant was collected and the Bradford method was used for protein quantification. Protein in the amount of 25 μg was loaded for sodium dodecyl sulphate–polyacrylamide gel electrophoresis (SDS-PAGE). The proteins were transferred to a polyvinylidene difluoride (PVDF) membrane and sealed with 5% skim milk at room temperature for 1 h; then, primary antibody was added and the membrane was incubated overnight at 4°C. The next day, the secondary antibody was added and incubated at room temperature for 1 h, and then, electrochemiluminescence (ECL) hypersensitive luminescence solution was added for developing.

Immunohistochemistry

Tissues were dewaxed and endogenous oxidase was inactivated with 3% hydrogen peroxide. After washing in PBS 3 times, the antigen was retrieved by microwave heating. The slices were placed in sodium citrate buffer with pH 6.0, heated to boiling in a microwave and then cooled. The slices were again microwaved in sodium citrate buffer with pH 6.0 and then washed with PBS. After cleaning, sections were removed and sealed for 10 min. Then, mouse anti-human *FCER1G*, *ITGA2* and *GP6* monoclonal antibodies (1:150) were added and incubated at 4°C for 12 h. After washing, biotin-labeled secondary antibodies were added and incubated at 4°C for 20 min each. After incubation and washing, the samples were washed again and immersed in DAB color developing solution for 5 min. Then, the samples were washed, re-dyed, dehydrated, sealed and observed under an optical microscope.

Statistical analyses

IBM SPSS v. 19.0 software (IBM Corp., Armonk, USA) was used for statistical analysis. The results were expressed as mean values ± standard deviation (SD). Differences between groups were compared using one-way analysis of variance (ANOVA) tests followed by Bonferroni post hoc test. The assumption for ANOVA was verified with the Brown–Forsythe test. A value of $p < 0.05$ was considered statistically significant.

Results

Anti-*GP6* inhibits vascular endothelial injury

After the successful establishment of the evaluation models, the rabbits were anesthetized with isopentane and sacrificed. Carotid artery tissue and cerebrovascular tissues were collected from the white rabbits, and H&E staining was used to analyze the pathological characteristics of the vascular endothelial injury. As shown in Fig. 1, in the control group, the smooth muscle cells were arranged neatly, tightly and orderly, the endothelial layer was continuous and there was no lipid deposition in the subcutaneous tissue. The structure of each layer was clear. In the CIS group, the endothelium was discontinuous, the intimal hyperplasia was serious, the tube wall was full of plaques, a large number of foam cells could be seen, the membranes in the middle and outside were irregularly thickened, and foam cell infiltration could be seen. In the anti-*GP6* group, endothelial cells were continuous, lipid deposition was observed under the intima, scattered thin plaques were observed, and no obvious foam cell deposition was observed. The thickness of the membrane was the same as that of the control group membrane, which was thinner than the CIS model group membrane.

Content of *Th1* and *Th17*

The content of *Th1* and *Th17* in blood was analyzed with FCM and the results are shown in Fig. 2. The *Th1* ($p < 0.01$, degrees of freedom (df) = 2, F = 337.7) and *Th17* ($p < 0.01$, df = 2, F = 150.6) content was significantly decreased in the CIS model group compared to the control group, while there was no marked difference compared to the anti-*GP6* group.

Results of immunohistochemistry

Immunohistochemistry was used to analyze the distribution and relative expression of *FCER1G*, *ITGA2* and *GP6* proteins in the carotid artery and cerebrovascular tissues of white rabbits. The proteins *FCER1G*, *ITGA2* and *GP6* were all distributed in the cell membrane
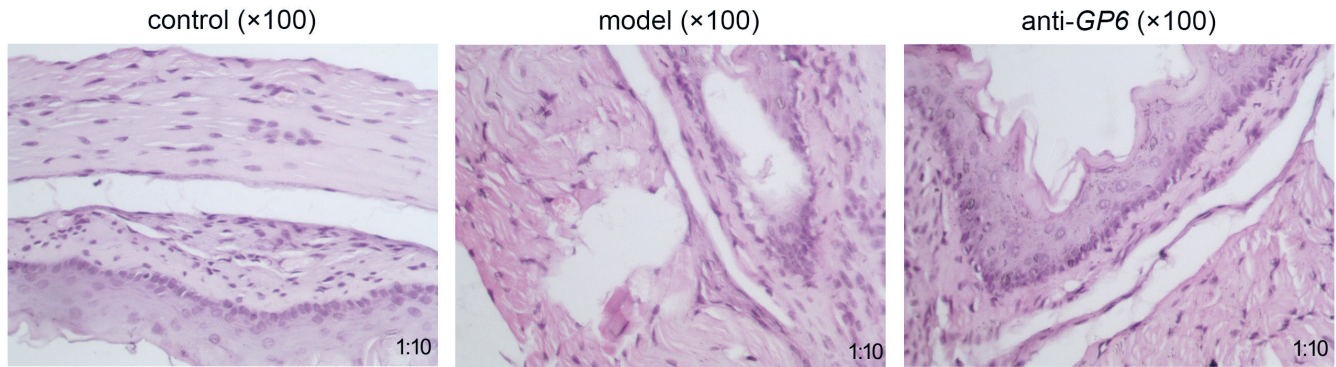
Fig. 1. The pathological features of vascular endothelial injury in the control, cerebral ischemic stroke (CIS) model and anti-*GP6* groups analyzed using H&E staining. In the control group, the smooth muscle cells were arranged neatly, tightly and orderly, the endothelial layer was continuous and there was no lipid deposition in the subcutaneous tissue; in the CIS model group, the endothelium was discontinuous, the intimal hyperplasia was serious, the tube wall was full of plaques, and a large number of foam cells could be seen; and in the anti-*GP6* group, scattered thin plaques were observed and no obvious foam cell deposition was observed
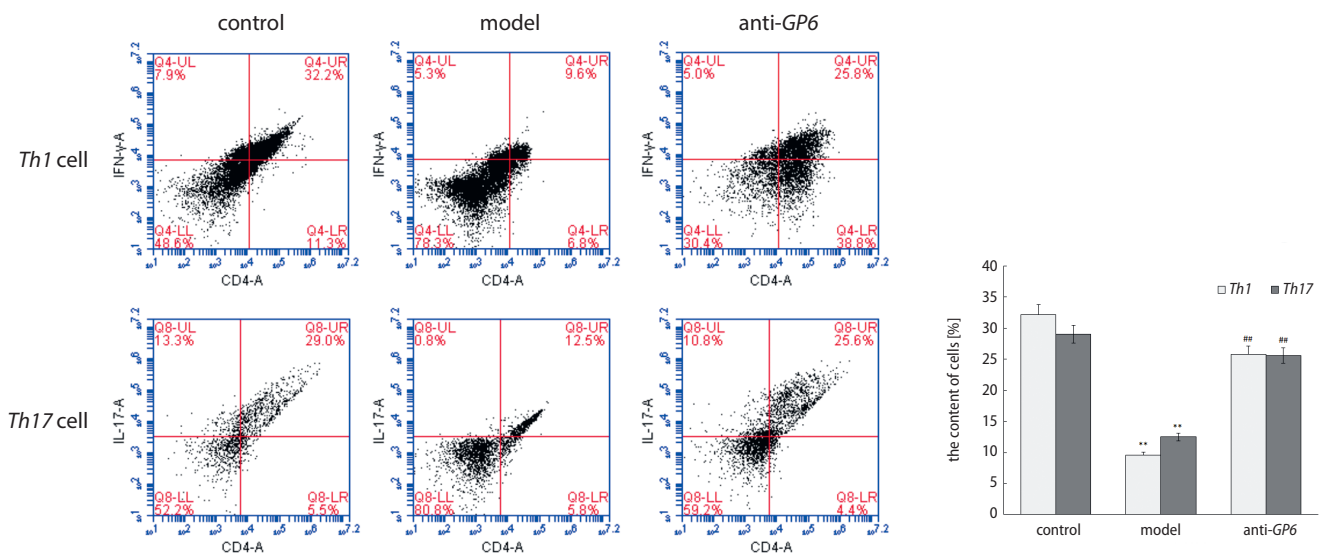
Fig. 2. The content of *Th1* and *Th17* in blood samples of rabbits from the control, cerebral ischemic stroke (CIS) model and anti-*GP6* groups determined with flow cytometry (FCM). The *Th1* and *Th17* content was significantly decreased in the CIS model compared to the control group and anti-*GP6* group

*p < 0.05 or ##p < 0.01, indicating the significant difference using one-way analysis of variance (ANOVA) followed by Bonferroni post hoc test.

(Fig. 3). The relative expression of *FCER1G*, *ITGA2* and *GP6* in the CIS model group was significantly higher compared to the control group and anti-*GP6* group. The relative expression of *FCER1G*, *ITGA2* and *GP6* did not significantly differ between the control group and anti-*GP6* group.

Expression of *GP6*, *FYN*, *PKA*, *pPTK2*, and *pFAK1*

Western blot was applied to determine the protein expression of *GP6*, *FYN*, *PKA*, *pPTK2*, and *pFAK1* in carotid artery tissues of rabbits from the control, CIS model and anti-*GP6* group. The protein expression of *GP6* (p < 0.001, df = 2, F = 392.9), *FYN* (p < 0.001, df = 2, F = 380.3), *PKA* (p < 0.001, df = 2, F = 304.3), *pPTK2* (p < 0.001, df = 2, F = 369.9), and *pFAK1* (p < 0.001, df = 2, F = 562.8) in the CIS model group were markedly higher compared

to those in the control group and anti-*GP6* group (Fig. 4). Moreover, the expression of *GP6*, *FYN*, *PKA*, *pPTK2*, and *pFAK1* were significantly upregulated in the anti-*GP6* group compared with the control group.

Discussion

With a remarkable rise in people's living standards and an accelerated pace of life, the onset of CIS is observed earlier than before and the incidence rate increases year after year. In particular, progressive CIS has a poor prognosis and high morbidity and mortality, which poses a serious threat to people's health and life safety, and burdens patients and families.[12,13] Carotid AS is an important risk factor for CIS and is closely related to the occurrence, development and recurrence of cerebral infarction.[14] To date, surgery
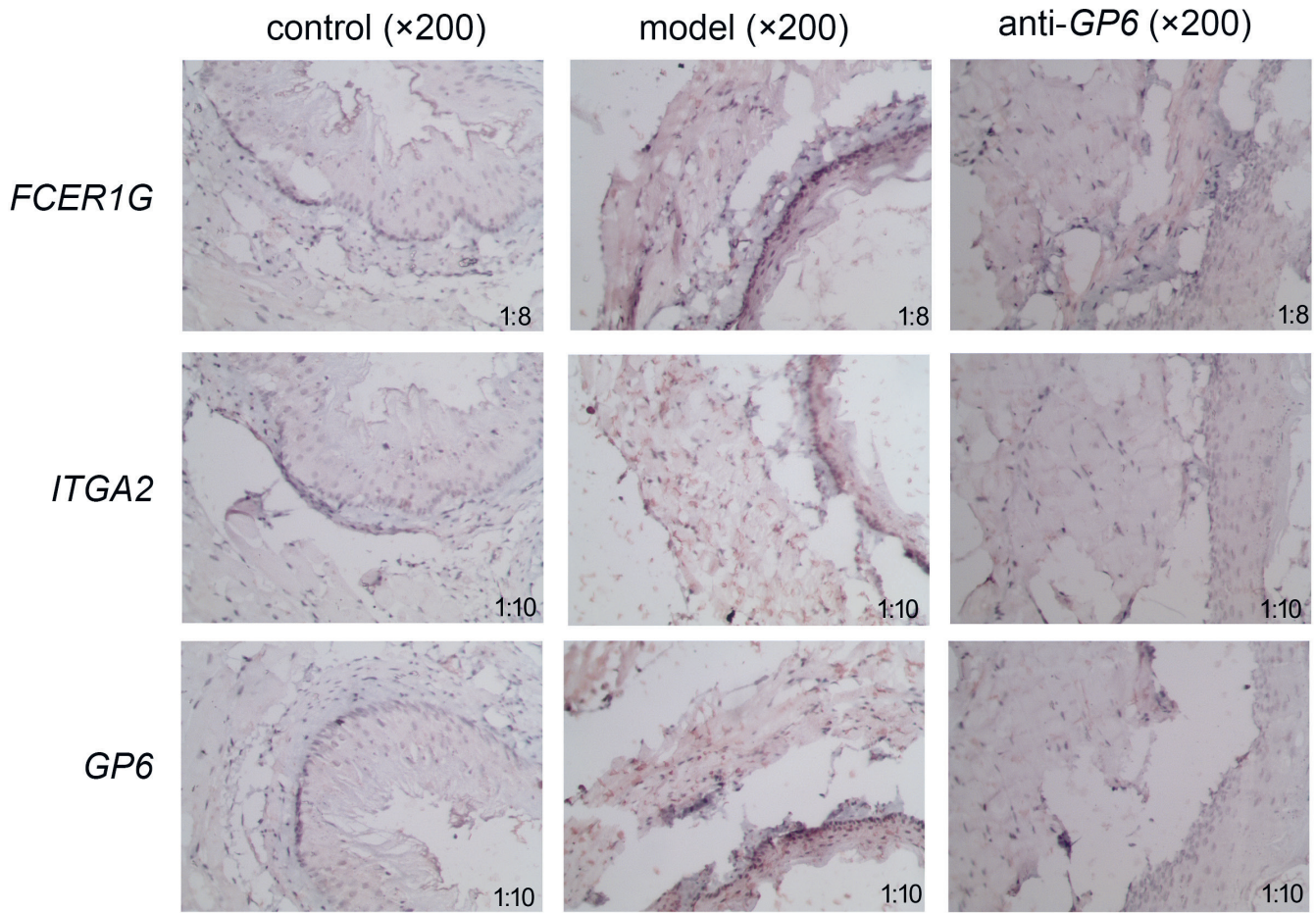
Fig. 3. Immunofluorescent staining of *FCER1G*, *ITGA2* and *GP6* proteins in the carotid artery and cerebrovascular tissues of white rabbits in the control, cerebral ischemic stroke (CIS) model and anti-*GP6* groups. The proteins *FCER1G*, *ITGA2* and *GP6* were all distributed in the cell membrane. The relative expression of *FCER1G*, *ITGA2* and *GP6* in the CIS model group was significantly higher compared to the control group and anti-*GP6* group
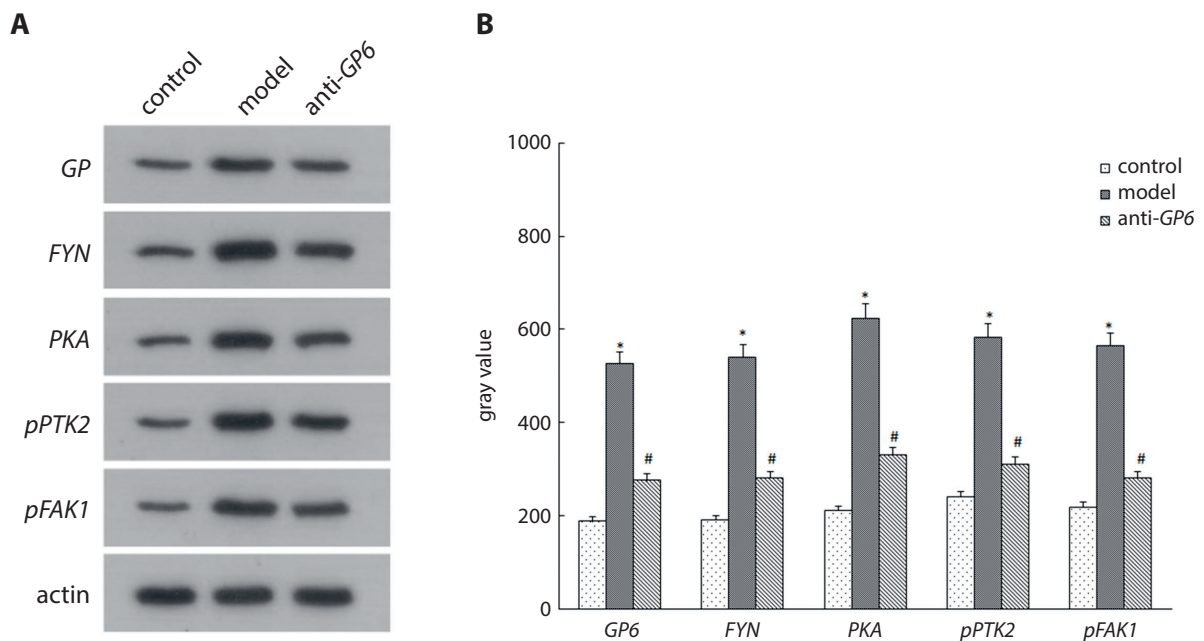
Fig. 4. The protein expression of *GP6*, *FYN*, *PKA*, *pPTK2*, and *pFAK1* in carotid artery tissues of rabbits in the control, cerebral ischemic stroke (CIS) model and anti-*GP6* groups measured with western blot assay. The protein expression of *GP6*, *FYN*, *PKA*, *pPTK2*, and *pFAK1* in the CIS model group was markedly higher compared to the control group and anti-*GP6* group

*p < 0.001 or #p < 0.01, indicating the significant difference using one-way analysis of variance (ANOVA) followed by Bonferroni post hoc test.

or endovascular treatment for patients with recent ischemic diseases has been dependent on the degree of narrowing of the responsible vessel. For many years, the extent of artery stenosis has been regarded as the most reliable index to predict the risk of stroke in patients with AS. Thromboembolism derived from atherosclerotic plaque is considered to be the main pathogenesis of CIS in most atherosclerotic patients. Plaque rupture can lead to platelet aggregation, local thrombosis or thromboembolism. Plaque itself can also cause thromboembolism.[15] Protein function analysis revealed that *GP6* is a platelet glycoprotein, which plays an important role in platelet coagulation, thrombosis and arterial embolization.[16] The *GP6* signaling pathway mainly activates *FYN* and *PKA*, phosphorylates PTK2/FAK1 and promotes platelet adhesion to damaged vascular endothelium.

Vascular endothelial cells have anticoagulant and fibrinolytic properties and can influence the chemotaxis and adhesion properties of cell membranes.[17] Under normal circumstances, vascular endothelial cells cover the inner surface of the entire vascular system, providing an anticoagulant interface that prevents platelets and other blood cells from adhering to the subcutaneous tissue and preventing activation of the clotting response. Endocrine dysfunction caused by endothelial cell injury plays a key role in the pathophysiological mechanism of the early formation and development of AS.[18] In this study, male New Zealand white rabbits were randomly divided into 3 groups: control, CIS model and anti-*GP6* group. Results of H&E staining analysis of the vascular endothelial injury showed that in the CIS model group, the endothelium was discontinuous, the intimal hyperplasia was serious, the tube wall was full of plaques, a large number of foam cells could be seen, the membranes in the middle and outside were irregularly thickened, and foam cell infiltration could be seen. However, the injury degree was reduced in the anti-*GP6* group compared to the CIS model group. Results of FCM showed that *Th1* and *Th17* content was significantly decreased in the CIS model group compared to the control group, while it did not markedly differ from the anti-*GP6* group. Atherosclerosis occurs for various reasons, including the involvement of macrophages, T lymphocytes, endothelial cells, smooth muscle cells, mast cells, and other cells. After entering the vascular wall, T lymphocytes are activated under antigen stimulation to produce inflammatory cytokines, which can aggravate the progression of AS by amplifying the inflammatory response. Different T cell subsets in the vascular wall are not only involved in the early plaque formation of AS but also promote the progression of AS, which is closely related to the pathological process of AS.[19] The CD4+T cells play a crucial role in the development of AS. According to biological characteristics and different cytokines produced, CD4+T cells are mainly divided into *Th1*, *Th2* and *Th17*. The *Th1* cells are differentiated from initial T cells in response to interleukin (IL)-12 and produce interferon gamma (IFN-γ), which acts as a defense against microorganisms in the cell.

The role of *Th17* cells in disease is mainly to promote defense against organ-specific autoimmune diseases and chronic infections. Results of animal experiments carried out by Davenport et al. showed that *Th1* and *Th2* immune responses were involved in the formation of atherosclerotic lesions.[20] Kim et al. assessed 124 patients with chest pain who underwent coronary angiography and found the expression of *Th1* and *Th17* cells in patients with stable angina pectoris was significantly increased, which indicated that *Th1* and *Th17* cells are associated with the development of AS.[21] Interleukin 17 (IL-17) is a major effector of *Th17* cells and an early promoter of T-cell-induced inflammatory response, which can amplify the inflammatory response. Immunohistochemistry results in our study showed the proteins *FCER1G*, *ITGA2* and *GP6* were all distributed in the cell membrane. The relative expression of *FCER1G*, *ITGA2* and *GP6* in the CIS model group was significantly higher compared to the control group and anti-*GP6* group. The *FCER1G* gene is located on chromosome 1q23 (1:161185024-161190489) 24 and encodes an 86-amino acid protein.[22] *ITGA2* is a protein-coding gene. Diseases associated with *ITGA2* include anus disease and thrombocytopenia.[23] Results from western blotting indicated that the protein expression of *GP6*, *FYN*, *PKA*, *pPTK2*, and *pFAK1* in the CIS model group was markedly higher compared to the control group and anti-*GP6* group. Protein kinases are enzymes that catalyze protein phosphorylation, which include an important protein kinase, protein kinase A (*PKA*).

Limitations

At present, a large number of studies have been carried out on the *GP6* gene in China and abroad. The consistent view is that *GP6* gene polymorphisms are related to platelet aggregation ability, but whether they lead to an increase or decrease in platelet aggregation, is still in question. If a polymorphism leads to an increase in platelet aggregation, then it is likely to be associated with thrombotic diseases. However, some scholars found that the ti3254c gene polymorphism of *GP6* is not significantly associated with the occurrence of coronary heart disease. Scholars generally agree that the expression of *GP6* is enhanced in patients with acute ischemic diseases such as stroke and myocardial infarction. However, regarding whether *GP6* gene polymorphisms are related to AS-based diseases (such as coronary heart disease and cerebral infarction), current research results are mostly negative and more in-depth studies are needed for verification. The safety of long-term drug use and the role of drug immunity and cardiovascular events need to be further explored. Chronic inflammation, which is repeated over a long time, can also lead to an inability to cure the disease. The presence of other pathways in the mechanism of *GP6* in the treatment of AS requires further study.

Conclusions

GP6 can promote the formation of cerebral ischemic stroke by upregulating the expression of *FCER1G*, *ITGA2*, *FYN*, *PKA*, *pPTK2*, and *pFAK1*. It may be a new treatment target for cerebral ischemic stroke.

ORCID iDs

Ye Gu https://orcid.org/0000-0002-9936-8125
Yihua Wu https://orcid.org/0000-0001-7119-1770
Liang Chen https://orcid.org/0000-0003-1978-3212

References

1. Caprio FZ, Sorond FA. Cerebrovascular disease. *Med Clin North Am*. 2019;103(2):295–308. doi:10.1016/j.mcna.2018.10.001
2. Xiang YH. Influencing factors of secondary early epileptic seizures in patients with acute cerebrovascular disease. *Pract J Cardiac Cerebral Pneumal Vasc Dis*. 2017;25(07):150–152.
3. Jibo LI, Jing LI, Liu WP. Analysis of clinical effect of nalmefene combined with Xingnaojing injection in the treatment of cerebrovascular disease with disturbance of consciousness. *Xinjiang Medical Journal*. 2018;48(12):1344–1345.
4. Celikbilek A, Ismailogullari S, Zararsiz G. Neutrophil to lymphocyte ratio predicts poor prognosis in ischemic cerebrovascular disease. *J Clin Lab Anal*. 2014;28(1):27–31. doi:10.1002/jcla.21639
5. Mutuberría LR, Capote RD. Benefits of therapeutic physical exercise in patients with sequelae of cerebrovascular disease. *Pflege*. 2012;21(3):172. doi:10.1024/1012-5302.21.3.172
6. Sibani S, Dipankar C, Arijit B, Mrinal Kanti G. Cerebral ischemic stroke: Cellular fate and therapeutic opportunities. *Front Biosci (Landmark Ed)*. 2019;24:435–450. PMID:30468665
7. Naitoh K, Hosaka Y, Shirakawa K, Furusako S. Establishment of immunoassay for platelet-derived soluble glycoprotein VI, a novel platelet marer. *J Immunol Methods*. 2015;418:52–60. doi:10.1016/j.jim.2015.01.010
8. Best D, Senis YA, Jarvis GE, Eagleton HJ, Watson SP. GPVI levels in platelets: Relationship to platelet function at high shear. *Blood*. 2003;102(8):2811–2818. doi:10.1182/blood-2003-01-0231
9. Kubisz P, Ivankova J, Skerenova M, Stasko J, Holly P. The prevalence of the platelet glycoprotein VI polymorphisms in patients with sticky platelet syndrome and ischemic stroke. *Hematology*. 2013;17(6):355–362. doi:10.1179/1024533212Z.000000000142
10. Sokol J, Biringer K, Skerenova M, et al. Platelet aggregation abnormalities in patients with fetal losses: The *GP6* gene polymorphism. *Fertil Steril*. 2012;98(5):1170–1174. doi:10.1016/j.fertnstert.2012.07.1108
11. Lecut C, Feeney LA, Kingsbury G, et al. Human platelet glycoprotein VI function is antagonized by monoclonal antibody-derived Fab fragments. *J Thromb Haemost*. 2010;1(12):2653–2662. doi:10.1111/j.1538-7836.2003.00495.x
12. Chen J, Cui C, Yang X, et al. MiR-126 affects brain–heart interaction after cerebral ischemic stroke. *Transl Stroke Res*. 2017;8(4):374–385. doi:10.1007/s12975-017-0520-z
13. Gao XL, Chen LY, Sun LQ, Xiao-Rong LI, Zheng GQ. Clinical efficacy and safety of edaravone combined with butylphthalide in treatment of acute cerebral ischemic stroke. *Chinese J Clin Pharmacol*. 2015;31(16):1569–1571.
14. Yang QH, Shen W, Jia XD, Ru JP, Du WZ. Correlation of ultrasound detection of carotid atherosclerosis plaque with ischemic cerebral stroke. *J Hainan Medical University*. 2016;22(015):153–155.
15. Fuster V, Badimon JJ, Chesebro JH, Fallon JT. Plaque rupture, thrombosis, and therapeutic implications. *Haemostasis*. 2010;26(Suppl 4):269–284. doi:10.1159/000217308
16. Kotulicová D, Chudy P, Skereňová M, Ivanková J, Dobrotová M, Kubisz P. Variability of *GP6* gene in patients with sticky platelet syndrome and deep venous thrombosis and/or pulmonary embolism. *Blood Coagul Fibrinolysis*. 2012;23(6):543–547. doi:10.1097/MBC.0b013e328355a808
17. Wang SW, Deng LX, Chen HY, Su ZQ, Ye SL, Xu WY. MiR-124 affects the apoptosis of brain vascular endothelial cells and ROS production through regulating PI3K/AKT signaling pathway. *Eur Rev Med Pharmacol Sci*. 2018;22(2):498–505. doi:10.26355/eurrev_201801_14201
18. Clemmons DR. Modifying IGF1 activity: an approach to treat endocrine disorders, atherosclerosis and cancer. *Nat Rev Drug Discov*. 2007;6(10):821–833. doi:10.1038/nrd2359
19. Tse K, Tse H, Sidney J, Sette A, Ley K. T cells in atherosclerosis. *Int Immunol*. 2013(11):615–622. doi:10.1093/intimm/dxt043
20. Davenport P, Tipping PG. The role of interleukin-4 and interleukin-12 in the progression of atherosclerosis in apolipoprotein E-deficient mice. *Am J Pathol*. 2003;163(3):1117–1125. doi:10.1016/S0002-9440(10)63471-2
21. Kim JD, Lee SH, Seo EH, et al. Role of *Th1* and *Th17* cells in the development and complexity of coronary artery disease: comparison analysis by the methods of flow cytometry and SYNTAX score. *Coron Artery Dis*. 2015;26(7):604–611. doi:10.1097/MCA.0000000000000289
22. Amo G, García-Menaya J, Campo P, et al. A nonsynonymous FCER1B SNP is associated with risk of developing allergic rhinitis and with IgE levels. *Sci Rep*. 2015;6(1):19724. doi:10.1038/srep19724
23. Felipe RLV, Tashi T, Koul P, Camp NJ, Prchal JT. Inherited giant platelet disorder, Kashmiri thrombocytopenia, a common syndrome found in Srinagar, India. *Blood*. 2014;124(21):4211. doi:10.1182/blood.V124.21.4211.4211

LncRNA *PCGEM1* mediates oxaliplatin resistance in hepatocellular carcinoma via *miR-129-5p/ETV1* axis in vitro

Jie Chen[1,2,A,D,F], Daiyue Yuan[2,A–C], Qingya Hao[2,C,D], Dongmei Zhu[2,C], Zhong Chen[1,3,E]

[1] Department Of General Surgery, The First Affiliated Hospital of Soochow University, Suzhou, China

[2] Department Of General Surgery, The Second Affiliated Hospital of Nantong University, China

[3] Department of General Surgery, Affiliated Hospital of Nantong University, China

A – research concept and design; B – collection and/or assembly of data; C – data analysis and interpretation;
D – writing the article; E – critical revision of the article; F – final approval of the article

Address for correspondence
Zhong Chen
E-mail: chenz9806@163.com

Abstract

Background. Hepatocellular carcinoma (HCC) is one of the most severe malignant cancers that leads to high death rate worldwide. Recent research revealed that long non-coding RNAs (lncRNAs) exert a critical role regarding chemoresistance in numerous cancers, including HCC.

Objectives. Our research aimed to explore the function and molecular mechanism of lncRNA *PCGEM1* on oxaliplatin resistance of HCC in vitro.

Materials and methods. Expression of the lncRNA *PCGEM1*, together with *miR-129-5p*, and the mRNA level of *ETV1* and drug resistance-related genes including *LRPA*, *MDR1* and *MDR3* were determined using quantitative real-time polymerase chain reaction (qRT-PCR) in an oxaliplatin-resistant HCC cell line (Hep3B/OXA). Cell Counting Kit-8 (CCK-8) was employed to assess the viability and cell survival rate, and transwell assays were performed to measure the number of migrated or invaded cells. In addition, the relation among lncRNA *PCGEM1*, *miR-129-5p* and *ETV1* were determined using luciferase assay.

Results. Our data indicated that *PCGEM1* and *ETV1* expression were enhanced in Hep3B/OXA cells. Furthermore, knockdown of lncRNA *PCGEM1* significantly decreased the migration, invasion and mRNA expressions of *LRPA*, *MDR1* and *MDR3*, and the cell viability in Hep3B/OXA cells. The starBase online tool and luciferase assays verified that *miR-129-5p* targeted *PCGEM1* and ETV1, signifying that *PCGEM1* could enhance *ETV1* expression via suppressing *miR-129-5p*.

Conclusions. Our findings demonstrated that *PCGEM1* modulated oxaliplatin resistance by targeting the *miR-129-5p/ETV1* pathway in HCC in vitro, suggesting a potential strategy for the treatment of chemoresistant HCC.

Key words: hepatocellular carcinoma, *miR-129-5p*, oxaliplatin resistance, *PCGEM1*, *ETV1*

832

J. Chen et al. LncRNA-PCGEM1 mediates carcinoma in vitro

Background

Hepatocellular carcinoma (HCC) is a severe type of malignant tumor, leading to a large number of cancer-related deaths worldwide.[1,2] It is an invasive and fast-growing tumor that leads to higher recurrence and metastasis.[3] Despite advancements in the therapeutic techniques for HCC such as radiotherapy, chemotherapy and surgery, the prognosis is still unsatisfactory, with an overall five-year survival rate of 15–40%.[4,5] The underlying mechanism behind the pathogenesis of HCC is complicated and needs to be investigated for promising prognosis and early-stage detection.[6] Therefore, novel targets and diagnostic indicators of HCC treatment are urgently needed.

Along with the progression of microarray analysis and sequencing, numerous novel non-coding RNAs have been discovered. Non-coding RNAs are sequences of nucleotides transcribed from chromatin and lack protein-coding capacity.[7] Long non-coding RNAs (lncRNAs) are a group of non-coding RNAs having a length of >200 nucleotides.[8] Previous research showed that lncRNAs exert critical functions in the pathogenesis of HCC.[9] For example, lncRNA UBE2CP3 was overexpressed in HCC and enhanced tumor metastasis through the modulation of EMT and induced migration and invasion.[10] Furthermore, other research revealed that overexpression of lncRNA UCA1 suppressed miR-216b expression and stimulated FGFR1/ERK pathways to enhance the pathogenesis of HCC.[11] Moreover, lncRNA AK021443 mediated the migration and proliferation of HCC cells via EMT regulation in vitro.[12] The lncRNA *PCGEM1* was identified to be highly expressed in prostate cancer, and acts to enhance its proliferation.[13,14] Also, *PCGEM1* was highly expressed in ovarian cancer tissues and enhanced the invasion, migration and proliferation, while decreasing the apoptosis rate.[15] Furthermore, *PCGEM1* induced metastasis and EMT via enhancing the SNAI1 expression in gastric cancer cells.[16] However, whether lncRNA *PCGEM1* exerts its function in the development and tumorigenesis of HCC remains unknown.

It has been previously reported that oxaliplatin-mediated chemotherapy prolonged survival and reduced mortality during treatment of HCC patients in an advanced stage of the disease.[17] Conversely, the resistance mechanism of oxaliplatin still needs to be elucidated. Numerous research has revealed that lncRNAs play a vital role in chemotherapy resistance in HCC. Several lncRNAs were highly expressed in chemoresistant HCC tissues and cells, and were shown to exert their function during oxaliplatin resistance and HCC pathogenesis.[18] For example, lncRNA ARSR increased doxorubicin resistance in HCC by regulating PTEN.[2] Conversely, lncRNA HULC increased chemosensitivity by inhibiting autophagy in HCC cells.[19]

Objectives

This study aimed to investigate the impact of lncRNA *PCGEM1* on oxaliplatin resistance in vitro in an HCC cell line. Our findings elucidated that lncRNA *PCGEM1* mediates oxaliplatin resistance in HCC via the *miR-129-5p/ETV1* axis, indicating that *PCGEM1* might be a therapeutic target for HCC treatment.

Materials and methods

Cell culture

The human liver cancer Hep3B cell line was acquired from American Type Cell Culture (ATCC, Manassas, USA) and cultured in Dulbecco's modified Eagle's medium (DMEM; Biocompare, San Francisco, USA) containing 100 units/mL penicillin, 100 µg/mL streptomycin (Thermo Fisher Scientific, Waltham, USA) and 10% fetal bovine serum (FBS; Biocompare) at 37°C in 5% CO_2.

Establishment of oxaliplatin-resistant Hep3B cells

Hep3B cells were exposed to increasing concentrations of oxaliplatin (2–25 µM) to establish the oxaliplatin-resistant Hep3B cells.[20] The IC_{50} of Hep3B cells was calculated after detection with Cell Counting Kit-8 (CCK-8) (Beyotime, Shanghai, China), and after that, the oxaliplatin (25 µM) group was selected as Hep3B/OXA. Hep3B and Hep3B/OXA cells were cultured in minimum essential medium (MEM) containing 10% FBS. A T25 culture flask was used to seed cells (2×10^6 cells/well) for 72 h per passage.

Cell transfection

Briefly, scrambled siRNA (si-control) and *PCGEM1* siRNAs (si-*PCGEM1*#1), (si-*PCGEM1*#2) and (si-*PCGEM1*#3), and pcDNA3.1 control (pcDNA/control) were all obtained from Invitrogen (Carlsbad, USA). The *miR-129-5p* mimics, mimic negative control (NC), *miR-129-5p* inhibitor, and inhibitor NC was bought from GeneCopoeia (Rockville, USA). *ETV1* mRNA 3'UTR and NC were obtained from Origene (Rockville, USA). Hep3B cells were cultured with 60–70% confluence at 37°C in 5% CO_2, and Lipofectamine 2000 (Invitrogen) was used to transfect these plasmids into the cells following the manufacturer's instructions (http://go.microsoft.com/fwlink/p/?LinkId=255141).

Mycoplasma detection

Hep3B cells and Hep3B/OXA cells were kept in an RPMI-1640 medium containing 10% FBS and antibiotic-antimycotic solution (Spectrum Chemical Manufacturing Corp.,

New Brunswick, USA) and cultured for 3 years with occasional freezing as previously described.[21] Blood agar plates and Mycoplasma IST2 kit (Biomereux Italia Spa, Florence, Italy) were used to perform titer of mycoplasmas as described previously.[21] Twelve well plates were used to add mycoplasmas (1×10^5 CFU/mL) into the mycoplasma-free Hep3B cells (2×10^3 cells/well). Infected cells were analyzed using MycoGuard™ Mycoplasma PCR detection kit (GeneCopoeia) for the detection of mycoplasmas using the polymerase chain reaction (PCR) method, as described previously.[21] Agarose gel electrophoresis was used to visualize amplified PCR products.

CCK-8 assay

Chemosensitivity and the rate of cell survival were examined using a CCK-8 assay. More specifically, 24-well plates were used to seed the cells at a density of 2×10^3 cells/well at 37°C. The CCK-8 solution (10 μL; Abcam, Cambridge, USA) was introduced into wells, and these plates were incubated for 1 h at 37°C. Proliferation was determined at 460 nm. The cell growth inhibition curve was detected by calculating the value of IC_{50} as (1-OD/$OD_{0\,\mu M}$) × 100%, as described previously.[22]

Transwell invasion and migration assay

Transwell chambers (Becton Dickinson, Franklin Lakes, USA) were used to perform invasion and migration assay on Hep3B/OXA cells. For performing the invasion assay, Hep3B/OXA cells were passaged in a serum-free media (200 μL) and kept in the higher compartment, followed by 600 μL of a medium comprising 10% FBS into the lower compartment. The cells were fixed with polyoxymethylene after incubation for 48 h. For the migration assay, 24-well plates were used to seed Hep3B/OXA cells, and 1×10^6 cells were re-suspended in a serum-free media (200 μL) and kept in the higher compartment. Media (600 μL) with 10% FBS were introduced into the lower compartment, and cells were incubated with 5% CO_2 for 48 h at 37°C. Finally, the invasion and migration of cells was visualized after staining with 20% Giemsa solution (Sigma–Aldrich, St. Louis, USA) and counted from 5 random chambers using an inverted microscope (Nikon Corp., Tokyo, Japan). All the experimentations were repeated in triplicate.

Luciferase assay

Online bioinformatics tools including miRcode (http://mircode.org/), starBase v. 2.0 (http://starbase.sysu.edu.cn/starbase2/index.php) and microRNA.org (https://bigd.big.ac.cn/databasecommons/database/id/1426) were used to predict the binding sites of *miR-129-5p* on *PCGEM1* as well as the *ETV1* binding sites on the *miR-129-5p* gene. Luciferase assay (BioAssay Systems, Hayward, USA) was

then performed to assess the luciferase activity according to the manufacturer's protocol (https://www.bioassaysys.com/Luciferase-Reporter-Assay-Kit-(1000-tests).html). A Mammalian Genomic DNA Miniprep Kit (Qiagen, Hilden, Germany) was used to generate the pGL3 plasmid (VWR, Radnor, USA), and once bound to their binding sites on the *miR-129-5p*, the RNA sequence of *PCGEM1* and 3'-UTR of *ETV1* were spliced into pGL3 to produce pGL3-*PCGEM1* (or *ETV1* mRNA) mutant or wild-type reporter vector. The 24-well plates were used to seed cells, and pGL3 mutant or wild type vector (100 ng) and *miR-129-5p* mimic or mimic NC, *miR-129-5p* inhibitor or inhibitor negative control (50 nmol/L) were transfected using Lipofectamine 2000 (Thermo Fisher Scientific) into the cells. Renilla luciferase gene was taken as a standard. All the experiments were performed in triplicate.

qRT-PCR

Total RNA was extracted using Ribozol RNA extraction reagent (VWR) following the manufacturer's protocol (https://us.vwr.com/store/product/7437721/vwr-life-science-ribozoltm-rna-extraction-reagent). A NanoDrop ND-1000 spectrophotometer (Thermo Fisher Scientific) was used to examine the purity and RNA concentration at 260/280 nm. Reverse transcription of total RNA (2 μg) into cDNA was performed using the SuperScript First-Stand Synthesis System. ABI PRISM 7500 and SYBR Premix ExTaq II kit (Thermo Fisher Scientific) was used to perform quantitative real-time PCR (qRT-PCR). Primers sequences are given below in Table 1. All the experiments were performed 3 times. *GAPDH* acted as the internal control, and the expressions of genes were measured using the $2^{-\Delta\Delta Ct}$ method.[23]

Table 1. The primer sequences for quantitative real-time polymerase chain reaction (qRT-PCR) analysis

Primers		Sequence
PCGEM1	forward	CTGTGTCTGCAACTTCCTCTAA
	reverse	TCCCAGTGCATCTCGTAGTA
miR-129-5p	forward	ACCCAGTGCGATTTGTCA
	reverse	ACTGTACTGGAAGATGGACC
ETV1	forward	TAGCCGTTCACTCCGCTATT
	reverse	CCTCGTTGATGTGACGTTCC
LRP1	forward	AATGGGCTAAGCCTGGACAT
	reverse	TGCCACTCCGATACTCAGTC
MDR1	forward	TCATTCGAGTAGCGGCTCTT
	reverse	TTCTTTGCTCCTCCATTGCG
MDR3	forward	TGCAGCCCACTTATTCATGC
	reverse	TTCTTCACCTCCAGGCTCAG
GAPDH	forward	GGTGTGAACCATGAGAAGTATGA
	reverse	GAGTCCTTCCACGATACCAAAG

834

J. Chen et al. LncRNA-PCGEM1 mediates carcinoma in vitro

Statistical analyses

Data are presented as the mean ± standard deviation (SD). IBM SPSS v. 19 (IBM Corp., Armonk, USA) and GraphPad Prism v. 8.0 (GraphPad Software, San Diego, USA) were used for statistical analyses of all data. The difference between the 2 groups was evaluated using Student's t-test while multiple-group comparisons were performed using analysis of variance (ANOVA) and Tukey's post hoc analysis. The general alpha value was set as 0.05. All the experimentations were performed 3 times.

Results

Effect of lncRNA *PCGEM1* and *ETV1* on oxaliplatin-resistant HCC cells

Hep3B cells were treated with oxaliplatin, and the *PCGEM1* expression was examined using qRT-PCR. Results indicated that *PCGEM1* expression was significantly enhanced in Hep3B/OXA cells compared to Hep3B cells without oxaliplatin treatment (Fig. 1A). The survival of Hep3B cells was assessed using a CCK-8 assay, and our data indicated that the percentage survival of Hep3B/OXA cells was greater than Hep3B control cells (Fig. 1B). Furthermore, *ETV1* mRNA expression was markedly enhanced in Hep3B/OXA cells compared to that of parental Hep3B cells (Fig. 1C). Next, oligonucleotides were
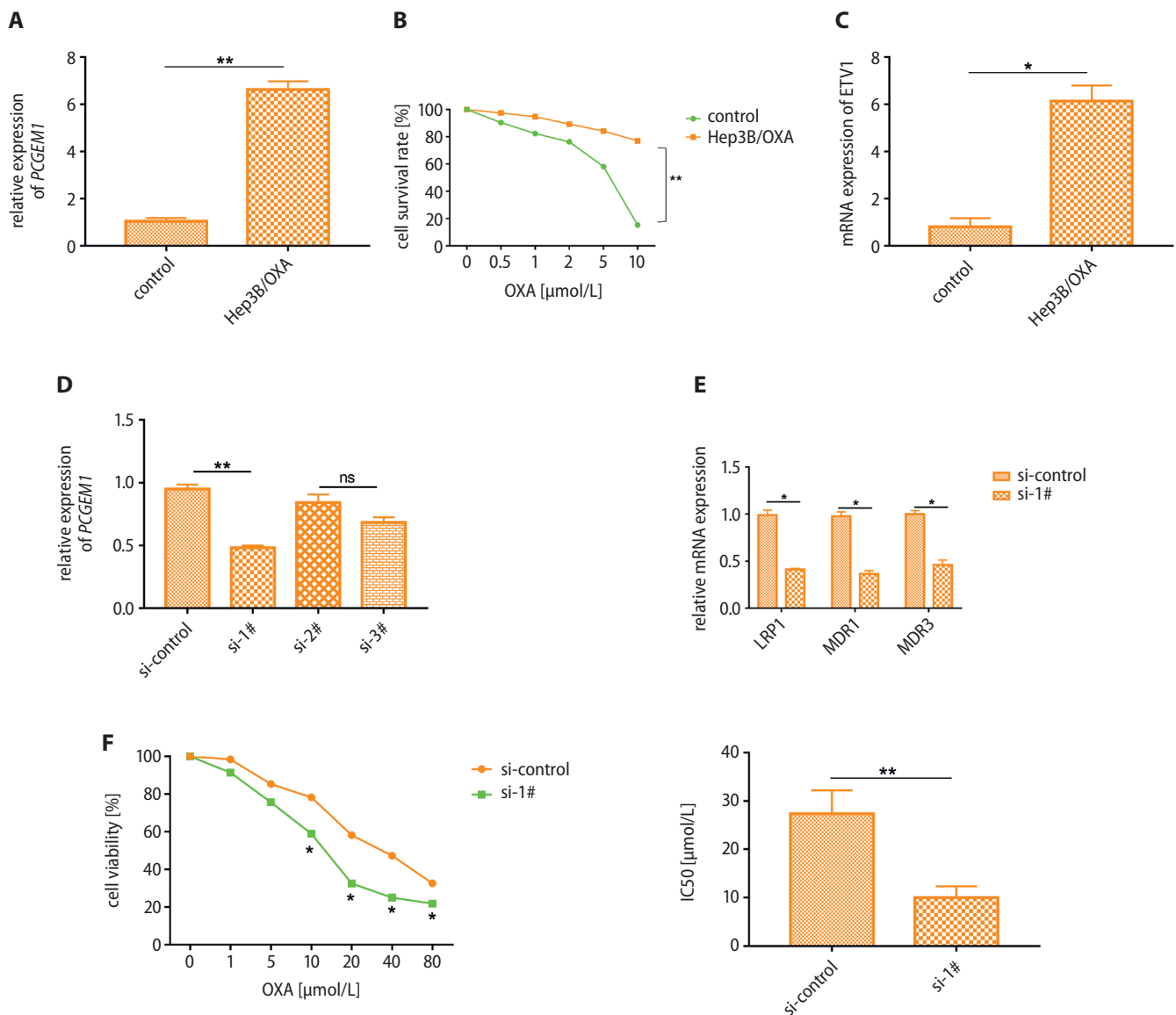
Fig. 1. Effect of lncRNA *PCGEM1* and *ETV1* in oxaliplatin-resistant hepatocellular carcinoma (HCC) cells. A. *PCGEM1* expression was determined in oxaliplatin-resistant Hep3B cells using quantitative real-time polymerase chain reaction (qRT-PCR); B. The cell survival rate was examined in oxaliplatin-resistant Hep3B cells using the Cell Counting Kit-8 (CCK-8) assay; C. The *ETV1* mRNA level in oxaliplatin-resistant Hep3B cells was examined using qRT-PCR; D. The *PCGEM1* expression was assessed after Hep3B cells were treated with interfering oligonucleotides (**$p < 0.01$, ns – not significant); E. qRT-PCR measured the mRNA level of *MDR1*, *MDR3* and *LRP1* (drug resistance-related genes); F. The IC$_{50}$ was measured in oxaliplatin-resistant Hep3B cells (*$p < 0.03$, **$p < 0.002$)

Fig. 2. Effect of *PCGEM1* knockdown on invasion and migration of oxaliplatin-resistant hepatocellular carcinoma (HCC) cells in vitro. A. Transwell assay detected the number of invasive cell in Hep3B/OXA cells transfected with *PCGEM1* siRNA compared to the cells transfected with empty vector (**p < 0.002); B. Transwell assay detected the number of migrative cell in Hep3B/OXA cells transfected with *PCGEM1* siRNA compared to the cells transfected with empty vector (**p < 0.002)

Fig. 3. *PCGEM1* directly targeted *miR-129-5p*. A and B. The binding sites between *PCGEM1* and *miR-129-5p* were predicted using online bioinformatic tools, including TargetScan website (http://www.targetscan.org) and starBase website (http://starbase.sysu.edu.cn/starbase2/index.php), and confirmed using a luciferase assay (*p < 0.03); C. The expression of *miR-129-5p* in Hep3B/OXA cells was examined using qRT-PCR (*p < 0.03); D. The *miR-129-5p* expression was determined in Hep3B/OXA cells transfected with empty vector or *PCGEM1* siRNA (*p < 0.03)

prepared and Hep3B/OXA cells were transfected with them to reduce the expression of *PCGEM1* (Fig. 1D). Moreover, our findings revealed that *PCGEM1* knockdown considerably decreased the mRNA expression of drug resistance-related genes, including low-density lipoprotein receptor-related protein 1 (*LRP1*), multidrug resistance gene 1 (*MDR1*) and multidrug resistance gene 3 (*MDR3*) compared to that of the control group (Fig. 1E). The CCK-8 assay was used to measure the cell growth inhibition curve by calculating the value of the inhibitory concentration (IC_{50}). Our findings elucidated that *PCGEM1* knockdown markedly suppressed the IC_{50} value in comparison to the control group (Fig. 1F). These data illustrated that *PCGEM1* knockdown markedly reduced the oxaliplatin resistance of HCC cells.

Effect of lncRNA *PCGEM1* on invasion and migration in the oxaliplatin-resistant HCC cells

Transwell assays indicated that *PCGEM1* knockdown considerably reduced the number of invasive cells in Hep3B/OXA cells compared to that of the empty vector group (Fig. 2A). Our findings also revealed that *PCGEM1* knockdown markedly reduced the number of migrating cells compared to the empty vector cells (Fig. 2B). These findings revealed that *PCGEM1* knockdown inhibited the invasion and migration in Hep3B/OXA cells.

MiR-129-5p was a target of PCGEM1

Online bioinformatics tools including miRcode (http://mircode.org/), starBase v. 2.0 (http://starbase.sysu.edu.cn/starbase2/index.php) and microRNA.org (https://bigd.big.ac.cn/databasecommons/database/id/1426), together with a luciferase assay, were used for the prediction and confirmation of binding between *PCGEM1* and *miR-129-5p*. Our data elucidated that the luciferase activity was significantly reduced in the *PCGEM1*-WT and *miR-129-5p* mimics group. At the same time, no significant change was observed in the rest of the groups (Fig. 3A,B). Moreover, *miR-129-5p* expression was reduced in Hep3B/OXA cells compared to that of parental Hep3B cells (Fig. 3C). Finally, *miR-129-5p* expression was significantly enhanced in Hep3B/OXA cells transfected with si-*PCGEM1* compared to that of the empty vector group (Fig. 3D).
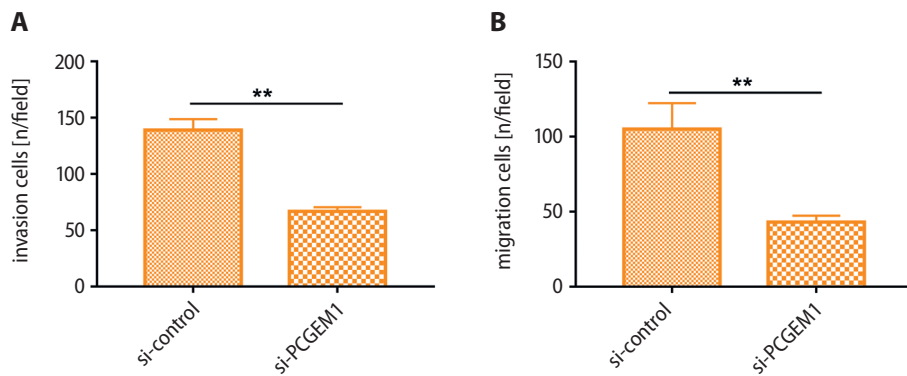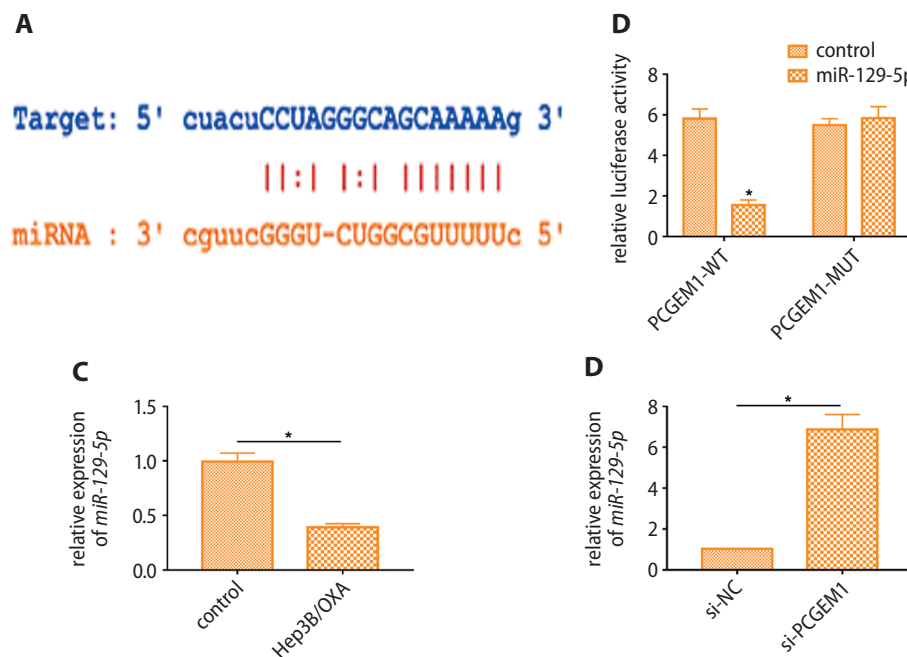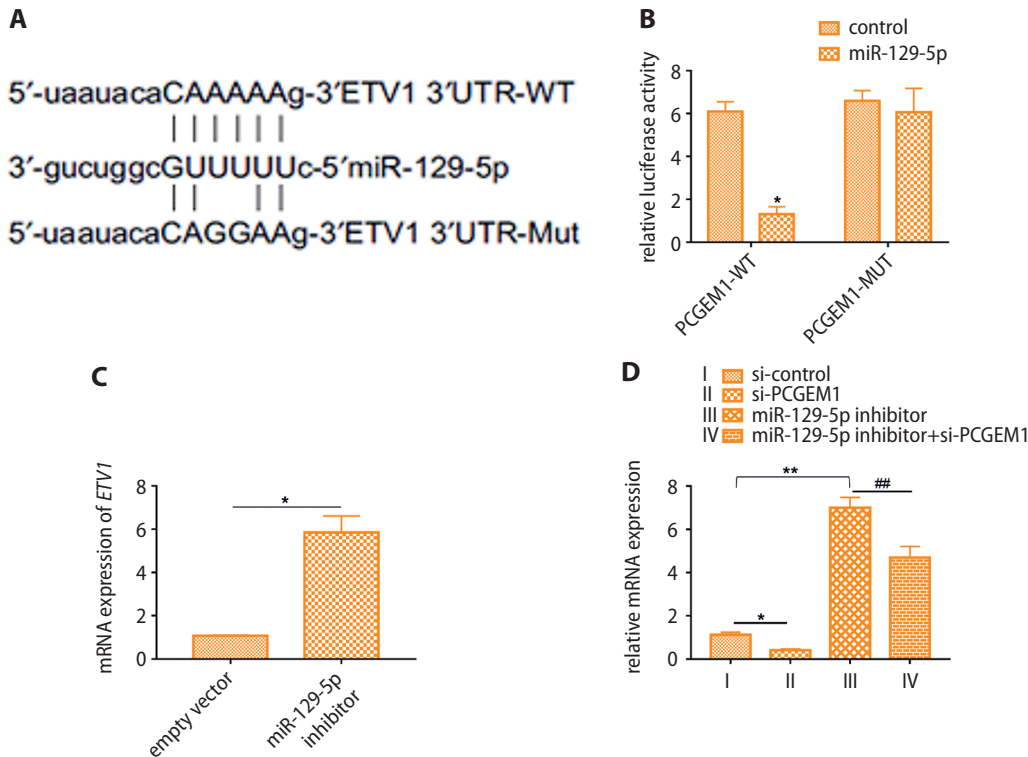
Fig. 4. LncRNA *PCGEM1* regulated *ETV1* expression by targeting *miR-129-5p*. A and B. The binding sites between *ETV1* and *miR-129-5p* were predicted using online bioinformatic tools including TargetScan website (http://www.targetscan.org) and starBase website (http://starbase.sysu.edu.cn/starbase2/index.php), and confirmed using a luciferase assay (*p < 0.03); C. The *ETV1* mRNA level was assessed in Hep3B/OXA cells transfected with *miR-129-5p* inhibitor using qRT-PCR (*p < 0.03, compared to si-control); D. The *ETV1* mRNA level was measured in Hep3B/OXA cells transfected with an empty vector, *miR-129-5p* inhibitor and *PCGEM1* siRNA (*p < 0.03, **p < 0.002 compared to si-control, ##p < 0.002 compared to *miR-129-5p* inhibitor)

LncRNA *PCGEM1* regulated *ETV1* expression via targeting *miR-129-5p*

The results from bioinformatic tools indicated that *miR-129-5p* shared binding sites with the 3'UTR of *ETV1* mRNA (Fig. 4A). Luciferase assay results revealed a decrease in luciferase activity after the co-transfection with *miR-129-5p* and *ETV1*-WT (100 ng), indicating molecular binding between *miR-129-5p* and *ETV1* (Fig. 4B). Furthermore, *ETV1* mRNA expression was increased in Hep3B/OXA cells transfected with *miR-129-5p* inhibitor (50 nmol/L) (Fig. 4C). Finally, the knockdown of *PCGEM1* reduced *ETV1* mRNA expression, while inhibition of *miR-129-5p* enhanced the mRNA level of *ETV1* in Hep3B/OXA cells (Fig. 4D).

Discussion

The HCC is a hepatic malignant neoplasm.[24] Despite great advancement in the therapeutic techniques for HCC, the overall outcomes remain unsatisfactory,[25] with a common obstacle being chemoresistance towards drugs such as oxaliplatin, doxorubicin and cisplatin, among others.[26] Our study explored the regulatory functions of *PCGEM1* in oxaliplatin resistance regarding *miR-129-5p*/*ETV1* interactions using oxaliplatin-resistant HCC cells (Hep3B/OXA) (Fig. 5).

The lncRNAs present a vital function in regulating tumorigenesis, as well as the chemoresistance of cancer cells.[27] Previous research has suggested that dysregulated

lncRNA expression might mediate potential chemoresistance.[28] Our findings revealed that the *PCGEM1* expression was enhanced in Hep3B/OXA cells compared to that of its parental cell line. Furthermore, knockdown of lncRNA *PCGEM1* decreased the mRNA expression levels of *LRP1*, *MDR1* and *MDR3* in Hep3B/OXA cells, indicating that silencing of *PCGEM1* might reduce the oxaliplatin resistance. Moreover, *PCGEM1* knockdown significantly inhibited the proliferation, migration and invasiveness of Hep3B/OXA cells, which was in accordance with the hypothesis that downregulation of *PCGEM1* might lead to the decrease in chemoresistance in vitro. Similar to our findings, it has been reported that downregulation of another lncRNA, lncRNA *PVT1* was able to inhibit tumor progression and reduced chemoresistance to cisplatin in colorectal cancer patients.[29] In HCC, lncRNA *HULC* was significantly upregulated in HCC cells after treatment with drugs including cisplatin and oxaliplatin, and
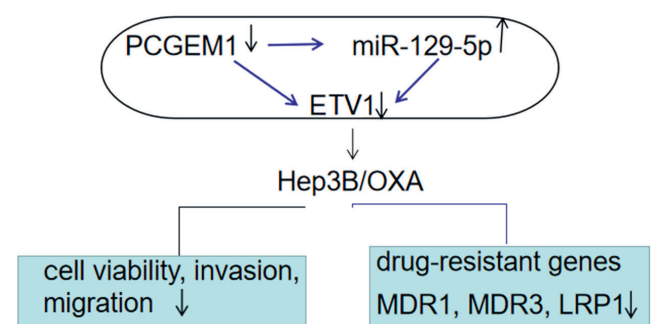

Fig. 5. The illustration of the hypothetical mechanism of *PCGEM1* in Hep3B/OXA cells

the additional knockdown of *HULC* enhanced chemoresistance of HCC cells through its interaction with *SIRT1*[19]. In this study, we found that the relative mRNA expression of *ETV1* was decreased by the knockdown of lncRNA *PCGEM1* in Hep3B/OXA cells. *ETV1* has been reported to function as an oncogene in various human malignant tumors.[30,31] A previous study indicated that *ETV1* enhanced the invasion, migration and proliferation of breast cancer cells.[32] Moreover, inhibitor of *ETV1* enhanced the cellular sensitivity to docetaxel in prostate cancer.[33] Similarly, ETV1 was reported to be modulated by Circ-ZNF609/miR-1224-3p in lung cancer cells.[34] We discovered that the expression of *ETV1* was positively regulated by *PCGEM1* in Hep3B/OXA cells, suggesting that knockdown of *PCGEM1* in HCC cells increased sensitivity to oxaliplatin, perhaps through the modulation of *ETV1*.

To predict the targeted sites between mRNA and lncRNA, bioinformatic prediction tools were used.[35] By using these online tools, we established that *miR-129-5p* targeted *PCGEM1*. The *miR-129-5p* overexpression has been shown previously to attenuate the proliferation of PC-3 cells,[36] while in prostate cancer, *miR-129-5p* was downregulated in tissues and cells in comparison with normal counterparts, and it specifically inhibits *ETV1*.[36] Furthermore, the upregulation of *miR-129-5p* was shown to curb the cell proliferation by suppressing *ETV1* in prostate cancer cells.[36] Finally, it was disclosed that *miR-129-5p* inhibited the development of colon cancer and osteosarcoma via regulating *HMGB1*.[37,38] In conclusion, our data revealed the impact of lncRNA *PCGEM1* in HCC oxaliplatin resistance in vitro. We have shown that *PCGEM1* and *miR-129-5p* expression levels were negatively correlated to each other, representing the enrichment and antagonistic function. *PCGEM1* downregulation led to an increase in *miR-129-5p* expression in Hep3B/OXA cells, while downregulation of *miR-129-5p* induced *ETV1* mRNA expression. In our work, *PCGEM1* downregulation reduced the oxaliplatin resistance in Hep3B/OXA cells via binding *miR-129-5p* and inhibiting *ETV1*.

Limitations

The limitation of this current study mainly exists in the absence of animal models. If respective animal models could be established to further validate the mechanism of the *PCGEM1/miR-129-5p/ETV1* pathway on HCC oxaliplatin resistance, the research would be more valuable and complete.

Conclusions

Our findings demonstrated the potential mechanism of the *PCGEM1/miR-129-5p/ETV1* pathway on HCC oxaliplatin resistance, suggesting the critical function of *PCGEM1* in HCC treatment and providing a new therapeutic target.

ORCID iDs

Jie Chen https://orcid.org/0000-0003-3904-4564
Daiyue Yuan https://orcid.org/0000-0002-2720-2337
Qingya Hao https://orcid.org/0000-0002-4205-2242
Dongmei Zhu https://orcid.org/0000-0001-7062-8475
Zhong Chen https://orcid.org/0000-0002-1598-9726

References

1. Brown ZJ, Heinrich B, Steinberg SM, Yu SJ, Greten TF. Safety in treatment of hepatocellular carcinoma with immune checkpoint inhibitors as compared to melanoma and non-small cell lung cancer. *J Immunother Cancer*. 2017;5(1):93. doi:10.1186/s40425-017-0298-2
2. Li M, Zhang M, Zhang ZL, et al. Induction of apoptosis by berberine in hepatocellular carcinoma HepG2 cells via downregulation of NF-κB. *Oncol Res*. 2017;25(2):233–239. doi:10.3727/096504016x14742891049073
3. Dika IE, Abou-Alfa GK. Treatment options after sorafenib failure in patients with hepatocellular carcinoma. *Clin Mol Hepatol*. 2017;23(4):273–279. doi:10.3350/cmh.2017.0108
4. Hocquelet A, Aubé C, Rode A, et al. Comparison of no-touch multi-bipolar vs monopolar radiofrequency ablation for small HCC. *J Hepatol*. 2017;66(1):67–74. doi:10.1016/j.jhep.2016.07.010
5. Huang X, Lu S. Impact of preoperative locoregional therapy on recurrence and patient survival following liver transplantation for hepatocellular carcinoma: A meta-analysis. *Scand J Gastroenterol*. 2017;52(2):143–149. doi:10.1080/00365521.2016.1236396
6. Margonis GA, Sasaki K, Andreatos N, et al. Prognostic impact of complications after resection of early stage hepatocellular carcinoma. *J Surg Oncol*. 2017;115(7):791–804. doi:10.1002/jso.24576
7. Meng YB, He X, Huang YF, Wu QN, Zhou YC, Hao DJ. Long noncoding RNA CRNDE promotes multiple myeloma cell growth by suppressing miR-451. *Oncol Res*. 2017;25(7):1207–1214. doi:10.3727/096504017x14886679715637
8. Qin N, Tong GF, Sun LW, Xu XL. Long noncoding RNA MEG3 suppresses glioma cell proliferation, migration, and invasion by acting as a competing endogenous RNA of miR-19a. *Oncol Res*. 2017;25(9):1471–1478. doi:10.3727/096504017x14886689179993
9. Liu K, Wu X, Zang X, et al. TRAF4 regulates migration, invasion, and epithelial–mesenchymal transition via PI3K/AKT signaling in hepatocellular carcinoma. *Oncol Res*. 2017;25(8):1329–1340. doi:10.3727/096504017x14876227286564
10. Cao SW, Huang JL, Chen J, et al. Long non-coding RNA UBE2CP3 promotes tumor metastasis by inducing epithelial-mesenchymal transition in hepatocellular carcinoma. *Oncotarget*. 2017;8(39):65370–65385. doi:10.18632/oncotarget.18524
11. Wang F, Ying HQ, He BS, et al. Upregulated lncRNA-UCA1 contributes to progression of hepatocellular carcinoma through inhibition of miR-216b and activation of FGFR1/ERK signaling pathway. *Oncotarget*. 2015;6(10):7899–7917. doi:10.18632/oncotarget.3219
12. Yang J, Li J, Liu B, et al. Long noncoding RNA AK021443 promotes cell proliferation and migration by regulating epithelial–mesenchymal transition in hepatocellular carcinoma cells. *DNA Cell Biol*. 2018;37(5):481–490. doi:10.1089/dna.2017.4030
13. Srikantan V, Zou Z, Petrovics G, et al. *PCGEM1*, a prostate-specific gene, is overexpressed in prostate cancer. *Proc Natl Acad Sci USA*. 2000;97(22):12216–12221. doi:10.1073/pnas.97.22.12216
14. Petrovics G, Zhang W, Makarem M, et al. Elevated expression of *PCGEM1*, a prostate-specific gene with cell growth-promoting function, is associated with high-risk prostate cancer patients. *Oncogene*. 2004;23(2):605–611. doi:10.1038/sj.onc.1207069
15. Chen S, Wang LL, Sun KX, et al. LncRNA *PCGEM1* induces ovarian carcinoma tumorigenesis and progression through RhoA pathway. *Cell Physiol Biochem*. 2018;47(4):1578–1588. doi:10.1159/000490931
16. Zhang J, Jin HY, Wu Y, et al. Hypoxia-induced LncRNA *PCGEM1* promotes invasion and metastasis of gastric cancer through regulating SNAI1. *Clin Transl Oncol*. 2019;21(9):1142–1151. doi:10.1007/s12094-019-02035-9
17. Seo SU, Min KJ, Woo SM, Kwon TK. Z-FL-COCHO, a cathepsin S inhibitor, enhances oxaliplatin-mediated apoptosis through the induction of endoplasmic reticulum stress. *Exp Mol Med*. 2018;50(8):107. doi:10.1038/s12276-018-0138-6

18. Yin X, Zheng SS, Zhang L, et al. Identification of long noncoding RNA expression profile in oxaliplatin-resistant hepatocellular carcinoma cells. *Gene.* 2017;596:53–88. doi:10.1016/j.gene.2016.10.008

19. Xiong H, Ni Z, He J, et al. LncRNA HULC triggers autophagy via stabilizing Sirt1 and attenuates the chemosensitivity of HCC cells. *Oncogene.* 2017;36(25):3528–3540. doi:10.1038/onc.2016.521

20. Bu Y, Jia QA, Ren ZG, et al. Maintenance of stemness in oxaliplatin-resistant hepatocellular carcinoma is associated with increased autocrine of IGF1. *PLoS One.* 2014;9(3):e89686. doi:10.1371/journal.pone.0089686

21. Kim MK, Kim WT, Lee HM, et al. Correction: Mapping of a mycoplasma-neutralizing epitope on the mycoplasmal p37 protein. *PLoS One.* 2017;12(2):e0172487. doi:10.1371/journal.pone.0172487

22. Ma J, Zeng S, Zhang Y, et al. BMP4 promotes oxaliplatin resistance by an induction of epithelial-mesenchymal transition via MEK1/ERK/ELK1 signaling in hepatocellular carcinoma. *Cancer Lett.* 2017;411:117–129. doi:10.1016/j.canlet.2017.09.041

23. Schmittgen TD, Livak KJ. Analyzing real-time PCR data by the comparative C(T) method. *Nat Protoc.* 2008;3(6):1101–1108. doi:10.1038/nprot.2008.73

24. Lu LC, Chang CJ, Hsu CH. Targeting myeloid-derived suppressor cells in the treatment of hepatocellular carcinoma: Current state and future perspectives. *J Hepatocell Carcinoma.* 2019;6:71–84. doi:10.2147/jhc.s159693

25. Flynn MJ, Sayed AA, Sharma R, Siddique A, Pinato DJ. Challenges and opportunities in the clinical development of immune checkpoint inhibitors for hepatocellular carcinoma. *Hepatology.* 2019;69(5):2258–2270. doi:10.1002/hep.30337

26. Liu L, Li N, Zhang Q, Zhou J, Lin L, He X. Inhibition of ERK1/2 signaling impairs the promoting effects of TGF-β1 on hepatocellular carcinoma cell invasion and epithelial–mesenchymal transition. *Oncol Res.* 2017;25(9):1607–1616. doi:10.3727/096504017x14938093512742

27. Liu Z, Zhang H. LncRNA plasmacytoma variant translocation 1 is an oncogene in bladder urothelial carcinoma. *Oncotarget.* 2017;8(38):64273–64282. doi:10.18632/oncotarget.19604

28. Chen G, Guo Z, Liu M, et al. Clinical value of capecitabine-based combination adjuvant chemotherapy in early breast cancer: A meta-analysis of randomized controlled trials. *Oncol Res.* 2017;25(9):1567–1578. doi:10.3727/096504017x14897173032733

29. Ping G, Xiong W, Zhang L, Li Y, Zhang Y, Zhao Y. Silencing long noncoding RNA PVT1 inhibits tumorigenesis and cisplatin resistance of colorectal cancer. *Am J Transl Res.* 2018;10(1):138–149.

30. Oh S, Shin S, Janknecht R. ETV1, 4 and 5: An oncogenic subfamily of ETS transcription factors. *Biochim Biophys Acta.* 2012;1826(1):1–12. doi:10.1016/j.bbcan.2012.02.002

31. Chi P, Chen Y, Zhang L, et al. ETV1 is a lineage survival factor that cooperates with KIT in gastrointestinal stromal tumours. *Nature.* 2010;467(7317):849–853. doi:10.1038/nature09409

32. Ouyang M, Wang H, Ma J, et al. COP1, the negative regulator of ETV1, influences prognosis in triple-negative breast cancer. *BMC Cancer.* 2015;15:132. doi:10.1186/s12885-015-1151-y

33. Yu L, Wu X, Chen M, et al. The effects and mechanism of YK-4-279 in combination with docetaxel on prostate cancer. *Int J Med Sci.* 2017;14(4):356–366. doi:10.7150/ijms.18382

34. Zuo Y, Shen W, Wang C, Niu N, Pu J. Circular RNA Circ-ZNF609 promotes lung adenocarcinoma proliferation by modulating miR-1224-3p/ETV1 signaling. *Cancer Manag Res.* 2020;12:2471–2479. doi:10.2147/cmar.s232260

35. Zhang G, Yang P. Bioinformatics genes and pathway analysis for chronic neuropathic pain after spinal cord injury. *Biomed Res Int.* 2017;2017:6423021. doi:10.1155/2017/6423021

36. Gao G, Xiu D, Yang B, et al. miR-129-5p inhibits prostate cancer proliferation via targeting ETV1. *Oncotargets Ther.* 2019;12:3531–3544. doi:10.2147/ott.s183435

37. Liu K, Huang J, Ni J, et al. MALAT1 promotes osteosarcoma development by regulation of HMGB1 via miR-142-3p and miR-129-5p. *Cell Cycle.* 2017;16(6):578–587. doi:10.1080/15384101.2017.1288324

38. Wu Q, Meng WY, Jie Y, Zhao H. LncRNA MALAT1 induces colon cancer development by regulating miR-129-5p/HMGB1 axis. *J Cell Physiol.* 2018;233(9):6750–6757. doi:10.1002/jcp.26383

LncRNA FEZF1-AS1 promotes colorectal cancer progression through regulating the miR-363-3p/PRRX1 pathway

Tongtong Zhang[A,D], Suyang Yu[B,C], Shipeng Zhao[E,F]

Department of Gastrointestinal Surgery, The Third Hospital Affiliated to Hebei Medical University, Shijiazhuang, China

A – research concept and design; B – collection and/or assembly of data; C – data analysis and interpretation;
D – writing the article; E – critical revision of the article; F – final approval of the article

Address for correspondence
Shipeng Zhao
E-mail: df452355@126.com

Abstract

Background. Long non-coding RNAs (lncRNAs) are involved in the development of many cancers, including colorectal cancer (CRC). FEZ family zinc finger 1 antisense RNA 1 (FEZF1-AS1) is a key lncRNA in the regulation of CRC progression, but its potential molecular mechanisms need to be further explored.

Objectives. To investigate the mechanism of lncRNA FEZF1-AS1 in the progression of CRC.

Materials and methods. Quantitative real-time polymerase chain reaction (qRT-PCR) was performed to measure FEZF1-AS1 and miR-363-3p expression. Cell proliferation, migration and invasion were analyzed using Cell Counting Kit-8 (CCK-8) and transwell assays. Protein expression of epithelial–mesenchymal transformation (EMT)-related markers and paired-related homeobox 1 (PRRX1) were determined using western blot analysis. The interactions among FEZF1-AS1, miR-363-3p and PRRX1 were verified with dual-luciferase reporter assay. A xenograft model was constructed in vivo to confirm the role of FEZF1-AS1 in CRC tumor growth.

Results. We demonstrated that FEZF1-AS1 expression was upregulated in CRC, and its silencing reduced CRC cell proliferation, migration, invasion, and EMT. MiR-363-3p could be inhibited by FEZF1-AS1, which inhibitor could reverse the suppressive effect of FEZF1-AS1 silencing on CRC progression. Paired-related homeobox 1 could be targeted by miR-363-3p, and the inhibitory effect of FEZF1-AS1 knockdown on CRC progression could also be eliminated by PRRX1 overexpression. Furthermore, interference of FEZF1-AS1 reduced the tumor growth of CRC in vivo.

Conclusions. Our data demonstrate that FEZF1-AS1 regulated PRRX1 expression to promote CRC progression via inhibition of miR-363-3p.

Key words: colorectal cancer, FEZF1-AS1, miR-363-3p, PRRX1

Background

Globally, colorectal cancer (CRC) is one of the most common malignant tumors, with more than 1.2 million new CRC patients diagnosed annually.[1,2] The age of CRC patient tends to be older (41–65 years), and is more common in females.[3] At present, the leading cause of death in CRC patients was tumor metastasis,[4] a process driven by epithelial–mesenchymal transformation (EMT).[5] Therefore, it is urgent to explore the mechanism affecting CRC metastasis.

Currently, increasing evidence reveals that long non-coding RNAs (lncRNAs) are involved in the regulation of cancer progression, including CRC.[6,7] The lncRNA is a kind of non-protein coding RNA with a length of more than 200 nucleotides (nts),[8] and mainly participates in the regulation of gene expression as a competitive endogenous RNA (ceRNA) that adsorbs microRNAs (miRNAs).[9,10] Studies have shown that a variety of lncRNAs (such as NKILA, BLACAT2 and MEG3) are abnormally expressed in CRC, which can modulate its occurrence and development.[11–13]

FEZ family zinc finger 1 antisense RNA 1 (FEZF1-AS1) was found to be aberrantly expressed in various cancers, such as prostate cancer, retinoblastoma and oral squamous cell carcinoma.[14–16] In nasopharyngeal carcinoma cells, FEZF1-AS1 silencing was discovered to significantly inhibit the EMT process of cancer cells, and played a role in promoting cancer cell proliferation and metastasis.[17] Furthermore, FEZF1-AS1 has been confirmed to up-regulate the invasion and EMT of human hepatocellular carcinoma cells.[18] However, few studies have examined the role and potential molecular mechanism of lncRNA FEZF1-AS1 in CRC.

Objectives

Our research aimed to explore the function and mechanism of FEZF1-AS1 in CRC, so as to provide new ideas for the pathogenesis and therapy of CRC.

Materials and methods

Patients and tissues

Seventy-one CRC patients were recruited from the Third Hospital Affiliated to Hebei Medical University (Shijiazhuang, China). The clinicopathological parameters of CRC patients are shown in Table 1. The CRC tumor tissues and adjacent normal tissues were preserved at –80°C. Each patient provided informed consent. This study was authorized by the Ethics Committee of the Third Hospital Affiliated to Hebei Medical University and was carried out in accordance with the 1964 Declaration of Helsinki.

Table 1. Correlation between FEZF1-AS1 expression and clinicopathological parameters of colorectal cancer (CRC) patients

Parameters	Patients (n, %)	FEZF1-AS1 high (n, %)	FEZF1-AS1 low (n, %)	p-value
Gender				
Female	29 (40.85)	12 (41.38)	17 (58.62)	0.192
Male	42 (59.15)	24 (57.14)	18 (42.86)	
Age [years]				
≥60	39 (54.93)	23 (58.97)	16 (41.03)	0.124
<60	32 (45.07)	13 (40.63)	19 (59.37)	
Tumor size [cm]				
≥4	47 (66.20)	27 (57.45)	20 (42.55)	0.112
<4	24 (33.80)	9 (37.50)	15 (62.50)	
TNM stage				
I–II	35 (49.30)	13 (37.14)	22 (62.86)	0.024*
III–IV	36 (50.70)	23 (63.89)	13 (36.11)	
Tumor grade				
T1–T2	30 (42.25)	10 (33.33)	20 (66.67)	0.012*
T3–T4	41 (57.75)	26 (63.41)	15 (36.59)	
Differentiation				
Poor and moderate	50 (70.42)	29 (58.00)	21 (42.00)	0.058
Well	21 (29.58)	7 (33.33)	14 (66.67)	
Distant metastasis				
Yes	19 (26.76)	15 (78.95)	4 (21.05)	0.004*
No	52 (73.24)	21 (40.38)	31 (59.62)	

Cell culture and transfection

The CRC cell lines (LOVO, HCT116, SW480, and SW620) and normal human intestinal epithelial cells (HIEC-6) were obtained from American Type Cell Culture (ATCC, Manassas, USA) and cultured in RPMI-1640 medium (Gibco, Waltham, USA) containing 10% fetal bovine serum (FBS; Gibco) and 1% penicillin-streptomycin at 37°C with 5% CO_2. Lentiviral short hairpin RNA (shRNA) against FEZF1-AS1 (sh-FEZF1-AS1) and its negative control (sh-NC), miR-363-3p mimic and inhibitor (miR-363-3p and anti-miR-363-3p) or their negative controls (miR-NC and anti-NC), FEZF1-AS1 and paired-related homeobox 1 (PRRX1) overexpression vectors or their negative controls (vector) were synthesized by Genechem (Shanghai, China). Cell transfection was performed using Lipofectamine 3000 (Invitrogen, Carlsbad, USA) according to the manufacturer's instructions.

qRT-PCR

Total RNA was isolated using TRIzol reagent (Invitrogen) and cDNA was synthesized using the Reverse Transcription Kit (HaiGene, Harbin, China). Quantitative real-time PCR (qRT-PCR) was carried out using SYBR Green reagent (HaiGene); β-actin or U6 was used as the endogenous control. The primers sequences that were used are as follows: FEZF1-AS1, Forward (F), 5'-AGGGGATCGACGAGTTGAGA-3' and Reverse (R), 5'-TTGTCCCCGAGTCATTGGTG-3';

PRRX1, F, 5'-TGATGCTTTTGTGCGAGAAGA-3' and R, 5'-AGGGAAGCGTTTTTATTGGCT-3'; β-actin, F, 5'-CATGTACGTTGCTATCCAGGC-3' and R, 5'-CTCCT-TAATGTCACGCACGAT-3'; miR-363-3p, F, 5'-TCGGCAG-GAATTGCACGGTATCCA-3' and R, 5'-CTCAACTGGT-GTCGTGGA-3'; U6 F 5'-GCTTCGGCAGCACATATAC-TAAAAT-3', R 5'-CGCTTCACGAATTTGCGTGTCAT-3'. Relative expression was determined using the $2^{-\Delta\Delta Ct}$ method.

CCK-8 assay

LOVO and HCT116 cells were seeded into 96-well plates. At a specific time point (0 h, 24 h, 48 h, and 72 h), an equal amount of Cell Counting Kit-8 (CCK-8) solution (Beyotime, Shanghai, China) was added to each well. The proliferation ability of cells was measured at an absorbance of 450 nm.

Transwell assay

Briefly, 8-μm polycarbonate membranes of Transwell chambers (Corning Inc., Corning, USA) were coated with BD Matrigel (Corning Inc.) for cell invasion, and uncoated for cell migration. Serum-free media was filled in the upper chambers, while media containing 10% FBS was added to the lower chambers. After 24 h, the cells were fixed and stained with crystal violet. The numbers of invading or migrating cells were counted with an inverted light microscope at ×100 magnification (Shoif, Shanghai, China).

Western blot analysis

The cells were lysed with lysis buffer (Beyotime). Proteins were separated using sodium dodecyl sulphate–polyacrylamide gel electrophoresis (SDS-PAGE) and transferred onto polyvinylidene fluoride (PVDF) membranes. After blocking with skim milk powder, the membranes were incubated with anti-E-cadherin (1:500; Yubo Bio, Shanghai, China), anti-N-cadherin (1:1000; Yubo), anti-vimentin (1:750; Yubo), anti-PRRX1 (1:500; Yubo), or anti-β-actin (1:750; Yubo) overnight at 4°C. Then, membrane were incubated with an horseradish peroxidase (HRP)-conjugated secondary antibody (1:1000; Yubo), and protein signals were observed using electrochemiluminescence ECL solution (Beyotime).

Dual-luciferase reporter assay

The wild-type (WT) and mutant-type (MUT) reporter vectors of FEZF1-AS1 or PRRX1 were constructed using pmirGLO reporter vector. Lipofectamine 3000 was used to transfect the above vectors into CRC cells with miR-363-3p mimic and miR-NC. Luciferase activities were measured using the Dual-Luciferase Assay Kit (Yubo) after transfection for 48 h.

Animal experiments

HCT116 cells transfected with sh-FEZF1-AS1 or sh-NC were administered subcutaneously into male BALB/c nude mice (purchased from Shanghai Laboratory Animals Center, Shanghai, China). Tumor volumes were calculated every 5 days. After 30 days, the tumors were removed for further analysis. All experiments involving animals were authorized by the Animal Care Committee of the Third Hospital Affiliated to Hebei Medical University and performed according to the Guide for the Care and Use of Laboratory Animals.

Statistical analyses

All experiments were performed in triplicate. Data are presented as the mean ± standard deviation (SD) and analyzed using a Student's t-test or one-way analysis of variance (ANOVA) followed by Tukey's post hoc test. Statistical analyses were performed using GraphPad Prism v. 5.0 software (GraphPad Software, San Diego, USA). According to the median cutoff of FEZF1-AS1 expression, patients were divided into low and high groups for analysis. The χ^2 test was used to estimate the correlation between FEZF1-AS1 expression and clinicopathological parameters of CRC patients. Kaplan–Meier analysis was used to analyze the association between FEZF1-AS1 expression and the overall survival of CRC patients, determined by the log-rank test. A value of $p < 0.05$ was defined as statistically significant.

Results

FEZF1-AS1 is highly expressed in CRC

Compared to normal adjacent tissues, we discovered that FEZF1-AS1 was upregulated in CRC tissues (Fig. 1A). Based on the median FEZF1-AS1 expression in CRC tissues, we divided tissues into those with high FEZF1-AS1 expression and low FEZF1-AS1 expression. Analysis of the correlations between FEZF1-AS1 and clinicopathological parameters of CRC patients demonstrated that high FEZF1-AS1 expression was positively correlated with TNM stage, tumor grade and distant metastasis in CRC patients (Table 1). Kaplan–Meier analysis revealed that high FEZF1-AS1 expression was associated with poor overall survival of CRC patients (Fig. 1B). Moreover, we also analyzed the expression of FEZF1-AS1 in CRC cell lines in vitro (LOVO, HCT116, SW480, and SW620) and normal intestinal epithelial cells (HIEC-6), and discovered that FEZF1-AS1 expression was promoted in 4 CRC cell lines (especially in LOVO and HCT116 cells) compared to that in HIEC-6 cells (Fig. 1C). These data suggest that *FEZF1-AS1* could act as an oncogene in CRC.
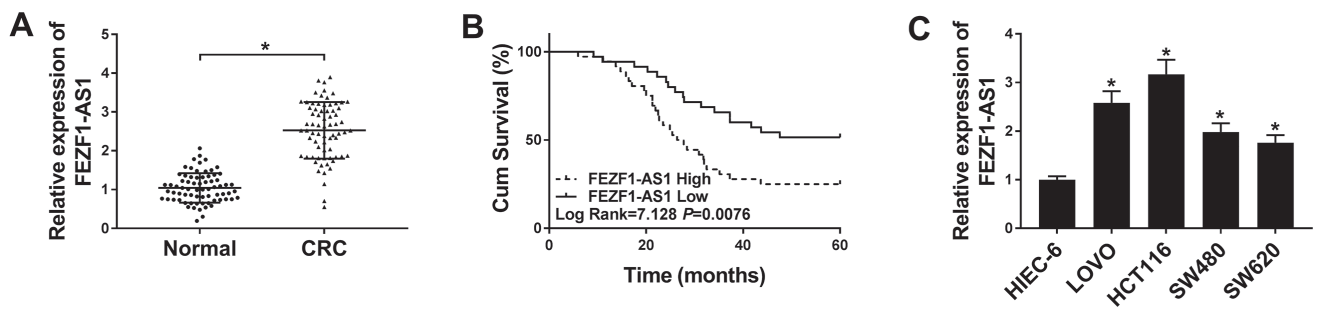
Fig. 1. FEZF1-AS1 expression in colorectal cancer (CRC) tissues and cells. A. Expression of FEZF1-AS1 in CRC tissues (CRC, n = 71) and adjacent normal tissues (normal, n = 71) was shown using quantitative real-time polymerase chain reaction (qRT-PCR); B. Kaplan–Meier survival analysis was used to investigate the overall survival of all CRC patients according to FEZF1-AS1 expression; C. FEZF1-AS1 expression in CRC cells (LOVO, HCT116, SW480, and SW620) and normal human intestinal epithelial cells (HIEC-6) was detected using qRT-PCR, *p < 0.05
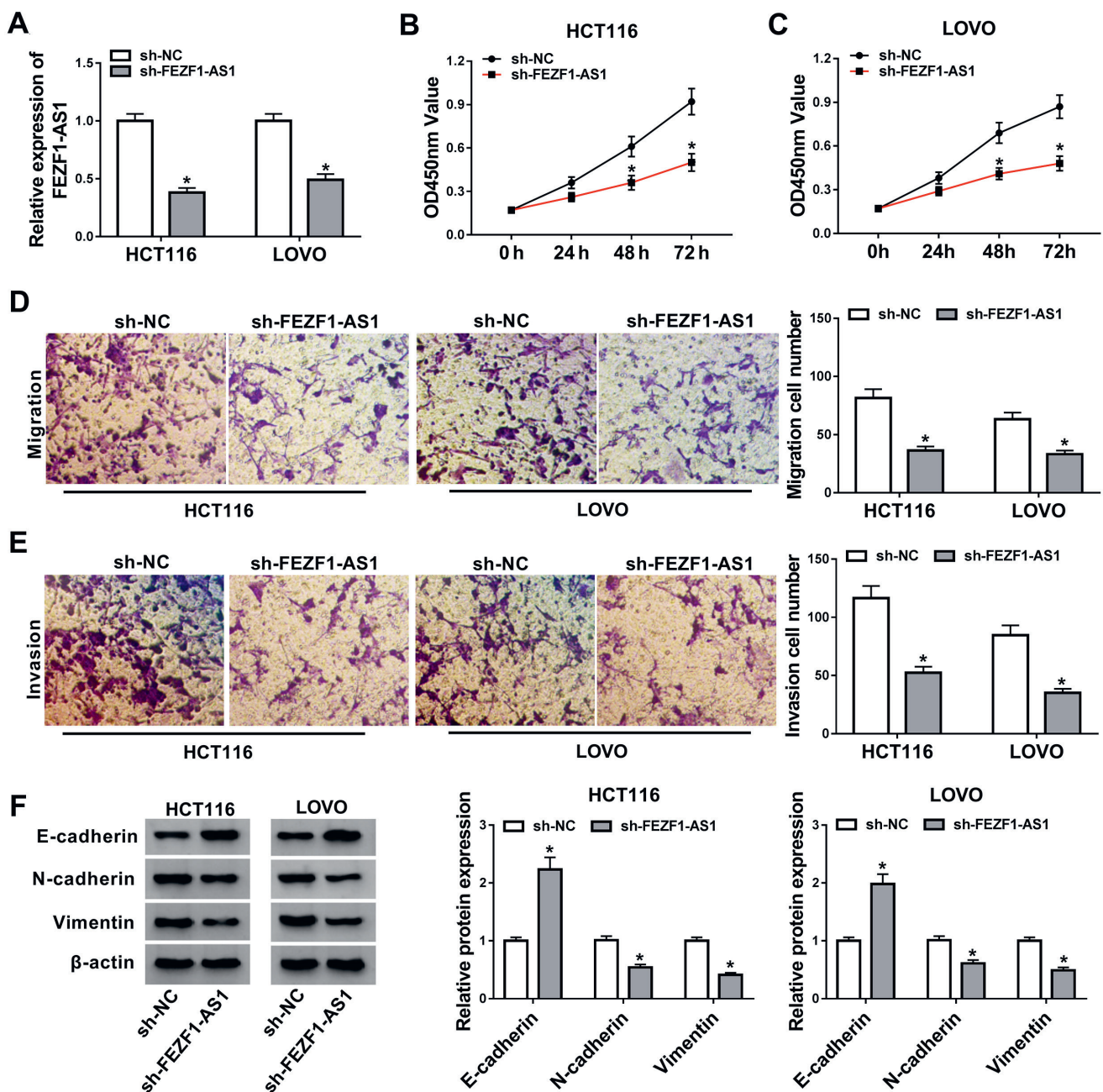
Fig. 2. FEZF1-AS1 knockdown regulated colorectal cancer (CRC) progression. HCT116 and LOVO cells were transfected with sh-FEZF1-AS1 and negative control (sh-NC). A. The quantitative real-time polymerase chain reaction (qRT-PCR) was used to measure FEZF1-AS1 expression; B and C. CRC cell proliferation was measured with Cell Counting Kit-8 (CCK-8) assay; D and E. Representative images and statistical results described cell migration and invasion abilities; F. Western blot analysis was performed to assess E-cadherin, N-cadherin and vimentin protein level, *p < 0.05
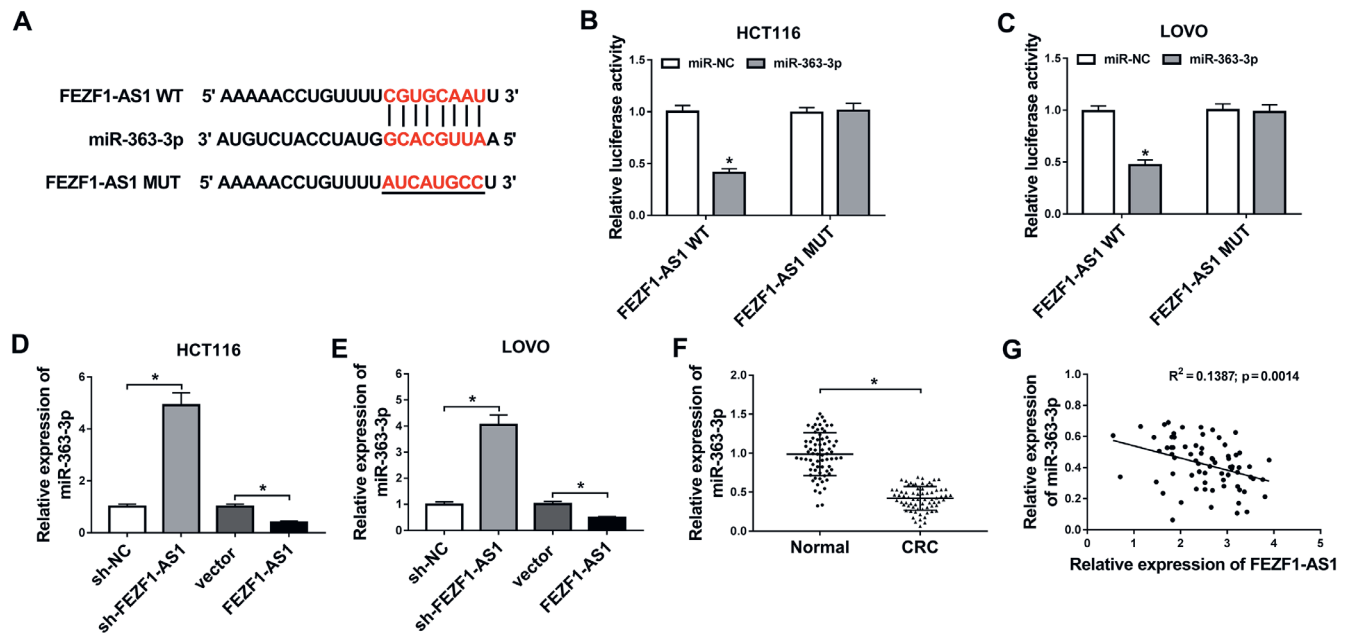
Fig. 3. MiR-363-3p could interact with FEZF1-AS1. A. The binding sites between FEZF1-AS1 and miR-363-3p; B and C. The interaction between FEZF1-AS1 and miR-363-3p was confirmed using dual-luciferase reporter assay; D and E. The expression of miR-363-3p in HCT116 and LOVO cells transfected with sh-FEZF1-AS1 and FEZF1-AS1 overexpression vector was determined using quantitative real-time polymerase chain reaction (qRT-PCR); F. miR-363-3p expression in colorectal cancer (CRC) tissues (CRC, n = 71) and adjacent normal tissues (normal, n = 71) was detected using qRT-PCR; G. The correlation analysis between miR-363-3p and FEZF1-AS1 expression were determined with Pearson correlation coefficient analysis, *p < 0.05

FEZF1-AS1 knockdown hindered CRC proliferation, migration, invasion, and EMT

To explore the effects of lncRNA FEZF1-AS1 on CRC progression, FEZF1-AS1 expression was silenced in HCT116 and LOVO cells using sh-FEZF1-AS1. The quantitative real-time polymerase chain reaction (qRT-PCR) results indicated that sh-FEZF1-AS1 had a significant silencing capacity on FEZF1-AS1 expression in both cells (Fig. 2A). The CCK-8 assay demonstrated that compared with the sh-NC group, downregulation of FEZF1-AS1 could suppress cell proliferation in HCT116 and LOVO cells (Fig. 2B,C). Furthermore, the ability of cells to migrate and invade was significantly reduced following silencing FEZF1-AS1 in HCT116 and LOVO cells (Fig. 2D,E). At the same time, we explored the levels of EMT-related proteins and found that the epithelial marker E-cadherin level was increased, while mesenchymal markers N-cadherin and vimentin levels were decreased in HCT116 and LOVO cells following FEZF1-AS1 silencing (Fig. 2F). Hence, these data demonstrated that silenced FEZF1-AS1 could hinder the proliferation, metastasis and EMT of CRC.

FEZF1-AS1 acted as miR-363-3p sponge

To further study the mechanism of FEZF1-AS1 in CRC progression, we predicted the potential targeted miRNAs of FEZF1-AS1 using the StarBase tool (http://starbase.sysu.edu.cn/). As shown in Fig. 3A, the potential complementary binding sites between FEZF1-AS1 and miR-363-3p are presented, and the WT and MUT FEZF1-AS1 vectors were constructed. Dual-luciferase reporter assay results showed that miR-363-3p mimic restrained the luciferase activity of FEZF1-AS1 WT vector, while not affecting that of the FEZF1-AS1 MUT vector in HCT116 and LOVO cells (Fig. 3B,C). Furthermore, we explored the impact of FEZF1-AS1 expression on miR-363-3p, and showed that FEZF1-AS1 knockdown could promote, while overexpression could inhibit the expression of miR-363-3p (Fig. 3D,E). Furthermore, we determined that miR-363-3p had a lower expression in CRC tissues (Fig. 3F), and correlation analysis showed that this was negatively correlated to FEZF1-AS1 expression (Fig. 3G). These results revealed that miR-363-3p could interact with FEZF1-AS1 in CRC cells.

MiR-363-3p inhibition reversed the suppressive effect of FEZF1-AS1 silencing on CRC progression

Subsequently, we verified the effect of miR-363-3p expression on CRC progression and confirmed whether FEZF1-AS1 regulated CRC progression by sponging miR-363-3p. Here, miR-NC or miR-363-3p mimic were transfected into HCT116 and LOVO cells, and sh-FEZF1-AS1 and anti-miR-363-3p were co-transfected into the same cells. MiR-363-3p mimic markedly increased miR-363-3p expression, and its inhibitor could also significantly reduce miR-363-3p expression in the presence of sh-FEZF1-AS1 (Fig. 4A,B). Results of the CCK-8 assay indicated that overexpression of miR-363-3p blocked the proliferation of CRC cells, while
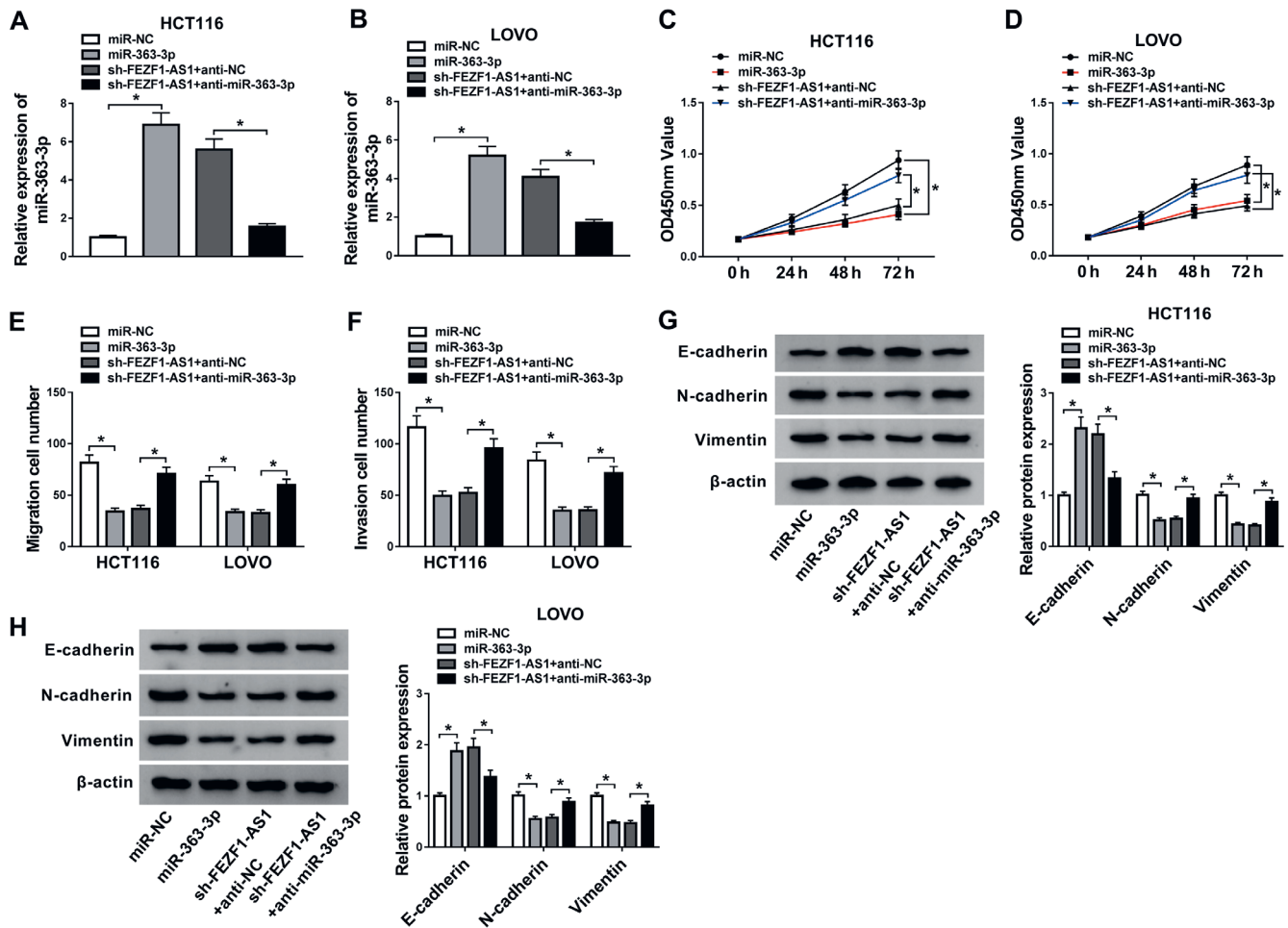
Fig. 4. miR-363-3p and FEZF1-AS1 regulated the progression of colorectal cancer (CRC) cells. The miR-363-3p mimic, miR-NC, sh-FEZF1-AS1, anti-NC, or anti-miR-363-3p were transfected into HCT116 and LOVO cells. A and B. Expression of miR-363-3p was determined using quantitative real-time polymerase chain reaction (qRT-PCR); C and D. Cell proliferation following transfection was measured with Cell Counting Kit-8 (CCK-8) assay; E and F. Cell migration and invasion of transfected cells in transwell assays; G and H. Protein levels of E-cadherin, N-cadherin and vimentin as assessed with western blot analysis, *p < 0.05

anti-miR-363-3p could inhibit CRC cell proliferation, as promoted by FEZF1-AS1 silencing (Fig. 4C,D). Similarly, transwell assay also revealed that miR-363-3p overexpression could hinder HCT116 and LOVO cell migration and invasion, while its inhibitor also could abolish the suppression effect of FEZF1-AS1 knockdown (Fig. 4E,F). Moreover, western blot analysis showed that the miR-363-3p increased E-cadherin protein level, while decreasing N-cadherin and vimentin protein levels in HCT116 and LOVO cells. Finally, miR-363-3p inhibitor could reverse the increased E-cadherin expression and the decreasing effect on N-cadherin and vimentin expression when FEZF1-AS1 was knocked down (Fig. 4G,H). Hence, these data indicated that FEZF1-AS1 sponged miR-363-3p to regulate CRC progression.

PRRX1 was a target of miR-363-3p

Then, StarBase tool was used to predict the downstream target of miR-363-3p, and PRRX1 3'UTR was found to have binding sites for miR-363-3p (Fig. 5A). Further experiments identified that miR-363-3p mimic suppressed

the luciferase activity of PRRX1 WT vector in HCT116 and LOVO cells, while not affecting that of the PRRX1 MUT vector (Fig. 5B,C). Furthermore, western blot analysis demonstrated that the protein level of PRRX1 was significantly reduced by miR-363-3p overexpression, and promoted by miR-363-3p inhibition in HCT116 and LOVO cells (Fig. 5D,E). These data suggested that miR-363-3p could target PRRX1 in CRC cells.

PRRX1 overexpression reversed the regulation of sh-FEZF1-AS1 on CRC progression

To verify whether PRRX1 was involved in the regulation of FEZF1-AS1 on CRC cell progression, sh-FEZF1-AS1 and PRRX1 overexpression vector were co-transfected into HCT116 and LOVO cells. The detection of PRRX1 protein level showed that knockdown of FEZF1-AS1 decreased the level of PRRX1, while this effect could be reversed by the overexpression of PRRX1 (Fig. 6A,B). The CCK-8 and transwell assays revealed that the aberrant overexpression of PRRX1 recovered the inhibiting
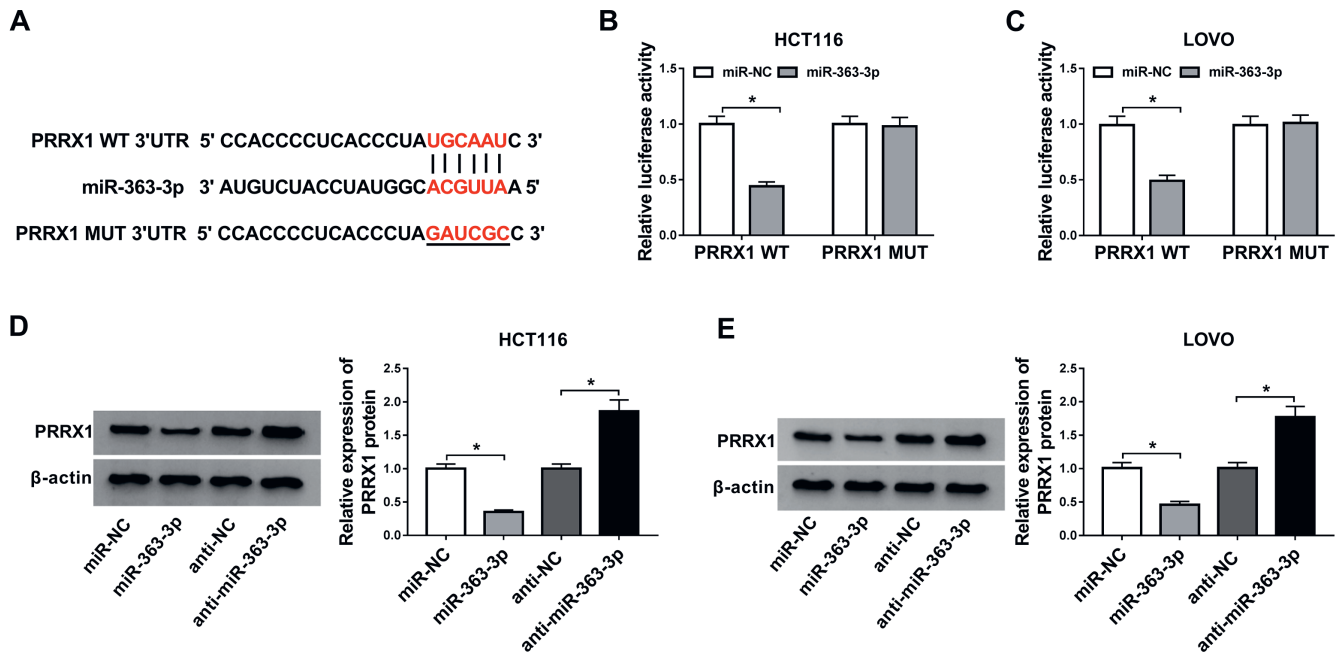
Fig. 5. PRRX1 was a target of miR-363-3p; A. The sequences of PRRX1-WT and PRRX1-MUT; B and C. Dual-luciferase reporter assay was employed to assess the interaction between PRRX1 and miR-363-3p; D and E. The protein level of PRRX1 in HCT116 and LOVO cells transfected with miR-363-3p mimic or inhibitor were examined with western blot analysis, *p < 0.05
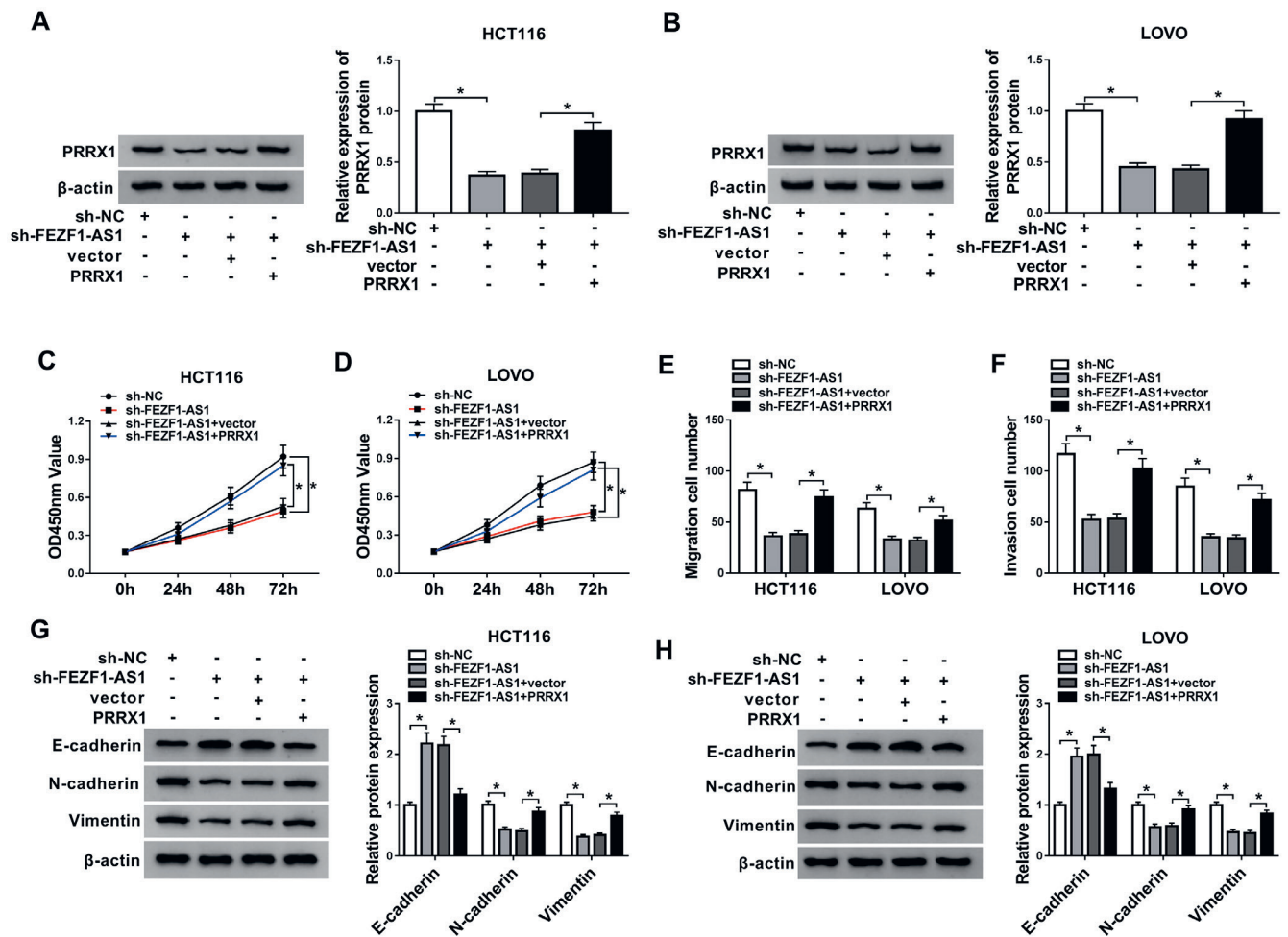
Fig. 6. PRRX1 overexpression regulated colorectal cancer (CRC) progression. HCT116 and LOVO cells were transfected with negative control (sh-NC), sh-FEZF1-AS1, sh-FEZF1-AS1 + vector, or sh-FEZF1-AS1 + PRRX1. A and B. Protein levels of PRRX1 as detected with western blot analysis; C and D. Cell proliferation of transfected cells using a Cell Counting Kit-8 (CCK-8) assay; E and F. Cell migration and invasion of transfected cells as measured using transwell assay; G and H. Western blot analysis was used to determine the E-cadherin, N-cadherin and vimentin protein levels, *p < 0.05
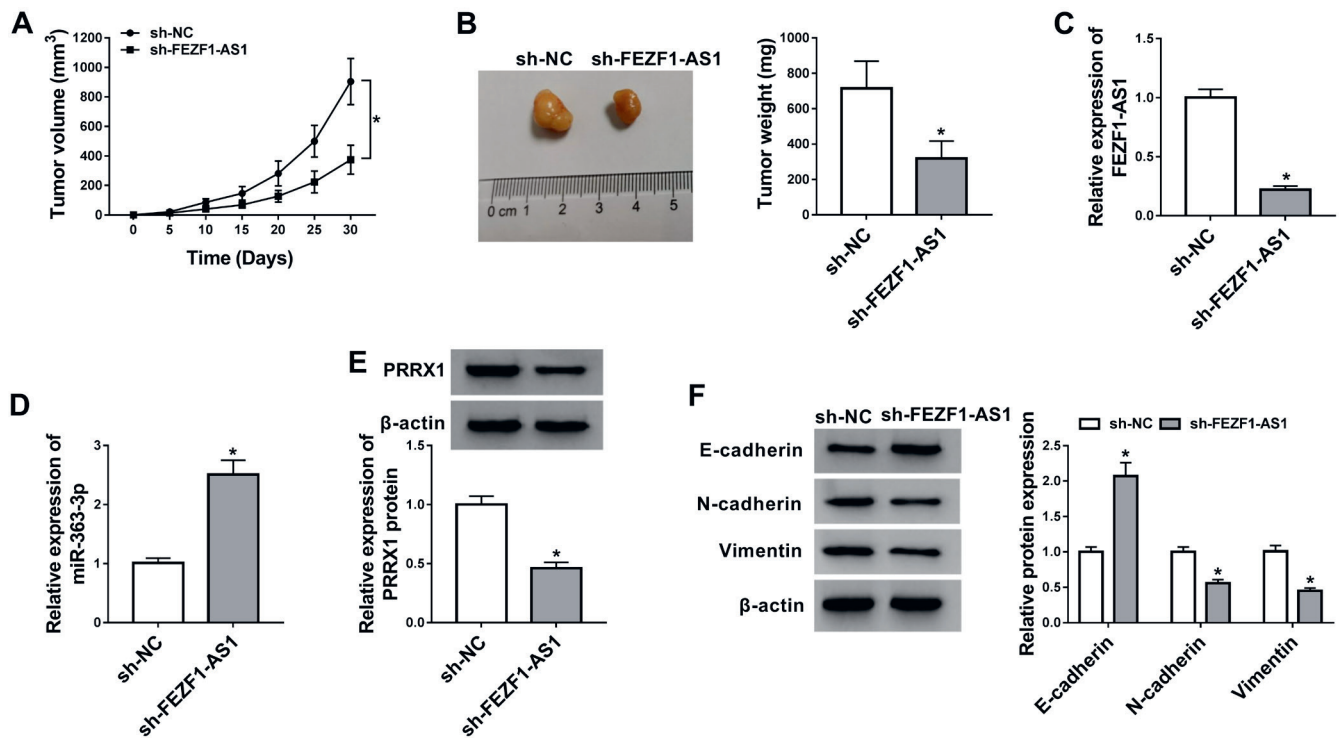
Fig. 7. FEZF1-AS1 silencing regulated colorectal cancer (CRC) tumor growth. Tumor volume (A) and tumor weight (B) were measured in mouse xenograft models; C and D. The FEZF1-AS1 and miR-363-3p expression levels were examined using quantitative real-time polymerase chain reaction (qRT-PCR); E, F. The PRRX1, E-cadherin, N-cadherin, and vimentin protein levels were measured using western blot analysis, *p < 0.05

effects of FEZF1-AS1 knockdown on CRC cell proliferation, migration and invasion (Fig. 6C–F). Furthermore, PRRX1 overexpression also reversed the promoting effect of FEZF1-AS1 knockdown on E-cadherin expression, and the inhibiting effect on N-cadherin and vimentin expression in HCT116 and LOVO cells (Fig. 6G,H). The above results suggest that PRRX1 participated in the regulation of FEZF1-AS1 on CRC progression.

Interference of FEZF1-AS1 reduced CRC tumor growth

To further confirm the influence of FEZF1-AS1 on CRC progression, HCT116 cells transfected with sh-FEZF1-AS1 were subcutaneously injected into nude mice. Following 30 days of monitoring, the tumor volume of the sh-FEZF1-AS1 group was reduced when compared to the sh-NC group (Fig. 7A). Furthermore, tumor weight also reduced in the sh-FEZF1-AS1 group (Fig. 7B). Through detecting the expression of FEZF1-AS1 and miR-363-3p in the tumors, we found that FEZF1-AS1 expression was significantly decreased (Fig. 7C), while miR-363-3p was markedly increased in the tumor tissues of the sh-FEZF1-AS1 group (Fig. 7D). Moreover, western blot analysis showed that FEZF1-AS1 knockdown could block the protein level of PRRX1 in tumor tissues of mice (Fig. 7E), promote the E-cadherin expression and reduce the N-cadherin and vimentin expression (Fig. 7F). These results confirmed that FEZF1-AS1 had a cancer-promoting effect in CRC.

Discussion

Recent studies have shown that lncRNAs functioned as tumor suppressors or promoters in CRC development and progression. For example, lncRNA *MIR17HG* promoted CRC progression,[19] and lncRNA *ROR1-AS1* enhanced CRC cell metastasis and proliferation, both of which played a role as oncogenes in CRC.[20] However, lncRNA GAS5 inhibited metastasis and promoted autophagy of CRC cells to suppress CRC.[21] In other CRC-related investigations, Bian et al. found that FEZF1-AS1 could bind to the PKM2 protein to promote aerobic glycolysis and activate STAT3 signaling to accelerate the progression of CRC.[22] Also, Chen et al. proposed that FEZF1-AS1 may promote FEZF1 and in turn facilitate CRC proliferation, migration and invasion.[23] Similar to these findings, our data confirmed that levels of lncRNA FEZF1-AS1 were significantly upregulated in CRC. Higher FEZF1-AS1 was related to TNM stage, tumor grade, distant metastasis, and overall survival rate of CRC patients. Functional experiments showed that FEZF1-AS1 knockdown restrained CRC cell proliferation, metastasis and EMT, and decreased CRC tumor growth. Consistent with the results of previous studies,[22,23] our results verified that *FEZF1-AS1* could be used as an oncogene in CRC, similar to its role in other cancers.[24,25]

To investigate the function of FEZF1-AS1 as a ceRNA, we performed bioinformatics predictions and found that miR-363-3p had complementary binding sites. Previous research has indicated that miR-363-3p took part

in the regulation of various cancers, including glioma, osteosarcoma and gastric cancer.[26–28] Furthermore, miR-363-3p has been shown to be related to the EMT process.[29,30] In this, miR-363-3p was confirmed to have decreased expression in CRC. FEZF1-AS1 silencing hindered miR-363-3p level in vitro and in vivo. Moreover, knockdown of FEZF1-AS1 had the same effect as miR-363-3p overexpression, both of which could promote the level of miR-363-3p and block proliferation, metastasis and EMT of CRC cells, while the miR-363-3p inhibitor could reverse the these effects. Therefore, we confirmed that miR-363-3p, as the absorption target of FEZF1-AS1, participates in the regulation of CRC progression though interactions with FEZF1-AS1.

Paired-related homeobox 1 was found to be an EMT inducer that participates in the metastasis of various cancers.[31,32] Investigations by Takahashi et al. suggested that PRRX1 induced EMT and was involved in metastasis and poor prognosis of CRC patients.[33] Interestingly, through prediction and verification, we discovered that PRRX1 was a target of miR-363-3p. Furthermore, we also found that PRRX1 overexpression reversed the inhibitory functions of FEZF1-AS1 silencing on CRC cell proliferation, metastasis and EMT. Additionally, we discovered that PRRX1 expression was positively regulated by FEZF1-AS1 in vitro and in vivo. These data suggested that FEZF1-AS1 regulated CRC progression by mediating the miR-363-3p/PRRX1 axis.

Limitations

The limitation of this study is that we did not further detect classical signaling pathways that might be involved in the modulation of FEZF1-AS1/miR-363-3p/PRRX1 axis in CRC.

Conclusions

Our studies suggested that lncRNA FEZF1-AS1 upregulated PRRX1 by sponging miR-363-3p to promote the proliferation, metastasis and EMT of CRC. The discovery of the FEZF1-AS1/miR-363-3p/PRRX1 axis elucidated the mechanism of FEZF1-AS1 in CRC and provided new avenues of investigation into the determination of CRC therapeutic targets.

ORCID iDs

Tongtong Zhang https://orcid.org/0000-0002-1121-021X
Suyang Yu https://orcid.org/0000-0002-9034-9294
Shipeng Zhao https://orcid.org/0000-0003-4522-2208

References

1. Brenner H, Kloor M, Pox CP. Colorectal cancer. *Lancet*. 2014;383(9927): 1490–1502. doi:10.1016/S0140-6736(13)61649-9
2. Siegel RL, Miller KD, Fedewa SA, et al. Colorectal cancer statistics, 2017. *CA Cancer J Clin*. 2017;67(3):177–193. doi:10.3322/caac.21395
3. Torre LA, Bray F, Siegel RL, Ferlay J, Lortet-Tieulent J, Jemal A. Global cancer statistics, 2012. *CA Cancer J Clin*. 2015;65(2):87–108. doi:10.3322/caac.21262
4. Qi L, Ding Y. Analysis of metastasis associated signal regulatory network in colorectal cancer. *Biochem Biophys Res Commun*. 2018;501(1): 113–118. doi:10.1016/j.bbrc.2018.04.186
5. Huang R, Zong X. Aberrant cancer metabolism in epithelial-mesenchymal transition and cancer metastasis: Mechanisms in cancer progression. *Crit Rev Oncol Hematol*. 2017;115:13–22. doi:10.1016/j.critrevonc.2017.04.005
6. Bhan A, Soleimani M, Mandal SS. Long noncoding RNA and cancer: A new paradigm. *Cancer Res*. 2017;77(15):3965–3981. doi:10.1158/0008-5472.CAN-16-2634
7. Wei L, Wang X, Lv L, Zheng Y, Zhang N, Yang M. The emerging role of noncoding RNAs in colorectal cancer chemoresistance. *Cell Oncol*. 2019;42(6):757–768. doi:10.1007/s13402-019-00466-8
8. Boon RA, Jae N, Holdt L, Dimmeler S. Long noncoding RNAs: From clinical genetics to therapeutic targets? *J Am Coll Cardiol*. 2016;67(10): 1214–1226. doi:10.1016/j.jacc.2015.12.051
9. Tay Y, Rinn J, Pandolfi PP. The multilayered complexity of ceRNA crosstalk and competition. *Nature*. 2014;505(7483):344–352. doi:10.1038/nature12986
10. Wilusz JE, Sunwoo H, Spector DL. Long noncoding RNAs: Functional surprises from the RNA world. *Genes Dev*. 2009;23(13):1494–1504. doi:10.1101/gad.1800909
11. Jiang P, Han X, Zheng Y, Sui J, Bi W. Long non-coding RNA NKILA serves as a biomarker in the early diagnosis and prognosis of patients with colorectal cancer. *Oncol Lett*. 2019;18(2):2109–2117. doi:10.3892/ol.2019.10524
12. Ren Y, Zhao C, He Y, Xu H, Min X. Long non-coding RNA bladder cancer-associated transcript 2 contributes to disease progression, chemoresistance and poor survival of patients with colorectal cancer. *Oncol Lett*. 2019;18(2):2050–2058. doi:10.3892/ol.2019.10487
13. Wang W, Xie Y, Chen F, et al. LncRNA MEG3 acts a biomarker and regulates cell functions by targeting ADAR1 in colorectal cancer. *World J Gastroenterol*. 2019;25(29):3972–3984. doi:10.3748/wjg.v25.i29.3972
14. Xu L, Hou TJ, Yang P. Mechanism of lncRNA FEZF1-AS1 in promoting the occurrence and development of oral squamous cell carcinoma through targeting miR-196a. *Eur Rev Med Pharmacol Sci*. 2019;23(15): 6505–6515. doi:10.26355/eurrev_201908_18534
15. Quan LJ, Wang WJ. FEZF1-AS1 functions as an oncogenic lncRNA in retinoblastoma. *Biosci Rep*. 2019;39(5):BSR20190754. doi:10.1042/BSR20190754
16. Zhu LF, Song LD, Xu Q, Zhan JF. Highly expressed long non-coding RNA FEZF1-AS1 promotes cells proliferation and metastasis through Notch signaling in prostate cancer. *Eur Rev Med Pharmacol Sci*. 2019;23(12):5122–5132. doi:10.26355/eurrev_201906_18176
17. Cheng Y. FEZF1-AS1 is a key regulator of cell cycle, epithelial-mesenchymal transition and Wnt/beta-catenin signaling in nasopharyngeal carcinoma cells. *Biosci Rep*. 2019;39(1):BSR20180906. doi:10.1042/BSR20180906
18. Wang YD, Sun XJ, Yin JJ, et al. Long non-coding RNA FEZF1-AS1 promotes cell invasion and epithelial–mesenchymal transition through JAK2/STAT3 signaling pathway in human hepatocellular carcinoma. *Biomed Pharmacother*. 2018;106:134–141. doi:10.1016/j.biopha.2018.05.116
19. Xu J, Meng Q, Li X, et al. Long non-coding RNA MIR17HG promotes colorectal cancer progression via miR-17-5p. *Cancer Res*. 2019;79(19): 4882–4895. doi:10.1158/0008-5472.CAN-18-3880
20. Liao T, Maierdan SL, Lv C. ROR1-AS1 promotes tumorigenesis of colorectal cancer via targeting Wnt/beta-catenin. *Eur Rev Med Pharmacol Sci*. 2019;23(3 Suppl):217–223. doi:10.26355/eurrev_201908_18650
21. Liu L, Wang HJ, Meng T, et al. lncRNA GAS5 inhibits cell migration and invasion and promotes autophagy by targeting miR-222-3p via the GAS5/PTEN-signaling pathway in CRC. *Mol Ther Nucleic Acids*. 2019;17:644–656. doi:10.1016/j.omtn.2019.06.009
22. Bian Z, Zhang J, Li M, et al. LncRNA-FEZF1-AS1 promotes tumor proliferation and metastasis in colorectal cancer by regulating PKM2 signaling. *Clin Cancer Res*. 2018;24(19):4808–4819. doi:10.1158/1078-0432.CCR-17-2967
23. Chen N, Guo D, Xu Q, et al. Long non-coding RNA FEZF1-AS1 facilitates cell proliferation and migration in colorectal carcinoma. *Oncotarget*. 2016;7(10):11271–11283. doi:10.18632/oncotarget.7168

24. Shi C, Sun L, Song Y. FEZF1-AS1: A novel vital oncogenic lncRNA in multiple human malignancies. *Biosci Rep*. 2019;39(6):BSR20191202. doi:10.1042/BSR20191202

25. Ou ZL, Zhang M, Ji LD, et al. Long noncoding RNA FEZF1-AS1 predicts poor prognosis and modulates pancreatic cancer cell proliferation and invasion through miR-142/HIF-1alpha and miR-133a/EGFR upon hypoxia/normoxia . *J Cell Physiol*. 2019. doi:10.1002/jcp.28188

26. Xu DX, Guo JJ, Zhu GY, Wu HJ, Zhang QS, Cui T. MiR-363-3p modulates cell growth and invasion in glioma by directly targeting pyruvate dehydrogenase B. *Eur Rev Med Pharmacol Sci*. 2018;22(16):5230–5239. doi:10.26355/eurrev_201808_15721

27. Wang K, Yan L, Lu F. miR-363-3p Inhibits osteosarcoma cell proliferation and invasion via targeting SOX4. *Oncol Res*. 2019;27(2):157–163. doi:10.3727/096504018X15190861873459

28. Song B, Yan J, Liu C, Zhou H, Zheng Y. Tumor suppressor role of miR-363-3p in gastric cancer. *Med Sci Monit*. 2015;21:4074–4080. doi:10.12659/msm.896556

29. Hu F, Min J, Cao X, et al. MiR-363-3p inhibits the epithelial-to-mes-enchymal transition and suppresses metastasis in colorectal cancer by targeting Sox4. *Biochem Biophys Res Commun*. 2016;474(1):35–42. doi:10.1016/j.bbrc.2016.04.055

30. Chang J, Gao F, Chu H, Lou L, Wang H, Chen Y. miR-363-3p inhibits migration, invasion, and epithelial-mesenchymal transition by targeting NEDD9 and SOX4 in non-small-cell lung cancer. *J Cell Physiol*. 2019;235(2):1808–1820. doi:10.1002/jcp.29099

31. Guo J, Fu Z, Wei J, Lu W, Feng J, Zhang S. PRRX1 promotes epithelial–mesenchymal transition through the Wnt/beta-catenin pathway in gastric cancer. *Med Oncol*. 2015;32(1):393. doi:10.1007/s12032-014-0393-x

32. Hirata H, Sugimachi K, Takahashi Y, et al. Downregulation of PRRX1 confers cancer stem cell-like properties and predicts poor prognosis in hepatocellular carcinoma. *Ann Surg Oncol*. 2015;22(Suppl 3):S1402–S1409. doi:10.1245/s10434-014-4242-0

33. Takahashi Y, Sawada G, Kurashige J, et al. Paired related homoeobox 1, a new EMT inducer, is involved in metastasis and poor prognosis in colorectal cancer. *Br J Cancer*. 2013;109(2):307–311. doi:10.1038/bjc.2013.339

Knockdown of miR-15b partially reverses the cisplatin resistance of NSCLC through the GSK-3β/MCL-1 pathway

Tianjian Lu[1,B–D], Weiping Lu[2,A,E,F], Chunyi Jia[3,B–D], Shanguang Lou[2,B,C], Yan Zhang[4,B,C]

[1] Department of Thoracic Surgery, West China Hospital, Sichuan University, Chengdu, China

[2] Department of Thoracic Surgery, Changchun Tumor Hospital, China

[3] Department of Thoracic Surgery, Jilin Tumor Hospital, Changchun, China

[4] Department of Anesthesia, Nanhua University, Hengyang, China

A – research concept and design; B – collection and/or assembly of data; C – data analysis and interpretation;
D – writing the article; E – critical revision of the article; F – final approval of the article

Address for correspondence
Weiping Lu
E-mail: weipinglu@tom.com

Abstract

Background. Induction of acquired drug resistance occurs frequently with cisplatin-based therapy for non-small cell lung cancer (NSCLC). As recent studies have demonstrated that deregulation of microRNAs (miRNAs) is associated with drug resistance in cancers, correcting the deregulation of miRNAs represents a promising strategy to reverse acquired resistance in NSCLC.

Objectives. This study investigated the functional role of miR-15b in cisplatin resistance in NSCLC.

Materials and methods. Cisplatin-resistant PC9 and A549 NSCLC cell lines (PC9-R and A549-R) were established through long-term exposure to cisplatin. Differences in miR-15b expression between cisplatin-resistant NSCLC cell lines and their parental cell lines were identified through quantitative real-time polymerase chain reaction (qRT-PCR). The effect of anti-miR-15b on the sensitivity of PC9-R and A549-R to cisplatin-induced cytotoxicity was evaluated using Cell Counting Kit-8 (CCK-8) assays. Regulation of GSK-3β by miR-15b was confirmed with luciferase reporter assays. Cell apoptosis and mitochondrial membrane potential (MMP) were measured using flow cytometry analysis.

Results. In PC9-R and A549-R cells, miR-15b was significantly overexpressed. However, knockdown of miR-15b clearly reduced cisplatin resistance in PC9-R and A549-R cells. Researching the mechanism, we proved that GSK-3β was the target of miR-15b. Knockdown of miR-15b significantly increased the expression GSK-3β and thus promoted the degradation of MCL-1, which is a key anti-apoptosis protein. As a result, anti-miR-15b expanded the cisplatin-induced apoptosis in cisplatin-resistant NSCLC cells.

Conclusions. Knockdown of miR-15b partially reversed cisplatin resistance in NSCLC cells through the GSK-3β/MCL-1 pathway.

Key words: NSCLC, cisplatin, GSK-3β, miR-15b, MCL-1

Background

Non-small-cell lung cancer (NSCLC) is the most common type of malignant tumor in the world. Despite current developments in medical technology, including surgery, radiotherapy and chemotherapy, no substantial change in survival has been seen, and NSCLC is still a leading cause of cancer-related deaths.[1,2] Therefore, NSCLC is a serious threat to human life. Today, chemotherapy is still an irreplaceable and valuable treatment for NSCLC patients without epidermal growth factor receptor (EGFR) mutation.[3,4] However, repeated chemotherapy usually reduces the sensitivity of cancer cells to the antineoplastic drugs.[5-7] Thus, drug resistance is a serious cause of poor prognoses in cancer patients, especially for NSCLC patients.[8,9] Overcoming the chemoresistance of NSCLC is an urgent need in current cancer therapy.

Today, cisplatin is still a frequently used platinum-based chemotherapeutic drug. Furthermore, cisplatin is still used as the first-line chemotherapeutic drug for patients with advanced NSCLC.[10] However, clinical application of cisplatin is limited by harsh side effects including nephrotoxicity, ototoxicity, neurotoxicity, bone marrow suppression, and digestive reaction.[11] Given this, combined treatment with sensitizing agents is desirable to increase the sensitivity of tumor cells to cisplatin.

As a broad-spectrum and cell cycle non-specific drug, cisplatin cross-links with DNAs to inhibit DNA replication and transcription. As a result, the initiated apoptotic process is accompanied by alterations of the outer mitochondrial membrane potential (MMP) and permeability. Finally, mitochondrial apoptosis occurs.[12,13] However, NSCLC cells usually acquired drug resistance to resist apoptotic pathways when they were under long-term cisplatin stress under the effect of cisplatin.[14,15] We aimed to explore the potential mechanisms and to reduce the cisplatin resistance of NSCLC.

MicroRNAs (miRNAs) are a group of short non-coding RNAs whose length is approx. 18–25 nucleotides.[16,17] They function as gene regulators via targeting mRNAs.[18,19] Since approx. 60% of all human genes are targeted by miRNAs, the miRNAs participate in various biological processes in cells.[20,21] Deregulation of miRNAs has been acknowledged to be responsible for tumorigenesis, cancer development and survival.[22,23] MiR-15b has been reported to function as an important member of cancer-related miRNAs. Studies indicate that miR-15b is frequently overexpressed in some cancers, including NSCLC.[24] Furthermore, previous research found that overexpression of miR-15b was associated with drug resistance in cancer.[25] Despite miR-15b having been shown to promote proliferation and invasion of NSCLC,[26] the role of miR-15b in chemoresistance in NSCLC is still unclear.

Objectives

The objective of this study was to investigate the functional role of miR-15b in cisplatin resistance in NSCLC. To achieve this, cisplatin-resistant NSCLC models were created to explore the potential role of miR-15b in cisplatin resistance.

Materials and methods

Cell lines

PC9 and A549, which are human NSCLC cell lines, were obtained from the Institute of Biochemistry and Cell Biology, Shanghai Institute for Biological Sciences, Chinese Academy of Sciences (Shanghai, China). Cells were maintained in RPMI-1640 medium (Gibco, Grand Island, USA) supplemented with 10% fetal bovine serum (FBS) in a 5% CO_2, 37°C incubator. To establish the cisplatin-resistant NSCLC cell models (PC9-R and A549-R), PC9 and A549 cells were exposed to increasing concentrations of cisplatin. In short, PC9 and A549 cell lines were initially treated with 0.5 μM cisplatin for 2 months. Then, the cisplatin concentration was increased by 0.1 μM every 2 weeks until the final concentration was 2 μM.

qRT-PCR

Relative expression of miR-15b, GSK-3β and MCL-1 was detected using quantitative reverse transcriptase real-time polymerase chain reaction (qRT-PCR) analysis. In short, Trizol Reagent (Life Technologies, Carlsbad, USA) was used to isolate the total RNAs of the cell lines. In order to detect miR-15b, cDNAs were synthesized with One Step PrimeScript miRNA cDNA Synthesis Kit (TaKaRa, Tokyo, Japan). In order to detect GSK-3β and MCL-1, cDNA was synthesized using M-MLV Reverse Transcriptase (Thermo Fisher Scientific, Waltham, USA) according to the manufacturer's instruction. Then, the relative expression of miR-15b, GSK-3β and MCL-1 was detected using TB Green® Premix Ex Taq™ II (TaKaRa) according to the manufacturer's instruction. Primers were obtained from Guangzhou RiboBio Co., Ltd. (Guangzhou, China) and had the following sequences: miR-15b, 5'-TAGCAGCACATCATGGTTTACA-3'; MCL-1 forward, 5'-TCGGACTCAACCTCTACTG-3' and reverse, 5'-GGCTTCCATCTCCTCAA-3'; GSK-3β forward, 5'-ACGCTCCCTGTGATTTAT-3' and reverse, 5'-CTCTGATTTGCTCCCTTG-3'. The PCR was performed under the following thermocycling conditions: 95°C for 30 s, followed by 40 cycles of 95°C for 5 s and 60°C for 34 s, and 1 cycle of 95°C for 15 s, 60°C for 60 s and 95°C for 15 s for dissociation. The fold change of miR-15b was normalized to U6 snRNA and the fold change of GSK-3β and MCL-1 was normalized to GAPDH with the comparative cycle threshold method ($2^{-\Delta\Delta CT}$).

Transfection

To knockdown the GSK-3β and MCL-1 directly, GSK-3β and MCL-1 siRNA were purchased from Santa Cruz Biotechnology (Santa Cruz, USA). To overexpress the GSK-3β and MCL-1 directly, the open reading frame of GSK-3β and MCL-1 without the 3'-UTR was amplified and cloned into the pcDNA3.1 vector (Life Technologies), respectively. miR-15b mimics (5'-UAGCAGCACAU-CAUGGUUUACA-3'), anti-miR-15b (5'-UGUAAAC-CAUGAUGUGCUGCUA-3') and negative control oligonucleotide (NCO, 5'-UGCACAGUUUAACCAGGAUUCA-3') were purchased from Genepharma Company (Shanghai, China). For transfection, plasmid (2 μg/mL) and RNA oligonucleotides (50 pmol/mL) were transfected into the NSCLC cells using Lipofectamine 2000 (Life Technologies) according to the manufacturer's instruction. Cells were collected and used for the following experiments 24 h after transfection.

Cell viability assay

$5 × 10^3$ transfected cells were seeded on 96-well plates. Then, different concentrations of cisplatin were used to treat these cells for 48 h. Subsequently, Cell Counting Kit-8 (CCK-8; 10 μL; Sigma–Aldrich, St. Louis, USA) was added to each well and incubated at 37°C for 2 h. The absorbance in each well was measured at 450 nm using an enzyme-linked immunosorbent assay (ELISA) microplate reader. Cell viability was calculated as follows: cell viability rate = optical density (OD) value in drug administration group/OD value in control group. The 50% inhibitory concentration (IC50) of cisplatin in the NSCLC cell lines was calculated according to the cell viability curves. Cell viability assays were repeated 3 times to calculate the IC50.

Luciferase reporter assay

According to the manufacturer's instruction, the GSK-3β 3' UTR containing the seed region of the miR-15b binding site (UGCUGCUU) was cloned into the pGL3 luciferase reporter vector (Promega, Madison, USA). The recombined luciferase reporter vector was named as pGL3-wt GSK-3β. The mutant plasmid, pGL3-mt GSK-3β, was created through mutating the seed region of the miR-15b binding site (UGCUGCUU to UGCACCUU) using a site-directed mutagenesis kit (TaKaRa). For luciferase reporter analysis, cells were co-transfected with the pGL3-wt GSK-3β (or pGL3-mt GSK-3β), Renilla luciferase pRL-TK vectors (Promega) and the miR-15b mimics (or anti-miR-15b) using Lipofectamine 2000. After 48 h incubation, luciferase activities were measured by using the Dual-Luciferase Reporter assay system (Promega). Relative firefly luciferase activities were determined through normalization to Renilla luciferase activities in each well.

Analysis of mitochondrial membrane potential and apoptosis

Treated cells were harvested and washed with PBS. For MMP analysis, cells were stained with JC-1 (Molecular Probes, Eugene, USA) followed by detection with flow cytometry (BD Biosciences, Franklin Lakes, USA). Cells that emitted red fluorescence were indicative of high mitochondrial membrane potential. To detect the apoptosis rate, the Annexin V-FITC Apoptosis Detection Kit (Sigma–Aldrich) was used according to the manufacturer's instructions. It is generally believed that Annexin V positive cells are the total number of apoptotic cells.

Statistical analyses

The data are expressed as mean ± standard deviation (SD) and obtained from 3 independent experiments. SPSS v. 15.0 (SPSS Inc., Chicago, USA) software was used for statistical analyses. Two-tailed t-tests were used to estimate the statistical difference between 2 groups. One-way analysis of variance (ANOVA) and Bonferroni post hoc tests were used to determine differences between three or more groups. A value of $p < 0.05$ was considered a significant difference.

Results

Overexpression of miR-15b in cisplatin-resistant NSCLC cells

We first evaluated the cisplatin resistance of PC9-R and A549-R cells. As shown in Fig. 1A, the cytotoxicity of cisplatin was slighter in PC9-R and A549-R cell lines compared to the PC9 and A549 cells. After analysis of the cell viability curves, we confirmed that the IC50 of cisplatin for PC9-R and A549-R was significantly higher than their parental cell lines PC9 and A549, respectively (Fig. 1B). After analysis of miR-15b, we found that miR-15b in PC9-R and A549-R cells was clearly overexpressed compared to the PC9 and A549 cells, respectively (Fig. 1C). These results suggested the potential role of miR-15b in determining the cisplatin resistance of NSCLC.

Knockdown of miR-15b reduced the cisplatin resistance in NSCLC cells

To investigate the role of miR-15b in the cisplatin resistance in NSCLC, we overexpressed the miR-15b directly in PC9 and A549 cells by transfecting the miR-15b mimics (Fig. 2A). Results of the cell viability assay showed that overexpression of miR-15b enhanced the resistance of PC9 and A549 cells to different concentrations of cisplatin (Fig. 2B). After analysis of the cell viability curves,
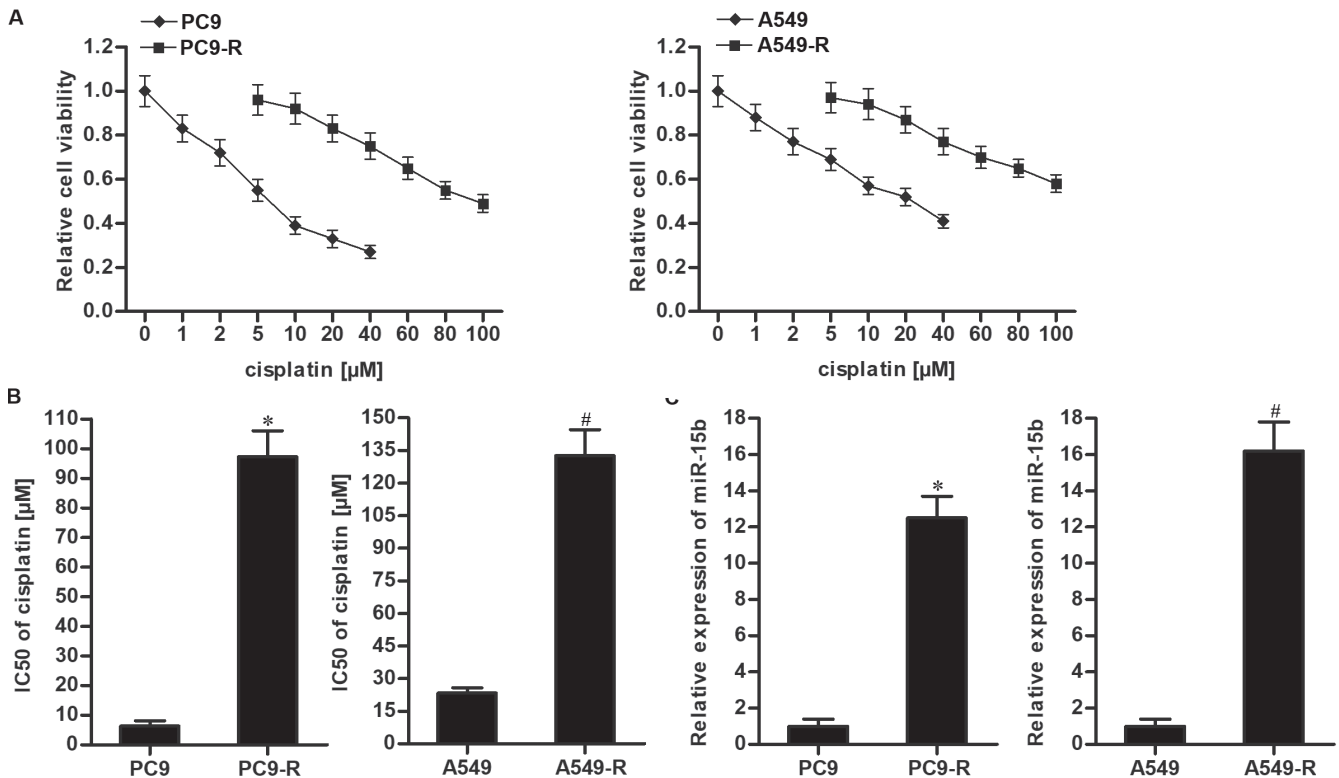
Fig. 1. Overexpression of miR-15b in cisplatin-resistant non-small-cell lung cancer (NSCLC) cells. A. Cisplatin sensitivity of cisplatin-resistant NSCLC cells (PC9-R and A549-R) and their parental NSCLC cells (PC9 and A549); B. IC50 of cisplatin in cisplatin-resistant NSCLC cells (PC9-R and A549-R) and their parental NSCLC cells (PC9 and A549); C. Differences of miR-15b expression between cisplatin-resistant NSCLC cells (PC9-R and A549-R) and their parental NSCLC cells (PC9 and A549). Data are presented as the means ±standard deviation (SD)

*p < 0.05 compared to PC9; #p < 0.05 compared to A549.

we confirmed that miR-15b increased the IC50 of cisplatin for PC9 and A549 cells (Fig. 2C). On the other hand, we knocked down miR-15b directly in PC9-R and A549-R cells through transfection with anti-miR-15b (Fig. 2D). We found that anti-miR-15b treatment increased the sensitivity of PC9-R and A549-R cells to different concentrations of cisplatin (Fig. 2E). After analysis of the cell viability curves, we confirmed that anti-miR-15b significantly decreased the IC50 of cisplatin for PC9-R and A549-R cells (Fig. 2F). Our data indicated that miR-15b partially determined the sensitivity of NSCLC cells to cisplatin. Furthermore, we demonstrated that knockdown of miR-15b can partially reverse cisplatin resistance in NSCLC.

MiR-15b targets GSK-3β in NSCLC

To explore how anti-miR-15b reduced the cisplatin resistance, miRanda (http://www.mirbase.org/), TargetScan (http://www.targetscan.org/vert_72/) and PicTar (https://pictar.mdc-berlin.de/cgi-bin/PicTar_vertebrate.cgi) databases were used to search for potential mRNA targets. The results showed that GSK-3β contained a putative binding site for miR-15b and was commonly predicted by all of these databases (Fig. 3A). Furthermore, in contrast to the overexpression of miR-15b in PC9-R and A549-R,

we found that the expression level of GSK-3β in PC9-R and A549-R cells was significantly lower than their parental PC9 and A549 cells (Fig. 3B). We therefore predicted that miR-15b targets GSK-3β in NSCLC. Subsequently, we altered the expression of miR-15b in PC9-R and A549-R cells using the miR-15b mimics and anti-miR-15b before detection of GSK-3β expression. We showed that miR-15b decreased the protein levels of GSK-3β, whereas anti-miR-15b increased the expression of GSK-3β (Fig. 3C). Furthermore, results of luciferase reporter assays showed that miR-15b significantly decreased the luciferase activities of pGL3-wt GSK-3β reporters, whereas anti-miR-15b clearly increased the luciferase activities of pGL3-wt GSK-3β reporters (Fig. 3D). Taken together, we confirmed that the expression of GSK-3β was regulated by miR-15b in PC9-R and A549-R cells.

Expression level of GSK-3β partially determines cisplatin resistance in NSCLC

To investigate the role of GSK-3β in cisplatin resistance in NSCLC, we performed gain-of-function and loss-of-function experiments using GSK-3β in NSCLC cells. We then found that GSK-3β siRNA treatment significantly reduced the cytotoxicity of cisplatin in PC9 and A549 cells
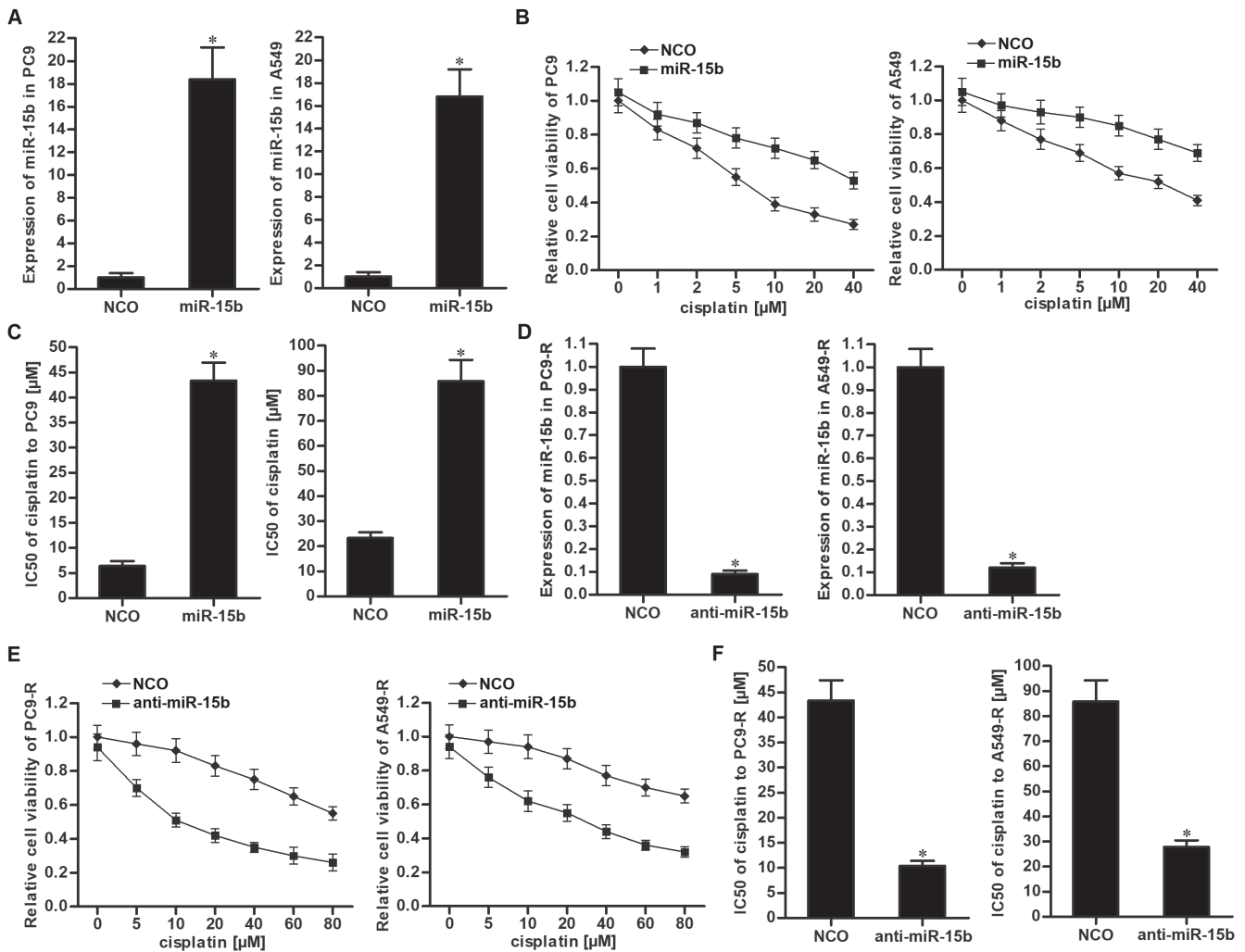
Fig. 2. Knockdown of miR-15b partially reversed cisplatin resistance in non-small-cell lung cancer (NSCLC). A. Transfection with miR-15b mimicked increased levels of miR-15b in PC9 and A549 cells; B. MiR-15b reduced the sensitivity of PC9 and A549 cells to cisplatin; C. MiR-15b increased the IC50 of cisplatin in PC9 and A549 cells; D. Transfection with anti-miR-15b decreased the level of miR-15b in PC9-R and A549-R cells; E. Anti-miR-15b reduced cisplatin resistance in PC9-R and A549-R cells; F. Anti-miR-15b decreased the IC50 of cisplatin in PC9-R and A549-R cells. Data are presented as the means ±standard deviation (SD)

*p < 0.05 compared to negative control oligonucleotide (NCO) group.

(Fig. 4A). On the other hand, we found that GSK-3β plasmid treatment clearly reduced cisplatin resistance in PC9-R and A549-R cells (Fig. 4B). These data indicated that reduction of GSK-3β was partially responsible for cisplatin resistance in PC9-R and A549-R cells.

Anti-miR-15b reduces cisplatin resistance in NSCLC by increasing GSK-3β expression

As anti-miR-15b significantly enhanced the effect of cisplatin in PC9-R and A549-R cells, we next investigated the role of GSK-3β in them. We found that cells treated with GSK-3β siRNA were resistant to the combination treatment with cisplatin and anti-miR-15b (Fig. 5A). We then confirmed that GSK-3β siRNA attenuated anti-miR-15b's reduction of the IC50 values for cisplatin in PC9-R and A549-R cells (Fig. 5B). Our data illustrate that anti-miR-15b partially reversed cisplatin resistance in NSCLC by increasing GSK-3β expression.

Anti-miR-15b inhibited the expression of MCL-1 by increasing GSK-3β expression

Previous research has indicated that GSK-3β induces degradation of MCL-1, which is a key anti-apoptotic protein.[27] In this study, we observed that MCL-1 was overexpressed in PC9-R and A549-R cells (Fig. 6A). Next, we found that direct knockdown of MCL-1 significantly enhanced the effect of cisplatin in PC9-R and A549-R cells (Fig. 6B). These data indicated that overexpression of MCL-1 was partially responsible for cisplatin resistance in NSCLC. On the other hand, we confirmed that anti-miR-15b inhibited the expression MCL-1, whereas knockdown of GSK-3β increased the MCL-1 level in PC9-R and A549-R cells that were co-treated with cisplatin and anti-miR-15b (Fig. 6C). We thus confirmed that anti-miR-15b inhibited the expression of MCL-1 through the GSK-3β pathway. Furthermore, we found that enforced expression of MCL-1 using the MCL-1 plasmid protected the PC9-R
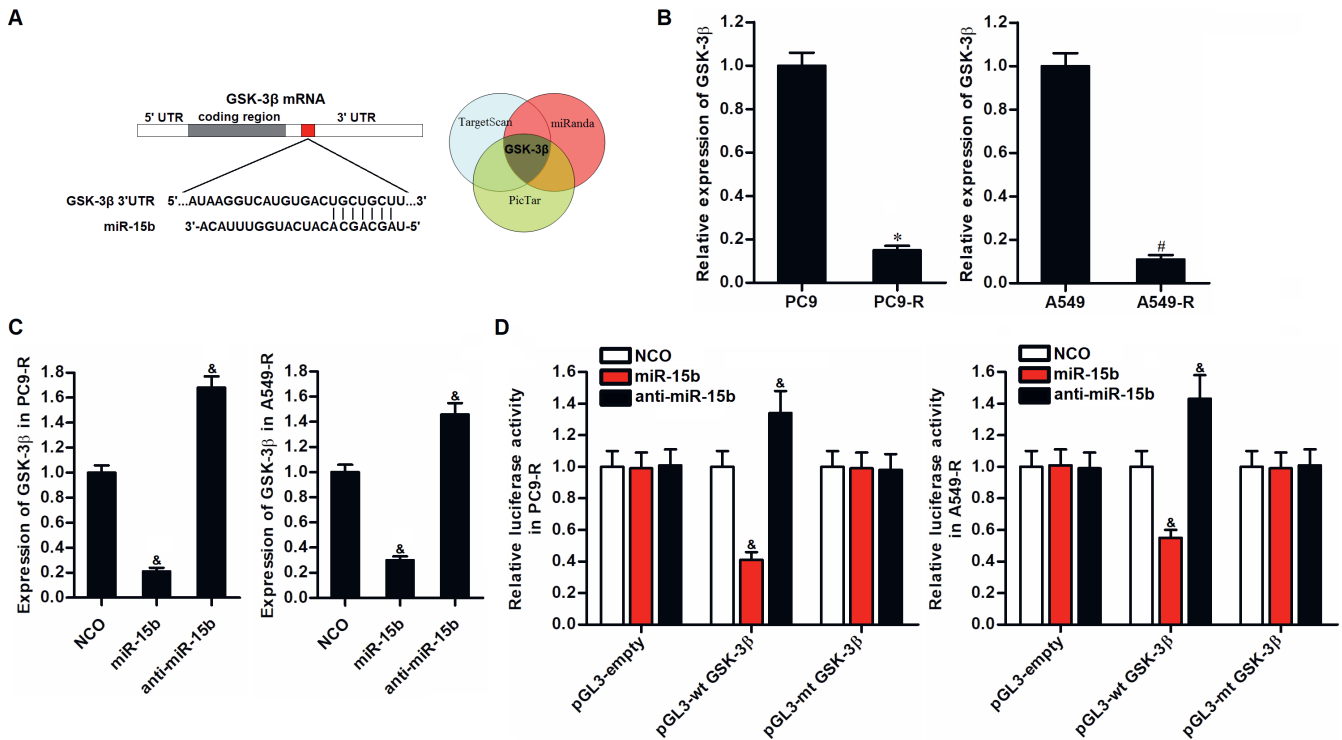
Fig. 3. GSK-3β was the target of miR-15b. A. Putative binding sequence of GSK-3β 3'-UTR paired with miR-15b; B. Expression of GSK-3β in cisplatin-resistant non-small-cell lung cancer (NSCLC) cells (PC9-R and A549-R) and their parental NSCLC cells (PC9 and A549); C. Effect of miR-15b and anti-miR-15b on the expression change of GSK-3β in PC9-R and A549-R cells; D. Effect of miR-15b and anti-miR-15b on the luciferase activities of pGL3-wt GSK-3β or pGL3-mt GSK-3β reporters. Data are presented as the means ±standard deviation (SD)

*$p < 0.05$ compared to PC9; #$p < 0.05$ compared to A549; &$p < 0.05$ compared to negative control oligonucleotide (NCO) group.
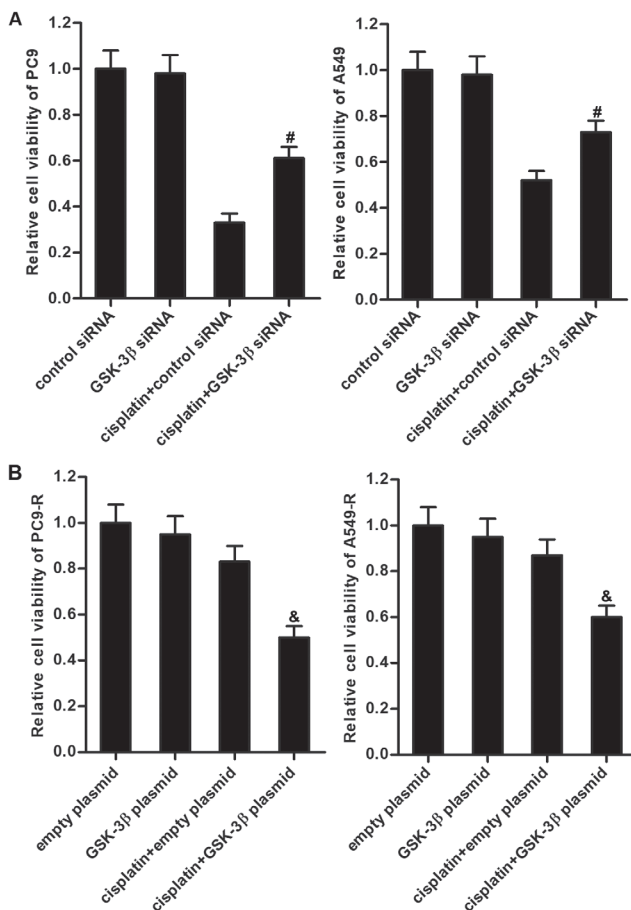
Fig. 4. Expression level of GSK-3β partially determined cisplatin resistance in non-small-cell lung cancer (NSCLC). A. GSK-3β siRNA decreased the cytotoxicity of cisplatin (20 μM) against PC9 and A549; B. GSK-3β plasmid increased the cytotoxicity of cisplatin (20 μM) against PC9-R and A549-R. The data are presented as the means ±standard deviation (SD)

#$p < 0.05$ compared to cisplatin+control siRNA group; &$p < 0.05$ compared to cisplatin+empty plasmid group.

and A549-R cells from the cytotoxicity induced by combination treatment with cisplatin and anti-miR-15b (Fig. 6D). These data illustrate that anti-miR-15b partially reduced cisplatin resistance in PC9-R and A549-R cells through the GSK-3β/MCL-1 pathway.

Anti-miR-15b enhanced the cisplatin-induced apoptosis of PC9-R and A549-R cells through the mitochondrial pathway

Our earlier results indicated that anti-miR-15b reduced cisplatin resistance in NSCLC. We next explored the role of anti-miR-15b in the cisplatin-induced apoptosis pathway. We showed that anti-miR-15b enhanced the effect of cisplatin in inducing the mitochondria collapse in PC9-R and A549-R cells (Fig. 7A). Accompanied by a decrease in mitochondrial membrane potential (MMP), the combination of cisplatin and anti-miR-15b induced significant
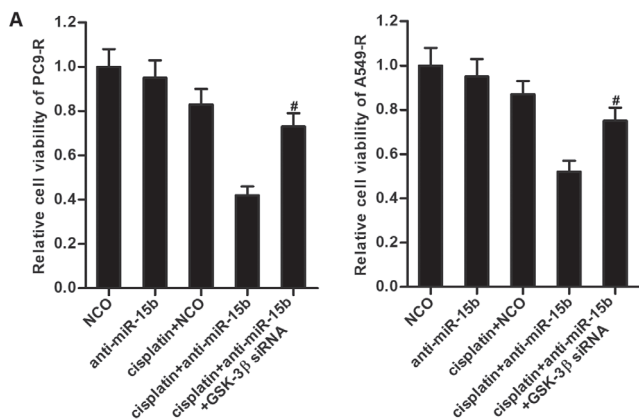
Fig. 5. Anti-miR-15b partially reversed cisplatin resistance in non-small-cell lung cancer (NSCLC) by increasing GSK-3β expression. A. Effect of GSK-3β siRNA on protection of PC9-R and A549-R cells from the cytotoxicity of co-treatment with cisplatin (20 μM) and anti-miR-15b; B. GSK-3β siRNA attenuated the effect of anti-miR-15b reducing the IC50 of cisplatin in PC9-R and A549-R cells. Data are presented as the means ±standard deviation (SD)

#p < 0.05 compared to cisplatin+anti-miR-15b group; &p < 0.05 compared to anti-miR-15b group.
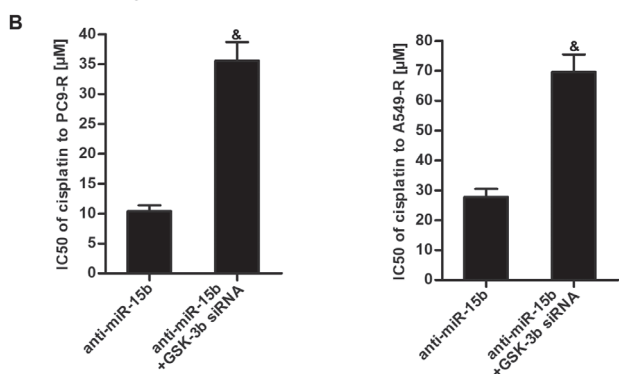
apoptosis of PC9-R and A549-R cells (Fig. 7B). Taken together, we demonstrated that anti-miR-15b enhanced the cisplatin-induced apoptosis of PC9-R and A549-R cells through the mitochondrial pathway.

Discussion

In this study, we continuously exposed NSCLC cell lines to cisplatin. As a result, these cells acquired resistance against cisplatin. Exploration of potential mechanisms and the use of novel approaches is needed to overcome cisplatin resistance in NSCLC. Recently, studies have indicated that chemoresistance in cancer is associated with deregulation of miRNAs. Correcting miRNA expression has been
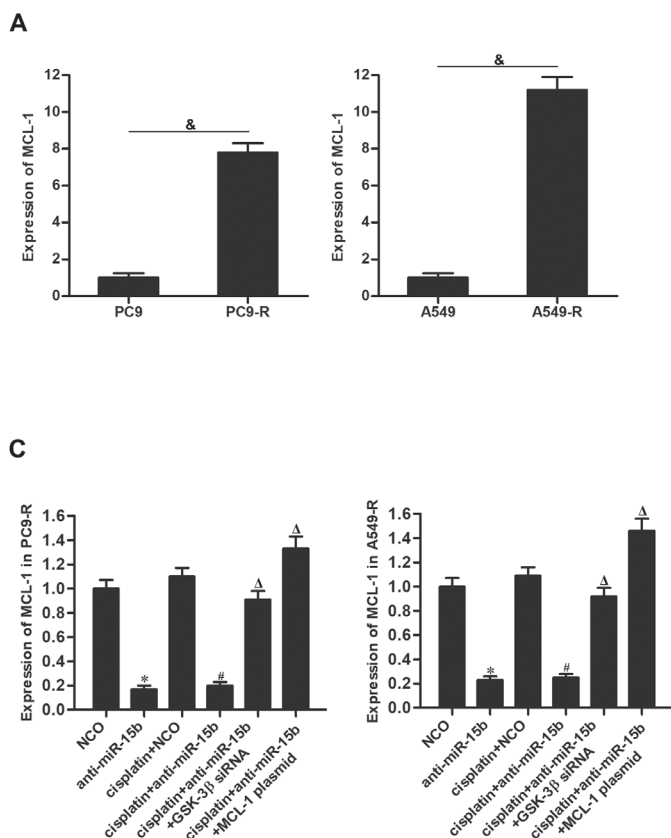
Fig. 6. Anti-miR-15b inhibited the expression of MCL-1 through an increase in GSK-3β expression. A. Difference of MCL-1 between cisplatin-resistant non-small-cell lung cancer (NSCLC) cells (PC9-R and A549-R) and their parental NSCLC cells (PC9 and A549); B. MCL-1 siRNA enhanced the cytotoxicity of cisplatin (20 μM) against PC9-R and A549-R cells; C. Effect of anti-miR-15b and GSK-3β siRNA on MCL-1 expression in PC9-R and A549-R cells; D. Effect of GSK-3β siRNA and MCL-1 plasmid on protection of PC9-R and A549-R cells from the cytotoxicity of co-treatment with cisplatin (20 μM) and anti-miR-15b. Data are presented as the means standard deviation (SD)

&p < 0.05; $p < 0.05 compared to cisplatin+control siRNA group; *p < 0.05 compared to negative control oligonucleotide (NCO) group; #p < 0.05 compared to cisplatin+NCO group; Δp < 0.05 compared to cisplatin+anti-miR-15b group.
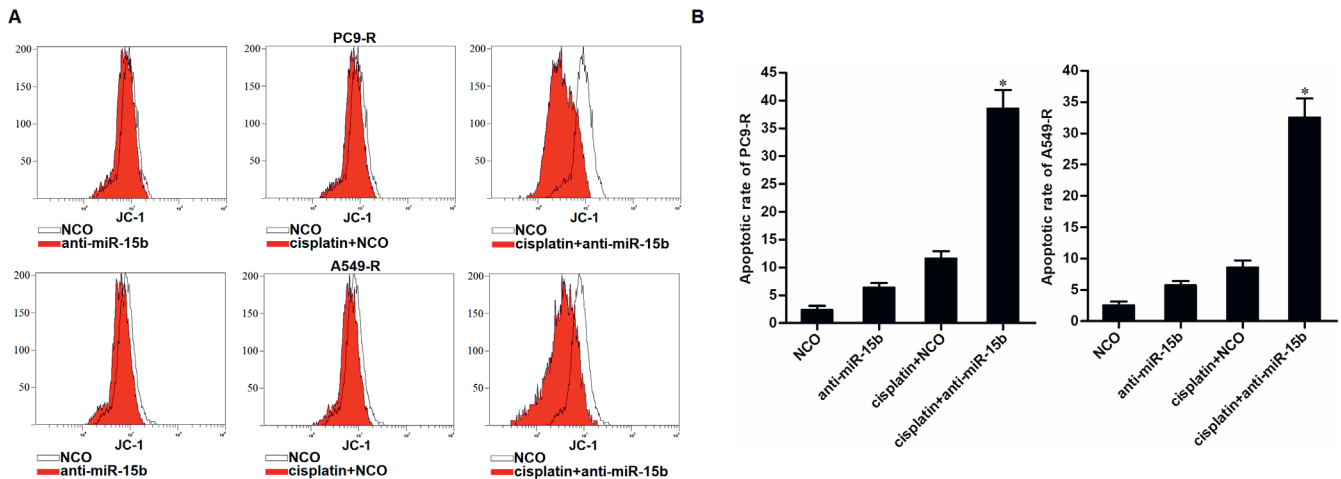
Fig. 7. Anti-miR-15b enhanced the cisplatin-induced apoptosis of PC9-R and A549-R cells through the mitochondrial pathway. A. Combination treatment with cisplatin (20 μM) and anti-miR-15b induced mitochondrial collapse in PC9-R and A549-R cells; B. Combination treatment with cisplatin (20 μM) and anti-miR-15b induced significant apoptosis of PC9-R and A549-R cells. Data are presented as the means ±standard deviation (SD)

*p < 0.05 compared to cisplatin+NCO group.

found to antagonize drug resistance in hepatocellular carcinoma,[28] prostate cancer[29] and breast cancer.[30] In NSCLC, studies have also revealed functions for miRNAs. For instance, miR-100 and miR-873 can confer resistance to ALK tyrosine kinase inhibitors in NSCLC cells.[31,32] MiRNAs have been recognized as a promising target for NSCLC treatment. MiR-15b was reported to function as a tumor promoter in some cancers including NSCLC.[24–26] However, the potential role of miR-15b in cisplatin resistance in NSCLC is still unclear. In the present study, we showed a significant overexpression of miR-15b in cisplatin-resistant NSCLC cells compared to their parental cells. Interestingly, we found that increased miR-15b expression can partially induce cisplatin resistance in routine NSCLC cell lines, whereas knockdown of miR-15b expression can reduce cisplatin resistance in cisplatin-resistant NSCLC cell lines. Our work confirmed that miR-15b partially determined the cisplatin sensitivity of NSCLC cells. MiR-15b may be a potential therapeutic target for improving the cisplatin-based chemotherapy in NSCLC.

GSK-3β is a serine/threonine protein kinase. Previous studies have indicated that inhibition of GSK-3β is responsible for occurrence, progression, metastasis, and drug resistance of multiple cancers such as colon cancer,[33] hepatocellular carcinoma[34] and breast cancer.[35] Therefore, GSK-3β functions as a tumor suppressor.

Drug resistance is a significant challenge to overcome. The mechanisms of drug resistance in cancer cells include at least one of the following: enhancement of DNA damage repair, enhancement of drug inactivation, dysregulation of growth factor signaling pathways, and/or dysregulation of survival-related genes.[36] Recent studies have indicated that GSK-3β induces degradation of MCL-1.[27,37] Therefore, deficiency of GSK-3β means overexpression of MCL-1. MCL-1 is a key anti-apoptotic protein belonging to the Bcl-2

family.[38] As MCL-1 is mainly located on the mitochondrial membrane, MCL-1 prevents the mitochondrial apoptosis of cancer cells by inactivating pro-apoptotic proteins such as Noxa and Puma. Overexpression of MCL-1 has been shown to be an important mechanism for the development of chemoresistance in cancer cells.[39,40]

In this study, a significant reduction of GSK-3β expression and an increase in MCL-1 expression was observed in cisplatin-resistant NSCLC cells compared to standard NSCLC cells. Furthermore, we confirmed that the downregulation of GSK-3β and overexpression of MCL-1 was responsible for cisplatin resistance in NSCLC. These data illustrated that the cisplatin-resistant NSCLC cells developed drug resistance through dysregulation of survival-related genes.

In summary, to obtain the drug resistance, the cisplatin-resistant NSCLC cells overexpressed miR-15b, reducing the expression level of GSK-3β. As a result, MCL-1 accumulated and the NSCLC cells gained resistance to cisplatin-induced apoptosis. According to the pathway, anti-miR-15b (miR-15b antisense oligonucleotides) was used to correct the overexpression of miR-15b in cisplatin-resistant NSCLC cells. As a result, expression of GSK-3β was increased and MCL-1 was degraded. Moreover, anti-miR-15b expanded mitochondrial apoptosis of NSCLC cells, which were under the stress of cisplatin. Taken together, this study provides the basis for potential intervention using miRNAs in cancer therapy.

Limitations

Although we have proved that knockdown of miR-15b reduces cisplatin resistance in NSCLC cell lines, the role of miR-15b in NSCLC patients is still unclear. Therefore, further study is required to clarify the effect of miR-15b on chemotherapy in vivo.

Conclusions

Our findings provide evidence that anti-miR-15b partially reversed cisplatin resistance in NSCLC through the GSK-3β/MCL-1 pathway. However, further studies are required to evaluate the approach of anti-miR-15b adjuvant treatment in clinical applications.

ORCID iDs

Tianjian Lu https://orcid.org/0000-0003-4894-3190
Weiping Lu https://orcid.org/0000-0002-6322-6897
Chunyi Jia https://orcid.org/0000-0002-6598-6902
Shanguang Lou https://orcid.org/0000-0002-5626-9565
Yan Zhang https://orcid.org/0000-0003-4246-157X

References

1. Siegel RL, Miller KD, Jemal A. Cancer statistics, 2019. *CA Cancer J Clin.* 2019;69(1):7–34. doi:10.3322/caac.21551
2. Torre LA, Siegel RL, Jemal A. Lung cancer statistics. *Adv Exp Med Biol.* 2016;893:1–19. doi:10.1007/978-3-319-24223-1_1
3. Hellyer JA, Wakelee HA. Adjuvant chemotherapy. *Thorac Surg Clin.* 2020;30(2):179–185. doi:10.1016/j.thorsurg.2020.01.003
4. Liu Y, He C, Huang X. Metformin partially reverses the carboplatin-resistance in NSCLC by inhibiting glucose metabolism. *Oncotarget.* 2017;8(43):75206–75216. doi:10.18632/oncotarget.20663
5. Cui Q, Wang JQ, Assaraf YG, et al. Modulating ROS to overcome multidrug resistance in cancer. *Drug Resist Updat.* 2018;41:1–25. doi:10.1016/j.drup.2018.11.001
6. Rotow J, Bivona TG. Understanding and targeting resistance mechanisms in NSCLC. *Nat Rev Cancer.* 2017;17(11):637–658. doi:10.1038/nrc.2017.84
7. Wang D, Zhao C, Xu F, et al. Cisplatin-resistant NSCLC cells induced by hypoxia transmit resistance to sensitive cells through exosomal PKM2. *Theranostics.* 2021;11(6):2860–2875. doi:10.7150/thno.51797
8. Mu Y, Hao X, Xing P, et al. Acquired resistance to osimertinib in patients with non-small-cell lung cancer: Mechanisms and clinical outcomes. *J Cancer Res Clin Oncol.* 2020;146(9):2427–2433. doi:10.1007/s00432-020-03239-1
9. Duan L, Perez RE, Chastain PD, et al. JMJD2 promotes acquired cisplatin resistance in non-small cell lung carcinoma cells. *Oncogene.* 2019;38(28):5643–5657. doi:10.1038/s41388-019-0814-6
10. Lai CL, Wei YF, Hsia TC, et al. S-1 plus cisplatin as first-line treatment of patients with advanced non-small cell lung cancer in Taiwan. *Asia Pac J Clin Oncol.* 2020;16(2):e68–e73. doi:10.1111/ajco.13294
11. Najafi M, Tavakol S, Zarrabi A, et al. Dual role of quercetin in enhancing the efficacy of cisplatin in chemotherapy and protection against its side effects: A review [published online ahead of print]. *Arch Physiol Biochem.* 2020;1–15. doi:10.1080/13813455.2020.1773864
12. Liu J, Tang Q, Li S, et al. Inhibition of HAX-1 by miR-125a reverses cisplatin resistance in laryngeal cancer stem cells. *Oncotarget.* 2016;7(52):86446–86456. doi:10.18632/oncotarget.13424
13. Matsumoto M, Nakajima W, Seike M, et al. Cisplatin-induced apoptosis in non-small-cell lung cancer cells is dependent on Bax- and Bak-induction pathway and synergistically activated by BH3-mimetic ABT-263 in p53 wild-type and mutant cells. *Biochem Biophys Res Commun.* 2016;473(2):490–496. doi:10.1016/j.bbrc.2016.03.053
14. Jiang T, Liu B, Wu D, et al. BCLAF1 induces cisplatin resistance in lung cancer cells. *Oncol Lett.* 2020;20(5):227. doi:10.3892/ol.2020.12090
15. Wang N, Song L, Xu Y, et al. Loss of Scribble confers cisplatin resistance during NSCLC chemotherapy via Nox2/ROS and Nrf2/PD-L1 signaling. *EBioMedicine.* 2019;47:65–77. doi:10.1016/j.ebiom.2019.08.057
16. Vu LT, Gong J, Pham TT, et al. MicroRNA exchange via extracellular vesicles in cancer. *Cell Prolif.* 2020;53(11):e12877. doi:10.1111/cpr.12877
17. Rupaimoole R, Slack FJ. MicroRNA therapeutics: Towards a new era for the management of cancer and other diseases. *Nat Rev Drug Discov.* 2017;16(3):203–222. doi:10.1038/nrd.2016.246
18. Creugny A, Fender A, Pfeffer S. Regulation of primary microRNA processing. *FEBS Lett.* 2018;592(12):1980–1996. doi:10.1002/1873-3468.13067
19. Miao J, Regenstein JM, Xu D, et al. The roles of microRNA in human cervical cancer. *Arch Biochem Biophys.* 2020;690:108480. doi:10.1016/j.abb.2020.108480
20. Saliminejad K, Khorram Khorshid HR, Soleymani Fard S, et al. An overview of microRNAs: Biology, functions, therapeutics, and analysis methods. *J Cell Physiol.* 2019;234(5):5451–5465. doi:10.1002/jcp.27486
21. Paliouras AR, Monteverde T, Garofalo M. Oncogene-induced regulation of microRNA expression: Implications for cancer initiation, progression and therapy. *Cancer Lett.* 2018;421:152–160. doi:10.1016/j.canlet.2018.02.029
22. Ghafouri-Fard S, Shoorei H, Taheri M. miRNA profile in ovarian cancer. *Exp Mol Pathol.* 2020;113:104381. doi:10.1016/j.yexmp.2020.104381
23. Li H, Zhang X, Jin Z, et al. MiR-122 promotes the development of colon cancer by targeting ALDOA in vitro. *Technol Cancer Res Treat.* 2019;18:1533033819871300. doi:10.1177/1533033819871300
24. Wang S, Zhang G, Zheng W, et al. MiR-454-3p and miR-374b-5p suppress migration and invasion of bladder cancer cells through targeting ZEB2. *Biosci Rep.* 2018;38(6):BSR20181436. doi:10.1042/BSR20181436
25. Lu L, Li Y, Wen H, et al. Overexpression of miR-15b promotes resistance to sunitinib in renal cell carcinoma. *J Cancer.* 2019;10(15):3389–3396. doi:10.7150/jca.31676
26. Wang J, Yao S, Diao Y, et al. miR-15b enhances the proliferation and migration of lung adenocarcinoma by targeting BCL2. *Thorac Cancer.* 2020;11(6):1396–1405. doi:10.1111/1759-7714.13382
27. Kang XH, Zhang JH, Zhang QQ, et al. Degradation of Mcl-1 through GSK-3β activation regulates apoptosis induced by bufalin in non-small cell lung cancer H1975 cells. *Cell Physiol Biochem.* 2017;41(5):2067–2076. doi:10.1159/000475438
28. Ji L, Lin Z, Wan Z, et al. MiR-486-3p mediates hepatocellular carcinoma sorafenib resistance by targeting FGFR4 and EGFR. *Cell Death Dis.* 2020;11(4):250. doi:10.1038/s41419-020-2413-4
29. Zhang JY, Li YN, Mu X, et al. Targeted regulation of miR-195 on MAP2K1 for suppressing ADM drug resistance in prostate cancer cells. *Eur Rev Med Pharmacol Sci.* 2020;24(15):7911. doi:10.26355/eurrev_202008_22445
30. Guan X, Guan Y. MiR-145-5p attenuates paclitaxel resistance and suppresses the progression in drug-resistant breast cancer cell lines. *Neoplasma.* 2020;67(5):972–981. doi:10.4149/neo_2020_190622N536
31. Lai Y, Kacal M, Kanony M, et al. MiR-100-5p confers resistance to ALK tyrosine kinase inhibitors crizotinib and lorlatinib in EML4-ALK-positive NSCLC. *Biochem Biophys Res Commun.* 2019;511(2):260–265. doi:10.1016/j.bbrc.2019.02.016
32. Jin S, He J, Li J, et al. MiR-873 inhibition enhances gefitinib resistance in non-small cell lung cancer cells by targeting glioma-associated oncogene homolog 1. *Thorac Cancer.* 2018;9(10):1262–1270. doi:10.1111/1759-7714.12830
33. Yu Z, Du J, Zhao Y, et al. A novel kinase inhibitor, LZT-106, downregulates Mcl-1 and sensitizes colorectal cancer cells to BH3 mimetic ABT-199 by targeting CDK9 and GSK-3β signaling. *Cancer Lett.* 2021;498:31–41. doi:10.1016/j.canlet.2020.10.001
34. Zhou ZJ, Luo CB, Xin HY, et al. MACROD2 deficiency promotes hepatocellular carcinoma growth and metastasis by activating GSK-3β/β-catenin signaling. *NPJ Genom Med.* 2020;5(1):15. doi:10.1038/s41525-020-0122-7
35. Zhang X, Zhong S, Xu Y, et al. MicroRNA-3646 contributes to docetaxel resistance in human breast cancer cells by GSK-3beta/beta-catenin signaling pathway. *PLoS One.* 2016;11(4):e0153194. doi:10.1371/journal.pone.0153194
36. Longley DB, Johnston PG. Molecular mechanisms of drug resistance. *J Pathol.* 2005;205(2):275–292. doi:10.1002/path.1706
37. Elgendy M, Cirò M, Hosseini A, et al. Combination of hypoglycemia and metformin impairs tumor metabolic plasticity and growth by modulating the PP2A-GSK3β-MCL-1 axis. *Cancer Cell.* 2019;35(5):798–815.e5. doi:10.1016/j.ccell.2019.03.007
38. Song X, Shen L, Tong J, et al. Mcl-1 inhibition overcomes intrinsic and acquired regorafenib resistance in colorectal cancer. *Theranostics.* 2020;10(18):8098–8110. doi:10.7150/thno.45363
39. Kehr S, Haydn T, Bierbrauer A, et al. Targeting BCL-2 proteins in pediatric cancer: Dual inhibition of BCL-X$_L$ and MCL-1 leads to rapid induction of intrinsic apoptosis. *Cancer Lett.* 2020;482:19–32. doi:10.1016/j.canlet.2020.02.041
40. Floros KV, Jacob S, Kurupi R, et al. Targeting transcription of MCL-1 sensitizes HER2-amplified breast cancers to HER2 inhibitors. *Cell Death Dis.* 2021;12(2):179. doi:10.1038/s41419-021-03457-6

Overexpression of HTRA1 increases the proliferation and migration of retinal pigment epithelium cells

Jinzi Zhou[1,A–E], Fenghua Chen[1,A–F], Aimin Yan[1,B,C,E,F], Xiaobo Xia[2,C,E,F]

[1] Department of Ophthalmology, The First People's Hospital of Guiyang, China

[2] Department of Ophthalmology, Xiangya Hospital Central South University, Changsha, China

A – research concept and design; B – collection and/or assembly of data; C – data analysis and interpretation;
D – writing the article; E – critical revision of the article; F – final approval of the article

Address for correspondence
Jinzi Zhou
E-mail: zjinzh1109@163.com

Conflict of interest
None declared

Abstract

Background. Age-related macular degeneration (AMD) mainly affects the central region of retina and has many late-stage manifestations.

Objectives. Age-related macular degeneration is a leading cause of irreversible blindness in older people. The main feature of AMD is retinal pigment epithelium (RPE) degeneration. In this study, we aimed to explore the influence of HTRA1 expression on the proliferation and migration of RPE cells.

Materials and methods. Human ARPE-19 cells were transfected with an HTRA1 overexpression lentivirus or HTRA1 siRNA to silence HtrA1 expression. Quantitave reverse-transcription polymerase chain reaction (qRT-PCR) and western blotting were used to verify the relative level of HTRA1 mRNA and expression of HTRA1 protein of transfected human ARPE-19 cells. The MTT clone formation and transwell assays were used to confirm the effect of HTRA1 expression on the proliferation, colony forming ability and migration of ARPE-19 cells.

Results. The proliferation capacity (shown as optical density value) of ARPE-19 cells in the HTRA1-overexpressing group at culture times of 24 h and 48 h were 0.595 ±0.032 and 0.867 ±0.037 respectively, which were much higher than in the mock group. However, the proliferative capacity of cells in the HTRA1-silenced group decreased with increasing time of culture, compared with the mock group. The number of cloned and migrating cells in the HTRA1-overexpressing group were much higher than in the mock group, whereas the numbers in the HTRA1-silenced group were significantly lower.

Conclusions. Overexpression of HTRA1 promotes proliferation and migration of RPE cells, which can help maintain the function of sensory neurons in the retina. Therefore, HTRA1 may be a suitable target for AMD treatments.

Key words: proliferation, migration, HtrA1, AMD, RPE

Background

Age-related macular degeneration (AMD) is an eye disease that mainly affects the central region of retina with many late-stage manifestations.[1] An abundance of cone photoreceptors in the retina can impact visual acuity. Previous studies have reported pathological changes during the development of AMD. However, the pathogenesis of AMD still needs to be explored further.[2] Retinal pigment epithelium (RPE) degeneration is one of the most important characteristics of AMD and plays a key role in regulating the neurosensory retina. The unusual structure of the RPE is closely related to the etiology of AMD.[3,4] Previous data have shown that age-related maculopathy susceptibility 2 (ARMS2) and HtrA serine peptidase 1 (HTRA1) located at chromosome 10q26 are closely associated with susceptibility to AMD.[5,6] Wang et al. speculated that HTRA1 might be an important risk factor in AMD.[7]

Human HTRA1 is a member of the serine protease family, which regulates protein quality and cell fate.[8] Aberrant expression of HTRA1 was found in a variety of tumors. Some studies have shown that overexpression of HTRA1 restrains tumor growth, indicating that HTRA1 might be a tumor-inhibiting factor.[9,10] HTRA1 may regulate the progression of AMD by mediating a variety of different pathways. Various substrates of HTRA1 have been identified, such as fibronectin, aggrecan and the transforming growth factor-beta (TGF-β) family.[11] Moreover, HTRA1 was shown to inhibit signaling via the TGF-β family.

Objectives

In this study, RPE cells were transfected with an HTRA1 overexpression lentivirus or HTRA1 siRNA. The effects of HTRA1 on the proliferation and migration of RPE cells were investigated.

Materials and methods

Cell culture

The human retinal pigment epithelial cell line ARPE-19 was purchased from Cell Repository, Chinese Academy of Sciences (Shanghai, China) and cultured in Dulbecco's modified Eagle's medium (DMEM) supplemented with 10% fetal bovine serum (FBS; Gibco, Carlsbad, USA), and 100 mg/L streptomycin and $1*10^{-5}$/UI penicillin (Gibco) at 37°C/5% CO_2.

Establishment of HTRA1-overexpressing cells

A pcDNA3 eukaryotic expression vector (Invitrogen, Carlsbad, USA) was used to establish stably transfected HTRA1-overexpressing cells. To construct the pcDNA3-HTRA1 plasmid, the full-length human HTRA1 gene *pB4* was digested with EcoRI and inserted into an EcoRI-cleaved pcDNA3 vector. ARPE-19 cells were transfected with pcDNA3 or pcDNA3-HTRA1 using the lipofection technique according to the manufacturer's protocol (Gibco BRL, Life Technologies, Rockville, USA).

Transfection of siRNAs

Human HTRA1 siRNA and scrambled control siRNA were purchased from Santa Cruz Biotechnology (Santa Cruz, USA). ARPE-19 cells were seeded onto multiple-well plates in DMEM containing 10% FBS and placed in a humidified incubator at 37°C and 5% CO_2. The cells were then transfected with 80 nM HTRA1 or non-target (control) siRNAs for 72 h using 2 μL/mL Lipofectamine 2000 Transfection Reagent (Invitrogen) according to the manufacturer's instructions.

Cell proliferation assay

Cells were seeded into 96-well plates at a density of 2×10^3 cells/well. The CCK-8 assay was used to indirectly determine cell growth.

qRT-PCR

Total RNA was isolated using the Total RNA Isolation System (Promega, Madison, USA). The cDNA was generated from 1 ug total RNA per sample using anchored oligo-dT primers (Reverse-iT First Strand Synthesis; ABgene, Thermo Fisher Scientific, Waltham, USA). Quantitative reverse-transcription polymerase chain reaction (qRT-PCR) was performed using a LightCycler and FastStart DNA Master SYBR Green 1 kit (Roche Applied Sciences, Basel, Switzerland).

Western blotting

Protein samples were extracted from cells and fractionated using 7.5–10% sodium dodecyl sulphate–polyacrylamide gel electrophoresis (SDS-PAGE). A primary antibody against HTRA1 (Stressgen Bioreagents, Ann Arbor, USA) was used, with glyceraldehyde-3-phosphate dehydrogenase (GAPDH; Research Diagnostics, Concord, USA) as an internal control.

Clone formation assay

Cells (100/well) were cultured in Roswell Park Memorial Institute (RPMI) 1640 medium supplemented with 10% FBS in six-well plates for 14 days. The number of clones (≥50 cells) was counted under a microscope.

Transwell assay

The transwell migration assay was performed in chemotaxis chambers containing 24 wells. A total of 5×10^4

cells were inoculated into the top chamber in DMEM (200 μL) without serum. The bottom chambers contained DMEM (600 μL) supplemented with 10% FBS. Cells that migrated through the pores to the bottom chamber were fixed in paraformaldehyde (4%) and stained with crystal violet. The number of cells was counted using a microscope (model DM4000B; Leica, Wetzlar, Germany).

Statistical analyses

One-way analysis of variance (ANOVA) and paired Student's t-tests were used and IBM SPSS v. 20.0 software (IBM Corp., Armonk, USA) was utilized. Significance level was defined as $p < 0.05$.

Results

Verification of transfection efficiency

Sequences of the constructed vector expressing HTRA1 (Fig. 1A) and HTRA1-shRNA (Fig. 1B) are shown. The HTRA1 mRNA and protein expression levels in each group were detected with qRT-PCR and western blot, respectively. The relative HTRA1 mRNA level in the HTRA1-overexpressed group was 0.291 ±0.035, which was significantly higher than in the mock group (0.075 ±0.014, $p < 0.01$). The HTRA1 mRNA expression in the sh-HTRA1#1 and sh-HTRA1#2 groups were 0.027 ±0.008 and 0.017 ±0.012, respectively, which were markedly lower than in the mock group ($p < 0.01$) and sh-Scb group (0.087 ±0.010) (Fig. 2A). The HTRA1 protein expression in the HTRA1-overexpressing group was much
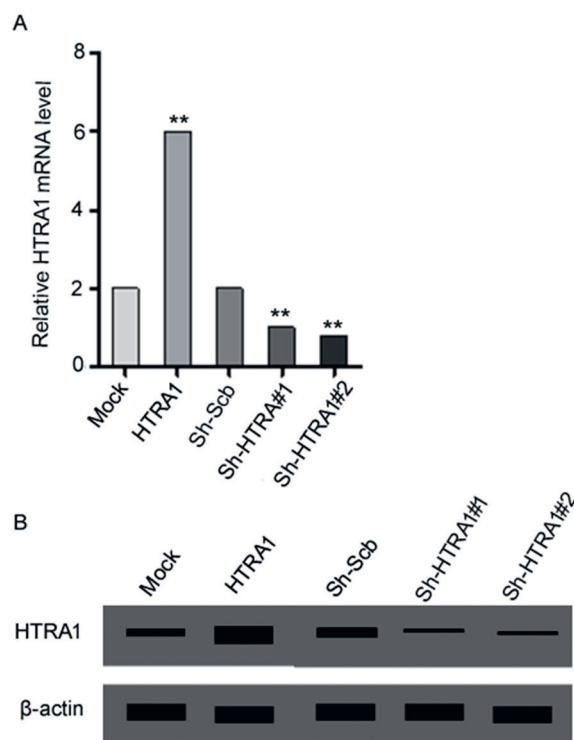
Fig. 2. Effect of plasmid or lentivirus transfection on HTRA1 expression. A. Relative HTRA1 mRNA level after transfection with HTRA1 overexpression lentivirus or HTRA1 siRNA plasmid (**$p < 0.01$ compared to mock group); B. Expression of HTRA1 protein in mock, HTRA1, shRNA-scb, and shRNA-HTRA1 groups

higher than in the mock group, indicating that the lentivirus transfection was successful (Fig. 2B). The HTRA1 protein level in the shRNA-HTRA1 groups were dramatically lower in comparison to the mock and sh-Scb groups ($p < 0.01$), suggesting that HTRA1 was knocked down by siRNA transfection.
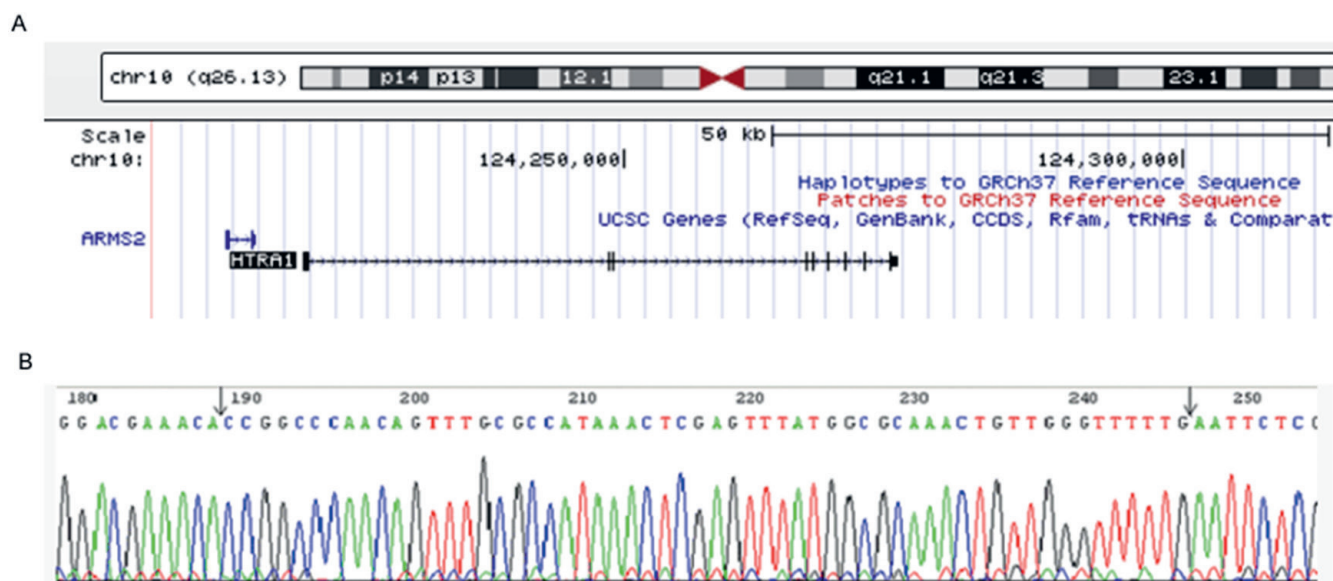
Fig. 1. Design of HTRA1 overexpression and silencing vectors. A. Constructed HTRA1 overexpression lentivirus; B. Constructed HTRA1-shRNA sequence

HTRA1 overexpression promotes proliferation of ARPE-19 cells

To investigate the effect of HTRA1 on the proliferation of ARPE-19 cells, CCK-8 was used to determine the proliferative capacity in all groups. As shown in Fig. 3, the proliferative capacity of ARPE-19 cells at 0 h in the mock, HTRA1-overexpressing (0.255 ±0.014), Sh-Scb (0.257 ±0.013), sh-HTRA1#1 (0.257 ±0.012), and sh-HTRA1#2 (0.257 ±0.016) groups were almost the same. As the culture time increased, the proliferative capacity of ARPE-19 cells in the HTRA1-overexpressing group significantly increased, compared with the mock group. At 24 h and 48 h, the optical density (OD) values in the HTRA1 group were 0.595 ±0.032 and 0.867 ±0.037, respectively, which were much higher than those in the mock group (0.460 ±0.028 and 0.646 ±0.035, respectively, $p < 0.01$). At 24 h and 48 h, the OD values in sh-HTRA1#1 group were 0.426 ±0.051 and 0.614 ±0.042, respectively, and 0.383 ±0.061 and 0.537 ±0.058, respectively, in the sh-HTRA1#2 group. The OD values in the sh-HTRA1#1 and sh-HTRA1#2 groups were significantly lower compared to the mock group at both time points ($p < 0.01$).

Overexpression of HTRA1 in ARPE-19 cells promotes invasion and vascular tube formation

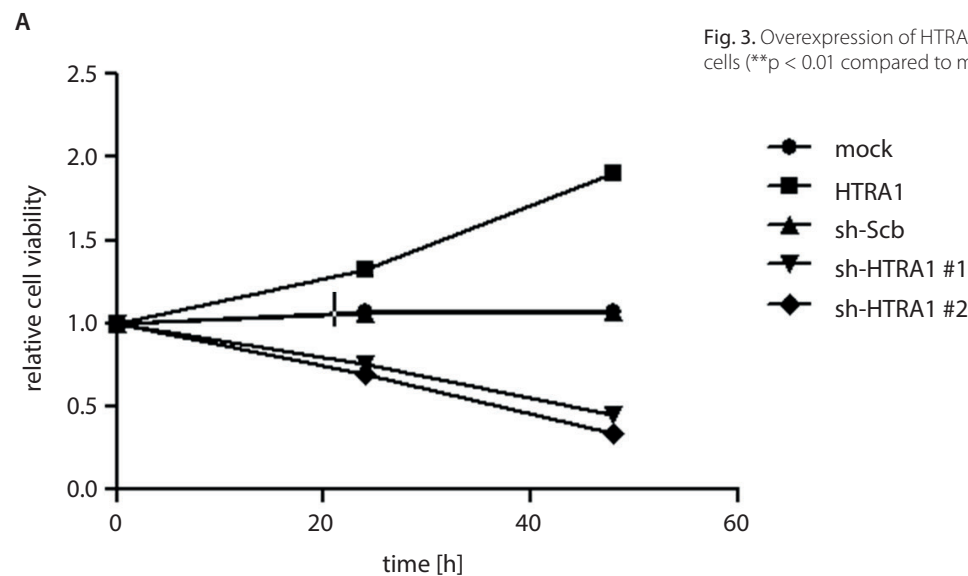To further explore the role of HTRA1 on AMD, we performed clone formation and transwell chamber analyses to assess the effect of HTRA1 overexpression or silencing on the cloning formation and migration of ARPE-19 cells. Compared with the mock group, the HTRA1-overexpressing group showed much more cloning cells in the clone formation assay, whereas the number of cells in the shRNA-HTRA1 groups were significantly lower than that in the mock and shRNA-scramble groups (Fig. 4A). These findings indicate that overexpression of HTRA1 in ARPE-19 cells promotes colony formation. The transwell migration assay results show that the number of migrating cells in the HTRA1-overexpressing group was much higher compared to the mock group, while the migration capacity of ARPE-19 cells in the shRNA-HTRA1 groups were lower compared to the mock and shRNA-scramble groups (Fig. 4B).

Discussion

The AMD is a major cause of irreversible blindness in the elderly population.[12] The key feature of AMD

A

Fig. 3. Overexpression of HTRA1 promotes the proliferation of ARPE-19 cells (**$p < 0.01$ compared to mock group)

B
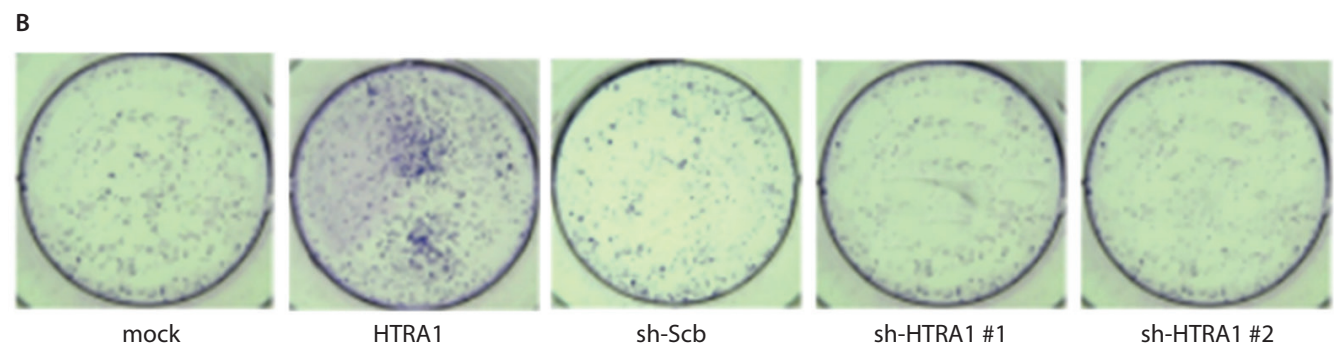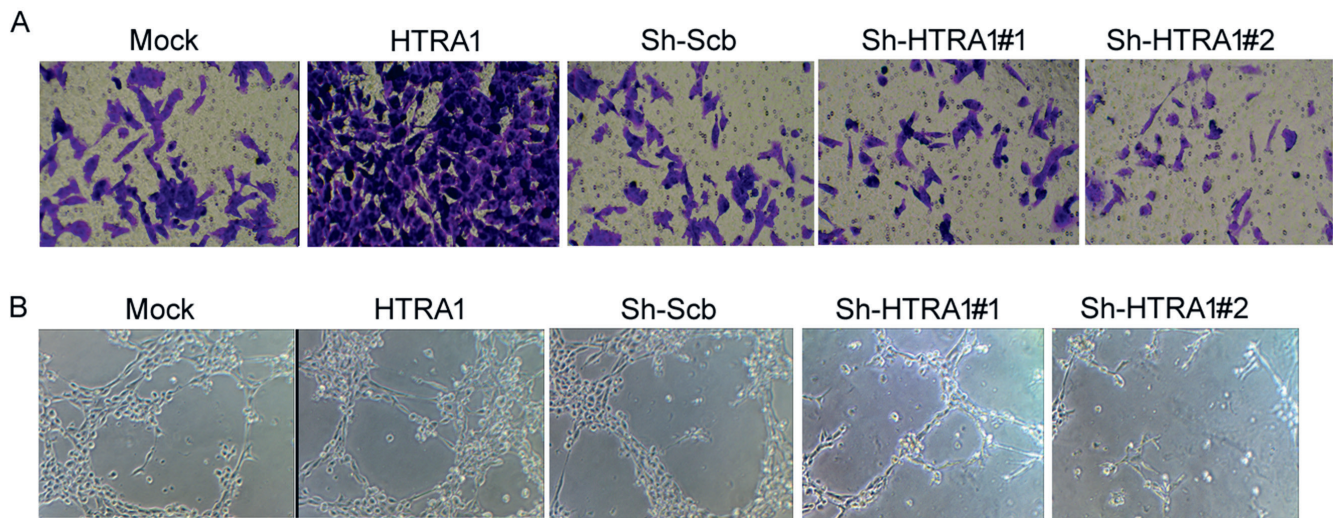
Fig. 4. Overexpression of HTRA1 promotes colony formation ability and migration of ARPE-19 cells. A. Colony formation in mock, HTRA1, shRNA-scb, and shRNA-HTRA1 groups; B. Migration of ARPE-19 cells in mock, HTRA1, shRNA-scb, and shRNA-HTRA1 groups

is degeneration of the RPE, which is located between retinal photoreceptors and choroidal capillaries. Dysfunction of RPE cells can destroy photoreceptors and disrupt the choroid vascular system.[13] In AMD, focal extracellular deposits in the Bruch's membrane are identified as drusen in ophthalmic testing. The presence of drusen and dense deposits are often considered to indicate the early stages of AMD.[14] The 2 key factors associated with the development of AMD are ARMS2 and HTRA1.[15] Specific HTRA1 alleles are related to neovascular lesion extent.[16] Increased expression of HTRA1 in the RPE of mice promoted the exudative form of AMD.[17] HTRA1 is a serine protease that controls protein quality and cell fate.[18] Previous studies have reported that HTRA1 might affect the occurrence and development of AMD by regulating extracellular matrix (ECM) proteoglycan degradation and TGF-β family activity.[19,20]

In this study, we explored the role of HTRA1 in ARPE-19 cells. The expression of HTRA1 in was increased or decreased by transfecting ARPE-19 cells with an HTRA1 overexpression plasmid or shRNA against HTRA1, respectively. Cell migration is an important part of the immune response and also plays a role in the development of diseases, including inflammation and tumor metastasis.[21] Indeed, cell migration is a key event of many physiological phenomena.[22] Cell viability, migration, and invasion are highly involved in cancer pathogenesis and other biological processes.[23] Control of cell proliferation is a fundamental aspect of tissue formation and regeneration.[24] To investigate the effect of HTRA1 on AMD, we assessed the proliferation, cloning formation, migration and angiogenic ability of ARPE-19 cells with overexpression or silencing of HTRA1. Our data show that overexpression of HTRA1 promotes proliferation, migration, cloning formation, and angiogenic ability of ARPE-19 cells, whereas HTRA1 silencing inhibits all these abilities.

Conclusions

Overexpression or silencing of HTRA1 affects the development of AMD. HTRA1 overexpression in ARPE-19 cells promoted proliferation, migration and vascular tube formation.

ORCID iDs

Jinzi Zhou https://orcid.org/0000-0002-4744-0252
Fenghua Chen https://orcid.org/0000-0002-8091-8078
Aimin Yan https://orcid.org/0000-0001-5165-9815
Xiaobo Xia https://orcid.org/0000-0002-2298-1482

References

1. Bandello F, Lafuma A, Berdeaux G. Public health impact of neovascular age-related macular degeneration treatments extrapolated from visual acuity. *Invest Ophthalmol Vis Sci.* 2007;48(1):96–103. doi:10.1167/iovs.06-0283
2. Ding X, Patel M, Chan CC. Molecular pathology of age-related macular degeneration. *Prog Retin Eye Res.* 2009;28(1):1–18. doi:10.1016/j.preteyeres.2008.10.001
3. Sonoda S, Sreekumar PG, Kase S, et al. Attainment of polarity promotes growth factor secretion by retinal, pigment epithelial cells: Relevance to age-related macular degeneration. *Aging (Albany NY).* 2010;2(1):28–42. doi:10.18632/aging.100111
4. Yu AL, Fuchshofer R, Kook D, Kampik A, Bloemendal H, Welge-Lüssen U. Subtoxic oxidative stress induces senescence in retinal pigment epithelial cells via TGF-β release. *Invest Opthalmol Vis Sci.* 2009;50(2):926–935. doi:10.1167/iovs.07-1003
5. Grassmann F, Heid IM, Weber BH; International AMD Genomics Consortium (IAMDGC). Recombinant haplotypes narrow the ARMS2/HTRA1 association signal for age-related macular degeneration. *Genetics.* 2017;205(2):919–924. doi:10.1534/genetics.116.195966
6. Fisher SA. Meta-analysis of genome scans of age-related macular degeneration. *Hum Mol Genet.* 2005;14(15):2257–2264. doi:10.1093/hmg/ddi230
7. Gaofeng W. Chromosome 10q26 locus and age-related macular degeneration: A progress update. *Exp Eye Res.* 2014;119:1–7. doi:10.1016/j.exer.2013.11.009
8. Grau S, Richards PJ, Kerr B, et al. The role of human HtrA1 in arthritic disease. *J Biol Chem.* 2006;281(10):6124–6129. doi:10.1074/jbc.M500361200

9. Chien J, Staub J, Hu SI, et al. A candidate tumor suppressor HtrA1 is downregulated in ovarian cancer. *Oncogene*. 2004;23(10):1636–1644. doi:10.1038/sj.onc.1207271

10. Catalano V, Muretto P, Aletti G, et al. Serine protease HtrA1 modulates chemotherapy-induced cytotoxicity. *J Clin Invest*. 2006;116(7):1994–2004. doi:10.1172/JCI27698

11. Friedrich U, Datta S, Schubert T, et al. Synonymous variants in HTRA1 implicated in AMD susceptibility impair its capacity to regulate TGF-β signaling. *Hum Mol Genet*. 2015;24(22):6361. doi:10.1093/hmg/ddv346

12. Resnikoff S, Pascolini D, Etya'Ale D, et al. Global data on visual impairment in the year 2002. *Bull World Health Organ*. 2004;82(11):844–851. PMID:15640920

13. Tarallo V, Hirano Y, Gelfand B, et al. DICER1 loss and Alu RNA induce age-related macular degeneration via the NLRP3 inflammasome and MyD88. *Cell*. 2012;149(4):847–859. doi:10.1016/j.cell.2012.03.036

14. Doyle SL, Campbell M, Ozaki E, et al. NLRP3 has a protective role in age-related macular degeneration through the induction of IL-18 by drusen components. *Nat Med*. 2012;18(5):791–798. doi:10.1038/nm.2717

15. Jakobsdottir J, Conley YP, Weeks DE, Mah TS, Ferrell RE, Gorin MB. Susceptibility genes for age-related maculopathy on chromosome 10q26. *Am J Hum Genet*. 2005;77(3):389–407. doi:10.1086/444437

16. Yang CH, Yang CH. The evolution of antivascular endothelial growth factor agents for the treatment of neovascular age-related macular degeneration. *Taiwan J Ophthalmol*. 2014;4(1):1–2. doi:10.1016/j.tjo.2014.01.002

17. Jones A, Kumar S, Zhang N, et al. Increased expression of multifunctional serine protease, HTRA1, in retinal pigment epithelium induces polypoidal choroidal vasculopathy in mice. *Proc Natl Acad Sci U S A*. 2011;108(35):14578–14583. doi:10.1073/pnas.1102853108

18. Oka C, Tsujimoto R, Kajikawa M, et al. HtrA1 serine protease inhibits signaling mediated by TGF-β family proteins. *Development*. 2004;131(5):1041–1053. doi:10.1242/dev.00999

19. Yang Z, Camp NJ, Sun H, et al. Variant of the HTRA1 gene increases susceptibility to age-related macular degeneration. *Science*. 2006;314(5801):992–993. doi:10.1126/science.1133811

20. Jacobo SMP, Deangelis MM, Kim IK, Kazlauskas A. Age-related macular degeneration-associated silent polymorphisms in HtrA1 impair its ability To antagonize insulin-like growth factor 1. *Mol Cell Biol*. 2013;33(10):1976–1990. doi:10.1128/MCB.01283-12

21. Kramer N, Walzl A, Unger C, et al. In vitro cell migration and invasion assays. *Mutat Res*. 2013;752(1):10–24. doi:10.1016/j.mrrev.2012.08.001

22. Stroka K, Jiang H, Chen SH, et al. Water permeation drives tumor cell migration in confined microenvironments. *Cell*. 2014;157(3):611–623. doi:10.1016/j.cell.2014.02.052

23. Ridha L, An W, Bea P, et al. Comparative analysis of dynamic cell viability, migration and invasion assessments by novel real-time technology and classic endpoint assays. *PLoS One*. 2012;7(10):e46536. doi:10.1371/journal.pone.0046536

24. Streichan SJ, Hoerner CR, Schneidt T, Holzer D, Hufnagel L. Spatial constraints control cell proliferation in tissues. *Proc Natl Acad Sci U S A*. 2014;111(15):5586–5591. doi:10.1073/pnas.1323016111

Reviews

Role of resistin in cardiovascular diseases: Implications for prevention and treatment

Maciej Rachwalik[1,A–F], Magdalena Hurkacz[2,A–F], Beata Sienkiewicz-Oleszkiewicz[2,A,B,E,F], Marek Jasiński[1,3,E,F]

[1] Department and Clinic of Cardiac Surgery, Wroclaw Medical University, Poland
[2] Department of Clinical Pharmacology, Wroclaw Medical University, Poland
[3] Children's Memorial Pediatric Health Institute, Warszawa, Poland

A – research concept and design; B – collection and/or assembly of data; C – data analysis and interpretation;
D – writing the article; E – critical revision of the article; F – final approval of the article

Address for correspondence
Maciej Rachwalik
E-mail: maciej.rachwalik@umed.wroc.pl

Abstract

Cardiovascular diseases (CVDs) are associated with socioeconomic and, most importantly, with clinical problems. Accordingly, the identification of early and specific biomarkers indicating metabolic changes that underlie disease development and/or progression is important and may improve preventive and treatment strategies. A recently discovered protein – resistin (ADSF, FIZZ3) – whose expression is increased in carbohydrate metabolism and adipose tissue disorders, seems to be worth of interest in this context. The current publication was based on a detailed review of available literature, including Medline, EBSCO, Scopus, and Cochrane Library databases. The search period was between January 1, 2001 and December 20, 2020. The following keywords were used: "resistin", "resistin AND cardiology" and "resistin AND cardiosurgery". Our review covered a total of 4476 records, 594 of which were review publications. The presented article summarizes the current knowledge on the role of resistin in prevention and treatment of CVDs. Available literature shows that resistin may be a predictor for various pathological states; however, data from some studies on the pathophysiological mechanisms of action are contradictory. There is a need for further investigations to explore the exact role of resistin in CVDs.

Key words: cardiovascular diseases, atherosclerosis, adipose tissue, cardiac surgery, resistin

Introduction

Over the last decade, the cultural and lifestyle changes in western civilizations and also the progressive aging of society led to a huge increase in the prevalence of diseases resulting from these phenomena. This causes tremendous financial costs that need to be incurred to ensure proper medical care and quality of life for all patients.

According to the World Health Organization (WHO) report, 55% of all 55.4 million deaths in 2019 were caused by 10 diseases that belong to 3 groups – cardiovascular (coronary artery disease (CAD) and stroke), pulmonary and neonatal diseases. Coronary artery disease is the leading cause of mortality accounting for 16% of all deaths.[1] Scientific research conducted in the 20th and 21st century led to the discovery of a number of agents (e.g., proteins such as neopterin, resistin and adiponectin) that are having a direct and indirect impact on the course of the above-mentioned diseases. Deeper knowledge is gained about the pathophysiological mechanisms in cells leading to metabolic diseases. This may enable better patient outcome and disease prevention.

This publication aims to assess the current knowledge on resistin as a biomarker in the prevention and treatment of heart diseases. Moreover, we will discuss the usefulness of measuring resistin level in everyday cardiological and cardiosurgical practice. We assessed the available scientific publications documenting the use of resistin as a biomarker for heart diseases and measurement of resistin levels for cardiovascular event screening in populations with risk factors.

Methodology

This article provides a review of the current publications (published until December 20, 2020). The following databases were searched using selected keywords and Medical Subject Headings (MeSH): Medline (using PubMed and EBSCO), Cochrane Library and Ovid Embase. The search terms were "resistin" and its synonyms (for example "adipose tissue-specific secretory factor", "adipocyte cysteine-rich secreted protein FIZZ3", "ADSF", "FIZZ3", "FIZZ3 protein", "protein found in inflammatory zone 3", "adipocyte-secreted factor", "adipocyte-specific secreted factor"). To achieve a comprehensive assessment, we did not state the date for the first publication and also performed a manual search. In PubMed, the term "resistin" yielded 4476 records (594 review articles). In 2020, 308 articles were published (31 reviews). Using the keywords "biomarkers AND cardiovascular prevention" to search for publications in databases resulted in 14,271 records (1198 in 2020). The term "resistin AND cardiology" generated 185 publications (17 published in 2020). The term "resistin AND cardiac surgery" resulted in 53 articles (5 published in 2020). In the Scopus database, the term "resistin"

appeared in 6911 publications (445 published in 2020) and the term "resistin AND cardiology" in 28 articles. Precisely 1402 records were reviews (6 of them published in 2020). In the Cochrane Library, the term "resistin" generated 526 results, while the term "resistin AND cardiology" 5 results. All of the articles were listed in the "trials" category. Additionally, a detailed search for publications was carried out using the keyword "resistin AND cardiovascular prevention AND biomarkers". In the PubMed database, 55 results were obtained, including only 7 for 2020. Similar keywords were used in the Scopus database search engine. Two hundred thirty-eight results for this query were obtained, of which 25 were published in 2020. In the EBSCO database, there were 80 and 7 results, respectively. There were no review publications.

The results of various studies show that there is a huge scientific interest in the role of resistin in the etiology of diseases, especially cardiovascular ones, but the usefulness of resistin as a biomarker in cardiac surgery is not fully established yet.

Results

The review of the publication database results indicates that most of the works focus on the current knowledge how this protein impacts the pathophysiological mechanism of various diseases. The few studies that tried to apply the knowledge of resistin levels as a prognostic factor for various phenomena in patients with heart disease seem to be promising. It is important to note that resistin can be obtained from both peripheral blood and adipose tissue, especially the epicardial adipose tissue. This opens potential pathways for future in-depth diagnosis of heart diseases and the use of resistin tests as a screening biomarker in cardiology and cardiac surgery. The results of several published studies will be presented in this paper.

Discovery of resistin, its structure and role in disease epidemiology

Adipokines are proteins structurally similar to cytokines and play an important role as biomarkers for lipid metabolism disturbances. Research performed on the influence of obesity on hormone secretion and metabolic syndrome development showed that adipose tissue plays an important role not only as a storage depot but also as a specific endocrine organ secreting functional proteins participating in different regulatory functions of the organism. The discovery of the *RETN* gene (encoding resistin) confirmed this function.[2] *RETN* (ADSF, FIZZ3, RETN1) was first discovered in mouse immune system genes. In humans, it is located on chromosome 19p13.2 and has 4 exons (the length of resistin pre-peptide in humans is 108 amino acid residues and it is 114 in mice). The first one has an approximate length of 1750 base pairs. The characteristic feature of this

family is the C-terminal stretch of 10 cysteine residues with identical spacing.[3] The mouse homolog of this protein is secreted by adipocytes and may be correlated with obesity and type 2 diabetes (T2D) development.[4] Genetic tests showed the presence of mRNA in the adipose tissue. Its expression is 418% higher in the abdominal adipose tissue than in adipose tissue from other parts of the body, for example from the thighs. McTernan et al. correlated this phenomenon with a greater risk of T2D and obesity.[5]

Resistin was discovered by Steppan et al. in 2001 while studying a new class of antidiabetic drugs – glitazones.[6] At the same time, Kim et al. showed that this protein secreted by adipocytes inhibits the proliferation of adipose cells.[7] Other authors discovered that resistin is one of the inflammation factors that have an impact on the reactivation of the respiratory system.[8] Before these studies were published, the main scientific interests focused on resistin as a factor influencing insulin resistance. Nowadays, it is thought to be a protein playing an important role in various pathomechanisms. The name resistin originates from the phrase "resistance to insulin". It is one of the resistin-like molecules (RELMs) proteins and was first discovered in mouse peripheral blood.[9] Different names for this protein can be found in the literature with resistin being the most frequently used followed by adipose-specific secretory factor (ADSF) and "protein found in inflammatory zone 3" (FIZZ3).[10]

The RELMs may influence signal pathways on a cell level, leading to changes in the concentrations of a variety of substances in tissues. Resistin has a multidirectional effect. Through its influence on the metabolism, it antagonizes the action of insulin and reduces glucose level in adipocytes and muscle cells.[8]

Resistin has 2 conformations: a trimer with molecular mass of 45 kDa and an oligomer with a molecular mass of 660 kDa. The influence of those 2 conformations on the activity of resistin has not yet been established.[11] The protein is present in the serum as oligomers with high or low molecular masses.[12] The multidirectional action of resistin on the metabolism is pleiotropic and directed through 3 mechanisms, i.e., paracrine, endocrine and autocrine mechanisms.[13]

It was shown that resistin is produced in human immune system cells, such as granulocytes, macrophages and monocytes. Moreover, the activity of this protein was observed in hematopoietic stem cells, the spleen, thymus, skeletal muscle system, digestive system, pancreas, placenta, and uterus.[14] More recent studies showed that *RETN* gene polymorphism may affect the course of treatment, especially in oncology.[15] It is suspected that a large number of cells and tissues may react to circulating resistin, which suggests that the protein may have an impact on a wide variety of pathological and physiological processes.

Resistin influences the inhibition of leptin activity through regulating the signal pathway inhibitor expression.[16] There is evidence that higher levels of this protein in adipose tissue promote the development of insulin resistance that is one

of the components of metabolic syndrome (MetS). This is now actively studied. Resistin changes the metabolism of carbohydrates, influencing liver enzyme activity. Banerjee et al. showed that resistin changes the activity of 5'AMP-activated protein kinase in the liver. The decrease of activity is connected with adenosine monophosphate (AMP) phosphorylation, which causes an increase in glucose release in the liver.[16] This protein accumulates in perivascular adipose tissue (PVAT). This tissue is endocrinally independent of other hormone influences according to studies. In diet-induced obesity, the dysfunction of PVAT leads to vascular diseases. Perivascular adipose tissue contains adipocytes, preadipocytes, mesenchymal stem cells, endothelial cells, and inflammatory cells. Mesenchymal stem cells from PVAT may differentiate into adipocytes, osteoblasts and endothelial cells. The composition of adipose tissue in obesity is different in different people in a given population, and the number of macrophages and lymphocytes T increases. This phenomenon is still being studied. Numerous inflammatory mediators released from epicardial adipose tissue (EAT) may affect the dynamics of atherosclerosis (AS) and ischemic heart disease (IHD) development.

Reference values of resistin levels in normal and pathological conditions

Resistin levels in healthy individuals are within the range of 7–22 ng/mL, and are on average 15 ng/mL. They increase with age and underlying pathological conditions, e.g., in diabetes it is 40 ng/mL.[17] Resistin levels depend on metabolic changes in the organism. According to Rajala et al., resistin levels are lower in a fasting state than after meals.[18] Obese individuals have higher resistin concentrations than slim ones.[19,20] Persons with diabetes and obese patients have increased plasma resistin levels.[12] In patients with MetS, the levels of this protein correlate with the levels of inflammation biomarkers and CAD.[21] In patients with osteoarthritis and rheumatoid arthritis, resistin levels are increased in the synovial fluid and tissue.[22]

The impact of resistin levels on insulin levels

One of the first observations related to resistin was that the levels of this protein were higher in mice with genetic or experimentally generated obesity.[9] In rats, resistin levels were higher in insulin resistance related to hepatic disturbances. The protein may influence the apoptosis of beta cells in their pancreas.[23,24] The extrapolation of this data to humans is difficult because of the different histologic composition of the adipose tissue, and the fact that the protein is synthesized in circulating blood monocytes. In contrast to mice, the synthesis of resistin in human white adipose tissue does not play an important role. It is worth mentioning that human and mouse resistin are approx. 60% homologous. Resistin has the ability to bind

the suppressor of cytokine signal proteins (SOCS), which are negative regulators of the JAK-STAT signal pathway. A correlation was found in relation to both dose and time. Through resistin induction, SOCS may increase insulin resistance, which corresponds to the impact of resistin on insulin activity in adipocytes.[25]

A study by Sheng et al. showed that the expression of resistin in hepatocytes leads to the development of insulin resistance in humans.[26] Resistin mRNA levels are higher in patients with T2D than in healthy volunteers.[27] Gharibeh et al. compared obese patients not suffering from T2D and those with diabetes. Higher levels of resistin were found in the latter group.[28] In patients with T2D and diabetic foot, resistin levels were even higher than in diabetic patients without this complication. In comparative studies conducted among obese people and patients with T2D, resistin expression was higher in the former, but not in the latter group.[29] In another study, a correlation of higher resistin levels and T2D was found. Moreover, a correlation with complications of gestational diabetes was found.[11] More studies on the impact of resistin levels on insulin resistance pathogenesis are needed to establish them as insulin resistance biomarkers in different patient groups.

Impact of resistin on the etiology of thrombosis

Recent studies show that in the pathophysiological mechanism of myocardial infarction (MI), thrombus building on the surface of plaque seems to play a key role in coronary arteries. Resistin probably plays an important role in this process, too. This role is connected with its influence on NO synthesis. Present theories pertain to the regulatory function of resistin on the endothelial nitric oxide synthase (eNOS) enzyme. This enzyme generates NO in the endothelium through the conversion of L-arginine into L-citrulline. The NO plays a role in platelet activity and in vivo studies are ongoing. Endogenous NO generated by eNOS is an important regulator of in vivo platelet activity in the vascular endothelium and has a minimal impact on inducible NOS and neuronal NOS.[30] The abovementioned theories need further validation in animal models. Resistin and oxidative stress may play a role in the pathogenesis of CAD, including acute coronary syndrome (ACS). The influence of resistin levels on the oxidative-reductive balance was evaluated in ACS to distinguish it from stable angina. Patients with ACS had higher resistin levels than those with stable angina (2.55 ±0.13 ng/mL compared to 1.53 ±0.12 ng/mL, respectively; p < 0.001).[31]

The impact of resistin levels on kidney diseases

A relationship between hyperresistinemia and renal function impairment was established in 2009.[32] Through the stimulation of proper signal pathways, cytokines may influence binding on the cell surface and triggering

signal pathways. In this way, they may influence cell function. The cytokine response takes place through the change in the number of receptors on the cell surface, regulation of the synthesis of other cytokines, and the change in gene activity and transcription.[33] Resistin influences the synthesis and release of endothelin-1 (ET-1) from endothelial cells, increases the production of cell adhesion molecules, and may decrease the synthesis of factor 3 connected with the tumor necrosis factor alpha (TNF-α) receptor. Endothelin-1 is a vascular factor synthesized in the endothelium that may be related to the development of AS.[34]

The impact of resistin levels on other diseases

In current studies, resistin is also thought to be connected with different cardiovascular diseases (CVDs), especially IHD.[35] Other studies show its potential relationship with oncologic diseases, asthma, Crohn's disease, and T2D.[32] Higher resistin levels were observed in patients with kidney failure.[36] Active cancer is connected with higher resistin activity, which may have an impact on its progression.[37] Resistin and other adipokines play an increasingly important role in the diagnosis of oncologic diseases. The research in the last 2 decades showed that their higher levels in serum are affecting breast cancer development in women with pre-existing obesity. Wang et al. showed a correlation between resistin levels and frequency of stromal tumor in breast cancer, especially in postmenopausal women with obesity.[38] Resistin together with other adipokines may be used as a predictor for complex breast cancer risk assessment in women.[39] Figure 1 shows the main mechanisms related to the influence of resistin on the human body and diseases in which it may play an important role.

Resistin as a potential biomarker of cardiovascular diseases treatment and prevention

The impact of resistin levels on the development of atherosclerosis

Cardiovascular diseases, especially IHD, are a leading cause of death in today's world. Atherosclerosis is an inflammatory disease. Monocytes migrate to the arterial endothelium where they differentiate into macrophages. The next step in this process is the invasion of large amounts of lipoproteins and further differentiation into foam cells, which may form a plaque. Importantly, resistin is synthesized not only in human adipocytes but also in macrophages.[40] This is supported by the fact that high resistin levels were observed in patients with ACS, where
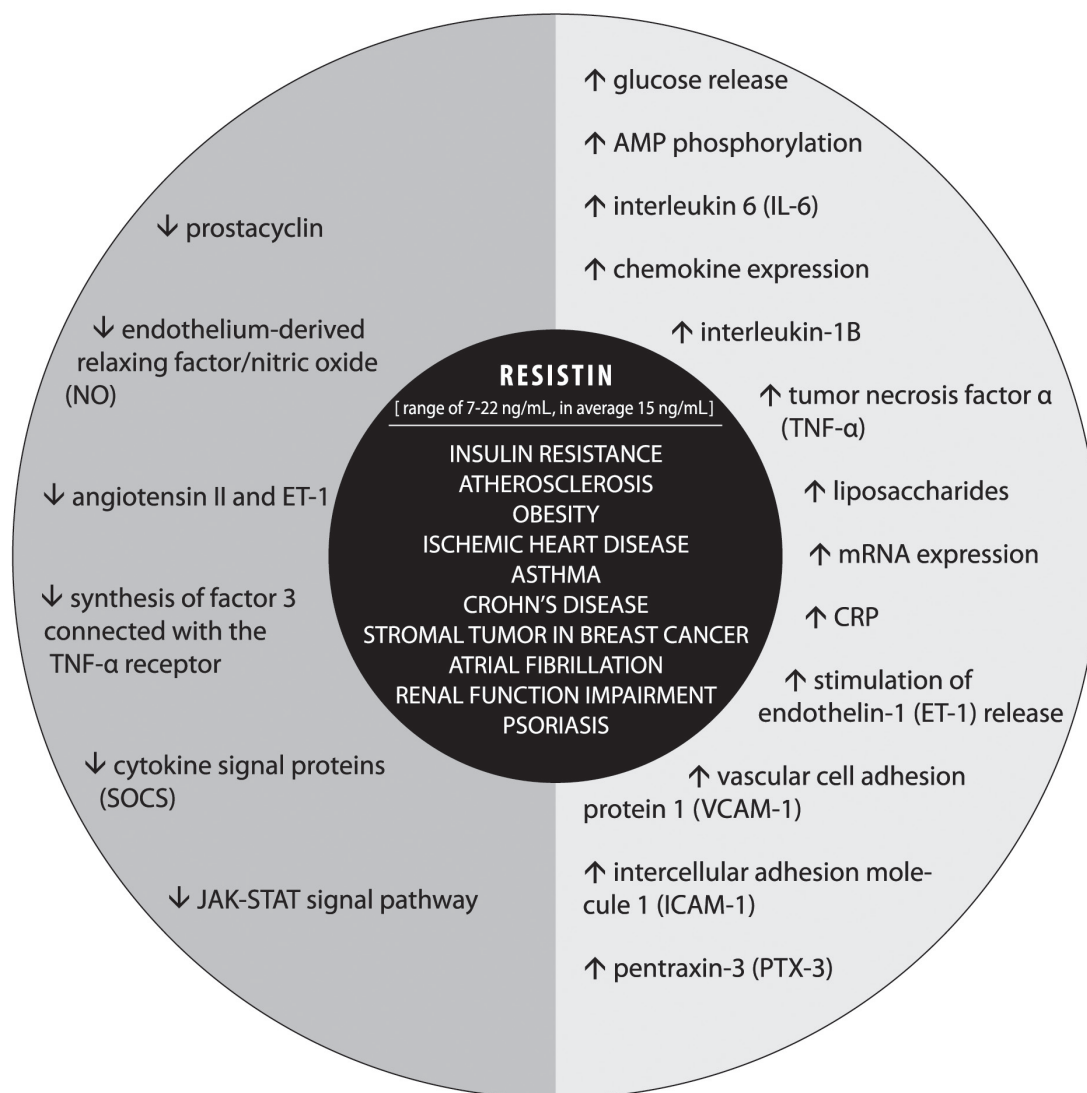
Fig. 1. The main mechanisms related to the influence of resistin on the human body and diseases in which it may play an important role

damage from plaques occurs. The cells infiltrate arteries and are a source of cytokines. As an adipokine, resistin induces cytokine and chemokine expression.[41]

Many studies showed a correlation between IHD and changes in plasma resistin levels as well as in pericardial perivascular tissue. Wang et al. showed higher plasma resistin levels in patients with ACS.[42] In a group of 220 patients with ACS, resistin levels were higher than in patients that qualified for elective cardiac procedures (1.18 ±0.48 μg/L compared to 0.49 ±0.40 μg/L; p < 0.01). Hu et al. published similar observations. In a group of 93 patients with ACS, resistin levels in patients with unstable angina were 12.09 ng/mL compared to 9.04 ng/mL in patients without signs of instability. Higher resistin levels were a syndrome of unstable angina. However, this study did not reveal a positive correlation between resistin concentrations and hypertension.[43] A positive correlation between resistin levels and high sensitivity C-reactive protein (CRP) levels and white blood cells (WBC) count was observed, which was also reported by other scientists.[44,45]

The impact of resistin levels on the etiology of atherosclerosis and endothelial function

The complicated mechanism of AS leads to an increase of lipid storage in blood vessels, proliferation of smooth muscle tissue cells, inflammatory cell invasion, and finally inflammation of blood vessels. Ischemic heart disease is caused by the progressive development of strictures in coronary vessels in the form of plaques, which are the places of damage and blood vessel stenosis. Literature shows that this process may be influenced by serum resistin levels.[46]

Initially, resistin was only associated with the influence on insulin resistance development. Further studies showed that the protein is involved in inflammatory processes in in vitro and in vivo conditions. Positive feedback is observed between the level of resistin and pro-inflammatory proteins such as interleukin (IL)-1B, IL-6, TNF-α, and liposaccharides, which significantly increase the expression

of resistin in peripheral blood mononuclear cells.[47] Resistin takes part in the communication between adipocytes and inflammatory cells.[48] An increase of mRNA expression and CRP secretion by peripheral blood mononuclear cells (PBMC) was shown.[49]

Free radicals are involved in the atherosclerotic process. Their production is connected with hyperresistinemia, the migration of monocytes to the inner membrane of the coronary vessels and their differentiation into macrophages. The consequence of monocyte migration is their stepwise differentiation into foam cells that accumulate the oxidated form of low-density lipoproteins (LDL). An additional factor of plaque formation is endothelial dysfunction. The process is multifactorial and modulated by cytokines, free radicals, growth factors, and cell adhesion molecules (influencing the tension of the coronary vascular wall and leukocyte adhesion).[11] In the development of AS, the mechanisms that mediate the adhesion, and release of inflammatory and anti-inflammatory cytokines are not fully known. Resistin may play a role in endothelial dysfunction through stimulation of ET-1 release.[50] It induces the expression of adhesive molecules, such as vascular cell adhesion protein 1 (VCAM-1), intercellular adhesion molecule 1 (ICAM-1) and pentraxin-3 (PTX-3), a pneumonia biomarker. Other proteins that inhibit the release of VCAM-1 and ICAM-1, additionally lowering insulin resistance, such as adiponectin, stand in contrast to the proatherogenic action of resistin. This shows that there is a balance between pro- and antiatherogenic factors; a balance between serum levels of resistin and adiponectin. An imbalance influences the development or inhibition of AS.[51] Endothelial dysfunction and endoplasmic reticulum stress was shown to influence resistin mRNA levels in a special mouse adipocyte cell line (3T3-L1) leading to the progression of AS in this model.[52] Coronary endothelial cells constitute a protective barrier against pathophysiological phenomena promoting AS. Prostacyclin, endothelium-derived relaxing factor/NO, angiotensin II, and ET-1 are substances synthesized and released by endothelial cells supporting their secretory properties.[53] The tight arrangement of the endothelial cells in the coronary vessels is additionally strengthened by endothelial cell junctions. Damage to this barrier leads to higher permeability for monocytes, macrophages, leucocytes, and cholesterol-transporting lipoproteins.[54] It was shown in a rabbit artery model that resistin synthesized in macrophages leads to the adhesion of monocytes to endothelial cells through the integration of integrin-alpha 4 and beta-1 in monocytes. This leads to VCAM-1 expression and longer-lasting monocytes on the plaque causing an increase in inflammation.[55]

In vitro studies showed that higher resistin levels may increase the permeability of endothelial cells. Epicardial adipose tissue is indicated as the source of resistin.[56] Other substances belonging to RELMs, especially RELM-beta, may play a similar role. Similar to resistin, RELM-beta is also a cysteine-rich protein.[57] Resistin influences also eNOS in endothelial cells. A correlation between the levels of this protein, lower mRNA expression and enzyme activity was shown. Nitric oxide concentration negatively correlated with resistin levels. The protein from endothelial cells increases the synthesis of reactive oxygen species (ROS) and suboxide anions.[58]

Kougias et al. showed that resistin acts as a pro-oxidant in endothelial dysfunction through lowering eNOS expression. A decrease of endothelial-dependent and independent vasorelaxation was noticed in prepared porcine coronary artery rings in vitro. This effect was significant when high levels of resistin (>40 ng/mL) were used.[59] Dick et al. confirmed the previously mentioned results using coronary arteries of dogs under general anesthesia and prepared parts of canine coronary artery rings. Resistin decreased the bradykinin-induced vasorelaxation, which led to the conclusion that this protein may influence the metabolism of endothelial cells. The experiment did not show that endothelial dysfunction caused by resistin influences the development of AS and the decrease of bradykinin activity was reported as moderate.[60] There are also some doubts as to whether the influence of resistin on human coronary arteries is the same as in other species such as pigs or dogs. Studies in mice were also performed. Transverse aortic vascular rings of mice (C57BL/6; n = 22) were exposed to various biological factors, including resistin. A decrease in vasorelaxation caused by insulin was observed. According to scientists, resistin acts mainly in the endothelium through the insulin-mediated IRS1 signal pathway, leading to Akt/eNOS phosphorylation and, in consequence, a decrease of NO-dependent vasorelaxation.[61] The abovementioned studies showed that resistin changes the vasomotor functions of coronary arteries in vivo and in vitro.

In 2014, Cabrera de Leon et al. published the results of a study on the impact of resistin levels on the occurrence of cardiovascular events. The study was conducted in a group of 6636 randomly selected people. It was shown that resistin levels in women were higher than in men, and, regardless of gender, these levels correlated with the frequency of cardiovascular events. The researchers also assessed other factors, such as: arterial hypertension, abdominal obesity, diabetes, dyslipidemia, and smoking.[62]

In 2015, Gencer et al. published a summary of results from a ten-year follow-up on the relationship between resistin and cardiovascular events. Exactly 3044 people aged 70–79 participated in the study. Cardiovascular events were defined as heart disease or stroke, whereas severe events were defined as death or MI. There was a significant correlation between the frequency and severity of cardiovascular events and plasma resistin levels.[63] Muse et al. investigated the relationship between resistin levels and the incidence of cardiovascular events in various ethnic groups in 1913 people, and found that the Hispanic group presented with a higher risk of cardiovascular events, which correlated with resistin levels.[64]

Resistin can be used as a peripheral blood biomarker for strokes. In a study performed in 46 patients with ischemic stroke, higher levels of resistin and chemerin (another adipokine) were noticed. Higher levels of resistin and chemerin significantly increased the risk of ischemic stroke. The severity of stroke was not influenced by the levels of the aforementioned adipokines.[65]

In a group of patients with heart diseases requiring surgical intervention, levels of pro-inflammatory proteins were measured before and after the surgical procedure. The study showed that higher resistin levels correlated with blood transfusions after valve replacement surgery and revascularization of the heart muscle.[66]

In the AVOCADO study (Aspirin Vs./Or Clopidogrel in Aspirin-resistant Diabetics inflammation Outcomes), patients with T2D and at least 2 other cardiovascular risk factors and receiving acetylsalicylic acid were examined. It was noted that patients with atrial fibrillation (AF) presented higher levels of resistin and adiponectin than patients without AF. However, none of the analyzed adipokines was a predictive factor for AF development.[67]

In another study carried out in 146 patients, resistin was indicated to play a potentially predictive role as a biomarker for AF. Twenty eight patients with AF presented higher serum resistin levels.[68]

There is a practical aspect of measuring resistin levels in epicardial tissue (sectioned during cardiovascular surgery) as that may be an indirect predictor for AF during postoperative care. In our previous study, 46 patients after coronary artery bypass grafting (CABG) were monitored for 3 days after the surgery and divided into 2 groups (with AF after the surgery and without AF after surgery). Resistin levels in perivascular adipose tissue in the area of the left coronary artery were significantly higher in patients with AF than in those without AF (p = 0.03). Multivariate stepwise regression analysis showed that resistin levels higher than 54 ng/g in the PVAT of the left coronary artery were independently connected with AF in the postoperative period.[69] Resistin may also be a biomarker for cardiovascular events in patients undergoing cardiosurgical procedures. In a study with 33 patients that had CAD after cardiac surgery, the patients were divided into 2 groups, in which the 1st group included patients that underwent MI in the past while the patients in the 2nd group did not. Epicardial fat tissue was collected from all patients during cardiac surgery. Multivariate analysis showed that MI correlated with being male, older age, and higher resistin levels in epicardial fat tissue compared to potentially healthy persons.[70]

The influence of resistin on different disease processes in the human body is multidirectional and leads to negative outcomes. This is why resistin may be a potential target for new therapeutic strategies. However, the role of resistin in pathophysiology needs to be fully evaluated. A potential method for this evaluation is the use of a new antibody against human resistin (hResistin). It may be used for the immunohistochemical evaluation of hResistin expression, localization and intracellular/extracellular compartmentalization in human tissues. The cross-sectional reactivity of this monoclonal antibody against hResistin immunoglobulin G1 class (IgG1) with proper human tissues was also verified. The results show that hResistin is widely spread and localized mainly in cytoplasmic macrophage granules in the interstitial parts of most human tissues. Marked hResistin was also observed in the cytoplasm of nervous system cells. Data show that the antibody binds to human resistin and may be potentially used in immunotherapy aiming to decrease free circulating hResistin levels in patients.[71]

In the etiology of CVDs, obesity and insulin resistance play a vital role. The treatment of those diseases

Table 1. Human studies showing evidence for the role of resistin in cardiac diseases

Analysis	Group	Evidence	References
Various markers, plasma resistin levels	6636 people (randomly selected)	Resistin levels correlated with the frequency of cardiovascular events	Cabrera et al.[62]
Plasma resistin levels	3044 people aged 70–79	Positive significant correlation with cardiovascular events	Gencer et al.[63]
Resistin levels, different ethnic groups	1913 people from various ethnic groups	Resistin plasma levels correlated with the incidence of cardiovascular events in the Hispanic group	Muse et al.[64]
Peripheral blood resistin levels	46 patients with ischemic stroke	Higher levels of resistin significantly increased the risk of ischemic stroke	Kazimierczak-Kabzińska et al.[65]
Various protein levels before and after surgical procedure	90 patients divided into 3 groups undergoing open heart surgeries	Higher resistin levels correlated with blood transfusion after valve replacement surgery and revascularization of the heart muscle	Saracevic et al.[66]
AVOCADO study	304 patients with type 2 diabetes with 2 additional cardiovascular risk factors and receiving acetylsalicylic acid	In type 2 diabetes, patients with AF had higher resistin concentrations than patients with no AF	Peller et al.[67]
Serum resistin levels	146 patients with AF	Resistin may play predictive role as biomarker for AF	Samanidis et al.[68]

AF – atrial fibrillation.

is connected with the use of statins which minimize the incidence of CVDs. Statins may be used in patients with T2D because they decrease resistin mRNA levels in PBMC and plasma resistin levels.[72] In addition, resistin plasma levels may also be decreased by the use of ramipril or amlodipine.[73] Promising reports show that those levels may also be decreased by the bolus administration of vitamin C that leads to lower oxidative stress.[74] A similar effect was observed in psoriasis patients treated with retinoids.[75]
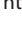
The review of available publications showed that the role of resistin as a marker in the etiology and treatment for heart diseases has increased in recent years, but the main interest lies in its role in metabolic, renal and oncological diseases. In the near future, new scientific data can be expected, which will also include issues related to cardiac surgery.

Table 1 provides an overview of relevant publications on the potential use of resistin as a biomarker in the treatment and prevention of heart diseases.

Conclusions

Publications show that resistin may be a predictor for various pathological states. Not all studies present precise and coherent data on the pathophysiological mechanisms of action. There is a need for further studies to explain the exact role of resistin in many diseases. Resistin could be a biomarker for cardiovascular events in patients undergoing cardiosurgical procedures. On the other hand, this protein may be a potential target for new therapeutic strategies.

ORCID iDs

Maciej Rachwalik   https://orcid.org/0000-0001-9714-4059
Magdalena Hurkacz   https://orcid.org/0000-0003-0846-3168
Beata Sienkiewicz-Oleszkiewicz   https://orcid.org/0000-0003-1912-0873
Marek Jasiński   https://orcid.org/0000-0002-9989-7748

References

1. WHO reveals leading causes of death and disability worldwide: 2000–2019 December 2020. Geneva, Switzerland: World Health Organization; 2020. https://www.who.int/news/item/09-12-2020-who-reveals-leading-causes-of-death-and-disability-worldwide-2000-2019. Accessed December 8, 2020.
2. Fasshauer M, Blüher M. Adipokines in health and disease. *Trends Pharmacol Sci.* 2015;36:461–470. doi:10.1016/j.tips.2015.04.014
3. Wang H, Chu WS, Hemphill C, Elbein SC. Human resistin gene: Molecular scanning and evaluation of association with insulin sensitivity and type 2 diabetes in Caucasians. *J Clin Endocrinol Metab.* 2002;87(6):2520–2524. doi:10.1210/jcem.87.6.8528
4. Berger A. Resistin: A new hormon that links obesity with type 2 diabetes. *BMJ.* 2001;322(7280):193. doi:10.1136/bmj.322.7280.193/c
5. McTernan C, McTernan P, Harte A, et al. Resistin, central obesity, and type 2 diabetes. *Lancet.* 2002;359(9300):46–47. doi:10.1016/s0140-6736(02)07281-1
6. Steppan CM, Bailey ST, Bhat S, et al. The hormone resistin links obesity to diabetes. *Nature.* 2001;409(6818):307–312. doi:10.1038/35053000
7. Kim KH, Lee K, Moon YS, Sul HS. A cysteine-rich adipose tissue-specific secretory factor inhibits adipocyte differentiation. *J Biol Chem.* 2001;276(14):11252–11256. doi:10.1074/jbc.C100028200
8. Borsuk A, Biernat W, Zięba D. Multidirectional action of resistin in the organism [in Polish]. *Postep Hig Med Dosw.* 2018;72:327–338.
9. Steppan CM, Brown EJ, Wright CM, et al. A family of tissue-specific resistin-like molecules. *Proc Natl Acad Sci U S A.* 2001;98(2):502–506. doi:10.1073/pnas.98.2.502
10. Al Hannan F, Culligan KG. Human resistin and the RELM of inflammation in diabesity. *Diabetol Metab Syndr.* 2015;7:54. doi:10.1186/s13098-015-0050-3
11. Codoner-Franch P, Alonso-Iglesias E. Resistin: Insulin resistance to malignancy. *Clin Chim Acta.* 2015;438:46–54. doi:10.1016/j.cca.2014.07.043
12. Gerber M, Boettner A, Seidel B, et al. Serum resistin levels of obese and lean children and adolescents: Biochemical analysis and clinical relevance. *J Clin Endocrinol Metab.* 2005;90(8):4503–4509. doi:10.1210/jc.2005-0437
13. Hsieh YY, Shen CH, Huang WS, et al. Resistin-induced stromal cell-derived factor-1 expression through Toll-like receptor 4 and activation of p38 MAPK/NFκB signaling pathway in gastric cancer cells. *J Biomed Sci.* 2014;21(1):59. doi:10.1186/1423-0127-21-59
14. Patel L, Buckels AC, Kinghorn IJ, et al. Resistin is expressed in human macrophages and directly regulated by PPAR gamma activators. *Biochem Biophys Res Commun.* 2003;300(2):472–476. doi:10.1016/s0006-291x(02)02841-3
15. Wang CQ, Tang CH, Tzeng HE, et al. Impacts of RETN genetic polymorphism on breast cancer development. *J Cancer.* 2020;11(10):2769–2777. doi:10.7150/jca.38088
16. Banerjee RR, Rangwala SM, Shapiro JS, et al. Regulation of fasted blood glucose by resistin. *Science.* 2004;303(5661):1195–1198. doi:10.1126/science.1092341
17. Fehmann HC, Heyn J. Plasma resistin levels in patients with type 1 and type 2 diabetes mellitus and in healthy controls. *Horm Metab Res.* 2002;34(11–12):671–673. doi:10.1055/s-2002-38241
18. Rajala MW, Qi Y, Patel HR, et al. Regulation of resistin expression and circulating levels in obesity, diabetes, and fasting. *Diabetes.* 2004;53(7):1671–1679. doi:10.2337/diabetes.53.7.1671
19. Nieva-Vazquez A, Pérez-Fuentes R, Torres-Rasgado E, López-López JG, Romero JR. Serum resistin levels are associated with adiposity and insulin sensitivity in obese Hispanic subjects. *Metab Syndr Relat Disord.* 2014;12(2):143–148. doi:10.1089/met.2013.0118
20. Joun BS, Yu KY, Park HJ, et al. Plasma resistin concentrations measured by enzyme-linked immunosorbent assay using a newly developed monoclonal antibody are elevated in individuals with type 2 diabetes mellitus. *J Clin Endocrinol Metab.* 2004;89(1):150–156. doi:10.1210/jc.2003-031121
21. Ohmori R, Momiyama Y, Kato R, et al. Associations between serum resistin levels and insulin resistance, inflammation, and coronary artery disease. *J Am Coll Cardiol.* 2005;46(2):379–380. doi:10.1016/j.jacc.2005.04.022
22. Schaffler A, Ehling A, Neumann E, et al. Adipocytokines in synovial fluid. *JAMA.* 2003;290(13):1709–1710. doi:10.1001/jama.290.13.1709-c
23. Rajala MW, Obici S, Scherer PE, Rossetti L. Adipose-derived resistin and gut-derived resistin-like molecule-beta selectively impair insulin action on glucose production. *J Clin Invest.* 2003;111(2):225–230. doi:10.1172/JCI16521
24. Gao C, Zhao D, Qiu J, et al. Resistin induces rat insulinoma cell RINm5F apoptosis. *Mol Biol Rep.* 2009;36(7):1703–1708. doi:10.1007/s11033-008-9371-8
25. Steppan CM, Wang J, Whiteman EL, Birnbaum MJ, Lazar MA. Activation of SOCS-3 by resistin. *Mol Cell Biol.* 2005;25(4):1569–1575. doi:10.1128/MCB.25.4.1569-1575.2005
26. Sheng CH, Di J, Jin Y, et al. Resistin is expressed in human hepatocytes and induces insulin resistance. *Endocrine.* 2008;33(2):135–143. doi:10.1007/s12020-008-9065-y
27. Tsiotra PC, Tsigos C, Anastasiou E, et al. Peripheral mononuclear cell resistin mRNA expression is increased in type 2 diabetic women. *Mediators Inflamm.* 2008;2008:892864. doi:10.1155/2008/892864
28. Gharibeh MY, Al Tawallbeh GM, Abboud MM, Radaideh A, Alhader AA, Khabour OF. Correlation of plasma resistin with obesity and insulin resistance in type 2 diabetic patients. *Diabetes Metab.* 2010;36:443–449. doi:10.3389/fphys.2019.01399
29. Laudes M, Oberhauser F, Schulte DM, et al. Visfatin/PBEF/Nampt and resistin expressions in circulating blood monocytes are differentially related to obesity and type 2 diabetes in humans. *Horm Metab Res.* 2010;42(4):268–273. doi:10.1055/s-0029-1243638

30. Moore C, Sanz-Rosa D, Emerson M. Distinct role and location of the endothelial isoform of nitric oxide synthase in regulating platelet aggregation in males and females in vivo. *Eur J Pharmacol*. 2011;651(1–3):152–158. doi:10.1016/j.ejphar.2010.11.011

31. Pourmoghaddas A, Elahifar A, Darabi F, Movahedian A, Amirpour A, Sarrafzadegan N. Resistin and prooxidant-antioxidant balance: Markers to discriminate acute coronary syndrome from stable angina. *ARYA Atheroscler*. 2020;16(2):46–54. doi:10.22122/arya.v16i2.1944

32. Filkova M, Haluzik M, Gay S, Senolt L. The role of resistin as a regulator of inflammation: Implications for various human pathologies. *Clin Immunol*. 2009;133(2):157–170. doi:10.1016/j.clim.2009.07.013

33. Verma S, Li SH, Wang CH, et al. Resistin promotes endothelial cell activation: Further evidence of adipokine-endothelial interaction. *Circulation*. 2003;108(6):736–740. doi:10.1161/01.CIR.0000084503.91330.49

34. Verma S, Li SH, Badiwala MV, et al. Endothelin antagonism and interleukin-6 inhibition attenuate the proatherogenic effects of C-reactive protein. *Circulation*. 2002;105(16):1890–1899. doi:10.1161/01.cir.0000015126.83143.b4

35. Libby P, Ridker PM, Hansson GK. Inflammation in atherosclerosis: From pathophysiology to practice. *J Am Coll Cardiol*. 2009;54(23):2129–2138. doi:10.1016/j.jacc.2009.09.009

36. Axelsson J, Bergsten A, Qureshi AR, et al. Elevated resistin levels in chronic kidney disease are associated with decreased glomerular filtration rate and inflammation, but not with insulin resistance. *Kidney Int*. 2006;69(3):596–604. doi:10.1038/sj.ki.5000089

37. Dalamaga M, Sotiropoulos G, Karmaniolas K, Pelekanos N, Papadavid E, Lekka A. Serum resistin: A biomarker of breast cancer in postmenopausal women? Association with clinicopathological characteristics, tumor markers, inflammatory and metabolic parameters. *Clin Biochem*. 2013;46(7–8):584–590. doi:10.1016/j.clinbiochem.2013.01.001

38. Wang YY, Hung AC, Lo S, Yuan SF. Adipocytokines visfatin and resistin in breast cancer: Clinical relevance, biological mechanisms, and therapeutic potential. *Cancer Lett*. 2021;498:229–239. doi:10.1016/j.canlet.2020.10.045

39. Wu X, Zhang X, Hao Y, Li J. Obesity-related protein biomarkers for predicting breast cancer risk: An overview of systematic reviews. *Breast Cancer*. 2021;28(1):25–39. doi:10.1007/s12282-020-01182-0

40. Tilg H, Moschen AR. Adipocytokines: Nediators linking adipose tissue, inflammation and immunity. *Nat Rev Immunol*. 2006;6(10):772–783. doi:10.1038/nri1937

41. Zhang Z, Xing X, Hensley G, et al. Resistin induces expression of proinflammatory cytokines and chemokines in human articular chondrocytes via transcription and messenger RNA stabilization. *Arthritis Rheum*. 2010;62(7):1993–2003. doi:10.1002/art.27473

42. Wang H, Chen DY, Cao J, He ZY, Zhu BP, Long M. High serum resistin level may be an indicator of the severity of coronary disease in acute coronary syndrome. *Chin Med Sci J*. 2009;24(3):161–166. doi:10.1016/s1001-9294(09)60082-1

43. Hu WL, Qiao SB, Hou Q, Yuan JS. Plasma resistin is increased in patients with unstable angina. *Chin Med J (Engl)*. 2007;120(10):871–875. PMID:17543176

44. Al-Daghri N, Chetty R, McTernan PG, et al. Serum resistin is associated with C-reactive protein & LDL cholesterol in type 2 diabetes and coronary artery disease in a Saudi population. *Cardiovasc Diabetol*. 2005;4:10–15. doi:10.1186/1475-2840-4-10

45. Bo S, Gambino R, Pagani A, et al. Relationships between human serum resistin, inflammatory markers and insulin resistance. *Int J Obes (Lond)*. 2005;29(11):1315–1320. doi:10.1038/sj.ijo.0803037

46. Taylor EB. The complex role of adipokines in obesity, inflammation, and autoimmunity. *Clin Sci*. 2021;135(6):731–752. doi:10.1042/CS20200895

47. Bokarewa M, Nagaev I, Dahlberg L, Smith U, Tarkowski A. Resistin, an adipokine with potent pro-inflammatory properties. *J Immunol*. 2005;174(9):5789–5795. doi:10.4049/jimmunol.174.9.5789

48. Biscetti F, Nardella E, Cecchini AL, Flex A, Landolfi R. Biomarkers of vascular disease in diabetes: The adipose-immune system cross talk. *Intern Emerg Med*. 2020;15(3):381–393. doi:10.1007/s11739-019-02270-6

49. Hu WL, Qian SB, Li LJ. Decreased C-reactive protein-induced resistin production in human monocytes by simvastatin. *Cytokine*. 2007;40(3):201–206. doi:10.1016/j.cyto.2007.09.011

50. Samsamshariat SZA, Sakhaei F, Salehizadeh L, Keshvari M, Asgary S. Relationship between resistin, endothelin-1, and flow-mediated dilation in patient with and without metabolic syndrome. *Adv Biomed Res*. 2019;8:16. doi:10.4103/abr.abr_126_18

51. Kawanami D, Maemura K, Takeda N, et al. Direct reciprocal effects of resistin and adiponectin on vascular endothelial cells: A new insight into adipocytokine-endothelial cell interactions. *Biochem Biophys Res Commun*. 2004;6;314(2):415–419. doi:10.1016/j.bbrc.2003.12.104

52. Lefterova MI, Mullican SE, Tomaru T, Qatanani M, Schupp M, Lazar MA. Endoplasmic reticulum stress regulates adipocyte resistin expression. *Diabetes*. 2009;58(8):1879–1886. doi:10.2337/db08-1706

53. Furchgott RF, Zawadzki JV. The obligatory role of endothelial cells in the relaxation of arterial smooth muscle by acetylcholine. *Nature*. 1980;288(5789):373–376. doi:10.1038/288373a0

54. Goshima Y, Okada Y, Torimoto K, Fujino Y, Tanaka Y. Changes in endothelial function during educational hospitalization and the contributor to improvement of endothelial function in type 2 diabetes mellitus. *Sci Rep*. 2020;21;10(1):15384. doi:10.1038/s41598-020-72341-8

55. Cho Y, Lee SE, Lee HC, et al. Adipokine resistin is a key player to modulate monocytes, endothelial cells, and smooth muscle cells, leading to progression of atherosclerosis in rabbit carotid artery. *J Am Coll Cardiol*. 2011;4;57(1):99–109. doi:10.1016/j.jacc.2010.07.035

56. Langheim S, Dreas L, Veschini L, et al. Increased expression and secretion of resistin in epicardial adipose tissue of patients with acute coronary syndrome. *Am J Physiol Heart Circ Physiol*. 2010;298:H746–H753. doi:10.1152/ajpheart.00617.2009

57. Mishra A, Wang M, Schlotman J, et al. Resistin-like molecule-beta is an allergen-induced cytokine with inflammatory and remodeling activity in the murine lung. *Am J Physiol Lung Cell Mol Physiol*. 2007;293(2):L305–L313. doi:10.1152/ajplung.00147.2007

58. Chen C, Jiang J, Lu JM, et al. Resistin decreases expression of endothelial nitric oxide synthase through oxidative stress in human coronary artery endothelial cells. *Am J Physiol Heart Circ Physiol*. 2010;299(1):H193–H201. doi:10.1152/ajpheart.00431.2009

59. Kougias P, Chai H, Lin PH, Lumsden AB, Yao Q, Chen C. Adipocyte-derived cytokine resistin causes endothelial dysfunction of porcine coronary arteries. *J Vasc Surg*. 2005;41(4):691–698. doi:10.1016/j.jvs.2004.12.046

60. Dick GM, Katz PS, Farias M III, et al. Resistin impairs endothelium-dependent dilation to bradykinin, but not acetylcholine, in the coronary circulation. *Am J Physiol Heart Circ Physiol*. 2006;291(6):H2997–H3002. doi:10.1152/ajpheart.01035.2005

61. Gentile MT, Vecchione C, Marino G, et al. Resistin impairs insulin-evoked vasodilation. *Diabetes*. 2008;57(3):577–583. doi:10.2337/db07-0557

62. Cabrera de Leon A, Gonzalez DA, Gonzalez Hernandez A, et al. The association of resistin with coronary disease in the general population. *J Atheroscler Thromb*. 2014;21(3):273–281. doi:10.5551/jat.19273

63. Gencer B, Auer R, de Rekeneire N, et al. Association between resistin levels and cardiovascular disease events in older adults: The health, aging and body composition study. *Atherosclerosis*. 2016;245:181–186. doi:10.1016/j.atherosclerosis.2015.12.004

64. Muse ED, Feldman DI, Blaha MJ, et al. The association of resistin with cardiovascular disease in the multi-ethnic study of atherosclerosis. *Atherosclerosis*. 2015;239(1):101–108. doi:10.1016/j.atherosclerosis.2014.12.044

65. Kazimierczak-Kabzińska A, Kajdaniuk D, Siemińska L, et al. Selected adipose tissue hormones in the blood of patients with ischaemic cerebral stroke. *Endokrynol Pol*. 2020;71(1):21–26. doi:10.5603/EP.a2019.0057

66. Saracevic A, Medved I, Hrabric Vlah S, Kozmar A, Bilic-Zulle L, Simundic AM. The association of systemic inflammatory markers with indicators of stress and cardiac necrosis in patients undergoing aortic valve replacement and revascularization surgeries. *Physiol Res*. 2020;69(2):261–274. doi:10.33549/physiolres.934243

67. Peller M, Kapłon-Cieślicka A, Rosiak M, et al. Are adipokines associated with atrial fibrillation in type 2 diabetes? *Endokrynol Pol*. 2020;71(1):34–41. doi:10.5603/EP.a2019.0059

68. Samanidis G, Gkogkos A, Bousounis S, Alexopoulos L, Perrea DN, Perreas K. Blood plasma resistin and atrial fibrillation in patients with cardiovascular disease. *Cardiol Res*. 2020;11(5):286–293. doi:10.14740/cr1121

69. Rachwalik M, Obremska M, Zyśko D, Matusiewicz M, Ściborski K, Jasiński M. The concentration of resistin in perivascular adipose tissue after CABG and postoperative atrial fibrillation. *BMC Cardiovasc Disord*. 2019;19(1):294. doi:10.1186/s12872-019-1254-5

70. Rachwalik M, Zyśko D, Diakowska D, Kustrzycki W. Increased content of resistin in epicardial adipose tissue of patients with advanced coronary atherosclerosis and history of myocardial infarction. *Thorac Cardiovasc Surg*. 2014;62(7):554–560. doi:10.1055/s-0034-1376403

874

M. Rachwalik et al. Resistin as a biomarker in cardiac surgery

71. Lin Q, Price SA, Skinner JT, et al. Systemic evaluation and localization of resistin expression in normal human tissues by a newly developed monoclonal antibody. *PLoS One.* 2020;15(7):e0235546. doi:10.1371/journal.pone.0235546

72. von Eynatten M, Schneider JG, Hadziselimovic S, et al. Adipocytokines as a novel target for the anti-inflammatory effect of atorvastatin in patients with type 2 diabetes. *Diabetes Care.* 2005;28(3):754–755. doi:10.2337/diacare.28.3.754

73. Westphal S, Borucki K, Taneva E, Makarova R, Luley C. Adipokines and treatment with niacin. *Metabolism.* 2006;55:1283–1285. doi:10.1016/j.metabol.2006.07.002

74. Krusinova E, Klementova M, Kopecky J, et al. Effect of acute hyperinsulinaemia with and without angiotensin II type 1 receptor blockade on resistin and adiponectin concentrations and expressions in healthy subjects. *Eur J Endocrinol*. 2007;157(4):443–449. doi:10.1530/EJE-07-0034

75. Corbetta S, Angioni R, Cattaneo A, Beck-Peccoz P, Spada A. Effects of retinoid therapy on insulin sensitivity, lipid profile and circulating adipocytokines. *Eur J Endocrinol*. 2006;154(1):83–86. doi:10.1530/eje.1.02057